Review of Tsunami Hazard in New Zealand (2013 Update)

Compiled by William Power

GNS Science Consultancy Report 2013/131
August 2013

Review of Tsunami Hazard in New Zealand (2013 Update)

Compiled by William Power

GNS Science Consultancy Report 2013/131
August 2013

DISCLAIMER

This report has been prepared by the Institute of Geological and Nuclear Sciences Limited (GNS Science) exclusively for and under contract to the Ministry of Civil Defence and Emergency Management. Unless otherwise agreed in writing by GNS Science, GNS Science accepts no responsibility for any use of, or reliance on any contents of this Report by any person other than the Ministry of Civil Defence and Emergency Management and shall not be liable to any person other than the Ministry of Civil Defence and Emergency Management, on any ground, for any loss, damage or expense arising from such use or reliance.

The data presented in this Report are available to GNS Science for other use from 13 September 2013.

BIBLIOGRAPHIC REFERENCE

Power, W. L. (compiler). 2013. Review of Tsunami Hazard in New Zealand (2013 Update), *GNS Science Consultancy Report* 2013/131. 222 p.

CONTENTS

EXECUTIVE SUMMARY IX

1.0 INTRODUCTION 1

1.1 SCOPE OF THIS REPORT 1
1.2 CONTRIBUTORS 1
1.3 STRUCTURE OF THE REPORT 2
1.4 WHAT IS A TSUNAMI? 3
1.5 WHAT DAMAGE DOES A TSUNAMI DO? 5

2.0 TSUNAMI IMPACTS 7

2.1 INTRODUCTION 7
2.2 TSUNAMI RISK 7
2.3 TSUNAMI IMPACT TYPES 8
2.4 ASSESSING THE COSTS OF TSUNAMI IMPACTS 12
2.4.1 Qualitative damage assessments 13
2.4.2 Semi-quantitative damage assessments 14
2.4.3 Quantitative damage assessments 14
2.4.4 Tsunami damage assessments – ex ante 14
2.4.5 Tsunami damage assessment – ex post 25
2.5 REFERENCES 28

3.0 PALEOTSUNAMI AND HISTORICAL TSUNAMI DATABASES 35

3.1 HISTORICAL TSUNAMI RECORDS 35
3.2 LARGE HISTORICAL TSUNAMI 39
3.3 RECENT TSUNAMI EVENTS 2005–2011 43
3.4 APPLICATION OF THE NEW ZEALAND HISTORICAL TSUNAMI RECORD 47
3.5 PALEOTSUNAMI RECORDS 47
3.5.1 Description of paleotsunami 47
3.5.2 The New Zealand paleotsunami database 49
3.5.3 Recent paleotsunami research 2005–2011 55
3.5.4 Summary of paleotsunami in New Zealand 59
3.6 REFERENCES 60

4.0 TSUNAMI MODELLING 63

4.1 NUMERICAL MODELS 63
4.2 TSUNAMI GENERATION 65
4.2.1 Submarine earthquakes 65
4.2.2 Landslides and volcanoes 67
4.3 PROPAGATION MODELLING 68
4.3.1 Modelling tsunami propagation numerically 69
4.3.2 Insights from propagation modelling 73
4.4 INUNDATION MODELLING 77
4.4.1 Numerical modelling of tsunami inundation 77
4.5 EMPIRICAL TSUNAMI MODELLING 79

4.5.1 Empirical modelling of tsunami heights 79
4.5.2 Empirical modelling of tsunami inundation 80
4.5.3 Deriving rules for defining tsunami evacuation zones 80
4.6 REAL-TIME TSUNAMI MODELLING AND FORECASTS 82
4.7 PROBLEMS AND LIMITATIONS OF TSUNAMI MODELLING 85
4.8 TSUNAMI MODELLING STUDIES RELEVANT TO NEW ZEALAND 85
4.8.1 Tsunami modelling studies in New Zealand 85
4.9 REFERENCES 86
5.0 DEFINING TSUNAMI SOURCES 91
5.1 DISTANT SOURCES 91
5.1.1 Earthquakes 91
5.1.2 Landslides 98
5.1.3 Volcanoes 99
5.1.4 Bolide impact 99
5.2 REGIONAL SOURCES 100
5.2.1 Earthquakes 100
5.2.2 Volcanoes 104
5.2.3 Landslides 105
5.3 LOCAL SOURCES 108
5.3.1 Earthquakes 108
5.3.2 Landslides 113
5.3.3 Volcanoes 117
5.4 REFERENCES 118
6.0 PROBABILISTIC MODELLING 125
6.1 INTRODUCTION AND MOTIVATION 125
6.2 METHODOLOGY OUTLINE 125
6.3 TYPES OF UNCERTAINTY AND VARIABILITY 127
6.4 SOURCE DEFINITION 127
6.5 TREATMENT OF VARIABLE SLIP AND MODELLING UNCERTAINTY 128
6.6 ESTIMATION OF TSUNAMI HEIGHTS 130
6.7 CALCULATION 131
6.8 DEAGGREGATION OF TSUNAMI SOURCES 131
6.9 RESULTS 132
6.10 COMMENTS AND DISCUSSION OF RESULTS 169
6.11 FUTURE WORK 170
6.12 REFERENCES 171
7.0 DISCUSSION AND CONCLUSIONS 173
7.1 SUMMARY 173
7.1.1 Subduction earthquakes 173
7.1.2 Probabilistic tsunami hazard model 173
7.2 DISCUSSION 173
7.2.1 Self-evacuation 173
7.3 RECOMMENDATIONS 174

EQUATIONS

Equation 4.1 79
Equation 4.2 80
Equation 4.3 80
Equation 6.1 129

FIGURES

Figure 2.1 The intersection of hazard, exposure, and vulnerability yields the risk (Reese and Schmidt, 2008). 8
Figure 2.2 Example of a qualitative risk analysis matrix (source: Standards Australia/Standards New Zealand, 2004). 14
Figure 2.3 Example of tsunami fragility functions (source: Reese et al., 2011); in this case for five different damage states. 17
Figure 2.4 Example of tsunami damage functions (source: Reese et al., 2007).....18
Figure 3.1 Distribution of tsunami that have been recorded on New Zealand shorelines from 1835–2011. 36
Figure 3.2 The distant source areas that have generated tsunami that have affected the New Zealand coastline (1835–2011). 37
Figure 3.3 The proximity of tsunami sources for tsunami that have affected the New Zealand coastline since 1835 (Downes, unpublished data). 38
Figure 3.4 The causes of tsunami that have affected the New Zealand coastline since 1835 (Downes, unpublished data).....39
Figure 3.5 Estimated tsunami runup values for the five largest tsunami in New Zealand between 1835 and 2011. 40
Figure 3.6 The location of the 2009 Dusky Sound earthquake and the locations where the tsunami was recorded.....44
Figure 3.7 Maximum peak-to-trough measurements of the 29th September, 2009, South Pacific tsunami. 45
Figure 3.8 Illustration of the arrival of the 2010 Chile tsunami on the Chatham Islands tide gauge. 46
Figure 3.9 Maximum peak-to-trough measurements of the 27th February 2010 Chile (Maule) tsunami at tide gauges around New Zealand. 46
Figure 3.10 The distribution of paleotsunami evidence around the New Zealand coastline from the New Zealand paleotsunami database (Goff, 2008; Goff et al., 2010c). 50
Figure 3.11 Estimated dates of paleotsunami deposits through time. Paleotsunami deposits have been binned into age ranges according to their midpoint age. 51
Figure 3.12 The distribution of paleotsunami evidence around the New Zealand coastline from the New Zealand paleotsunami database (Goff, 2008; Goff et al., 2010c). 52
Figure 3.13 The distribution of paleotsunami evidence around the New Zealand coastline from the New Zealand paleotsunami database (Goff, 2008; Goff et al., 2009b). 53
Figure 3.14 The distribution of paleotsunami evidence around the New Zealand coastline from the New Zealand paleotsunami database (Goff, 2008; Goff et al., 2009b). 55
Figure 3.15 The locations of recent paleotsunami studies in New Zealand from 2005–2011.....56
Figure 4.1 Seafloor deformation for the 27 March 1947 Gisborne earthquake (MW7.1) computed using a uniform slip model (left model) and a variable slip model (right panel). 66
Figure 4.2 The modelled maximum tsunami elevations of the 27 March 1947 offshore Gisborne earthquake (MW7.1). 67

Figure 4.3 Modelled distribution of maximum tsunami elevations throughout the Pacific for the 2010 Chilean tsunami event (numerical simulations by tsunami scientists at GNS Science, New Zealand). 69
Figure 4.4 Comparisons between the modelled sea surface fluctuations and the measurements at DART buoys for the 2010 Chilean tsunami (numerical simulations by tsunami scientists at GNS Science, New Zealand). 70
Figure 4.5 Modelled maximum tsunami elevations in the Pacific for the 11 March 2011 Tohoku earthquake in Japan 71
Figure 4.6 Comparison between the tsunami sea-level fluctuations over time derived from modelling and the measurements made at DART buoys (filtered) throughout the Pacific for the 2011 Tohoku event in Japan. 72
Figure 4.7 Measurements of the 11 March 2011 (UTC) Japan tsunami at coastal tsunami gauges in New Zealand. 73
Figure 4.8 A series of images illustrating the propagation of a tsunami generated by an earthquake on the Lachlan fault 74
Figure 4.9 A comparison of two scenarios for South American tsunami affecting New Zealand, illustrating the effect that directivity of the source can have on distant locations. 75
Figure 4.10 The modelled flow depth in the Gisborne area for an MW9.0 scenario event involving rupture of the whole Hikurangi margin. 78
Figure 4.11 The modelled flow depth in Gisborne area for an MW9.0 scenario event involving rupture of the whole Hikurangi margin. 78
Figure 4.12 Water level plotted as a function of distance from the coast, using field survey data from the districts of Lhok Nga and Banda Aceh, as recorded by Lavigne et al. 81
Figure 4.13 DART buoys in deep oceans (NCTR, USA). At DART buoys, sea levels are measured by bottom pressure recorders and transmitted to related data centers in real time. 83
Figure 4.14 User interface of WebSIFT (NCTR, USA) and the forecasted tsunami amplitude and arrival time for the 29 September 2009 Samoa event. 83
Figure 4.15 Web-based user interface of GDACS (http://www.gdacs.org/). 84
Figure 5.1 Subduction margins in the circum-Pacific region. 93
Figure 5.2 (Left) Paleotsunami deposits and their height distribution for the event with an inferred date of ~1450AD (Goff, 2008; Goff et al., 2010); (Right) maximum water level distribution (offshore) in modeled MW 9.4 Kermadec Trench scenario (Power et al., 2012). 103
Figure 5.3 Distribution of submarine volcanoes along the southern Kermadec arc between 30°S and 36°30'S (after Wright et al., 2006). 107
Figure 5.4 Location of possible volcano sources for tsunami along the southern Kermadec arc. 108
Figure 5.5 Schematic cross-section through the Hikurangi subduction zone. 110
Figure 6.1 Simplified flow-chart representation of the Monte-Carlo modelling scheme. 126
Figure 6.2 Representation of the Monte-Carlo modelling scheme. 126
Figure 6.3 Hazard curves for 300 samples of the uncertain parameters, illustrating how the 16th, 50th and 84th percentiles of uncertainty are calculated for one coastal section. 127
Figure 6.4 Illustration of the steps by which the tabulated fault properties are used to create synthetic earthquake catalogues. 128
Figure 6.5 Area map and tsunami hazard curve for Auckland East. 134
Figure 6.6 Deaggregation of tsunami sources for Auckland East Coast at 500 yr (top) and 2500 yr (bottom) return periods. 135
Figure 6.7 Area map and tsunami hazard curve for Auckland West Coast. 136

Figure 6.8 Deaggregation of tsunami sources for Auckland West Coast at 500 yr (top) and 2500 yr (bottom) return periods. 137
Figure 6.9 Area map and tsunami hazard curve for Christchurch. 138
Figure 6.10 Deaggregation of tsunami sources for Christchurch at 500 yr (top) and 2500 yr (bottom) return periods. 139
Figure 6.11 Area map and tsunami hazard curve for Dunedin. 140
Figure 6.12 Deaggregation of tsunami sources for Dunedin at 500 yr (top) and 2500 yr (bottom) return periods. 141
Figure 6.13 Area map and tsunami hazard curve for Gisborne. 142
Figure 6.14 Deaggregation of tsunami sources for Gisborne at 500 yr (top) and 2500 yr (bottom) return periods. 143
Figure 6.15 Area map and tsunami hazard curve for Invercargill. 144
Figure 6.16 Deaggregation of tsunami sources for Invercargill at 500 yr (top) and 2500 yr (bottom) return periods. 145
Figure 6.17 Area map and tsunami hazard curve for Kapiti Coast. 146
Figure 6.18 Deaggregation of tsunami sources for Kapiti Coast at 500 yr (top) and 2500 yr (bottom) return periods. 147
Figure 6.19 Area map and tsunami hazard curve for Napier. 148
Figure 6.20 Deaggregation of tsunami sources for Napier at 500 yr (top) and 2500 yr (bottom) return periods. 149
Figure 6.21 Area map and tsunami hazard curve for Nelson. 150
Figure 6.22 Deaggregation of tsunami sources for Nelson at 500 yr (top) and 2500 yr (bottom) return periods. 151
Figure 6.23 Area map and tsunami hazard curve for New Plymouth. 152
Figure 6.24 Deaggregation of tsunami sources for New Plymouth at 500 yr (top) and 2500 yr (bottom) return periods. 153
Figure 6.25 Area map and tsunami hazard curve for Porirua. 154
Figure 6.26 Deaggregation of tsunami sources for Porirua at 500 yr (top) and 2500 yr (bottom) return periods. 155
Figure 6.27 Area map and tsunami hazard curve for Tauranga. 156
Figure 6.28 Deaggregation of tsunami sources for Tauranga at 500 yr (top) and 2500 yr (bottom) return periods. 157
Figure 6.29 Area map and tsunami hazard curve for Timaru. 158
Figure 6.30 Deaggregation of tsunami sources for Timaru at 500 yr (top) and 2500 yr (bottom) return periods. 159
Figure 6.31 Area map and tsunami hazard curve for Wellington. 160
Figure 6.32 Deaggregation of tsunami sources for Wellington at 500 yr (top) and 2500 yr (bottom) return periods. 161
Figure 6.33 Area map and tsunami hazard curve for Whakatane. 162
Figure 6.34 Deaggregation of tsunami sources for Whakatane at 500 yr (top) and 2500 yr (bottom) return periods. 163
Figure 6.35 Area map and tsunami hazard curve for Whangarei. 164
Figure 6.36 Deaggregation of tsunami sources for Whangarei at 500 yr (top) and 2500 yr (bottom) return periods. 165

Figure 6.37 Expected maximum tsunami height in metres at 100 year return period, shown at median (50th percentile) and 84th percentile of epistemic uncertainty. See comment on the Wairarapa coast in Section 6.10. 166

Figure 6.38 Expected maximum tsunami height in metres at 500 year return period, shown at median (50th percentile) and 84th percentile of epistemic uncertainty. 167

Figure 6.39 Expected maximum tsunami height in metres at 2500 year return period, shown at median (50th percentile) and 84th percentile of epistemic uncertainty. 168

TABLES

Table 1.1 Summary of damage that can be caused by tsunami waves. 6

Table 2.1 Potential direct impacts of tsunami. 10

Table 2.2 Summary of main indirect and intangible impacts of tsunami. 11

Table 2.3 Summary of existing damage and fragility functions (extended from Grezio and Tonini, 2011). 21

Table 2.4 Summary of existing studies of methods for predicting casualties. 23

Table 2.5 Damage state classification (Reese et al., 2011). 26

Table 3.1 Validity rankings for historical tsunami of New Zealand 1985–2011. 35

Table 5.1 Large South American earthquakes that have produced tsunami with maximum tsunami heights greater than 8 m locally (extracted from Gusiakov, 2001; additional information on the 2001 and 2010 earthquakes from the NGDC tsunami database). 95

Table 5.2 Summary of available data from Kermadec chain volcanoes. * = local sources < 100 km from New Zealand. 106

Table 5.3 Summary parameters of the largest submarine landslides documented on the New Zealand margin. 114

Table 6.1 Standard deviations associated with random adjustments to the synthetic catalogue to create a catalogue of 'effective magnitudes'. The fault-specific uncertainty covers uncertainties that are specific to the modelling of each fault, while the method bias covers uncertainties that cause a systematic bias across all faults. Units are in the M_w scale. 129

Table 6.2 New Zealand local faults ranked by rate of moment release. 170

APPENDICES

APPENDIX 1: REFERENCES TO TSUNAMI-RELATED PUBLICATIONS RELEVANT TO NEW ZEALAND 177

APPENDIX 2: BOLIDE FREQUENCY AND MAGNITUDE 197

APPENDIX 3: SUBDUCTION ZONE PARAMETERS, AS USED IN THE TSUNAMI SOURCE MODEL 199

APPENDIX 4: CRUSTAL FAULT PARAMETERS, AS USED IN THE TSUNAMI SOURCE MODEL 201

APPENDIX 5: TENTATIVELY IDENTIFIED LOCAL FAULTS 207

A5.1 OUTER RISE FAULTS 207
A5.2 TARANAKI BASIN FAULTS 208
A5.3 OFFSHORE WEST COAST FAULTS 209

APPENDIX 6: A PROBABILISTIC METHODOLOGY FOR ESTIMATING HAZARD FROM TSUNAMI GENERATED BY SUBMARINE LANDSLIDES 211

A6.1 REFERENCES 212

APPENDIX 7: ADDITIONAL HAZARD MODEL INFORMATION 213

A7.1 SUMMARY TABLE OF UNCERTAINTIES AND VARIABILITIES 213
A7.2 GENERATION OF SYNTHETIC CATALOGUES 214
A7.3 EXPLANATION AND DERIVATION OF COEFFICIENTS DESCRIBING VARIABILITY AND UNCERTAINTY USING AN 'EFFECTIVE MAGNITUDE' APPROACH 215
A7.4 ESTIMATION OF TSUNAMI HEIGHTS 218
A7.5 REFERENCES 221

EQUATIONS

Equation A 2.1 197
Equation A 2.2 197
Equation A 2.3 197
Equation A 7.1 216
Equation A 7.2 218
Equation A 7.3 219
Equation A 7.4 219
Equation A 7.5 220
Equation A 7.6 220

APPENDIX FIGURES

Figure A 2.1 Estimated volume of water displaced by a bolide hitting ocean within 1000 and within 3000 km of Wellington for various return periods. 198

Figure A 5.1 Assumed location of Hikurangi Outer Rise faults as used for this study. 207

Figure A 5.2 Assumed locations of tentatively identified Taranaki Basin faults. 208

Figure A 5.3 Assumed locations of west coast South Island faults. 209

Figure A 7.1 Hazard curves for 300 samples of epistemic uncertainty, illustrating how the 16th, 50th and 84th percentiles of uncertainty are calculated. 221

APPENDIX TABLES

Table A 1.1 A brief summary of tsunami modelling and inundation studies in New Zealand. 177

Table A 1.2 Tsunami research and modelling studies relevant to New Zealand. 183

Table A 3.1 Properties of subduction zone sources. Mmax is the maximum value of M_w, C is the coupling coefficient, and B-value is the Gutenberg-Richter B-value. 199

Table A 4.1 Crustal faults properties. Fault Name and NZSHM_Number are as used in the National Seismic Hazard Model (Stirling et al., 2012). NZSHM_Number can be used to identify fault locations using the figures in Stirling et al. (2012). 201

Table A 5.1 Assumed Hikurangi Outer Rise fault properties. 208

Table A 5.2 Assumed Taranaki Basin fault properties. 209

Table A 5.3 Assumed west coast South Island fault properties. 210

Table A 7.1 Summary table of uncertainties and variabilities. 213

Table A 7.2 Standard deviations associated with stochastic adjustments to the synthetic catalogue to create a catalogue of 'effective magnitudes' 215

Table A 7.3 Magnitudes of scenario events used for modelling of local subduction zones 219

EXECUTIVE SUMMARY

In this report we have examined all likely sources of tsunami that could affect New Zealand, and evaluated their potential to generate tsunami, the likely waves produced, and the likely size of tsunami at the New Zealand coast. This review builds on the 2005 *Review of Tsunami Hazard and Risk in New Zealand*, and summarises the current state of knowledge, highlighting the results of new research and changes in scientific understanding between 2005 and 2013. A substantially revised probabilistic hazard model has been constructed for this report, which for the first time estimates the tsunami hazard for all parts of the New Zealand coastline.

This report focuses on quantifying tsunami hazard, i.e., the likely size of tsunami for specified timescales, along with estimates of uncertainty. It does not provide estimates of risk, i.e., expected costs of damage and numbers of casualties. Every effort has been made to assign realistic parameters for seismic tsunami sources in terms of their likely earthquake magnitudes and frequencies, but there are large uncertainties. Our probabilistic method incorporates these uncertainties throughout the analysis, so that the results contain realistic 'error bars'.

The hazard posed by tsunami generated by landslides and volcanic activity has been carefully considered. At this time it has not been possible to quantify the hazard from these sources, though research work towards this goal is being undertaken. For most parts of New Zealand, the hazard posed from these tsunami sources on time frames of up to 2500 years is considered secondary to the hazard from earthquake-generated tsunami. This is consistent with the global experience of tsunami, in which relatively few events in the instrumental era have been attributed to landslide and volcanic sources relative to the number of earthquake-generated tsunami.

The 2011 Tohoku tsunami in Japan illustrates some of the key changes in scientific knowledge since 2005. That event was the latest in a sequence, starting with the 2004 Indian Ocean tsunami and the subsequent 2009 South Pacific tsunami, that were produced by earthquakes substantially larger than had been considered likely to occur at those locations. These earthquakes contradicted previous geophysical assumptions about the maximum magnitudes of earthquakes that could be created on tectonic plate boundaries. There are now far fewer restrictions on possible maximum magnitudes than was previously thought to be the case, and the new probabilistic model attempts to account for this. It is now known that there was a similar tsunami in Japan in AD 869, indicating that the interval between the largest earthquakes there is over a thousand years. The tectonic plates in Japan are converging twice as fast as those around New Zealand, which suggests that the interval between the largest earthquakes on our local plate interfaces could be in excess of two thousand years. The important implication here is that our brief historical record of 200 years can, on its own, provide very little guidance in estimating the magnitude of the largest earthquakes that New Zealand may experience.

To improve estimates of the earthquake potential of subduction plate interfaces around New Zealand, where one plate is pushed below another, we must study the evidence of prehistoric tsunami and earthquakes (paleotsunami and paleoearthquakes) in the geological record, and work with the global community to find new, statistically valid, geophysical estimates.

The movement between the tectonic plates in the Tohoku tsunami was very non-uniform—in some areas the plates moved more than 50 metres whereas in many other areas the movement was much less, typically around 5 to 10 metres. This ‘non-uniform slip’ has important implications for tsunami, as the distribution of movement between the plates affects the motion of the seabed, which determines the size of tsunami. The probabilistic model in this report attempts to incorporate the effects of this phenomenon to a first level of approximation; this is at the cutting-edge of current science and the analysis represents a first attempt at tackling this important problem.

The greater uncertainty that now exists regarding the maximum size of earthquakes on plate boundaries close to New Zealand, has led to an increase in the estimated hazard from tsunami triggered by local and regional sources. While for most parts of New Zealand the overall levels of tsunami hazard have not changed greatly from the assessed hazard levels in the 2005 report, the estimated hazard has generally increased in those areas most exposed to tsunami from local subduction zones – notably the east-facing coasts of the North Island, and the southwest corner of the South Island.

1.0 INTRODUCTION

1.1 SCOPE OF THIS REPORT

Following the disastrous tsunami in the Indian Ocean on December 26, 2004 the New Zealand Government resolved to consider the risk of such events in New Zealand. The Ministry of Civil Defence & Emergency Management commissioned a report from the Institute for Geological and Nuclear Sciences (now GNS Science) to answer this question. The report "Review of Tsunami Hazard and Risk in New Zealand" was compiled by Kelvin Berryman and completed in 2005.

In the period between 2005 and 2012 much research has been undertaken on the subject of New Zealand's tsunami hazard. A new report was commissioned by the Ministry of Civil Defence & Emergency Management to update the findings of the original 2005 report with this new information. The new report builds upon the findings and structure of the original. Like the original it represents the work of many scientists, and it directly incorporates material from the original report where the present understanding is unchanged.

This report is a synthesis of available data on the hazard of distant, regional and local tsunami in New Zealand. It includes summaries of geologically and historically derived information on the occurrence of tsunami, and of numerical modelling studies. A revised probabilistic model of tsunami hazard has been developed for this report which incorporates new information on tsunami sources resulting from studies since 2005. It also differs from the 2005 hazard model by developing hazard estimates for the entire coast, not only the major cities.

Estimates of expected casualties and damage costs have not been included in this report. It is anticipated that the Riskscape project (see Section 2.4.4.2) will use the tsunami hazard model developed here to produce revised estimates of tsunami risk.

1.2 CONTRIBUTORS

Many people have worked on this project. The project also draws heavily on the 2005 report, particularly in the area of tsunami sources. The following researchers are acknowledged for their contribution to writing the following chapters of this report:

Introduction (2013 update): William Power[1]

Tsunami Impacts: Stefan Reese[2,3]

Historical and pre-historical tsunami databases: Kate Clark[1]

Tsunami Modelling: Xiaoming Wang[1], William Power[1]

Tsunami Sources (2013 update): Laura Wallace[1,4], William Power[1], Joshu Mountjoy[2]

Probabilistic Modelling: William Power[1], Joshu Mountjoy[2]

Discussion and Conclusions: William Power[1]

---

1 GNS Science
2 NIWA
3 SwissRe
4 University of Texas

The following are additionally acknowledged for their scientific contribution to this report in the following areas:

Tsunami Sources: Philip Barnes[2], Kelvin Berryman[1], Nicola Litchfield[1], Andy Nicol[1], Martin Reyners[1], Aggeliki Barberopoulou[1], Stuart Fraser[1, 5]

Probabilistic Modelling: Christof Mueller[1], Stuart Fraser[1,5], Biljana Lukovic[1]

The following are additionally acknowledged for their contributions to the 2005 report on which this report draws:

Warwick Smith[1], Mark Stirling[1], David Heron[1], Gaye Downes[1], Ursula Cochran[1], Willem de Lange[6], James Goff[1, 7], Scott Nichol[8], Roy Walters[2], Terry Webb[1], Russell Robinson[1], John Beavan[1], Rob Langridge[1], Geoffroy Lamarche[2], Arne Pallentin[2], Mauri McSaveney[1], Nick Perrin[1], Ian Wright[2], Alistair Barnett[9], Doug Ramsay[2], Jim Cousins[1], Andrew King[1].

Project management was provided by: Ursula Cochran[1] and Hannah Brackley[1], and document editing and preparation by: Eileen McSaveney[1] and Kat Hammond[1]. Reviewing was performed by Emily Lane[2], David Burbidge[10] and Kenji Satake[11].

1.3 STRUCTURE OF THE REPORT

In this Chapter 1 we briefly describe the structure of the report, what tsunami are, how they are generated, and what damage they can do. Chapter 2 describes the impacts of tsunami and how they may be quantified to evaluate tsunami risk. In the following chapter on historical and paleotsunami (Chapter 3) we present the current state of knowledge about tsunami that have occurred in our relatively recent recorded history and earlier tsunami that have left evidence in the form of sedimentary deposits.

Chapter 4 describes techniques for numerical modelling of tsunami, and summarises modelling work that has been done for New Zealand. Chapter 5 on Tsunami Sources characterises the set of possible causes of tsunami, whether generated by earthquake, landslide, volcano or bolide impact, and whether this occurs close to New Zealand or far overseas.

A nationwide model of tsunami hazard was developed for this report. The model, the input data it uses, and the results it produces are the subject of Chapter 6. Finally in Chapter 7 there is a discussion about the findings of the report and conclusions are drawn, including a series of recommendations for further research.

---

5 Massey University
6 Waikato University
7 University of New South Wales
8 University of Auckland
9 Barnett & McMurray Ltd
10 Geoscience Australia
11 Earthquake Research Institute, University of Tokyo

1.4 WHAT IS A TSUNAMI?

A tsunami is a natural phenomenon consisting of a series of waves generated when a large volume of water in the sea, or in a lake, is rapidly displaced. Tsunami are known for their capacity to violently inundate coastlines, causing devastating property damage, injuries, and loss of life. The principal sources of tsunami are:

- large submarine or coastal earthquakes (in which significant uplift or subsidence of the seafloor or coast occurs)
- underwater landslides (which may be triggered by an earthquake, or volcanic activity)
- large landslides from coastal or lakeside cliffs
- volcanic eruptions (e.g., under-water explosions or caldera collapse[12], pyroclastic flows[13] and atmospheric pressure waves)
- meteor (bolide) splashdown, or an atmospheric air-burst over the ocean.

In a tsunami, the whole water column from the ocean floor to its surface is affected, the initial disturbance creating a series of waves radiating outwards, until the waves either dissipate or collide with a shoreline. Tsunami waves can arrive at nearby shores within minutes, or travel across the deep ocean basins at speeds in excess of 500 kilometres per hour (km/hr). Very large sources (disturbances) are required to cause tsunami that are damaging at great distances from the source. For example, the 1960 magnitude[14] (M) 9.5 Chile earthquake, which had a rupture length of several hundred kilometres, produced a 25 metre (m) high tsunami locally, over 10 m in Hawaii, and nearly 4 m in New Zealand. On the other hand, tsunami that are generated locally do not need such a large source to be large and damaging at nearby shores. For example, the 1947 M7.1 earthquake off Gisborne affected 120 km of coastline, with a tsunami of 10 m maximum height occurring along tens of kilometres of coast north of Gisborne.

The amplitude of tsunami waves[15] in deep water is generally less than one metre, producing only a gentle rise and fall of the sea surface that is not noticed by ships, nor able to be seen by aircraft, although new satellites with sea-surface elevation technology can detect large tsunami in the deep ocean. When tsunami waves reach shallower waters, their speed decreases rapidly from their deep-ocean values, and at the same time their height increases

---

[12] CALDERA COLLAPSE refers to the formation of a large depression when the underlying magma chamber of a volcano collapses during or following an eruption or explosion. The collapsed caldera is a crater-shaped depression which may be many hundreds of square kilometres in area, and many hundreds of metres deep. The collapse needs to occur suddenly to cause a tsunami.

[13] A PYROCLASTIC FLOW is a ground-hugging avalanche of hot ash, pumice, rock fragments, and volcanic gas that rushes down the side of a volcano at hundreds of km/hr, and can have temperatures greater than 500°C. In a coastal setting, such flows cause tsunami when they enter the sea. Pyroclastic flows can also occur from underwater volcanoes.

[14] The MAGNITUDE of an earthquake is a measure of its energy. There are several methods for estimating the magnitude, which often give slightly different results. At present the most widely used form of the magnitude is the moment magnitude M_w. In this report M is used to signify an approximate generic magnitude in situations where there is significant uncertainty; this is often the case when discussing earthquakes that occurred before the instrumental era.

[15] TSUNAMI HEIGHT (m) is the vertical height of waves above the tide level at the time of the tsunami (offshore it is approximately the same as the AMPLITUDE). It is far from constant, and increases substantially as the wave approaches the shoreline, and as the tsunami travels onshore.The term "WAVE HEIGHT" is also often used, but there is a potential ambiguity as many scientists define WAVE HEIGHT as the peak-to-trough height of a wave (approximately twice the amplitude). Note that this is a change in terminology from the 2005 Tsunami Hazard and Risk Review, intended to bring greater consistency with international usage of these terms.

(as the front of each wave slows down and the back of the wave, which is moving faster, catches up on the front, piling the water higher). A tsunami wave that is only half a metre high in the open ocean can increase to a devastating 10 m high wave travelling at 10-40 km/hr at impact with the shore.

Tsunami waves differ from the usual waves we see breaking on the beach or in the deep ocean, particularly in the distance between successive waves, because tsunami waves occupy the whole ocean depth and not just the top few tens of metres as in storm waves. Both of these factors contribute to the huge momentum of water in a tsunami at the coast. The distance between successive tsunami waves (called wavelength) can vary from several kilometres to over 400 km, rather than around 100 metres for normal waves at the beach. The time between successive tsunami wave crests (called period) can vary from several minutes to a few hours, rather than the few seconds usual for beach waves. Hence, when tsunami waves reach the shore, they continue to flood inland over many minutes, and then the waves may retreat over as many minutes, before the arrival of the next wave. The waves may come in at irregular intervals, often without complete withdrawal of the inundating water from previous waves due to retardation of the outflow and impoundments. The first wave to arrive may not be the largest wave.

New Zealand's location astride a plate boundary means that it experiences many large earthquakes. Some cause large tsunami. New Zealand's coasts are also exposed to tsunami from submarine and coastal landslides, and from island and submarine volcanoes. In addition, tsunami generated by large earthquakes at distant locations, such as South America, or western North America and the Aleutians in the north Pacific Ocean, can also be damaging in New Zealand.

Tsunami with run-up heights[16] of a metre or more have occurred about once every 10 years on average somewhere around New Zealand, a similar frequency to Hawaii and Indonesia, but about one third that in Japan. Smaller tsunami occur more frequently, the smallest of which are only detectable on sea-level recorders.

New Zealand can expect tsunami in the future. Some coasts are more at risk than others because of their proximity to areas of high local seismic activity, or exposure to tsunami from more distant sources. No part of the New Zealand coastline is completely free from tsunami hazard.

[16] TSUNAMI RUN-UP (m), a measure much used in tsunami-hazard assessment, is the elevation of inundation above the instantaneous sea level at the time of impact at the farthest inland limit of inundation. This measure has a drawback in that its relationship with the amplitude of the waves at the shore depends markedly on the characteristics of waves and on the local slopes, vegetation, and buildings on the beach and foreshore areas, so it is highly site-specific.

1.5 WHAT DAMAGE DOES A TSUNAMI DO?

Tsunami damage and casualties are usually from four main factors (see also Table 1.1 and further discussion in Chapter 2):

- Impact of swiftly-flowing torrent (up to 40 km/hr), or travelling bores[17], on vessels in navigable waterways, canal estates and marinas, and on buildings, infrastructure and people where coastal margins are inundated. Torrents (inundating and receding) and bores can also cause substantial erosion both of the coast and the sea-floor. They can scour roads and railways, land and associated vegetation. The receding flows, or "out-rush", when a large tsunami wave recedes are often the main cause of drowning, as people are swept out to sea.
- Debris impacts—many casualties and much building damage arise from the high impulsive impacts of floating debris picked up and carried by the in-rush (inundating) and out-rush (receding) flows.
- Fire and contamination—fire may occur when fuel installations are floated or breached by debris, or when home heaters are overturned. Breached fuel tanks, and broken or flooded sewerage pipes or works can cause contamination. Homes and many businesses contain harmful chemicals that can be spilled.
- Inundation and saltwater-contamination by the ponding of potentially large volumes of seawater will cause medium- to long-term damage to buildings, electronics, fittings, and to farmland.

[17] Tsunamis often form bores in harbours, man-made waterways, and in coastal rivers and streams. A bore can be a smooth or turbulent, non-breaking step-like increase in water height resulting in wall-like change in water levels from normal to some higher level. They can travel 3 or more kilometres up a river with the water many metres above the normal level, sometimes well over the bank height, causing damage to bridges and wharves, and causing water to flood nearby flat areas.

Table 1.1 Summary of damage that can be caused by tsunami waves.

People and animals	Built environment	Natural environment	Shipping
• Washed off feet • Drowned, especially in out-wash • Injured by debris or impact with structures • Skin may be removed by the “sand-blast” effect of suspended particles • Injury/illness due to contact with contaminated water	• Damaged by inundation and deposition of sand • Damaged by floating debris (including cars and boats) • Wooden buildings floated and damaged • Reinforced concrete buildings damaged (with on-land water levels of 4m+) • Reinforced buildings badly damaged (with on land water levels of 10m+) • Coastal wharves, coastal defences (seawalls/gabions) and bridges damaged or destroyed • Riverside wharves and bridges damaged or destroyed 3 km or more upstream by bores • Walls, fences, road surfaces, power/telegraph poles damaged or destroyed • Oil spills from overturned vehicles, heaters or floated storage tanks, with consequent fire danger • Aqua-culture rafts, etc. damaged • Sewerage systems obstructed, or damaged, with consequent contamination	• Erosion or deposition • Trees snapped or uprooted • Long-term sea-water contamination effects (salt) • Sewage contamination • Fish and shellfish thrown ashore, with consequent contamination • Disturbance, siltation, contamination of the near shore marine environment with subsequent reduction in fish stocks	• Ship and boat damage by impact with wharves, breakwaters or other boats • Ship and boat damage by complete withdrawal of water, or too rapid a return of water to allow floating • Ships and boats torn from moorings and thrown on shore • Buoys moved • Channels altered by scouring and deposition • Shipping lanes littered with floating debris • Oil spills from overturned boats and wharf installations with consequent fire danger • Port and marina docking facilities and breakwaters

2.0 TSUNAMI IMPACTS

2.1 INTRODUCTION

Compared to other perils tsunami are rare events, but they can be extremely destructive. Coastlines have always been a favoured location for human settlements, and coastal communities have continued to develop in recent times. Consequently, more people and facilities are now at risk from tsunami. Tsunami risk is a function of three factors: 1) the nature and extent of the tsunami hazard; 2) the characteristics of the coastline; and 3) the degree of exposure and vulnerability of people and the built environment (United States National Tsunami Hazard Mitigation Program, 2001).

Unlike earthquakes, where damage is normally confined to a smaller area, tsunami impact long stretches of coastlines, often entire ocean basins. They usually extend inland for a few hundred metres, possibly up to several kilometres in low-lying areas. Onshore behaviour and characteristics of tsunami are also quite distinct from other coastal hazards (Yeh, 2009). Inundation depth, run-up and consequently the level of damage vary significantly over short distances due to a number of factors, including the topography and geomorphology of the coast—near-shore bathymetry, beach slope, coastal orientation and configuration, and direction of the arriving waves (Ghobarah et al., 2006; Reese et al., 2007; Rossetto et al., 2007). In addition, the complex interactions between tsunami and the land surface cause unique wave patterns, with large-scale reflection and refraction (Salinas et al., 2005). Bays, sounds, inlets, rivers, streams, offshore canyons, islands, or artificial channels can amplify the wave height and exacerbate local damage.

2.2 TSUNAMI RISK

The simplest definition of risk is

$$R = F \times D$$

where F is the frequency or likelihood of an event occurring and D is the damage or consequences (Standards Australia and Standards New Zealand, 2004; Hollenstein, 2005). Hollenstein (2005) recommends extending the definition for natural hazard applications by defining the hazard as probability P (or its reciprocal, the return period) and an intensity I. He also splits the consequences into two factors—exposure E (describing the spatial and temporal distribution of the assets) and vulnerability V. The vulnerability provides a means to estimate impacts; it is the relative fragility to damage or harm of the exposed assets or people, to the hazard at that magnitude. For example, for a given hazard exposure, some assets may remain undamaged due to their strength or the hazard protection measures in place, whereas other weaker or more vulnerable structures may suffer a degree of damage.

That results in the following risk definition:

$$R = P \times I \times E \times V$$

Sometimes vulnerability is further broken down into vulnerability and resilience and / or adaptive capacity (Malone, 2009). Despite these slight variations (see Thywissen, 2006 for comparisons), hazard, exposure (magnitude of the hazard that is manifest at the location of assets) and vulnerability are the three common key components of a risk analysis (Figure 2.1).

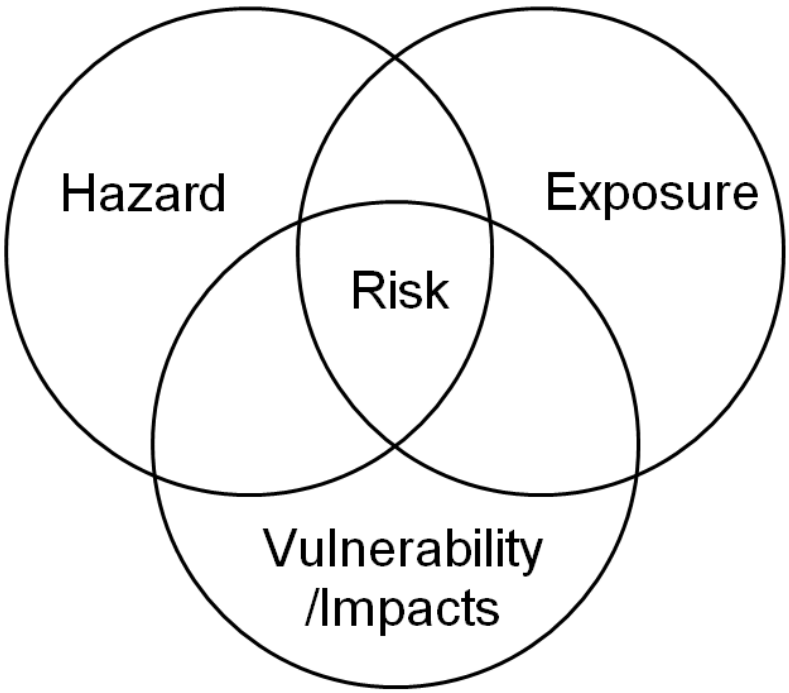

Figure 2.1 The intersection of hazard, exposure, and vulnerability yields the risk (Reese and Schmidt, 2008).

Risk analyses have become almost a standard procedure in dealing with natural hazards. They provide a powerful aid in decision making and offer a structured, systematic and consistent method in order to understand, characterize and quantify risk so it can be managed.

All three components, the hazard assessment as well as the exposure and vulnerability analysis include data collection, modelling, and monitoring of vulnerability factors. From these three assessments, the specific risk can be derived.

2.3 TSUNAMI IMPACT TYPES

In the breakdown of risk given in the previous section, vulnerability refers to the possible impacts of the tsunami. These impacts can be further subdivided into different types. There are many different ways that tsunami impacts have been subdivided, depending on what aspects are being focussed on.

Generally, the effects of any disaster can be categorised into tangible and intangible effects, and into direct and indirect effects (Bureau of Transport Economics, 2001; ECLAC, 2003; UNDP, 2004; Smith and Petley, 2009). Direct effects are the first order and most visible consequences due to the immediate impact, such as structural damage, or if intangible, damage to archaeological sites for instance. Indirect effects emerge later as a consequence of the event, but not due to the direct impact; examples are the disruption of economic and social activities (Bureau of Transport Economics, 2001; Smith and Petley, 2009). Tangible effects can be quantified monetarily, whereas intangible effects cannot. Instead of direct and indirect effects, the terms damages and losses are sometimes used (ECLAC, 2003): Direct damages are the costs of “totally or partially destroyed physical assets and indirect losses are losses in the flows within the economy that arise from the temporary absence of the damaged assets” (ECLAC, 2003). ECLAC (2003) also uses a third category, macroeconomic effects. However, macroeconomic effects are normally covered by assessing direct and indirect impacts. Hence, it is just a complementary way to assess these impacts from a

different perspective. They should not be added to direct and indirect impact estimates, as this results in double counting (McKenzie et al., 2005). UNDP (2004) on the other hand classifies “short- and long-term impacts of a disaster on the overall economy and socio-economic conditions (fiscal and monetary performance, effects of relocated workforce, etc.)” as secondary effects. Table 2.1 shows a summary of possible types of direct tsunami damage, depending on the nature of the impact. Table 2.2 summarises the main indirect and intangible impacts of tsunami.

Another categorisation of the direct effects of the tsunami focuses on what aspect of the tsunami caused the damage. Sometimes, most of the damage is caused by the advancing wave front or surge. In other situations, the greatest damage is caused by debris impact, the outflow of water back to the sea, or erosion that can undermine the foundations of structures built along coastlines. Yalciner et al. (2011) classify these factors into i) primary and ii) secondary tsunami impacts:

“Primary impacts of tsunamis are based on (drag, lift and inertia) forces which are caused by hydrostatic and hydrodynamic impacts due to the motion of the water. The forces causing primary impact depend on the shape and characteristics of the structure, flow depth and flow characteristics.

Secondary impacts of tsunamis are caused in general by dragging of objects, debris flow and driftwood, contaminants together with flowing water. Scour around structure foundations can also cause damage. The resonant oscillations of basins can continue the agitations and cause additional damage inside the basins. The contact with water results in damage of certain building components, e.g., insulation, internal lining, floors, electrical system components such as switches, fuse boxes, control panels, air conditioning, hot water cylinders, etc. In some cases fire can also be observed as a secondary impact of tsunami.”

Table 2.1 Potential direct impacts of tsunami.

	People and animals	Built environment	Natural environment
Inundation	Drowning	Damage by inundation/water contact	Disturbance of marine habitats (coral reefs, seagrass beds, lagoons, mangroves, intertidal flats)
		Failure of mechanical equipment, electrical and communication systems and equipment	Loss of protected areas
		Structural damage due to hydrostatic forces (e.g. pressure on outside walls)	Disturbance of terrestrial habitats (forests, wetlands, riverine areas, beaches, dunes, surface and groundwater, soils)
		Damage due to buoyancy (flotation or uplift forces)	Damage to farmland and yield
		Saturation causing slope instability (e.g. stopbanks)	
Currents	Washed off feet	Structures washed away due to hydrodynamic forces (pushing forces and drag)	Loss of coastline/beach, dunes, seagrass beds, etc. due to erosion
	Impact with structures	Walls, fences, road surfaces, railways, ports/harbours, power, telecom poles, gas, oil or water pipelines damaged or destroyed	Breaking and overturning of trees
		Scouring of building or bridge foundations, power poles, coastal or river defences, railways and road embankments	Fish and shellfish thrown ashore, with consequent contamination
		Scattering and subsidence of concrete blocks	Destruction and loss of rafts, fishes and shells in aquaculture
		Ship, boat and wharf damage	Harbour change in water depth (erosion and accumulation)
		Damage to farms buried by sands	Disturbance, soil erosion and siltation
Debris	Injured or killed by debris	Structural damage by debris impact	Hazardous waste
		Rails and roads buried by sediment and debris	Build-up of marine debris
Contamination /Fire	Injury/illness due to contact with contaminated water	Oil spills from vehicles, ships, heaters, storage tanks	Salinisation
		Contamination due to sewage	Contamination of near-shore environment
		Fire from gas or electricity leaks	Eutrophication
		Damage from sediment deposition	
		Fire from waterborne flammable materials	

Table 2.2 Summary of main indirect and intangible impacts of tsunami.

Indirect			
Social	**Infrastructure**	**Economic**	**Intangible**
Increased costs for medical treatment and care	Disruption of networks (roads, lifelines, etc.)	Disruption to flows of goods and services	Inconvenience of disruption of services
Disruption of households (e.g. extra travel costs, temporary accommodation, etc.)	Loss or reduction of earnings and income	Costs of relocation	Health effects
		Additional costs in public sector (e.g. extra staff, training, etc.)	
Increased debts	Loss of production and services		Loss of memorabilia
Increased poverty	Clean-up costs	Disruption of businesses	Loss of confidence
Costs of relocation	Increased operating and distribution costs	Loss or reduction of earnings and income	Loss of contracts
Additional heating costs	Costs of demolition and debris removal	Loss of production and services	Stress, trauma, depression
Loss of jobs / livelihood	Increase in water and sanitation operating costs	Costs of emergency response and relief	Loss of environmental assets
Loss or reduction of earnings and income	Increase communications service during recovery phase	Clean-up costs	Loss of heritage/cultural assets
Increased prices for food, energy, and other products		Decrease in tourism	Loss of tourist attractions
Decreased land-prices		Losses in yields (crop and livestock)	Decrease in air and water quality
Disruption of provision of basic public services (education, health, cultural, etc.)		Revenue losses to federal, regional and local governments (from reduced tax base)	Degradation of landscape quality, loss of biodiversity and soil erosion
Increased operating costs		Costs of higher unemployment	Reduced quality of life, and inequities in the distribution of impacts and disaster relief
		Fewer businesses (due to bankruptcies, etc.)	Lack of food and drinking water
		Costs of responding to new situation (e.g. tourism campaign)	Reduced investor confidence
		Costs of demolition and debris removal	Social conflicts
		Downstream effects of relocation and restructuring on economy and workforce (decline of GDP, decrease in exports, inflation)	

2.4 ASSESSING THE COSTS OF TSUNAMI IMPACTS

Natural disasters are a significant and rising cost to communities and will be exacerbated in most cases by climate change. A rising sea level acts as a kind of a multiplier: as the base sea level is higher, so too will be the elevation of the tsunami as measured relative to the landscape (n.b. measures to mitigate other hazards exacerbated by sea level rise, such as storm surge, may also reduce tsunami risk). Having good information on the costs of natural disasters serves various purposes. According to the Bureau of Transport Economics (2001) “every dollar spent on mitigation is worth two dollars of response and recovery”. Damage or risk assessments / analysis can help assess the effectiveness of different mitigation measures, since they focus on potential damage rather than on individual hazards (Hollenstein, 2005). Emergency managers and planners are also demanding increasingly more quantitative information on possible consequences and the risks associated with different hazards, including tsunami, to be in a position to compare the impacts across the different hazards before making investment decisions on risk reduction for their region (Blong, 2003; Durham, 2003; Reese and Smart, 2008).The economic viability of communities also depends upon the continued operation of infrastructure and essential services. Hence, it is critical to know the risks from natural hazards in order to minimize them.

The cost of tsunami impacts is usually assessed using damage or impact analyses. These are normally part of a comprehensive risk assessment process, which in return should be embedded in an overall risk management framework. The terms “risk analysis”, “risk assessment”, and “risk evaluation” are not consistently used in natural hazard literature. The determination of consequences and likelihood, and hence the level of risk, is normally described as risk analysis (Standards Australia and Standards New Zealand, 2004; ISDR, 2004). However, other authors use the term risk assessment (Dilley, 2005; Hollenstein, 2005). According to the Australian and New Zealand Risk Management Standard (Standards Australia and Standards New Zealand, 2004) risk assessment also includes the process to “determine risk management priorities by evaluating and comparing the level of risk against predetermined standards, target risk levels or other criteria” (see also ISDR, 2004). For the rest of this chapter we will use the terms risk analysis and damage assessment as part of a risk analysis process, because the focus of this chapter lies on the impacts of tsunami.

Damage assessments can be categorised as either ex ante (i.e., occurring before a disaster has occurred and so using either scenarios or probabilistic representations of the hazard) or ex post, occurring after a specific disaster has occurred as a form of post-disaster survey. Ex ante and ex post assessments are essentially the prediction / verification cycle that characterises scientific endeavour. As such, ex post assessments serve to verify how well past ex ante assessments predicted the consequences of a specific disaster and also to provide information for the next round of ex ante assessments in anticipation of future disasters.

If conducted ex-post, these assessments are essential to prioritise relief and rehabilitation needs (McKenzie et al., 2005). They are also necessary for validating scientific models and understanding the limitations and uncertainties of the models and the outputs they produce. This can only be achieved if sufficient validation data is available. Natural disasters provide an invaluable opportunity to capture such data for hazard exposure and risk modelling. However, detailed and comprehensive tsunami impact data is still limited (Douglas, 2007). Apart from validation, post-event assessments also improve our understanding of vulnerability to natural hazards. Observed damage provides useful insights into the factors contributing to building and infrastructure vulnerability and consequential community risk.

Tsunami damage assessments, both ex-ante and ex-post, were very sparse prior to the 2004 Indian Ocean tsunami (Hatori, 1984; Shuto, 1993; Izuka and Matsutomi, 2000; Matsutomi et al., 2001; Papadopoulos and Imamura, 2001). Since the 2004 tsunami, the number of studies has increased significantly. All components of risk, including exposure and vulnerability, can be analysed quantitatively, semi-quantitatively or qualitatively. For each category, examples can be found in the literature:

Qualitative damage analysis (Dalrymple and Kriebel, 2005; EERI, 2005; Stansfield, 2005; Ghobarah et al., 2006;Saatcioglu, 2007; Rosetto et al., 2007; Kaplan et al., 2009);

Semi-quantitative/ index-based approach (Dominey-Howes and Papathoma, 2007; Dall'Osso et al., 2009; Omira et al., 2010; Strunz et al., 2011).

Quantitative using fragility or vulnerability functions (Kimura et al., 2006; Peiris, 2006; Ruangrassamee et al., 2006; Reese et al., 2007; Dias et al., 2009; Koshimura et al., 2009; Koshimura et al., 2009a; Leone et al., 2010; Matsutomi et al., 2010; Murao and Nakazato, 2010;Reese et al., 2011; Suppasri et al., 2011, Valencia et al., 2011[18]) or experimental studies / loadings-based assessments (Okada et al., 2005; Yeh et al., 2005; Palermo and Nistor, 2008; Thusyanthan and Gopal, 2008;Pimanmas et al., 2010; Nistor et al., 2011)

2.4.1 Qualitative damage assessments

All approaches have their advantages and disadvantages. A **qualitative tsunami damage assessment** is descriptive rather than numerical and can rely on relatively coarse data and judgments in order to describe damage or categorise it into order-of-magnitude bands. This approach is resource efficient but fairly subjective. This can be an adequate approach if quantitative precision is not needed, initial screening is required, or numerical, detailed data is not available (Ale, 2002; Standards Australia and New Zealand, 2004). However, the results cannot be compared with other events or hazards, and they are also not suited as baseline data for cost-benefit analysis or to evaluate risk reduction measures. All the above examples are ex-post assessments and summarise impacts and findings from historic events.

For ex-ante analysis, risk matrices (Figure 2.2) are the most common tools. They provide a systematic method for assigning a hazard level to a failure event, based on the severity and frequency of the event. This allows the establishment of risk categories for given combinations of frequency, magnitude and estimated consequences. This approach makes it possible to link the risk analysis results back to risk management actions and decision making. The Australian/New Zealand Risk Management Standard (2004) gives comprehensive instructions on how to use risk matrices.

[18] see Grezio and Tonini (2011) for a comparison of existing tsunami fragility functions.

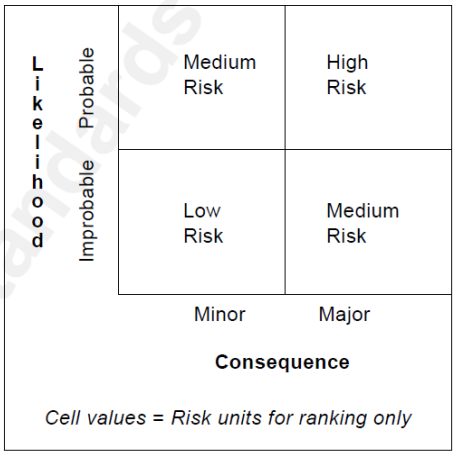

Figure 2.2 Example of a qualitative risk analysis matrix (source: Standards Australia/Standards New Zealand, 2004).

2.4.2 Semi-quantitative damage assessments

Semi-quantitative tsunami assessments provide an intermediate level between the descriptive evaluation of qualitative damage / risk assessment and the numerical evaluation of quantitative risk assessment, by evaluating risks with a score and producing rankings. It is more sophisticated than a qualitative assessment, as it is more consistent and rigorous in assessing and comparing risks and risk management strategies. It requires more data and mathematical skills than a qualitative approach, and avoids some of the greater ambiguities that a qualitative risk assessment may produce (FAO/WHO, 2009). On the other hand, these rankings are not always realistic, nor do the rankings always reflect an accurate relationship to the actual magnitude or consequence of the tsunami (Standards Australia and Standards New Zealand, 2004).

2.4.3 Quantitative damage assessments

"Quantitative assessment can be either deterministic (i.e., single values such as means or percentiles are used to describe model variables) or probabilistic (i.e., probability distributions are used to describe model variables)" (FAO/WHO, 2009). They use numerical values for both consequences and likelihood, using data from experimental studies, and synthetic or historic data (Standards Australia and Standards New Zealand, 2004). They provide more in-depth information and allow cost-benefit analysis to be based on the results. It is important to understand that the results are only as good as the input data, which means the best approach always depends on the circumstances, data and resources available.

2.4.4 Tsunami damage assessments – ex ante

Ex ante tsunami damage assessments are built up using the components of risk described in Section 2.2 above. Depending on how qualitative the assessment is, these components may be broken down into smaller parts and assigned individual values. Qualitative assessments tend to use more broad-brush approaches that may lump several components together. Below we briefly touch on the hazard and the exposure components, but focus mainly on the vulnerability component of the risk.

2.4.4.1 Tsunami hazard

Every disaster starts with a hazard, in this case a tsunami. Much of the rest of this report is dedicated to understanding and quantifying the tsunami hazard. A detailed understanding of what events have occurred in the past (including prehistoric events) and their effects provides the basis for understanding what could or will happen in the future (see Chapter 3). In order to quantify tsunami risk, each magnitude is tied to a specific return period or its inverse, frequency. “The latter ensemble is the magnitude-frequency relationship of a tsunami and it is always an inherent characteristic of a specific locality or region” (Thywissen, 2006). Numerical modelling can simulate events, and compute the wave propagation and its effects on structures that have to be protected.

2.4.4.2 Tsunami exposure

Tsunami exposure is another pre-requisite to quantify the risk of tsunami. In the context of natural disasters, exposure is understood as the number of people and/or other elements at risk that can be affected by a tsunami event (Thywissen, 2006). In an uninhabited area the human exposure is zero, although other elements such as agricultural assets, cultural or natural environments may be at risk. It is the exposure that drives the damage, not the vulnerability. However, vulnerability determines the severity of the impact.

Assessing an area’s tsunami exposure requires a good understanding of the elements at risk within the study area. Elements at risk or assets are spatial-temporal phenomena, valued by human society, and under threat of being damaged by hazards, e.g. buildings, lifelines, business disruption, economic impacts, etc. (Schmidt et al., 2011). The knowledge of the distribution of people, the location and function of critical infrastructure, and the spatial extent, distribution and types of buildings, are the key to determining their exposure to tsunami (Strunz et al., 2011). Also relevant are attributes that characterise the assets and describe their vulnerability pertinent to the specific hazard, e.g. floor height, which determines when the water enters a building.

A consistent national database of the building stock and infrastructure is not currently available in New Zealand. Such a database is essential to conduct damage assessments or risk analysis. The database must be sufficiently detailed to allow robust estimates of loss to be made. Even though most of the required information does exist somewhere, there are currently no joint or governmental efforts to establish such a database. RiskScape, an initiative by GNS Science and the National Institute of Water and Atmospheric Research Ltd. (NIWA) is in the process of developing a national building database as part of the programme. The database will be a key element of the multi-hazard loss modelling tool that is RiskScape. An important part of this database is the building inventory, which will be derived from a national property dataset maintained by Quotable Value Limited (QV), a New Zealand state-owned enterprise for property valuation and information. The inventory is available as point datasets of property centroids with a range of attributes attached to it such as building age, number of storeys, building material, etc. Additional attributes that QV does not hold, such as floor heights or roof pitch, have to be added, based on survey information and proxies. RiskScape will allow users to update the database when additional or more detailed local information is available, so that, with time, the QV data gets replaced with local and more detailed information. The compilation of infrastructure data is significantly more challenging, as most of the data is held by private companies, in different formats with inconsistent information. In some cases there might also be commercial security concerns, so that access has to be restricted.

2.4.4.3 Tsunami vulnerability

Vulnerability refers to the potential for casualties, destruction, disruption or other form of damage or loss with respect to a particular element/asset. Vulnerability is in some ways a predictive parameter and describes the susceptibility of the element at risk. It identifies what may happen to the element under conditions of a particular hazard (Canon et al., 2005). "Vulnerability is a permanent and dynamic feature that is revealed during an event to an extent that depends on the magnitude of the harmful event. This means that vulnerability can often only be measured indirectly and retrospectively, and the dimension normally used for this indirect measure is damage or more general harm. What is normally seen in the aftermath of a disaster is not the vulnerability per se, but the harm done." (Thywissen, 2006). Risk combines vulnerability with the probable frequency of impact to be expected from a known magnitude of a tsunami or other hazard. Vulnerability should not be confused with exposure; they are two separate, but complementary components of risk (Alexander, 2000).

The vulnerability of an element at risk can be characterised by the relationship between the magnitude of the hazard and the damage it causes. The most common quantitative method to describe vulnerability and estimate potential damage is the fragility and damage function. They are also referred to by a variety of other names, including depth-damage functions or stage-damage curves. According to Douglas (2007) and Schultz et al. (2010), fragility functions are key components in a risk analysis framework because they permit rational decision making for both immediate evacuation due to an incoming tsunami as well as for long-term hazard planning and mitigation. As such, they are the backbone of rigorous risk and damage estimation. Fragility functions were first introduced for conducting seismic risk assessments at nuclear power plants (Kennedy et al., 1980; Kaplan et al., 1983).

Reese et al. (2011) state that, "**fragility functions** describe a (probabilistic) relationship between demand and damage". Therefore, in the case of structures subjected to tsunami, the demand on structures needs to be quantified as a function of one or more predictor variables such as water depth, velocity, and entrained debris. The observed building and infrastructure damage needs to be catalogued in sufficient detail to enable the post-tsunami damage state (e.g., minor, major, complete damage) of the structure to be obtained, as well as details regarding the building/infrastructure itself, to examine the dependence of fragility on structure type".

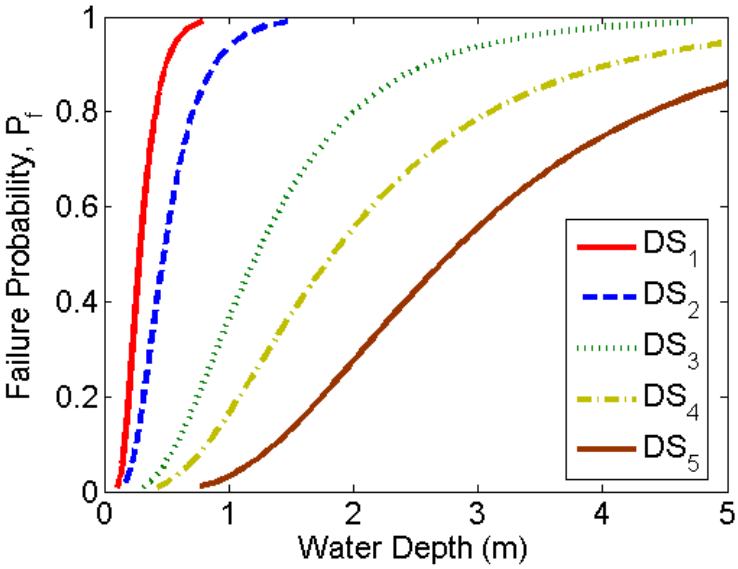

Figure 2.3 Example of tsunami fragility functions (source: Reese et al., 2011); in this case for five different damage states.

For each damage state DSi, the failure probability gives the probability that the building is damaged to at least that state when inundated to a given water depth.

Damage curves or functions, on the other hand, relate tsunami characteristics such as inundation depth, velocity or duration to the percentage damage (relative to replacement cost) for a variety of elements such as buildings, cars, and household goods (Reese and Ramsay, 2010).

Fragility or damage functions are typically based on either:

- Empirical curves developed from historical tsunami and damage survey data, or
- Synthetic functions (hypothetical curves) based on expert opinion developed independently from specific tsunami and damage survey data.

Both methods have their advantages and disadvantages (see Middelmann-Fernandes, 2010). RiskScape for instance uses a combination of both, as it has been found that synthetic damage curves calibrated against observed damage gave the most accurate results (McBean et al., 1986). However, unlike earthquakes, our knowledge about and experience with tsunami vulnerability is limited, and consequently the majority of existing fragility functions are simple empirical ones.

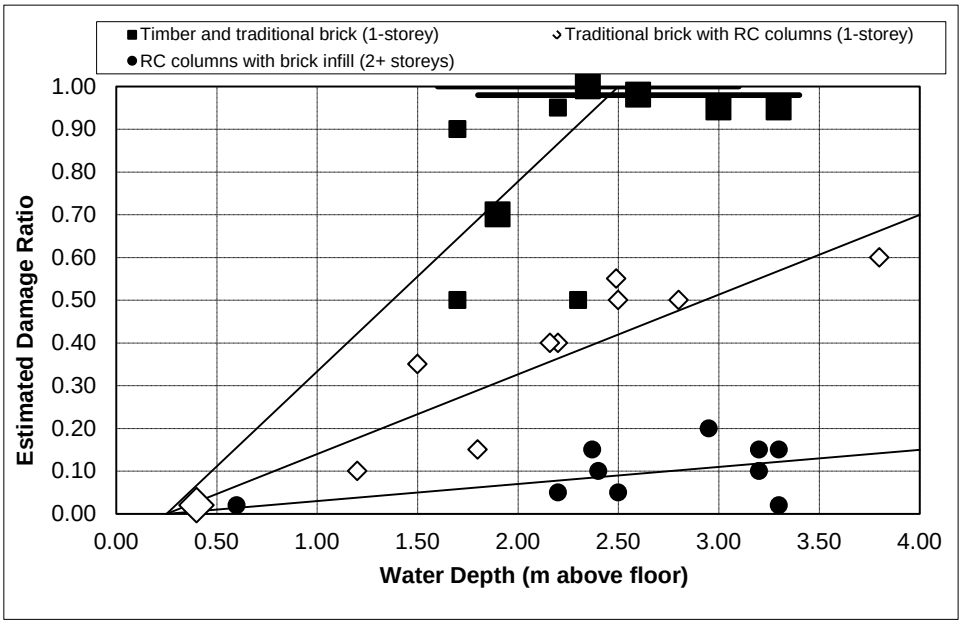

Figure 2.4 Example of tsunami damage functions (source: Reese et al., 2007).

2.4.4.4 Building damage

Table 2.3 gives an overview of existing tsunami studies that quantify building vulnerability and tsunami building damage. Most of the sixteen studies use fragility functions as the preferred method, four use damage functions, and two use judgement criteria (defined tsunami demand parameter thresholds such as critical flow depth or velocity that causes damage or collapse). The majority of the studies use data from the 2004 Indian Ocean tsunami, either collected in field surveys or derived from image interpretation. A few studies have also used numerical modelling to corroborate field data and calculate the hydrological parameters such as flow velocities. This is because usually only inundation depth is recorded in the field. All of the studies use inundation depth as a tsunami demand parameter; only a few have addressed vulnerability due to other predictors such as velocity, debris, etc.

Which of the damage or fragility functions are best suited for the New Zealand building stock? The answer is unfortunately not simple. Why do Murao and Nakazato's (2010) damage curves, for instance, estimate 45% damage at 4 m inundation, whereas Peiris' (2006) shows 80% and Kimura et al.'s (2006) 100% at the same depth? Even though the study areas are more or less the same (certain districts in Sri Lanka) the authors used different sources both for their building data (e.g., field surveys, questionnaires and third party) and inundation data (field surveys, modelling and third party). Given the dependence of the final result on these derived functions, it is important to evaluate the accuracy and reliability of the data. Nonetheless, there is always an uncertainty associated with empirical functions, because they are extremely site-dependent and not applicable to other areas without an expert's adjustment to account for regional and structural differences. There may also be bias due to the specific circumstances of the event the data is based on. If the fragility functions rely on just one demand parameter, for instance inundation depth, and velocity is neglected, the effect is buried in the fragility functions and contributes to the uncertainty (Reese et al., 2011). For these reasons, synthetic fragility functions are often used instead of empirical functions (Middelmann-Fernandez, 2010).

"Empirical fragility functions also often do not take into account mechanical properties of the structure. Because of the time constraints of field surveys, comprehensive structural inspections of buildings are often not feasible. If these differences in the structural capacity

are ignored, and the functions are applied to individual structures or smaller clusters of buildings, not all buildings of the same type will suffer the same level of damage for a given event intensity and damage might be under or overestimated. Some of the fragility functions are also based on a relatively small number of field observations and are hence subject to greater uncertainty" (Reese et al., 2011). All these aspects must be taken into account before applying empirical fragility functions to other areas.

Apart from damage and fragility functions and judgement criteria or thresholds, calculating the tsunami load that impacts on a building is another approach to quantify tsunami building damage. Either field survey data is used or physical model laboratory tests are conducted to calculate the load of a tsunami wave. The information is also used for improving the design of coastal structures (Thusyanthan and Gopal, 2008). According to Palermo and Nistor (2008), three parameters are relevant for tsunami-induced forces: (1) Inundation depth, (2) flow velocity, and (3) flow direction. There are static and dynamic loads, the (1) hydrostatic force, (2) hydrodynamic drag force, (3) surge force, (4) buoyancy force and (5) debris impact (Okada et al., 2005; Palermo and Nistor, 2008). Okada et al. (2005) give an overview of previous studies on tsunami wave pressure and forces. Grundy (2008) also notes that it is equally important to address vulnerability to scour, sediment deposit and impact from debris.

Tsunami-induced lateral forces can meet or exceed seismic forces (Palermo and Nistor, 2008), in particular for low-rise buildings (Okada et al., 2005). According to Chan (1994), a water depth of 1.3 m and a velocity of 1.7 m/s results in a maximum wall pressure of 29 kPa, while a 70 cm depth and a velocity of 2 m/s give a peak pressure of 5 kPa (Hattori et al., 1994). That equals the horizontal bracing demand stipulated for an average one-storey house in New Zealand (Berryman, 2005). However, Thurston and King (2003) have shown that if a house is constructed to the New Zealand building code, it may be up to twice as strong as the bracing demand required for a high wind zone. The actual horizontal strength could be in the range 10-40 kPa/m (Berryman, 2005). This is still well below the impact that a tsunami can cause. Thusyanthan and Gopal (2008) have calculated a peak load of 127.5 kPa at a wave velocity of 5 m/s from a wave tank experiment.

The problem with applying this approach is that building strength varies. Matsutomi et al. (2010) states that wooden buildings in Japan and Samoa will be completely destroyed at a drag force of between 9.7 and 17.6 kPa/m, which corresponds with an inundation depth of 2 m or a velocity of 2.9 m/s. For stone/brick buildings, the thresholds lies at 118-215 kPa/m or 7 m inundation depth and 5.5 m/s velocity respectively. There are not only these obvious differences between countries, but also within New Zealand. In order to apply this loadings approach, one would have to define a typical house for each category. However, due to variations in construction methods and techniques, quality of workmanship, ignorance of building codes and standards, deterioration, etc., most buildings, even of the same type and material, will have different strengths. Ideally this approach should quantify the range of strengths that similar sorts of buildings could withstand. This would explain part of the uncertainty encompassed in the fragility functions.

In the absence of robust, well-constructed and validated fragility models, semi-quantitative approaches are a good alternative. The Papathoma Tsunami Vulnerability Assessment (PTVA) Model for instance is such a semi-quantitative approach (see Papathoma et al., 2003; Dominey-Howes and Papathoma, 2007; Dall'Osso et al., 2009). It provides a Relative Vulnerability Index (RVI) for every single building, which can help planners and emergency managers in their decision-making process. The model takes into account all the main factors that influence building vulnerability (Dominey-Howes and Papathoma, 2007;

Middelmann-Fernandez, 2010; Reese et al., 2011) such as number of stories, building material, ground floor openings, shielding and foundations, as well as the shape and orientation of the building. These authors also introduced a multi-criteria approach for weighting the various attributes in order to limit concerns about subjective ranking of attributes (Dall'Osso et al., 2009). This makes the PTVA model a useful tool for the assessment of building vulnerability. Limitations are the high data demands, with detailed information about each building required, as well as not accounting for secondary tsunami impacts such as debris.

2.4.4.5 Casualties

Quantifying disaster-related casualties helps emergency response coordinators and other public health officials respond to the needs of disaster victims (e.g., allocating resources) and develop policies for reducing the injuries and mortality due to future disasters. Understanding disaster impact and casualty factors can aid in anticipating the consequences of future disasters and in developing risk reduction strategies (Doocy et al., 2007).

The causes of injuries and deaths from tsunami are manifold. The most frequent reasons are drowning, people being swept away by fast moving water and impact from debris causing injuries to the head, spinal, thoracic and abdominal regions. Survivable injuries often include near-drowning, aspiration pneumonia, or orthopaedic injuries such as fractures, sprains and strains (Hogan and Burstein, 2007). Warning and evacuation can significantly decrease the number of casualties. A large percentage of tsunami victims are women, the elderly and children, who are often too weak to swim against the bore or not able to escape as fast as other people (Nishikiori et al., 2006; McAdoo et al., 2008; Reese et al., 2011). Nishikiori et al. (2006) identified being indoors at the time of the tsunami and the house destruction level as other risk factors.

Table 2.3 Summary of existing damage and fragility functions (extended from Grezio and Tonini, 2011).

Reference	Tsunami event	Methodology	Demand parameter	Data	Building categories
Hatori (1984) [in Koshimura et al. 2009]	Meiji Sanriku 1896; Showa Sanriku 1933, Chile 1960	Fragility functions	Inundation depth	Field survey	Unknown
Shuto (1993)	Meiji Sanriku 1896	Fragility functions	Inundation depth	Field survey	Unknown
Iizuka and Matsutomi (200) [in Shuto & Arish 2006]	Unknown	Thresholds	Inundation depth (m) Flow velocity (m/s) Hydrodynamic force (KN/m2)	Unknown	Wood Concrete block Reinforced concrete
Kimura et al (2006) [in Murao & Nakazato 2010]	Indian Ocean Tsunami 2004	Damage functions	Inundation depth (m)	Questionnaires	Unknown
Namegaya and Tsuji (2006) [in Koshimura et al. 2009]	Indian Ocean Tsunami 2004	Fragility functions	Inundation depth (m)	Image Interpretation	Unknown
Peiris (2006)	Indian Ocean Tsunami 2004	Fragility functions	Inundation depth (m)	Field survey	Masonry residential
Ruangrassamee et al. (2006)	Indian Ocean Tsunami 2004		Inundation depth Distance from shore	Field survey	Reinforced concrete
Reese et al. (2007)	Java 2006	Damage functions	Inundation depth (m)	Field survey	Timber/Bamboo Brick traditional Brick traditional with reinforced columns Reinforced concrete frame with brick infill walls
Dias et al (2009)	Indian Ocean Tsunami 2004	Fragility functions	Inundation depth (m)	Field survey, Stats	Masonry residential (temporary and permanent materials)
Koshimura et al. (2009)	Indian Ocean Tsunami 2004	Fragility functions	Inundation depth (m) Flow velocity (m/s) Hydrodynamic force (KN/m2)	Field survey, image interpretation and numerical modelling	Low rise wooden houses Timber constructions Non-engineered reinforced constructions
Matsutomi et al. (2010)	Samoa 2009	Thresholds	Inundation depth (m) Flow velocity (m/s)	Field survey and flow experiments	Wood Stone, bricks, concrete-block

Reference	Tsunami event	Methodology	Demand parameter	Data	Building categories
			Hydrodynamic force (KN/m2)		Reinforced concrete
Murao & Nakazato (2010)	Indian Ocean Tsunami 2004	Damage functions	Inundation depth	Field survey	Non-solid (timber frame and masonry) Solid (reinforced concrete, steel)
Leone et al. (2011)	Indian Ocean Tsunami 2004	Fragility functions	Inundation depth (m)	Field survey and photo interpretation	Wood Brick Brick with reinforced columns Reinforced concrete collective structures (weak) Reinforced concrete collective structures (strong)
Reese et al. (2011)	Samoa 2009	Fragility functions	Inundation depth (m) Debris Shielding	Field survey	Generic Timber residential Masonry residential Reinforced concrete residential Shielded/unshielded – masonry residential Debris/non debris – masonry residential
Suppasri et al. (2011)	Indian Ocean Tsunami 2004	Fragility functions	Inundation depth (m) Flow velocity (m/s) Hydrodynamic force (KN/m2)	Image interpretation and numerical modelling	Mixed type Reinforced concrete Wood
Valencia et al. 2011	Indian Ocean Tsunami 2004	Damage functions	Inundation depth	Field survey and photo interpretation	Light constructions Brick/masonry Brick with reinforced columns and masonry infill Non-engineered reinforced concrete

Table 2.4 Summary of existing studies of methods for predicting casualties.

Reference	Tsunami event	People vulnerability
Miyano & Ro (1992) [in Shuto & Arish 2006]	Tonankai 1944	Percentage of deaths and injuries as function of percentage of destroyed buildings
Shuto (1993)	Meiji Sanriku 1896	Deaths as a percentage of destroyed buildings
Kawata (2001)	Meiji Sanriku 1897, Sanriku 1933, Tou-Nankai 1944, Nankai 1946, Hokkaido Nansai-Oki 1993	Death rate as function of tsunami height
EEFIT (2005)	Indian Ocean Tsunami 2004	Total casualties (sum of deaths, missing and injuries) as a function of number of total damage to houses
Doocy et al. (2007)	Indian Ocean Tsunami 2004	District level mortality rates as a function of environmental indicators
Oya et al. (2006) [in Shuto & Arish 2006]	Indian Ocean Tsunami 2004	Percentage deaths as function of tsunami height
Koshimura et al. (2006)	Synthetic model	Tsunami casualty index
Reese et al. (2007)	Java 2006	Percentage casualties (death and injuries) as function of inundation depth Number of death as function of number of collapsed houses
Koshimura et al. (2009, 2009a)	Indian Ocean Tsunami 2004	Death ratio (death and missing) as function of inundation depth
Leone et al. (2010)	Indian Ocean Tsunami 2004	Percentage of dead and missing people as function of percentage of total destruction

In a similar treatment to flooding, most studies use a correlation between the casualty rate and the inundation depth. More recently there has been a tendency to relate casualties to levels of damage. Table 2.4 gives a summary of existing casualty studies.

Comparing the three studies that have correlated the inundation depth with fatality rates gives significantly different results. While Reese et al. (2007) and Koshimura et al. (2009, 2009a) both estimate a fatality rate of 6% for an inundation depth of 2 m, Oya et al. (2001; in Shuto and Arish, 2006) gives a range of 0.01–0.3%. For a depth of 4 m, the differences are even bigger, with Reese et al. (2007) estimating 14%, Koshimura et al. (2009) 52% and Oya et al. (2001; in Shuto and Arish, 2006) between 0.01 and 20%.

Relating the casualties with the number of destroyed buildings shows a similar variance. For instance, for 500 destroyed buildings, Miyano and Ro (1992; in Shuto and Arish, 2006) estimate 39 casualties, Reese et al. (2007) 154, Leone et al. (2011) 574, EEFIT (2005) 287 and Shuto (1993) 3500. It should be noted though, that some of the studies include injuries and/or missing people, while others only give estimates for the fatalities. However, it highlights that casualty estimation is even more subject to tsunami characteristics and site specific factors. The tsunami casualty rate, even if the tsunami height is the same, has significant variation within each event and depends on the location within each community. How many people have (self-)evacuated, was there any warning prior to the arrival of the tsunami, were the people in buildings or outdoors, etc.? Consequently, every casualty function represents specific circumstances, both in terms of the hydrological characteristics and the specifics of the location. Hence, Koshimura et al. (2006) recommend combining various factors.

The most significant factor is likely to be whether the residents in a community take part in the evacuation or not (including self-evacuation). Koshimura et al. (2006) use a tsunami casualty index indicating the casualty potential at a location. The index is based on the local hydrodynamic characteristics of the tsunami inundation flow and a human body model (physical characteristics of evacuees such as weight and height). This approach does still not include all relevant factors, as suggested in some flood casualty studies (see McClelland and Bowles, 2002; Priest et al., 2007; Tapsell et al., 2009; Reese and Ramsay, 2010) but is certainly a step towards more accurate casualty estimation.

2.4.4.6 Other tsunami damage

The 2004 Indian Ocean Tsunami and the more recent 2011 tsunami in Japan have shown that damage to infrastructure and lifelines can be immense. A community's resilience to a disaster is greatly affected by the continued operation of infrastructure and some essential services. Some of these are essential for emergency operations, some are linked to the provision of basic needs—food, water, shelter, and others are important for public health. The economic viability of communities depends upon the continued operation of these utilities. Hence, it is critical to be able to quantify the risk to lifelines and the economy from tsunami in order to minimize them. However, hardly any quantification methods exist yet, other than for buildings and people. Shuto and Arish (2006) are one of the few who have developed additional (damage) functions, such as for fishing boats, destruction of road- and railway embankments and oil-related fires.

2.4.5 Tsunami damage assessment – ex post

(source: Yalciner and Reese, 2011)

The assessment of damage to the built environment after a tsunami has occurred is crucial for better understanding of planning and design specifications. The most common method of ex-post damage assessments is structural surveys, which investigate the performance of the built environment. These surveys examine the relevant factors associated with damage and failure of buildings and other structures due to the tsunami. They provide valuable information about the tsunami resistance of structures and the adequacy of current building standards and practices. In addition, they also help to improve emergency response and identify specific opportunities to mitigate the impacts of future tsunami.

The built environment includes all human-made structures, ranging from residential, commercial or industrial buildings to lifelines.

A list of the key structures is given in the following.

- Residential buildings
- Commercial buildings and centres
- Industrial buildings and complexes
- Educational buildings
- Health services
- Social, cultural and public assembly areas
- Emergency services
- Communication centres
- Infrastructure (roads, fresh and waste water networks, electricity, oil, gas and communications networks)
- Tourism, tourist facilities
- Marine and land transportation terminals (piers, quays, warehouses, lifelines etc.)
- Historical or cultural buildings and monuments
- Military areas
- Storage facilities (including tanks)
- Solid waste storages

Impacts to buildings are manifold, ranging from damage to windows, doors, interior and exterior walls, structural walls/frames, and foundation damage/scouring, or even total collapse. Infrastructure damage includes damage to telecommunication, electricity, roads, rail and other networks; flood structures and networks and other public utilities.

Collecting comprehensive and detailed data about structural damage will improve model-based estimates of structural and non-structural damage, casualties, and economic losses. A field investigator looking at structural damage is expected to assess the type and level of damage to buildings and infrastructure. It is important that damage is documented for a sufficient number of similar buildings or infrastructure elements in the same area—damaged

and undamaged—so that both an average level of damage and the variety of the damage can be determined. It is important to note what did not fail, as well as what did.

The following information should be collected in order to determine the damage level of the building (Yalciner and Reese, 2011):

- Building use
- Type of structure
- Building material
- Address and/or GPS coordinates
- Distance from the shore
- Number of storeys
- Size
- Wall cladding material
- Roof cladding material
- Age
- Floor height above ground
- Foundation type
- Foundation height
- Sheltered / exposed
- Orientation to the tsunami waves
- Nearby ground characteristics
- Possible debris, sediment impacts
- A photo of each surveyed building should be taken

If infrastructure and other structures are inspected (e.g. roads, piers, etc.), all the relevant information from the above list should also be collected.

According to Yalciner and Reese (2011) “the observed building and infrastructure damage needs to be catalogued in sufficient detail to enable the post-tsunami damage state (e.g., minor, major, complete damage) of the structure. It is therefore common to classify the damage into the following categories”: (Table 2.5)

Table 2.5 Damage state classification (Reese et al., 2011).

Damage State (DS)		**DS description**
DS_0	None	None
DS_1	Light	Non-structural damage only
DS_2	Minor	Significant non-structural damage, minor structural damage
DS_3	Moderate	Significant structural and non-structural damage
DS_4	Severe	Irreparable structural damage, will require demolition
DS_5	Collapse	Complete structural collapse

This allows the assignment of a repair cost, or repair cost ratio (denoted as loss functions) to each damage state if needed.

How structures perform is dependent on the building material and construction type, but it is also a function of the tsunami characteristics such as inundation depth, flow and impact velocity, duration of the inundation and any entrained sediment or debris. Thus, it is necessary to collect not only the details and attributes of the surveyed building or infrastructure element, but also hydraulic information for each surveyed structure. The following information should also be collected if possible:

- Inundation depth (flow depth)
- Maximum water elevation in inundation zone
- Flow velocity
- Direction of incoming tsunami waves
- Inundation duration
- Flow directions in inundation zone
- Evidence of debris

Yalciner and Reese (2011) also state that “in addition to identifying damage to individual structures, field investigators should consider performing an overall building survey on a representative sample basis. Geo-coded spatial data sufficient to make a map of what types of buildings and infrastructure are/were available in each area and the type and extent of damage at each sample building and element should also be collected. Any survey should produce a damage map for each area that includes measurements of the hazard intensity (e.g., inundation depth) and the level of damage.

To ensure a consistent survey and damage assessment, a standardized survey template and damage scale templates should be used throughout”.

2.5 REFERENCES

Ale, B.J.M. (2002). Risk Assessment practices in the Netherlands. *Safety Science* 40, 105-126.

Alexander, D. (2000). Confronting Catastrophe - New Perspectives on Natural Disasters. Oxford University Press, Oxford, p. 282.

Berryman, K. (Compiler; 2005). Review of tsunami hazard and risk in New Zealand [online]. Institute of Geological & Nuclear Sciences client report 2005/104, 139pp. Available at: www.civildefence.govt.nz [Accessed 20 May 2011].

Blong, R. (2003). A new damage index. *Natural Hazards*, 30 (1): 1–23.

Bureau of Transport Economics (2001). Economic costs of natural disasters in Australia. Report 103, Bureau of Transport Economics, Commonwealth of Australia, Canberra.

Cannon, T.; Twigg, J.; Rowell, J. (2005). Social Vulnerability, Sustainable Livelihoods and Disasters [online]. Report to DFID Conflict and Humanitarian Assistance Department (CHAD) and Sustainable Livelihoods Support Office. London. Available at: http://www.proventionconsortium.org/themes/default/pdfs/CRA/DFIDSocialvulnerability_meth.pdf [Accessed 17 May 2011]

Chan, E.S. (1994). Mechanics of deep water plunging-wave impacts on vertical structures. *Coastal engineering*, 22(1-2):115-133.

Dall'Osso, F., Gonella, M., Gabbianelli, G., Withycombe, G., Dominey-Howes, D. (2009). A revised (PTVA) model for assessing the vulnerability of buildings to tsunami damage. *Nat. Hazards Earth Syst. Sci.*, 9: 1557-1565.

Dalrymple, R.A., Kriebel, D.L. (2005). Lessons in Engineering from The Tsunami in Thailand. *The Bridge*, 35: 4-13.

Dias, W.P.S., Yapa, H.D., Peiris, L.M.N. (2009). Tsunami vulnerability functions from field surveys and Monte Carlo simulation. *Civil Engineering and Environmental Systems*, 26 (2):181-194, doi: 10.1080/10286600802435918.

Dilley, M. (2005). Natural Disaster Hotspots: A Global Risk Analysis [online]. Synthesis Report, International Bank for Reconstruction and Development/The World Bank and Columbia University. Available at: http://www.ldeo.columbia.edu/chrr/research/hotspots/ [Accessed 19 May 2011]

Dominey-Howes, D., Papathoma, M. (2007). Validating a Tsunami Vulnerability Assessment Model (the PTVA Model) Using Field Data from the 2004 Indian Ocean Tsunami. *Natural Hazards*, 40: 113-136

Doocy, S., Gorokhovich, Y., Burnham, G., Balk, D. Robinson, C. (2007). Tsunami Mortality Estimates and Vulnerability Mapping in Aceh, Indonesia. *American Journal of Public Health*, Supplement 1, Vol 97 (S1):146-151.

Douglas, J. (2007). Physical vulnerability modelling in natural hazard risk assessment. *Nat. Hazards Earth Syst. Sci.*, 7: 283–288.

Durham, K. (2003). Treating the Risks in Cairns. *Natural Hazards*, 30 (2): 251–261.

Economic Commission for Latin America and the Caribbean (ECLAC) (2003). Handbook for Estimating the Socio-economic and Environmental Effects of Disasters.

EERI (Earthquake Engineering Research Institute) (2005). The Great Sumatra Earthquake and Indian Ocean Tsunami of December 26, 2004. Report #6.

EEFIT (2005). The Indian Ocean Tsunami 26 December 2004: Mission findings in Sri Lanka & Thailand. London.

FAO/WHO (2009). Risk Characterization of Microbiological Hazards in Food: Guidelines. *Microbiological Risk Assessment Series* No. 17. Rome. 116pp.

Ghobarah, A., Saatcioglu, M. Nistor, I. (2006). The impact of the 26 December 2004 earthquake and tsunami on structures and infrastructure. *Engineering Structures*, 28: 312–326.

Grezio, A., Tonini, R. (2011). Tsunami fragility curves and tsunami vulnerability:state of the art [online]. Draft. Available at: http://bymur.bo.ingv.it/frames/uploads/tsunami_vulnerability_report_v1.pdf [Accessed 24 May 2011].

Grundy, P. (2008). Strategies for Disaster Risk Reduction on Coasts.Paper at the third IFED Forum, Shoal Bay, Australia, 12-15 December 2007. Available at: http://www.ifed.ethz.ch/events/Forum07/Paper/Grundy_paper.pdf [Accessed 09 May 2011].

Hatori, T. (1984). On the damage to houses due to tsunamis. *Bulletin of the Earthquake Research Institute* 59(3): 433-439 (in Japanese).

Hattori, M., Arami, A., Yui, T. (1994). Wave impact pressures on vertical walls under breaking waves of various types. *Coastal Engineering*, 22(1-2):79-114.

Hogan, D.E., Burstein, J.L. (2007). Disaster medicine. Kluwer, Philadelphia.

Hollenstein, K. (2005). Reconsidering the risk assessment concept: Standardizing the impact description as a building block for vulnerability assessment. *Natural Hazards and Earth System Sciences*, 5, 301–307.

International Strategy for Disaster Reduction, ISDR (2004). Living with risk. Geneva.

Izuka, H., Matsutomi, H. (2000). Damage estimation due to tsunami inundation flow. *Proceedings of Coastal Engineering, JSCE*, Vol.47, 381-385 (in Japanese).

Kaplan, M., Renaud, F.G., Lüchters, G. (2009).Vulnerability assessment and protective effects of coastal vegetation during the 2004 Tsunami in Sri Lanka. *Nat. Hazards Earth Syst. Sci*., 9: 1479–1494.

Kaplan, S., Perla, H.G., Bley, D.C. (1983).A methodology for seismic analysis at nuclear power plants. *Risk Analysis,* 3(3):169–180.

Kawata, Y. (2001). Disaster mitigation due to next Nankai earthquake tsunamis occurring in around 2035. ITS Proceedings, Session 1, Number 1-8:315-329.

Kennedy, R.P., Cornell, C.A., Campbell, R.D., Kaplan, S., Perla, H.F. (1980).Probabilistic seismic safety study of an existing nuclear power plant. *Nuclear Engineering and Design*, 59(1980):315–338.

Kimura, K., Ishimi, K., Sato, S., Fukuda, T., Mikami, T., Kikuchi, S. (2006). Verification of tsunami wave source model and formulation of a vulnerability function for buildings based on the investigation of actual damage due to the Sumatran earthquake and tsunami: subject area being the damage at Matara city, Sri Lanka. *Coastal Engineering Committee*, Vol.53: 301-305 (in Japanese).

Koshimura, S., Katada, T., Mofjeld, H.O., Kawata, Y. (2006). A method for estimating casualties due to the tsunami inundation flow. *Nat. Hazards*, 39(2): 265–274.

Koshimura, S., Namegaya, Y., Yanagisawa, H., (2009). Tsunami Fragility - A New Measure to Identify Tsunami Damage. *Journal of Disaster Research*, 4 (6): 479-488.

Koshimura, S., Oie, T., Yanagisawa, H., Imamura, F. (2009a). Developing Fragility Functions for Tsunami Damage Estimation Using Numerical Model and Post-Tsunami Data from Banda Aceh, Indonesia. *Coastal Engineering Journal*, Vol. 51, No. 3 (2009) 243–273.

Leone, F., Lavigne, F., Paris, R., Denain, J-C., Vinet, F. (2010). A spatial analysis of the December 26th, 2004 tsunami-induced damages: Lessons learned for a better risk assessment integrating buildings vulnerability. *Applied Geography*, doi:10.1016/j.apgeog.2010.07.009.

Malone, E. (2009). Vulnerability and Resilience in the Face of Climate Change: Current Research and Needs for Population Information [online]. Report for Population Action International, Washington. Available at: http://www.populationaction.org/Publications/Working_Papers/Vulnerability_and_Resilience/Malone_resilience.pdf [Accessed 14 May 2011].

Matsutomi, H., Okamoto, K., Harada, K. (2010). Inundation Flow Velocity of Tsunami on Land and its Practical Use [online]. No 32 (2010): Proceedings of 32nd Conference on Coastal Engineering, Shanghai, China, 2010. Available at: http://journals.tdl.org/ICCE/article/viewFile/1141/pdf_215. [Accessed 22 May 2011].

Matsutomi, H., Shuto, N., Imamura, F., Takahashi, T. (2001). Field Survey of the 1996 Irian Jaya Earthquake Tsunami in Biak Island. *Natural Hazards,* 24: 199–212.

McAdoo, B.G., Moore, A., Baumwoll, J. (2008). Indigenous knowledge and the near field population response during the 2007 Solomon Islands tsunami. *Nat Hazards*. DOI 10.1007/s11069-008-9249-z.

McBean, E., Fortin, M., Gorrie, J. (1986). A critical analysis of residential flood damage estimation curves. *Can. J. Civ. Eng*., 13: 86–94.

McClelland, D.M., Bowles, D.S. (2002). Estimating Life Loss for Dam Safety Risk Assessment - a Review and New Approach. Institute for Water Resources, U.S. Army Corps of Engineers, Alexandria, VA.

McKenzie, E., Prasad, B., Kaloumaira, A. (2005). Economic Impact of Natural Disasters on Development in the Pacific [online]. Volume 2: Economic Assessment Tools. Available at: http://www.ausaid.gov.au/publications/pdf/impact_pacific_tools.pdf [Accessed 15 May 2011].

Middelmann-Fernandes, M.H. (2010). Flood damage estimation beyond stage-damage functions: an Australian example. *Journal of Flood Risk Management*, 3: 88-96.

Murao, O., Nakazato, H. (2010). Vulnerability Functions for Buildings Based on Damage Survey Data in Sri Lanka after the 2004 Indian Ocean Tsunami. Proceedings of the International Conference on Sustainable Built Environment (ICSBE-2010), Kandy, 13-14 December 2010, p.371-378.

Namegaya, Y., Tsuji, Y. (2006). Distributions of the Swept Away Houses in Banda Aceh City, Indonesia, due to the 2004 Indian Ocean Tsunami Estimated by Satellite Images. *Annual Journalof Coastal Engineering*, JSCE, Vol.53: 286-290 (in Japanese).

Nishikiori, N., Abe, T., Costa, D.G.M., Dharmaratne, S.D., Kunii,O., Moji, K. (2006). Who died as a result of the tsunami? – Risk factors of mortality among internally displaced persons in Sri Lanka: a retrospective cohort analysis. *BMC Public Health, (*6): 73.doi: 10.1186/1471-2458-6-73.

Nistor, I, Palermo, D., Al-Faesly, T., Cornett, A. (2011). Investigations and Experimental Modelling of the Tsunami-Induced Extreme Hydrodynamic Forces on Structures [online]. Proceedings of 34th International Association of Hydraulic Engineering (IAHR) Congress, Brisbane, Australia, July, 2011.

Okada, T., Sugano, T., Ishikawa, T., Takai, S., Tateno, T. (2005). Tsunami Loads and Structural Design of Tsunami Refuge Buildings. The Building Centre of Japan.Tokyo.

Omira, R., Baptista, M.A., Miranda, J.M., Toto, E., Catita, C., Catalaõ, J. (2010). Tsunami vulnerability assessment of Casablanca-Morocco using numerical modelling and GIS tools. *Nat Hazards*, 54:75–95

Palermo, D., Nistor, I. (2008). Tsunami – induced loading on Structures. *Structure*. (3), 10-13.

Papadopoulos, G.A., Imamura, F. (2001).A proposal for a new tsunami intensity scale. Proceedings of International Tsunami Symposium 2001, IUGG, 569-577.

Papathoma, M., Dominey-Howes, D., Zong, Y., Smith, D. (2003).Assessing tsunami vulnerability, an example from Herakleio, Crete. *Nat.Hazards Earth Syst. Sci.,* 3, 377–389.

Peiris, N. (2006). Vulnerability functions for tsunami loss estimation. First European Conference on Earthquake Engineering and Seismology, Geneva, Switzerland, 3-8 September 2006. Paper No. 1121.

Pimanmas, A., Joyklad, P., Warnitchai, P. (2010). Structural Design guideline for tsunami evacuation shelter. *Journal of Earthquake and Tsunami*. (4), 269-284.

Priest, S., Wilson, T., Tapsell, S., Penning-Rowsell, E., Viavattene, C., Fernandez-Bilbao, A. (2007). Building a model to estimate Risk to Life for European flood events. Floodsite Final Report, T10-07-10.

Reese, S., Cousins, W.J., Power, W.L., Palmer, N.G., Tejakusuma, I.G., Nugrahadi, S. (2007). Tsunami vulnerability of buildings and people in South Java.Field observations after the July 2006 Java tsunami.*Nat. Hazards Earth Syst. Sci*., 7 (5): 573-589.

Reese, S., Schmidt, J. (2008).Tsunami and flood hazard exposure of city council infrastructure in Christchurch City. NIWA client report: WLG-2008-67.Unpublished.

Reese, S., Smart, G. (2008). High resolution inundation modelling as part of a multi-hazard loss modelling tool. In: Samuels, P., Huntington, S. Allsop, W. and J. Harrop (eds): Flood Risk Management. Research and Practice. Proceedings of the European Conference on Flood Risk Management Research into Practice (FloodRisk 2008), Oxford, Uk, 30.09-02.10.2008, pp. 1663-1668.

Reese, S., Ramsay, D. (2010). Riskscape: Flood fragility methodology. NIWA technical report, WLG-2010-45.

Reese, S. Bradley, B.A., Bind, J., Smart G.M., Power, WJ.,Sturman, J.D. (2011). Empirical building fragilities from observed damage in the 2009 South Pacific tsunami.*Earth Science Reviews*, Special issue.doi:10.1016/j.earscirev.2011.01.009

Rossetto, T., Peiris, N., Pomonis, A., Wilkinson, S.M., Del Re, D., Koo, R., Gallocher, S. (2007). The Indian Ocean tsunami of December 26, 2004: observations in Sri Lanka and Thailand. *Nat Hazards*, 42:105–124.

Ruangrassamee, H., Yanagisawa, P. Foytong, P. Lukkunaprasit, Koshimura, S., Imamura, F. (2006). Investigation of tsunami-induced damage and fragility of buildings in Thailand after the December 2004 Indian Ocean tsunami. *Earthquake Spectra*, 22 (S3):S377–S401.

Saatcioglu, M., Ghobarah, A., Nistor, I.(2007).Performance of Structures Affected by the 2004 Sumatra Tsunami in Thailand and Indonesia. In: T. S. Murty, U. Aswathanarayana and N. Nirupama (Editors), The Indian Ocena Tsunami. Francis & Taylor, London, pp. 297-321.

Salinas, S.V., Low, K.K., Liew, S.C. (2005). Quick Analysis of Wave Patterns Generated by Tsunami Waves and Captured by SPOT Imagery. Geoscience and Remote Sensing Symposium, 2005.IGARSS '05.Proceedings. 2005 IEEE International,(5), p.3634-3636.

Schmidt, J., Matcham, J., Reese, S., King, A., Bell, R., Smart, G., Cousins, J. Smith, W., Heron, D. (2011). Quantitative multi-risk analysis for natural hazards: a framework for multi-risk modelling. *Nat Hazards*. DOI: 10.1007/s11069-011-9721-z

Schultz, M.T., Gouldby, B.P., Simm, J.D., Wibowo, J.L. (2010). Beyond the Factor of Safety: Developing Fragility Curves to Characterize System Reliability. USACE Water Resources Infrastructure Program, Final report ERDC SR-10-1.

Shuto, N. (1993). Tsunami intensity and disasters. In: Tinti, S. (ed.). Tsunamis in the World. Kluwer Academic Publisher, Dortrecht, 197-216.

Shuto, N., Arish, N. (2006). Tsunamis, Disasters and Countermeasures.Paper at the International Workshop on Fundamentals of Coastal Effects of Tsunamis [online], December 26-28, 2006, Hilo Hawaii. Available at: http://tsunami.orst.edu/workshop/2006/doc/premeeting/Shuto.pdf [Accessed 17 May 2011].

Smith, K., Petley, D.N. (2009). Environmental Hazards.Assessing risk and reducing disaster.5th Edition. Routledge. New York.

Standards Australia/Standards New Zealand (2004). Risk Management Guidelines. Companion AS/NZS 4360:2004. Sydney & Wellington.

Stansfield, K. (2005). Effects of the Asian tsunami on structures.*The Structural Engineer*, 83(11): 20-21.

Strunz, G., Post, J., Zosseder, K., Wegscheider, S., Mück, M., Riedlinger, T., Mehl, H., Dech, S., Birkmann, J., Gebert, N., Harjono, H., Anwar, H.Z., Sumaryono, Khomarudin, R.M., Muhari, A. (2011). Tsunami risk assessment in Indonesia. *Nat. Hazards Earth Syst. Sci*., 11, 67–82.

Suppasri,A., Koshimura, S., Imamura, F. (2011). Developing tsunami fragility curves based on the satellite remote sensing and the numerical modeling of the 2004 Indian Ocean tsunami in Thailand. *Nat. Hazards Earth Syst. Sci*., 11, 173–189.

Tapsell, S.M, Priest, S.J., Wilson, T., Viavattene, C., Penning-Rowsell, E.C. (2009). A new model to estimate risk to life for European flood events. In: In: Samuels, P., Huntington, S. Allsop, W. & J. Harrop (eds): Flood Risk Management. Research and Practice. Proceedings of the European Conference on Flood Risk Management Research into Practice (FloodRisk 2008), Oxford, Uk, 30.09-02.10.2008, pp. 933-943.

Thurston, S.J., King, A.B. (2003). Full sized house cyclic racking test. Proceedings 2003 Pacific Conference on Earthquake Engineering, 13-15 February 2003, Christchurch.New Zealand Society for Earthquake Engineering. Paper No. 029

Thusyanthan, N.I., Gopal, S.P. (2008). Tsunami wave loading on coastal houses: a model approach. Proceedings of ICE, *Civil Engineer* 161, paper 07-00037, 77-86. Doi:10.1680/cien.2008.161.277

Thywissen, K. (2006). Components of Risk.A Comparative Glossary. 'Studies of the University: Research, Counsel, Education'. Publication Series of UNU-EHS, No. 2/2006.

United Nations Development Programme (UNDP) (2004). Reducing Disaster Risk: A Challenge for Development [online]. New York: United Nation Development Programme, Bureau for Crisis Prevention and Recovery. Available at: http://www.undp.org/cpr/whats_new/rdr_english.pdf [Accessed 14 May 2011].

United States National Tsunami Hazard Mitigation Program (2001). Designing for Tsunamis. Seven Principles for Planning and Designing for Tsunami Hazards. Available at: http://nthmp-history.pmel.noaa.gov/Designing_for_Tsunamis.pdf [Accessed 16 May 2011].

Valencia, N., Gardi, A., Gauraz, A. L., Leone, F., and Guillande, R. (2011). New tsunami damage functions developed in the framework of SCHEMA project: application to Euro-Mediterranean coasts. *Natural Hazards and Earth System Science*.in review.

Yalciner, A., Reese, S., Koshimura, F.I. (2011). Tsunami coastal impact, damage information, and engineering aspects. In: UNESCO-IOC .Post-tsunami survey field guide.Second Edition.IOC Manuals and Guides No.XY. Paris, UNESCO.

Yalciner, A., Reese, S. (in press). Structural damage surveys. In: UNESCO-IOC .Post-tsunami survey field guide.Second Edition.IOC Manuals and Guides No.XY. Paris, UNESCO, 2011.

Yeh, H., Robertson, I., Preuss, J. (2005). Development of Design Guidelines for Structures that Serve as Tsunami Vertical Evacuation Sites. Report No 2005-4, Washington Dept. of Natural Resources.

Yeh, H. (2009). Tsunami impacts on coastlines. In: Bernard, E.N. & Robinson, A.R, (eds): The sea. Tsunamis.Harvard University Press, Cambridge, p.333-370.

This page is intentionally left blank.

3.0 PALEOTSUNAMI AND HISTORICAL TSUNAMI DATABASES

3.1 HISTORICAL TSUNAMI RECORDS

The New Zealand historical tsunami database has been compiled by Gaye Downes (GNS Science). This is currently an unpublished database but work is in progress to publish it as an online, searchable database. In this section we summarise the New Zealand historical tsunami database by analysing the distribution of tsunami through time and the sources of the tsunami. Brief descriptions of the most significant historical tsunami are given. The New Zealand historical tsunami database assigns a "validity" ranking of 0–4 for tsunami reports, with 4 being a definite tsunami and 0 being an erroneous tsunami report. For our analysis we only use tsunami with a validity ranking ≥2 (Table 3.1).

Table 3.1 Validity rankings for historical tsunami of New Zealand 1985–2011. Very doubtful or erroneously attributed tsunami of validity "0" and "1" (shaded grey) are noted in the historical tsunami database but are excluded from the analysis undertaken in this report. *All the "3"-level tsunami are pre-1932 except for a tsunami on Tasman Lake (Aoraki-Mt Cook) on 22nd February, 2011, which was caused by ice-calving from the Tasman Glacier. The ice calving was triggered by the M6.3 Christchurch earthquake, but it is debatable whether this was a true tsunami.

Validity		# tsunami	Notes on ages
4	Definite tsunami	60	
3	Probable tsunami	8	Most pre-1932*
2	Questionable/unlikely	12	All pre-1928
1	Very doubtful/highly unlikely	15	All pre-1993
0	Erroneous tsunami report	6	All pre-1870

New Zealand has been affected by at least 80 tsunami from 1835–2011 (Downes, unpublished data). Figure 3.1 shows the distribution of tsunami through time during this historical period. The rates of tsunami appear relatively steady at approximately 4–5 per decade up until c. 2000. From 2000 onward the frequency of tsunami appears to increase, but this is largely due to an increase in data collection from tide gauges. The tide gauges record fluctuations caused by tsunami that would not have been noticed by human observation alone. In the period from c. 1970–2000, the database contains a mixture of tide gauge records and newspaper or written reports of tsunami. Prior to c. 1970 the historical tsunami database is largely reliant upon newspaper reports and writings in historical documents, which are naturally skewed towards recording tsunami that were damaging or very noticeable.

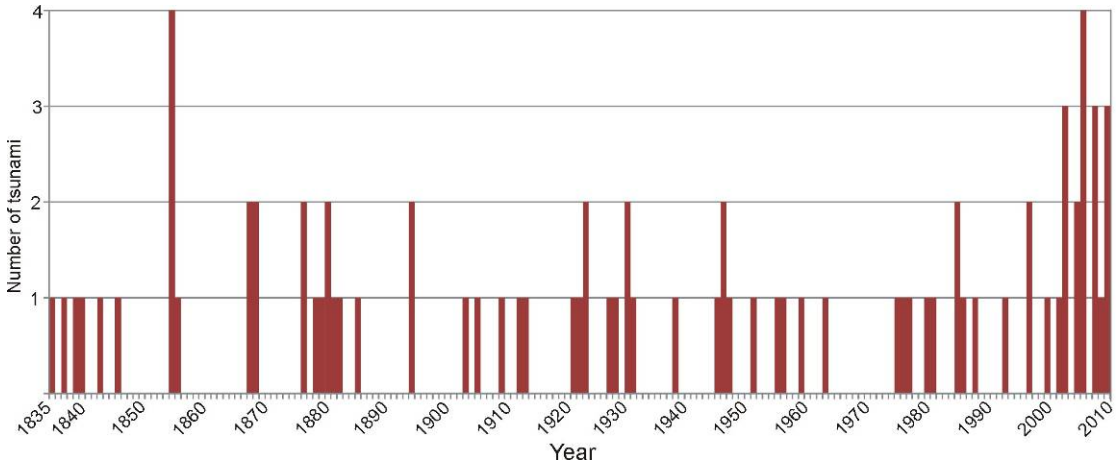

Figure 3.1 Distribution of tsunami that have been recorded on New Zealand shorelines from 1835–2011. Data from the New Zealand historical tsunami database (Downes et al., unpublished data). This analysis excludes tsunami of low validity ranking (see Table 3.1).

Of the 80 tsunami to have affected New Zealand in historical times (post-1835):

- 27 were from distant sources (> 3 hours tsunami travel time, Figure 3.2)
- 12 were from regional sources (1–3 hours tsunami travel time)
- 28 were from local sources (< 1 hour tsunami travel time)
- 13 were from unknown sources.

The ring of subduction zones around the Pacific Ocean is responsible for most of the distant-source tsunami to affect New Zealand (Figure 3.2). Tsunami from the South American margin along Peru and Chile are most frequent, but New Zealand is also affected by tsunami from the Alaska-Aleutian margin, and the Kamchatka-Kuril-Japan margin, and the south Pacific subduction zones of the Solomon Islands and the Tonga-Kermadec trench (Figure 3.2). Tsunami generated at the Sumatra subduction zone (the M_W9.3 Indian Ocean tsunami, 2004) and by the Krakatau volcanic eruption (1883) were recorded in New Zealand but did not cause any significant damage.

Regional-source tsunami are typically from the Puysegur trench, southwest of New Zealand and the Tonga-Kermadec trench, northeast of New Zealand (depending on the distance from New Zealand, tsunami generated on the Tonga-Kermadec trench can be classified as distant- or regional-source). Local-source tsunami are predominantly associated with upper plate faults or the plate interface along the Hikurangi subduction zone or the Fiordland-Puysegur subduction zone. Exceptions to this are tsunami that were generated by the M_W 6.4 1922 Motunau (north Canterbury) earthquake, the M_W 7.3 Buller earthquake and landslide-generated tsunami on Lake Taupo in 1846 and 1910.

Figure 3.3 shows the distribution of locations around New Zealand that have been impacted by historical tsunami, and the proximity of the tsunami source (note that a single tsunami can affect multiple points along the coastline, so there are many more data points on Figure 3.3 than there were individual tsunami). The Northland to Bay of Plenty region has been dominantly affected by distant-source tsunami, with rare regional-source tsunami. The East Coast of the North Island from East Cape to Wellington has been affected by both distant- and local-source tsunami. The northwest Nelson area and Fiordland coast have mostly been impacted by local-source tsunami. All other areas, including the Chatham Islands have been dominantly affected by distant-source tsunami (Figure 3.3).

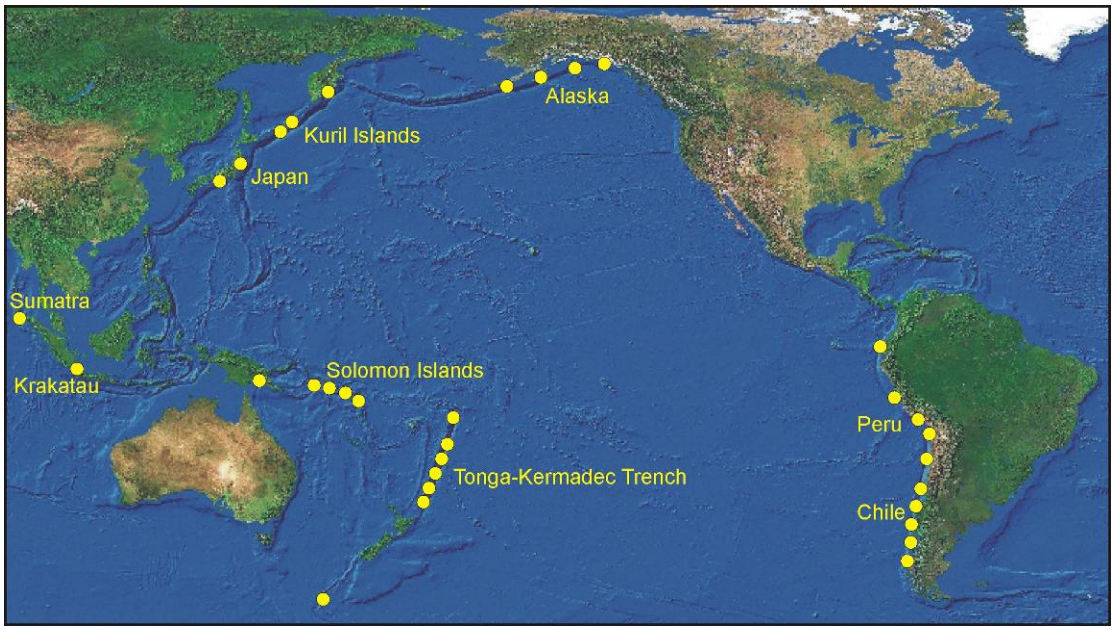

Figure 3.2 The distant source areas that have generated tsunami that have affected the New Zealand coastline (1835–2011). Each yellow dot represents an event. The dots are in the approximate source location but they do not accurately represent earthquake epicentres. All distant sources were earthquakes, except Krakatau, which was a volcanic eruption. Note that tsunami triggered at the Tonga-Kermadec Trench may be classified as regional if their source is close to New Zealand.

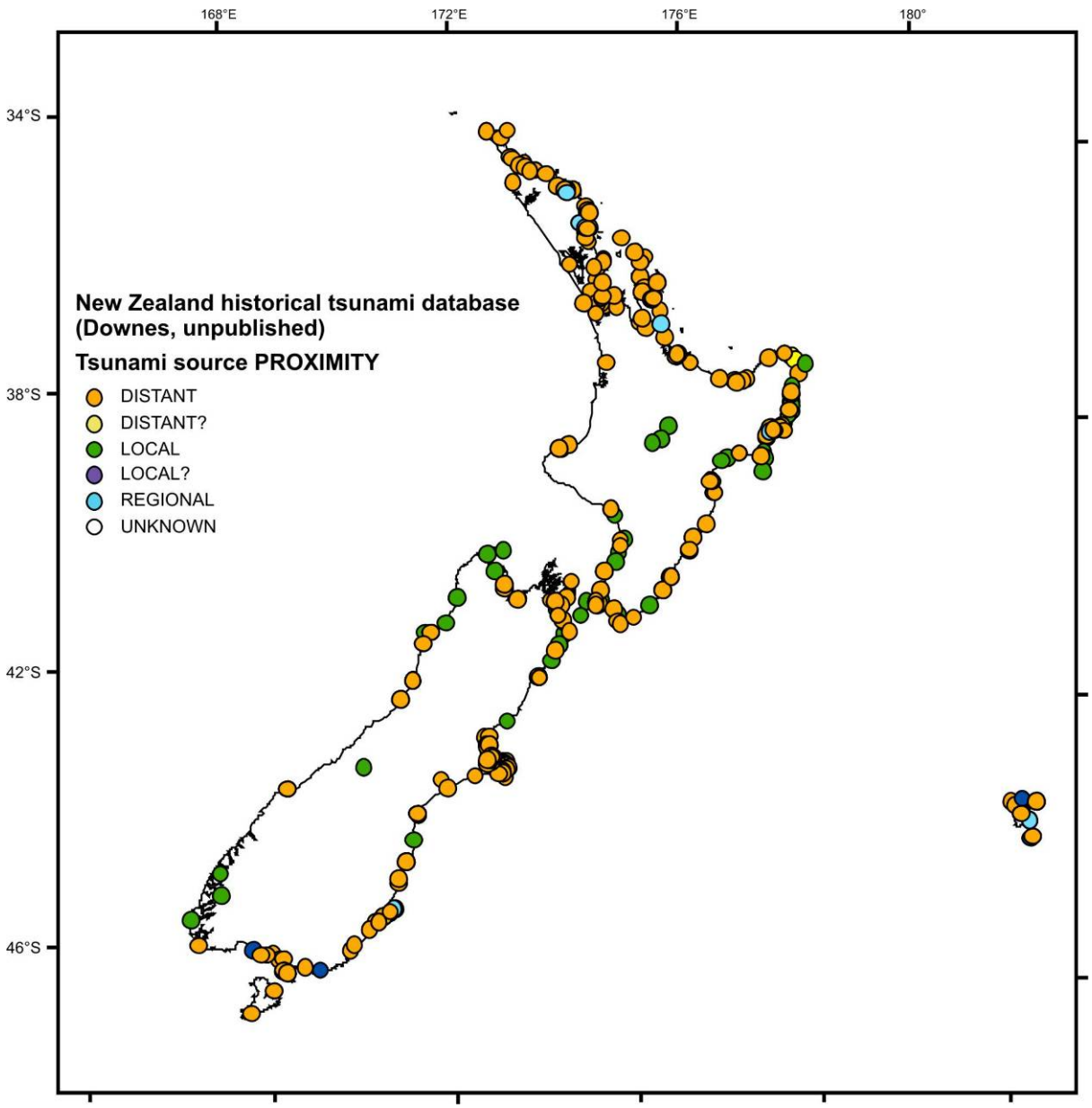

Figure 3.3 The proximity of tsunami sources for tsunami that have affected the New Zealand coastline since 1835 (Downes, unpublished data). Distant source: > 3 hours travel time; regional source: 1–3 hours travel time; local source: < 1 hour travel time. Note that an individual tsunami event may affect the coastline at multiple points, so each data point does not represent a separate event. Points overlap in some locations but are intended to give a general impression (specific location details are recorded in the database).

Most historical tsunami that have affected New Zealand shorelines have been caused by earthquakes (Figure 3.4). Of the 80 tsunami to have impacted New Zealand, 44 were definitely caused by earthquakes, 9 were caused by earthquakes and associated landslides, and 8 tsunami were caused by landslides alone. One tsunami was a meteo-tsunami caused by the Krakatau eruption in 1883. Meteo-tsunami are generated by air-pressure disturbances (e.g. the blast from the Krakatau eruption); there are three other suspected meteo-tsunami in the historical database. Five tsunami have no known cause, and the remainder of the tsunami (13 events) have uncertain causes but are suspected to have resulted from earthquakes and/or landslides. The distribution of tsunami generated by different causes seems to have no particular spatial pattern (Figure 3.4).

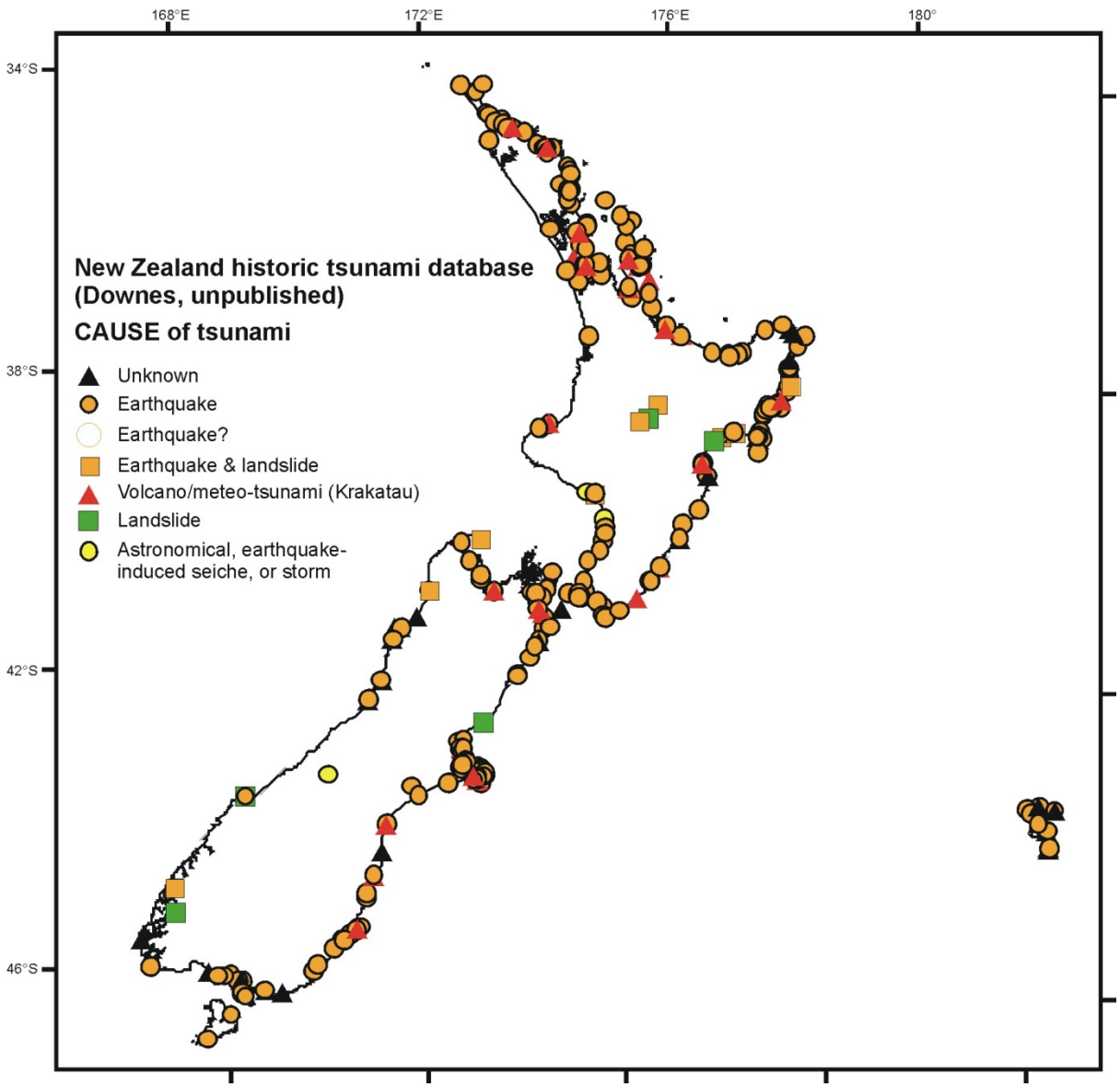

Figure 3.4 The causes of tsunami that have affected the New Zealand coastline since 1835 (Downes, unpublished data). Note that an individual tsunami event may affect the coastline at multiple points, so each data point does not represent a separate event. Points overlap in some locations but are intended to give a general impression (specific location details are recorded in the database).

3.2 LARGE HISTORICAL TSUNAMI

According to the historical tsunami database (Downes, unpublished) the five largest historical tsunami in New Zealand were generated by: the M_W8.2 Wairarapa earthquake in 1855, a M_W7.1 earthquake 50 km offshore of Gisborne in March 1947, and distant earthquakes in South America in 1868, 1877 and 1960 (Figure 3.5).

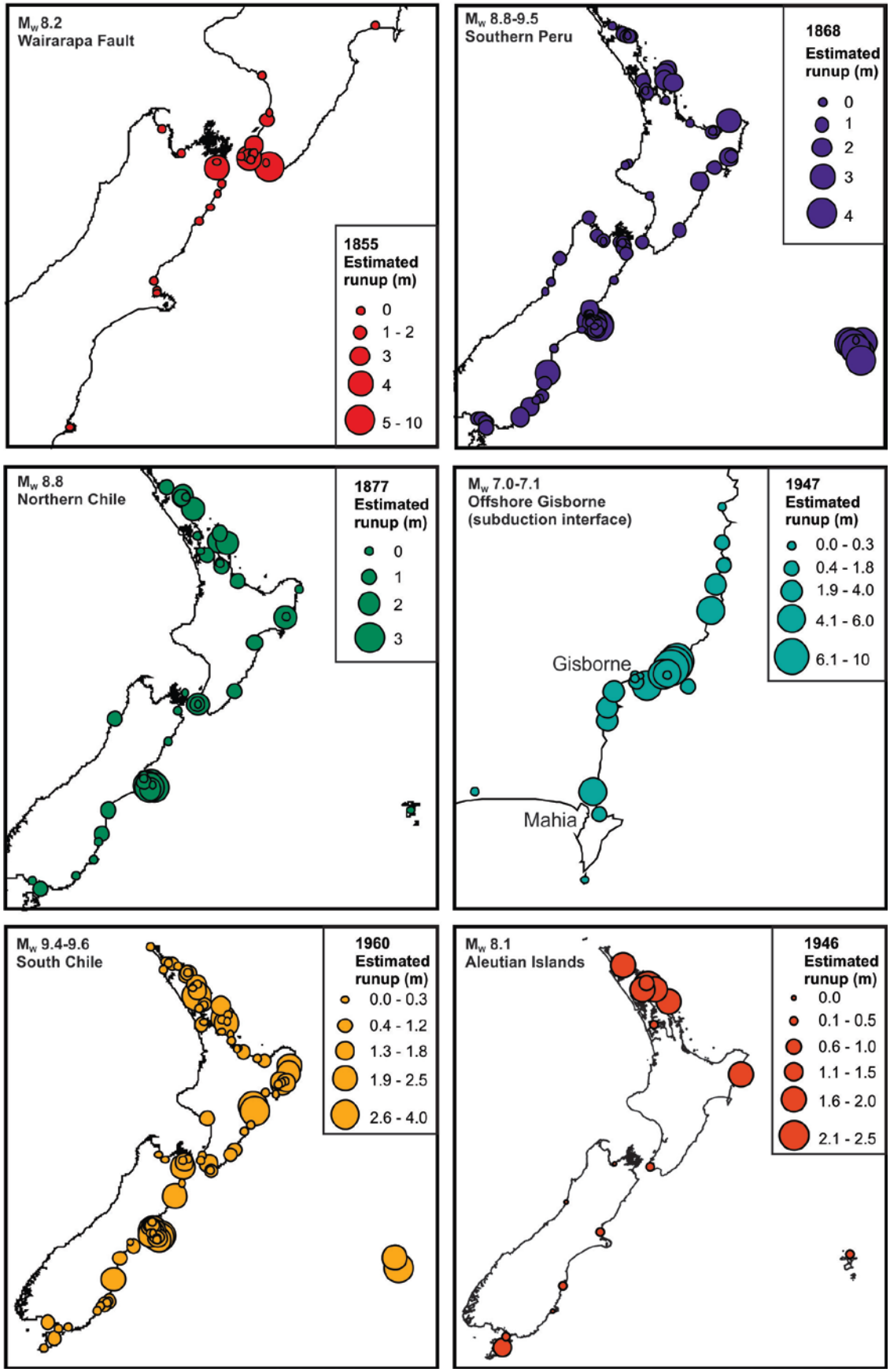

Figure 3.5 Estimated tsunami runup values for the five largest tsunami in New Zealand between 1835 and 2011. Note the scale varies between boxes. Local-source tsunami have high runups, but are typically smaller in spatial extent, distant-source tsunami have widespread effects but lower runups. The runup values are from the New Zealand historical tsunami database (Downes et al., unpublished data), and include a combination of actual measured values and estimates based on descriptions given in newspaper (and other) reports.

1855 Wairarapa Earthquake

The 1855 earthquake, which ruptured the Wairarapa Fault east of Wellington, generated a tsunami with a maximum known run-up of 10 m at Te Kopi in eastern Palliser Bay and up to 4–5 m in several locations in Wellington and along the northern Marlborough coast (Figure 3.5). The Rongotai isthmus and Miramar were reportedly covered in water to about one metre depth, rushing in from Lyall Bay and from Evans Bay. In Lambton Quay, the tsunami was 2–2.5 m high, washing into shops that fronted on to what was then the beach. Waves swept around Wellington Harbour and through Cook Strait for more than 12 hours, being observed as far south as the Clarence River Mouth and at least as far north as Otaki, where the run-up was probably about 2–3 metres. It is estimated that at least 300–500 km of coastline was affected, with run-ups of 1 m or more. The first waves arrived within minutes in Wellington and within an hour of the earthquake at Otaki and Marlborough. While submarine and coastal landslides may have contributed to the tsunami, the coseismic displacement of the sea bed, by as much as 6 m vertically upward near Turakirae Head on the south Wellington coast, was probably the main cause. Tides continued to be disturbed for the following week, possibly because of large aftershocks, perhaps with accompanying landslides.

1868, 1877 & 1960 South American Earthquakes

Three tsunami, in 1868, 1877, and 1960 generated by great ($M_W \geq 8$) earthquakes in South America caused widespread damage and disruption along the east coast of the North and South Islands and in the Chatham Islands (Figure 3.5). The 1868 tsunami caused the only death in New Zealand attributable to tsunami since European settlement. The tsunami was generated by a magnitude ~M9.1 earthquake off southern Peru/northern Chile. The greatest near-source run-up recorded for the 1868 tsunami was 18 m (Integrated Tsunami Database for the World Ocean). In New Zealand, run-ups of 1–4 m occurred on the mainland, and up to 10 m in the Chatham Islands. Considerable damage to houses, boats, shops, wharves, jetties, and boatsheds occurred along the whole eastern seaboard. At Tupuanga (Tupuangi) on the northwest coast of Chatham Island, the dwellings of an entire Māori village were washed away, the 60–70 residents escaping after the first of three large waves reached the floor of their dwellings. The tsunami severely impacted Great Barrier Island, eastern Bay of Plenty, Napier, Canterbury (especially Banks Peninsula), and Oamaru. It even reached the West Coast with waves of 1-2 m reported in Westport. Damage was more limited than could have been expected because the largest waves of the tsunami arrived within an hour or two of low tide at locations south of Napier. Smaller waves that occurred near high tide also caused damage.

The 1877 tsunami was caused by a magnitude ~M9 earthquake off northern Chile, about 400 km south of the source of the 1868 event. The tsunami was up to 21 m high near its source, but in New Zealand the effects were generally not as extensive or as well recorded in historical documents as the 1868 tsunami. Nevertheless, the tsunami had peak run-ups of 3.5 m. Many of the places strongly affected in 1868 were again affected in 1877, but there were some notable differences showing the effect of the source location (Figure 3.5). The tsunami was again evident for several days, and again damage was limited by the largest waves arriving at or near low tide along a large part of the east coast.

The 1960 tsunami was generated by a massive, M_W9.4–9.6 earthquake in the subduction zone off central Chile. It was the largest earthquake in the 20th century. According to the Integrated Tsunami DataBase (ITDB), it caused a large local tsunami (maximum run-up 25 m) that resulted in US$550 million in damage and 1,000 deaths. Another US$24 million in

damage and 61 deaths occurred in Hawaii, and in Japan the waves were more than 6 m high and caused 199 fatalities and US$50 million in damage. There is as yet no estimate of the cost of the damage in New Zealand. As with the 1868 event, run-ups of 1–4 m occurred along the whole eastern seaboard from Northland to Southland, and in the Chatham Islands (Figure 3.5). In places, some of the largest waves of the tsunami arrived within an hour or two of low tide, particularly in the lower half of the North Island and northern half of the South Island. Considerable damage was done to houses, boats, shops, wharves, jetties, port facilities, and boatsheds, as well as threatening the lives of several people in Hawke's Bay, Gisborne and Banks Peninsula.

1947 Gisborne Earthquakes

In March 1947, a 120 km long stretch of coast, from Mahia Peninsula northwards, was struck by a tsunami, 30 minutes after a moderately felt earthquake. The earthquake was located about 50 km offshore from the coastline north of Gisborne and 10–15 km west of the Hikurangi Trough. Although described by some as severe and prolonged, the earthquake was not widely felt along the nearest coast and the shaking caused no damage. The maximum intensity of MMI 4 (on the Modified Mercalli Intensity scale) is considerably less than the expected intensity for the earthquake's moment magnitude M_W7.0–7.1 and surface wave magnitude M_S7.2, and was even somewhat low for its local magnitude of M_L5.9. This type of earthquake is called a tsunami earthquake. Tsunami earthquakes are characterised by a slow rupture pattern and produce tsunami of greater size than expected, given the earthquake magnitude (M_S).

The March 1947 tsunami was not only observed along the coastline from Mahia Peninsula to Tokomaru Bay (Figure 3.5), but also probably at Waitangi, and possibly at Tuapeka, in the Chatham Islands. The maximum run-up height of the March 1947 tsunami was ~10 m at a near-deserted beach about 20 km north of Gisborne (Figure 3.5). Here, the 16 m span wooden bridge on the main road near Pouawa was swept 800 m inland and all except one room of the only house nearby was destroyed, with the five occupants surviving. The Tatapōuri Hotel and other houses were damaged further south and near Mahia. Another tsunami earthquake (M_L5.6, M_S7.2, M_W6.9–7.1; Doser and Webb, 2003) in May 1947 in a similar source area to the March event produced a tsunami that again impacted the Gisborne region coastline. Estimated runups of up to 6 m occurred at Waihau Bay and up to 5 m at Tolaga Bay; minor damage was reported.

The tsunami earthquakes of March and May 1947 have been the subject of recent investigation by GNS Science (Bell et al., 2009; Wang et al., 2009). Bell et al. (2009) proposed a source model for the March 1947 event involving rupture on or near a subducted seamount located on the shallow part of the plate interface. This unusual situation produced an anomalously large tsunami because the physical presence of the seamount promoted shallow rupture (hence more deformation of the seafloor), the concave profile over the seamount focussed the tsunami waves toward a narrow stretch of coastline, and the slow rupture occurred at a similar speed to the tsunami wave propagation, resulting in water "piling-up" and amplifying the tsunami. Tsunami earthquakes similar to the 1947 events are a problem for public tsunami hazard awareness because the relatively low severity of ground shaking associated with such earthquakes may not alert people to the need to evacuate, yet such earthquakes can produce anomalously large tsunami with short travel-times, so self-evacuation is the best form of mitigation.

Further discussion of the 1947 earthquakes appears in Sections 4.2.1 and Section 5.3.1.2.

1947 Aleutian Island Earthquake

A tsunami generated by the 1946 M7.4 earthquake in the Aleutian Islands caused minor damage and 1–2 m run-ups over limited parts of the New Zealand coastline. This event is important, as it is the only distant earthquake under M_W8.5 to have had a significant effect in New Zealand. The 1946 Aleutian earthquake was a tsunami earthquake similar to, but much more distant than, the 1947 Gisborne earthquakes described above. In the near-source area of the Aleutian earthquake, tsunami runups of up to 42 m were recorded, and far-field effects were felt across the Pacific, including 159 deaths in Hawaii (Okal and Hébert, 2007; Okal et al., 2003). In New Zealand the greatest impact on the main islands was along the east coast of the northern North Island (north of Whangarei), with water heights above sea level at the time reaching 1.2 m and causing minor damage to a bridge at Tutukaka. Great Barrier Island, Tolaga Bay and Stewart Island were also affected, with inundation heights of about 1–1.2 m above sea level.

3.3 RECENT TSUNAMI EVENTS 2005–2011

In the period from 2005–2011 (since the 2005 report of Berryman) there have been four tsunami to have affected New Zealand shorelines. These were the July 15th, 2009, Dusky Sound tsunami, the September 29th, 2009, South Pacific tsunami, the February 27th, 2010, Chile tsunami and the March 11th, 2011, Tohoku (Japan) tsunami. None of these tsunami caused any significant damage in New Zealand, but the potential threat level was high and Civil Defence warnings were issued in all cases.

15th July, 2009, Dusky Sound tsunami

On July 15th, 2009, a M_W7.8 earthquake on the subduction interface beneath southern Fiordland created a tsunami that affected the near-field region of Dusky Sound (Figure 3.6) (Beavan et al., 2010a; Clark et al., 2011c; Prasetya et al., 2011). The earthquake ruptured an ~80 x 50 km^2 patch of the plate interface (Beavan et al., 2010a) and it was the largest earthquake in New Zealand since the 1931 Napier earthquake. It was only because it occurred in the remote and largely unpopulated area of Dusky Sound that there was not significant injury or damage caused by the earthquake and tsunami. The earthquake occurred at night (9:22 pm). The ensuing tsunami was recorded by eyewitnesses on boats within Dusky Sound, and recorded instrumentally by a DART buoy in the Tasman Sea and by tide gauges in New Zealand and Australia (Figure 3.6) (Prasetya et al., 2011). The largest instrumental record was 0.98 m peak-to-trough at Jackson Bay, south Westland, ~ 260 km from the epicentre (Figure 3.6).

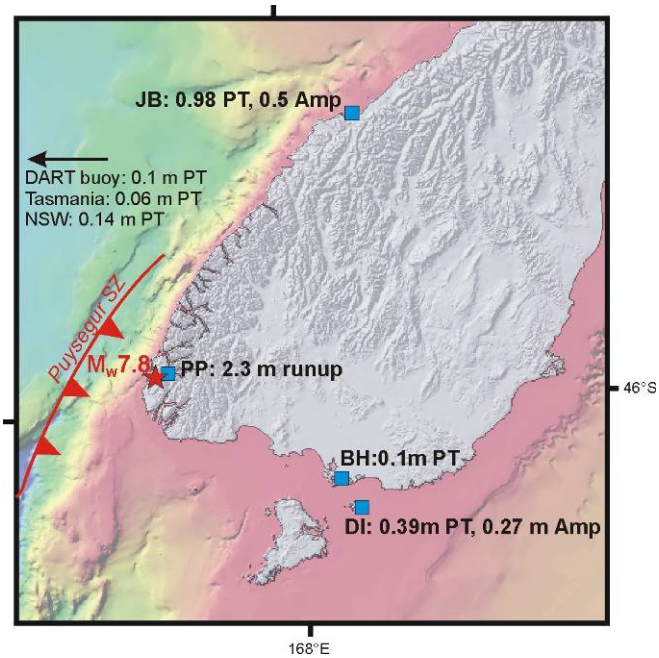

Figure 3.6 The location of the 2009 Dusky Sound earthquake and the locations where the tsunami was recorded (JB: Jackson Bay, PP: Passage Point, BH: Bluff Harbour, DI: Dog Island). PT: peak-to-trough tsunami measurement; Amp: tsunami amplitude.

Within Dusky Sound strong currents pulled on boat anchor lines, vessels hit the seafloor and turbulent water was observed, but no damage was caused. Post-tsunami field reconnaissance in Dusky Sound found very little disturbance to the shoreline, except in one location where the tsunami deposited shells and starfish 2.3 m above, and 8 m inland of the high tide line (Clark et al., 2011c). Tsunami modelling suggests the tsunami elevations in the near-field area would have been 0.5–2 m, with flow speeds of 3 m/sec (Prasetya et al., 2011). No tsunami damage was recorded, probably due to the absence of shoreline infrastructure and the coincidence of the tsunami with a low tide.

29th September, 2009, South Pacific tsunami

The September 2009 South Pacific tsunami was triggered by an earthquake doublet (two near-synchronous earthquakes) of M_W8.0 and M_W8.1 at the northern end of the Tonga Trench (Beavan et al., 2010b). Within 10–15 minutes of the earthquake, tsunami struck Samoa, American Samoa and the northern islands of Tonga, causing 189 fatalities and millions of dollars of damage.

The tsunami was first recorded in New Zealand 4.2 hours after the earthquake at Moturiki Island (Tauranga) and on the Chatham Islands (Figure 3.7; this analysis only includes sea-level gauge data from NIWA; the Geonet-operated tide gauge data has not yet been analysed for this event). Other parts of New Zealand took up to eight hours for the tsunami to arrive. The maximum peak-to-trough measurement was 0.89 m recorded at Kaingaroa on Chatham Island, the mainland of New Zealand generally saw peak-to-trough measurements of 0.3–0.6 m (Figure 3.7). The maximum height waves arrived 5–19 hours after the earthquake.

Within minutes of the earthquakes the Pacific Tsunami Warning Centre issued a tsunami warning for the wider South Pacific, including New Zealand.

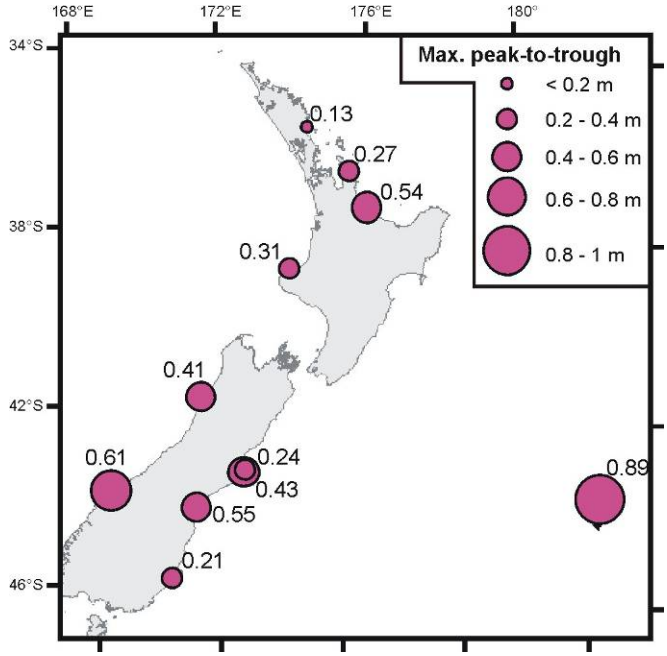

Figure 3.7 Maximum peak-to-trough measurements of the 29th September, 2009, South Pacific tsunami. This coverage only includes sea-level gauge data provided by NIWA (Rob Bell). The Geonet-operated tide gauges have not yet been analysed for this event.

27th February, 2010, Chile (Maule) tsunami

The 27th February, 2010, Chile tsunami (also called the Maule tsunami) was triggered by a M_W8.8 earthquake on the central Chile subduction zone. A ~500 km long segment of the plate interface slipped up to 15 m in the earthquake (Vigny et al., 2011). In Chile the death toll was 521, with 124 of those due to the tsunami. Hundreds of kilometres of the Chilean coast was affected by the tsunami, which had a maximum runup of 29 m (Fritz et al., in press). The eastern Pacific islands of the Juan Fernandez Archipelago and Easter Island also suffered tsunami damage.

In New Zealand the first tsunami waves were detected on tide gauges on the Chatham Islands 11.6 hours after the earthquake. The tsunami arrived on the east coast of the New Zealand mainland 13–14 hours after the earthquake and the first arrivals reached the west coast 16–18 hours after the earthquake. The maximum peak-to-trough values for the tsunami were 1.93 m (Lyttleton), 1.9 m (Chatham Islands, Figure 3.8) and 1.8 m (Gisborne, Figure 3.9). The maximum tsunami peak-to-trough heights arrived 20 hours after the earthquake at Lyttleton, 13.6 hours at the Chatham Islands, and 21.4 hours at Gisborne, so there was a time lag of 2 to 7 hours between the first tsunami waves and the largest tsunami waves. Gisborne had the highest amplitude measurement of 1.05 m.

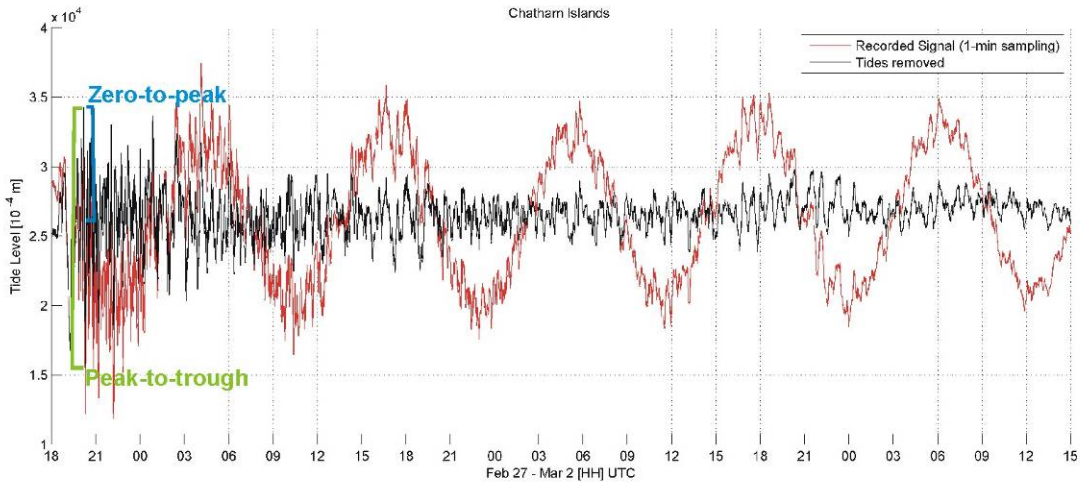

Figure 3.8 Illustration of the arrival of the 2010 Chile tsunami on the Chatham Islands tide gauge. The red line is the tide gauge reading and the black line shows fluctuations with the tidal effect removed. The green bar illustrates how the peak-to-trough value is obtained, and the blue line illustrates the amplitude measurement.

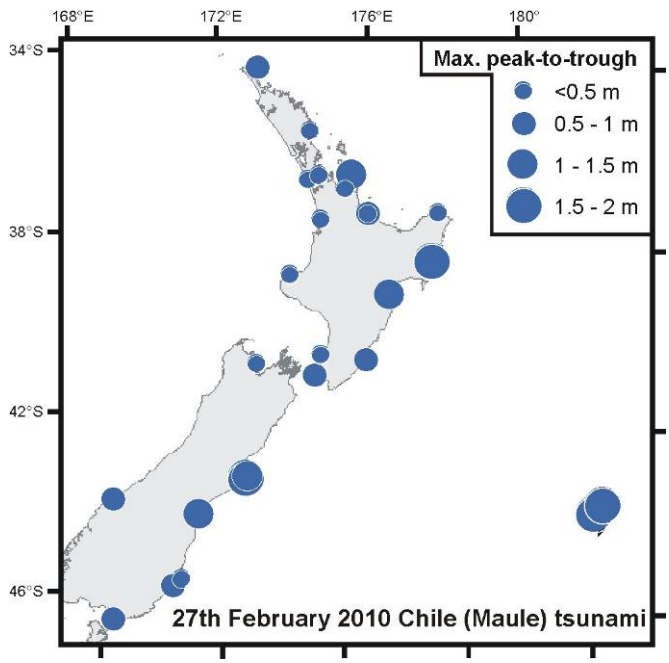

Figure 3.9 Maximum peak-to-trough measurements of the 27th February 2010 Chile (Maule) tsunami at tide gauges around New Zealand. Data processed by Paul Lehmann.

Immediately following the Maule earthquake, a Pacific-wide tsunami warning was issued by the Pacific Tsunami Warning Centre. The New Zealand Ministry of Civil Defence & Emergency Management issued a tsunami warning for New Zealand. There was sufficient delay between the tsunami generation and arrival that the tsunami warnings were well-publicised in New Zealand and many coastal activities on the Sunday morning were cancelled.

11th March, 2011, Japan (Tohoku) tsunami

The Tohoku tsunami of 11th March, 2011, was triggered by a M_W 9.0 earthquake at the Japan trench (Simons et al., 2011). In the near-field the tsunami was devastating, causing 15,700 deaths, with 4,600 people missing (as of 28th August, 2011, IOC-UNESCO Bulletin). The tsunami affected >2000 km of the Japan coastline; over 290 km of the coast had tsunami runups of >20 m, with a maximum runup of 39.7 m reported (Mori et al., 2011). The maximum instrumentally recorded amplitudes around New Zealand were up to about 1 m, and inundation of a small residential area occurred in Port Charles on the Coromandel Peninsula. The impacts of the tsunami on New Zealand are summarized in Borrero et al. (2012).

3.4 APPLICATION OF THE NEW ZEALAND HISTORICAL TSUNAMI RECORD

The written historical record covers only 165 years, and this is too short a time to reflect the full range of possible events that New Zealand might experience. Many large earthquakes have recurrence intervals in hundreds of years for the smaller events (M_W8.5) to several thousand years for the largest earthquakes (e.g. M_W9.5). Also, the historical record of small tsunami, or tsunami in the early years of our history, in sparsely populated places, or in remote places, such as Fiordland, is almost certainly incomplete. Nevertheless, New Zealand's historical tsunami database is one of the most comprehensive databases in the South Pacific.

The frequencies of occurrence for distant, regional and local source tsunami of specified run-up somewhere in New Zealand based on the historical record are only first estimates, and may severely under- or overestimate the hazard. The historical record contains no local volcanic events, no great (M>8) local or regional plate interface earthquakes, and large earthquakes have occurred on only a small proportion of a large number of local sources. To calibrate frequency relationship requires multiple events of each type.

For risk management, and to provide all the necessary information for appropriate response in a tsunami warning situation, the historical record is at best indicative. It is, however, very useful for understanding the behaviour of tsunami in New Zealand, for public education, and for calibrating and validating numerical models. Paleotsunami can be used to supplement the historic record and New Zealand's paleotsunami record will be described in the next section.

3.5 PALEOTSUNAMI RECORDS

3.5.1 Description of paleotsunami

Paleotsunami are tsunami that occurred prior to written records. The evidence for their occurrence typically comes from the sediments and debris that they deposited in the coastal zone (tsunami deposits), occasionally from the marks of erosion they left in the landscape, or from archaeological sites and oral traditions (see, e.g., Atwater, 1987; Nanayama et al., 2003). Studies of coastal sediments can be used to build up a record of paleotsunami that inundated coasts in the past. Such records extend the tsunami record much further back in time than the historical and instrumental record, thereby improving our knowledge of tsunami hazard. Tsunami deposits, in addition to providing evidence for the occurrence of past tsunami inundation, can also provide information about their sources, and their frequency and magnitude in the following ways:

Sources

- The aspect and length of coast over which a tsunami deposit is found can provide information about the direction and distance offshore of the source (and thereby whether it was a local, regional or distant event).
- The type of source can sometimes be inferred from co-existence of the tsunami deposit with physical evidence of deformation (e.g. subsidence and liquefaction features imply a local earthquake source).
- Correlation of the deposit with a known tsunami-causing event can be used to infer a source where high-resolution age control is available.

Frequency

- Where a long geological record of tsunami deposits exists, it is possible to estimate recurrence intervals for paleotsunami. This type of information is particularly important where no large tsunami have occurred in historical times, but where large events are represented in the geological record frequently enough to suggest they will occur again in the future.

Magnitude

- Sedimentary deposits are usually evidence of large paleotsunami because small tsunami are unlikely to leave obvious evidence of their occurrence in the geological record.
- The physical extent of tsunami deposits along and across coastal topography, as well as the height above sea level that deposits reach, provide minimum estimates for tsunami inundation distance and run-up height once any vertical tectonic movement is accounted for.

Although paleotsunami datasets have a unique contribution to make to tsunami hazard assessment, there are some major limitations that must be taken into account. For a start, paleotsunami datasets will always be incomplete because:

- Many paleotsunami are not represented in the geological record:
  - Not all tsunami leave a recognisable deposit.
  - Not all deposits are preserved for long periods of time.
- Many paleotsunami cannot be identified:
  - Not all deposits contain unique tsunami signatures.
  - Deposition is patchy, so evidence may be missing from a particular site.
  - Storm surge deposits may be misinterpreted as tsunami deposits and vice versa.

Despite the limitations of paleotsunami research, it has a vital role in identifying areas that have been impacted by tsunami. With detailed work, the source, magnitude and frequency of past tsunami can be elucidated. Paleotsunami research extends the record of events beyond the historical period, which is too short to capture the full range of events that can potentially affect the New Zealand coastline.

3.5.2 The New Zealand paleotsunami database

Paleotsunami research since the 2004 Indian Ocean tsunami has increased markedly, both internationally and in New Zealand. In New Zealand, paleotsunami have been identified at many places around the coastline as a result of targeted research by a few scientists. Identification of paleotsunami in New Zealand has provided evidence for the occurrence of past large events and has improved awareness of New Zealand's tsunami risk. Despite the recent increase in paleotsunami research, there is still a lack of coverage of key sites and little detail at many of the sites that have been studied. Paleotsunami research is time-consuming, so the focus of many studies has been on the initial identification of tsunami deposits. Additional work that is crucial for the assessment of tsunami source, frequency and magnitude, such as detailed mapping of the extent of the deposit, high-resolution age control, and investigation of multiple events at any one site, is yet to be carried out in many cases.

Recently a paleotsunami database[19] for New Zealand has been compiled by Goff (2008) and Goff et al. (2010c). This database describes 293 observations around the New Zealand coastline of likely-to-possible paleotsunami, which are related to between 35 and 40 paleotsunami (i.e., there are multiple observations that are attributed to the same event).

The New Zealand paleotsunami database contains a mixture of formally published research (peer-reviewed journal articles), non-formally published research (e.g. student theses, newsletters, reports, conference proceedings) and unpublished work (e.g. personal communications). A significant number of the database entries are based on the compilers' reinterpretation of published work which described deposits but did not specifically relate them to tsunami. These entries indicate further study is required to confirm or refute their interpretation as paleotsunami. Despite the variable quality of the source material and debate about interpreting paleotsunami deposits, the New Zealand paleotsunami database is a valuable resource for describing the distribution of features of potential-to-likely paleotsunami around the New Zealand coastline. Later in this section we will describe some recent and well-verified paleotsunami studies from around the New Zealand coastline.

Geographic distribution and validity of paleotsunami deposits

Figure 3.10 shows the distribution of sites with paleotsunami evidence around the New Zealand coast. This figure shows the sites based on the validity of the evidence: larger dots in warm colours show the sites with excellent evidence for paleotsunami, smaller dots in cooler colours show sites with less certain evidence. In general a wealth of paleotsunami evidence exists along the east coast of the North Island (with the exception of the East Cape region), in the Wellington region, along parts of the east coast of the South Island, and on the Chatham Islands. Paleotsunami evidence also exists along the west coast of New Zealand but is less abundant than east coast records. The spatial distribution of paleotsunami evidence is approximately consistent with the distribution of historical tsunami observations (compare Figure 3.10 with Figure 3.3). It is also consistent with the location of New Zealand's most active offshore faults (the Hikurangi margin, Cook Strait, Bay of Plenty) and with the direction of tsunami coming from Pacific Rim subduction zone sources.

[19] The Goff (2008) and Goff et al. (2010c) database includes information about historical events, but we exclude these from our description of the paleotsunami database because the Downes et al. (in prep) historical tsunami database (used in the previous sections) is a more comprehensive resource.

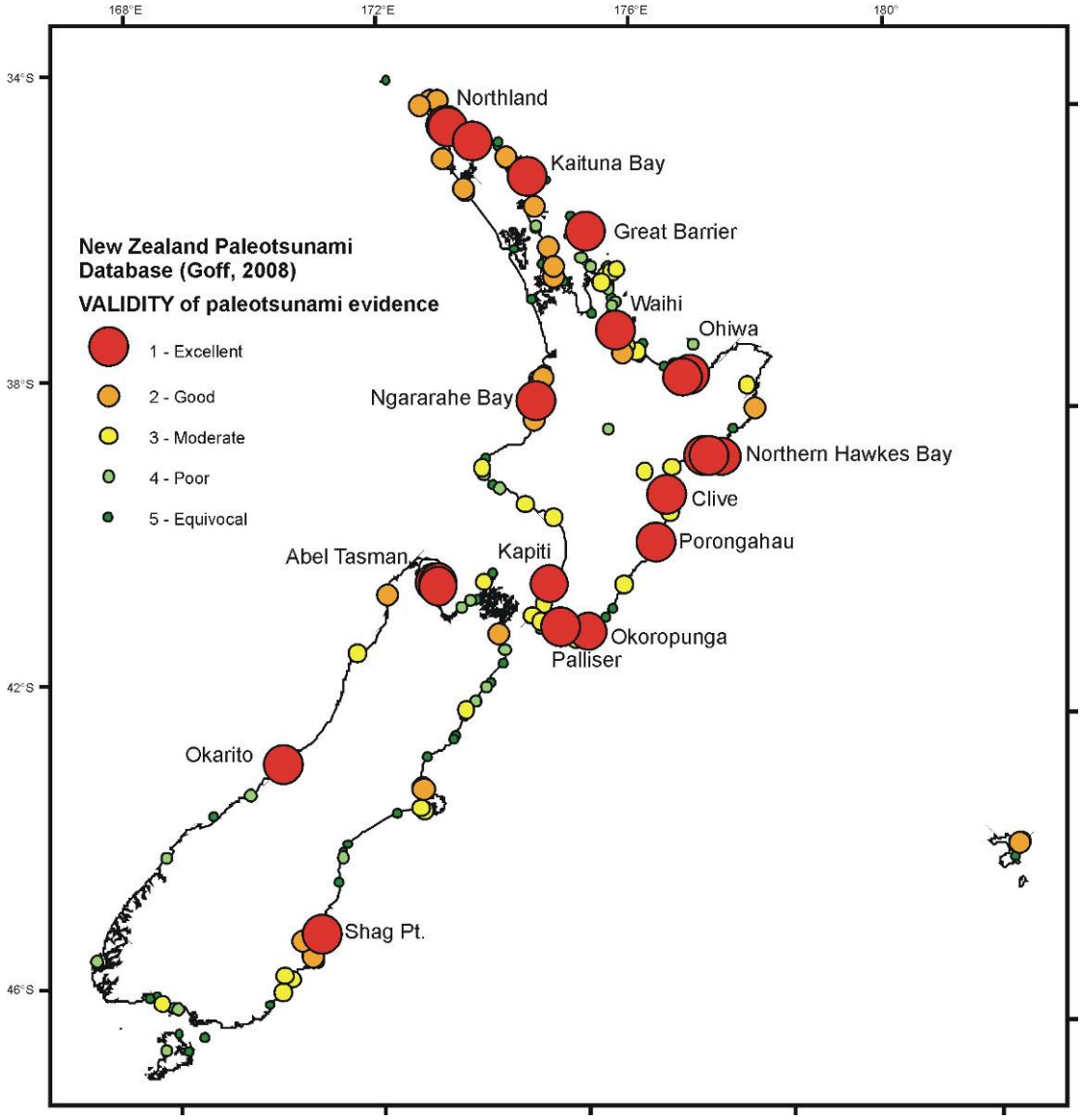

Figure 3.10 The distribution of paleotsunami evidence around the New Zealand coastline from the New Zealand paleotsunami database (Goff, 2008; Goff et al., 2010c). The symbols are graduated according to the validity of the data.

Ages of paleotsunami deposits

Ages of paleotsunami in the New Zealand paleotsunami database are shown in Figure 3.11 and Figure 3.12. Paleotsunami evidence is usually associated with an age range; sometimes relatively small (±50 years) but in most cases larger (>200 to 1000's of years). In Figure 3.11 and Figure 3.12 the midpoint of the age ranges plotted. Much evidence of paleotsunami (~160 entries in the database) is estimated to be related to tsunami that occurred between 1300AD and 1600AD (Figure 3.11). Tsunami within this age range are spread around the New Zealand coastline (Figure 3.12). However, much of this evidence probably relates to the same tsunami, particularly where the sites occur in proximity (Figure 3.12). In most cases the age estimate is a relative age and not based on absolute dating methods such as radiocarbon dating. In many instances, a deposit has been dated in one location then deposits nearby in a similar stratigraphic position are assumed to be of the same age. There are 52 entries in the database related to tsunami >2000 years old. The oldest estimated paleotsunami evidence is 2.51 Ma (Goff et al., 2012), and is inferred to be related to the Eltanin asteroid impact.

- The age distribution of the evidence for paleotsunami deposits in New Zealand raises some interesting questions. In general one would expect the evidence for paleotsunami to increase toward the present day because more recent events would leave fresher, more distinctive deposits/erosion scars, the deposits would be shallower (i.e., closer to the surface so more accessible for geological studies), and there would be less opportunity for the evidence to be reworked. The fact that paleotsunami evidence in New Zealand is most frequent at ~1500AD and then tapers off is unusual. Many well-studied paleotsunami deposits are reliably dated to this time period so it is likely there was a cluster of large tsunami in the 14th and 15th centuries. However, there may be some inflation of the frequency at this time through inaccurate correlations. This could occur when one deposit that is well-dated is used for correlation to a number of other deposits in the same region without independent verification of age.

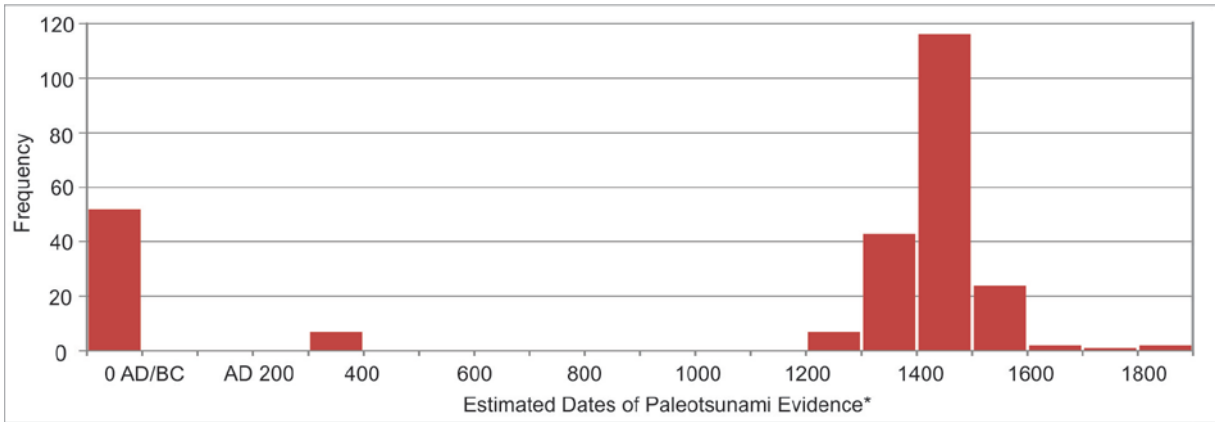

Figure 3.11 Estimated dates of paleotsunami deposits through time. Paleotsunami deposits have been binned into age ranges according to their midpoint age. Note that multiple records of paleotsunami deposits may relate to the same tsunami event. This plot excludes information from Māori oral records that have an age range estimate of AD 1250–1800.

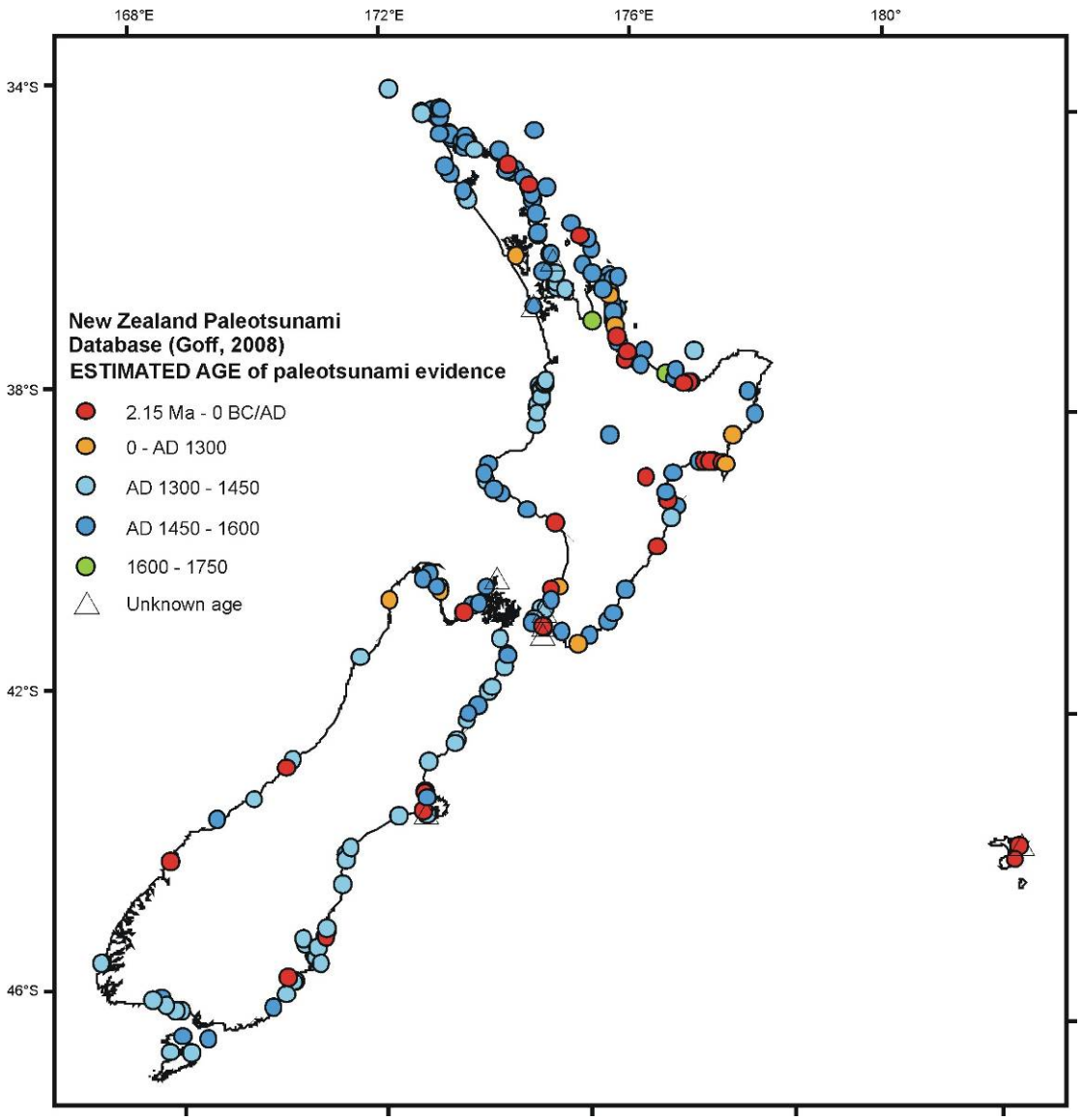

Figure 3.12 The distribution of paleotsunami evidence around the New Zealand coastline from the New Zealand paleotsunami database (Goff, 2008; Goff et al., 2010c). The symbols are coloured according to the estimated date of the paleotsunami.

Elevation of paleotsunami deposits

The present-day elevation of paleotsunami deposits can yield information about the minimum height of the tsunami. The elevation of discrete deposits or erosional features can be measured, and, once vertical tectonic movement is taken into account, the measurements can be used to estimate the minimum runup of the paleotsunami. The elevations of deposits in the New Zealand paleotsunami database are shown in Figure 3.13. The red to yellow dots show deposits above present-day mean sea level. The blue dots show sites where paleotsunami deposits have been found in cores. Many types of paleotsunami evidence do not have a measurable elevation (hollow squares, Figure 3.13); this evidence includes Māori oral records and secondary geomorphic changes such as sand dune remobilisation.

The highest inferred-paleotsunami deposits are 60–65 m and occur on the west coast of the Waikato region. While this is an alarmingly high elevation, the evidence consists of a pebble layer within sand dunes. This type of data is of debateable paleotsunami origin; it is often assigned a paleotsunami origin because few other explanations are satisfactory. It is however unsatisfactory to conclude proof of a paleotsunami origin through lack of alternative

explanations, but to date there has been little rigorous investigation of such pebble layers to understand their mechanism of deposition.

Most paleotsunami deposits are between 0–5 m above sea level. While this does not seem high, it should be remembered that the deposit elevation gives a minimum wave runup and the tsunami may have been many metres higher. Many of the most reliable indicators of paleotsunami have been found in core samples, e.g. Cochran et al. (2005); Goff et al. (2010b); Nichol et al. (2007b). The core samples usually come from back-barrier wetlands and extend to below mean sea level, so they are not a useful proxy for runup measurements (but they can reliably indicate minimum inundation distance).

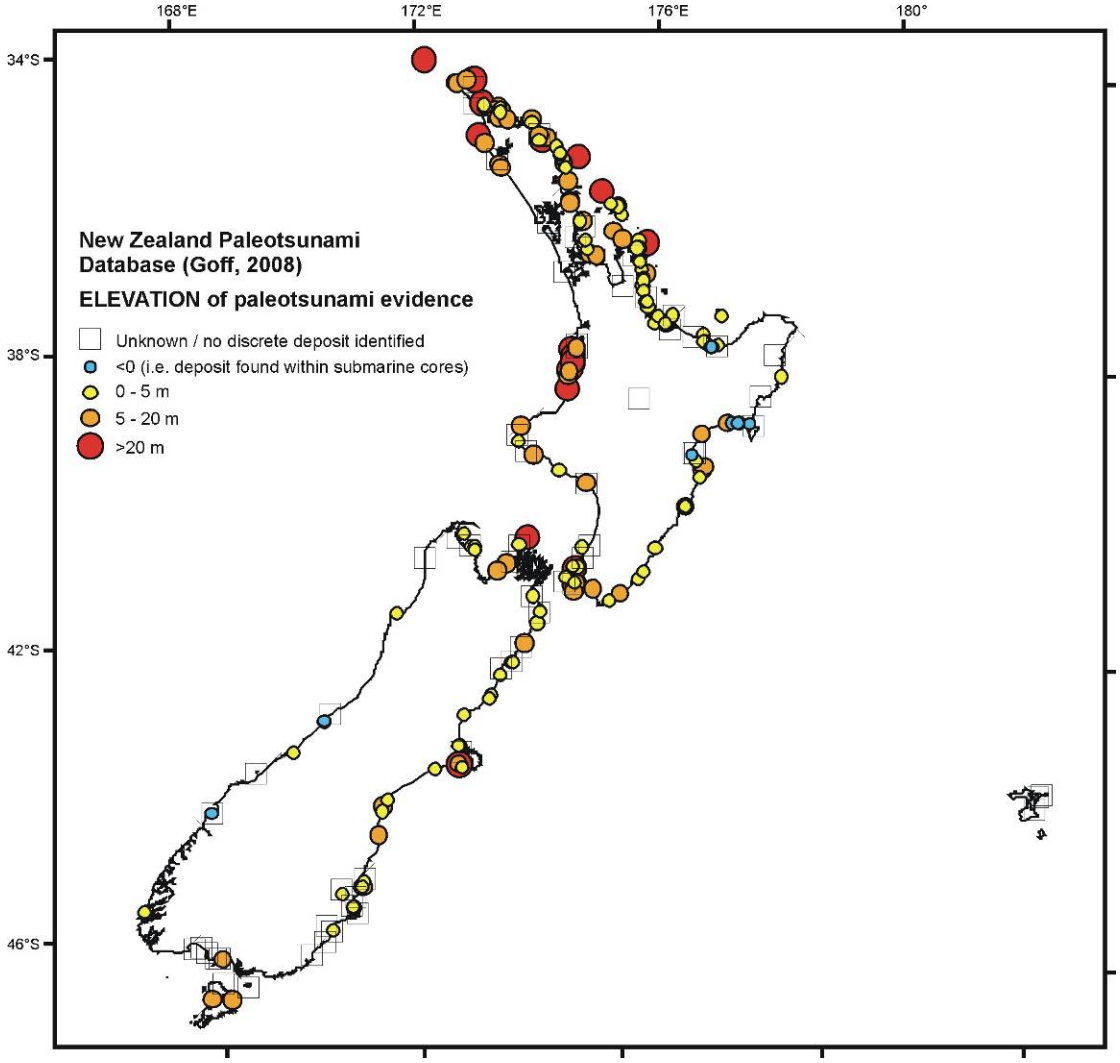

Figure 3.13 The distribution of paleotsunami evidence around the New Zealand coastline from the New Zealand paleotsunami database (Goff, 2008; Goff et al., 2009b). The symbols are coloured according to the elevation at which the paleotsunami evidence is found. Empty square boxes indicate evidence that lacks elevation data, for example Māori oral records, or evidence of secondary dune mobilisation.

Inferred sources of paleotsunami

Due to the nature of the evidence it is difficult to confidently identify the source of a paleotsunami. Hence, we treat all causes in the paleotsunami database as “inferred”. Techniques to identify the source of a tsunami include:

- Correlation to known historical earthquakes from other locations. For example, a paleotsunami deposit on the Chatham Islands has been correlated with a large earthquake in 1604 in South America (Goff et al., 2010a).
- Association with evidence of a paleoearthquake, volcanic eruption or landslide. For example, two paleotsunami sand layers found in wetland cores in northern Hawke’s Bay are inferred to be related to paleoearthquakes because they occur in association with a sudden (coseismic) subsidence event (Cochran et al., 2005). Correlation of paleotsunami deposits in Abel Tasman National Park and Kapiti Island to the c. AD 200 Taupo eruption has been suggested by Lowe and de Lange (2000).
- Extensive mapping of a paleotsunami deposit such that various source models can be tested. An example of this has been attempted by Goff et al. (2010b), who compiled evidence for three paleotsunami to have impacted the northern half of the North Island. They inferred that the distribution of two paleotsunami deposits matched a Tonga-Kermadec trench earthquake source, and one potentially matched an earthquake source in the Fiji region or a large volcanic eruption in the New Hebrides island group. This technique requires extensive mapping and accurate dating which has rarely been carried out.

Figure 3.14 shows the inferred causes of paleotsunami evidence around the New Zealand coastline. Most paleotsunami evidence is related to earthquake sources (64% of entries in the database). There are smaller numbers of paleotsunami related to land or submarine landslides and volcanic eruptions, and one inferred asteroid impact (at 2.51 Ma) and many examples of paleotsunami evidence with no inferred cause.

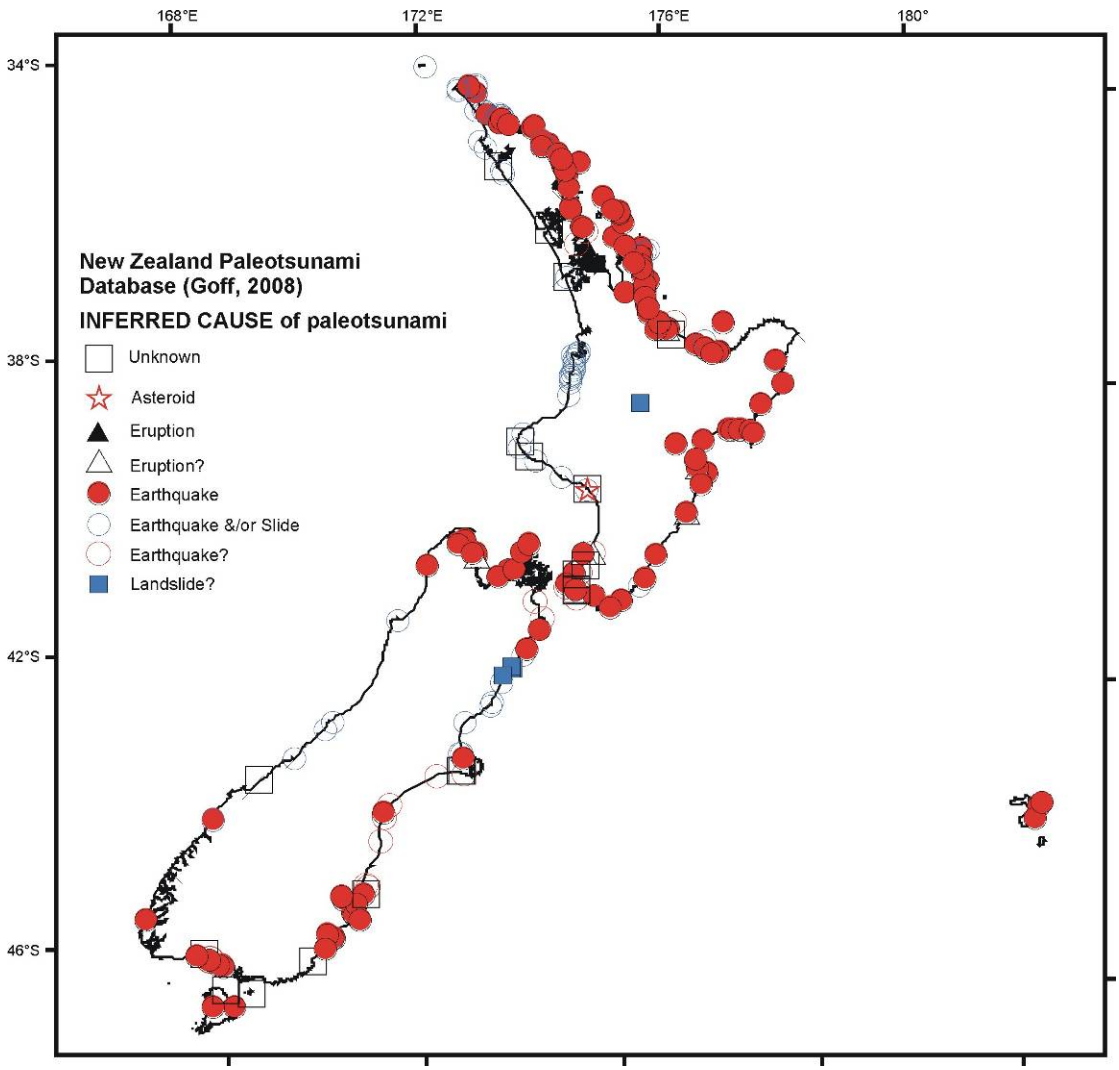

Figure 3.14 The distribution of paleotsunami evidence around the New Zealand coastline from the New Zealand paleotsunami database (Goff, 2008; Goff et al., 2009b). The symbols indicate the inferred cause of the tsunami.

3.5.3 Recent paleotsunami research 2005–2011

Since the 2005 review of tsunami hazard and risk in New Zealand (Berryman, 2005), the amount of paleotsunami research in New Zealand has increased in line with a global increase following the 2004 Indian Ocean tsunami. Techniques have improved due to better knowledge of modern and prehistorical tsunami deposits. In this section we review some of the recently published research (Figure 3.15).

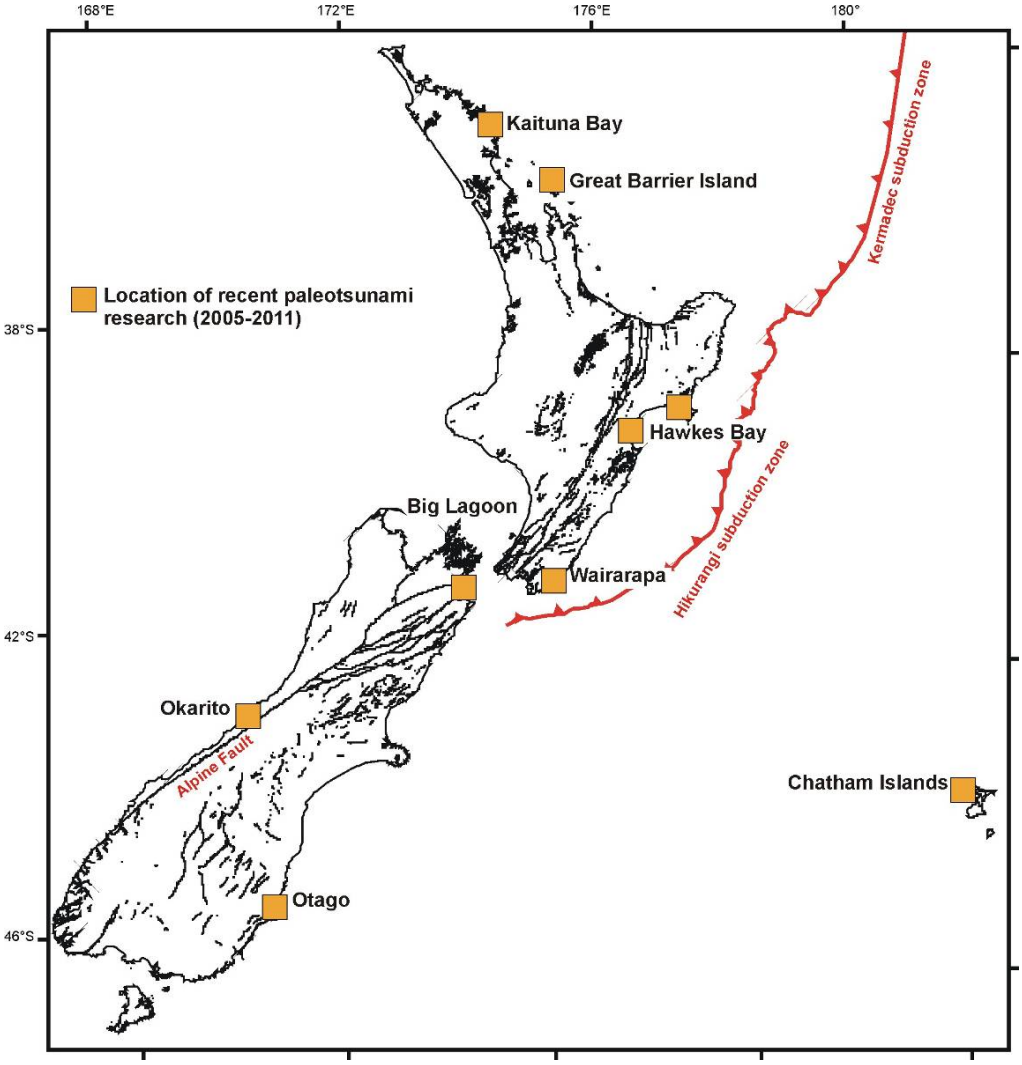

Figure 3.15 The locations of recent paleotsunami studies in New Zealand from 2005–2011. The black lines onshore represent the active faults of New Zealand. The red line shows the Hikurangi-Kermadec trench.

Northern Hawke's Bay: Studies by Cochran et al. (2006), and Cochran et al. (2005) have found evidence for two paleotsunami associated with coseismic subsidence events. The tsunami deposits were found in cores from coastal wetlands, and the deposits were characterised by anomalously coarse grain size, chaotically mixed sediment, sharp lower contacts and fossils derived from seaward of the site. Both tsunami deposits were associated with a change in the wetland environment due to a large earthquake. A significant amount of radiocarbon data was obtained and the paleotsunami were dated at c. 7100 and 5550 years BP. By tracing out the extent of earthquake-related deformation, it was inferred the most likely source of the earthquake was a large event (~M7.9) on the Hikurangi margin plate interface. The Cochran et al. (2006) study is significant because it is the first to provide good evidence that the Hikurangi subduction zone has produced large earthquakes and tsunami in the past. Work is continuing on this project at a new location in southern Hawkes Bay which also shows evidence of paleotsunami deposits.

Okarito Lagoon, Westland: Nichol et al. (2007a) obtained sediment cores from Okarito Lagoon on the west coast of the South Island that suggest occurrence of a paleotsunami c. AD 1320–1495. The evidence for the paleotsunami consists of coarser-grained sediment overlying a buried soil and it is associated with an increase in lagoon salinity. Some key diagnostic criteria (e.g. evidence of transport from a seaward environment) are absent from the inferred paleotsunami deposit, and there are several other scenarios that could explain

an increase in lagoon salinity. The age of the deposit overlaps with the timing of a large earthquake on the Alpine Fault. Therefore Nichol et al. (2007a) infer the cause of the subsidence and tsunami to be an Alpine Fault earthquake.

Great Barrier Island: A sediment core from a back-barrier wetland at Harataonga Bay, Great Barrier Island, contains evidence of a paleotsunami at c. 3000 years BP (Nichol et al., 2007b). The paleotsunami deposit is characterised by its coarser grain size and unusual magnetic properties (which suggest the sand came from a seaward source). Nearby, earlier work had identified a gravel layer within sand dunes that had also been inferred to be a paleotsunami deposit (Nichol et al., 2003). While neither deposit in isolation is unequivocal evidence for paleotsunami, their proximity does suggest a common source, thus making paleotsunami a more likely cause. The significance of the Great Barrier Island studies is that the gravel deposits reach up to 14 m above sea level, and the wetland at Harataonga Bay has a stationary 15 m foredune, implying the paleotsunami had a runup of >15 m. Nichol et al. (2003) speculate the source of the tsunami could have been an earthquake along the Hikurangi subduction zone or a volcanic eruption along the Kermadec arc. The heights are consistent with modelling of an earthquake on the Tonga-Kermadec subduction zone (Power et al., 2012; Lane et al., 2012).

Otago coast: The geomorphology of Blueskin Bay and Long Beach, north of Dunedin, was studied by Goff et al. (2009a). Goff et al. (2009a) identified coastal landforms consistent with formation due to erosion and scouring by tsunami (e.g. scour fans and sand dune breaches). At Long Beach, a sand layer was also identified and tentatively assigned a tsunami origin, though it was not characterised in sufficient detail to be considered a strong case for a paleotsunami deposit. Correlations to dated Māori artefacts suggest the inferred paleotsunami occurred sometime in the 14th to early 15th century; they suggest a Puyseygur subduction zone earthquake (Goff et al., 2009a).

Chatham Islands: The sedimentary evidence for the AD 1868 tsunami (see section 3.1) on the Chatham Islands was investigated by Goff et al. (2010a). At the same location where 1868 sediments were identified, an older, thicker sandsheet was identified. This sandsheet contained many indicators of tsunami deposition (e.g. erosional base, fining upward, rip-up clasts, unusual paleoecology). The changing pollen assemblages placed some age constraints and Goff et al. (2010a) correlated the event to an AD 1604 earthquake in Peru. Interestingly, a study at another location on the Chathams Island by Nichol et al. (2010) found evidence of the AD 1868 tsunami but no others, even though they had a sedimentary core dating back to 43,000 years BP.

Kaituna Bay, Northland: Cores from a wetland at Kaituna Bay contain evidence for three paleotsunami in the past 8000 years (Goff et al., 2010b). The paleotsunami deposits were well-characterised using multiple techniques (e.g. grain size, geochemistry, microfossils) but relatively poorly dated. Goff et al. (2010b) correlated the paleotsunami deposits at Kaituna Bay to other inferred paleotsunami deposits of a similar age around the North Island and used the spatial distribution of the deposits to infer the earthquake source. The events at c. 6500 and 2800 years BP were inferred to be from a Tonga-Kermadec trench earthquake source. The event at c. 1450AD had a wider distribution than the earlier events and was also correlated to inferred paleotsunami deposits in the northern west coast of the North Island. Goff et al. (2010b) suggested a volcanic eruption in the New Hebrides island group may have been the source of that event. The dating of older paleotsunami deposits at Kaituna Bay (and those around the North Island that they were correlated to) has large uncertainties (up to ± 3000 years). Further radiocarbon dating (with lower uncertainties) is necessary to provide

confidence that the regionally-distributed paleotsunami deposits were from a single (and very large) event.

Wairarapa coast: The east coast of the Wairarapa region from Cape Palliser to Cape Turnagain displays a sequence of uplifted Holocene marine terraces. In a study of the ages of the marine terraces (which indicate the timing of past large earthquakes along this coast) Berryman et al. (2011) found evidence of paleotsunami. Thirty-five radiocarbon ages were collected from the marine terraces and approximately 20% of these were anomalously young for their elevation. The anomalously young samples on high terraces often coincided with the age at which lower terraces had been uplifted. It was suggested by Berryman et al. (2011) that the young samples represent paleotsunami deposits that were emplaced by tsunami triggered by the same earthquakes that uplifted younger terraces. The research into the inferred paleotsunami deposits has not yet been comprehensive enough to be confident of their origin, but the Berryman et al. (2011) study corroborates previous paleotsunami studies along the Wairarapa coast (e.g. Goff et al., 2004).

Big Lagoon, Blenheim: The Big Lagoon area near Blenheim is the subject of an ongoing study examining evidence for earthquake-related subsidence. Multiple cores have been taken from the lagoon margins and these cores show evidence of paleotsunami deposits. Clark et al. (2011a) identified a sand layer at 3.1 m depth with anomalous microfossil assemblages and a chaotic, poorly sorted sedimentology. It was not well-dated (between 2,000–7,000 years) but it will be the subject of further studies. More recently Clark et al. (unpublished data) have identified a sand layer in Big Lagoon containing evidence for landward-transported marine microfossil assemblages, dated at c. 800 years BP. Like the northern Hawke's Bay study sites of Cochran et al. (2005, 2006) and the Wairarapa coast (Berryman et al., 2011, Goff et al., 2004), the Big Lagoon site is significant because it may hold evidence of paleotsunami related to large subduction earthquakes along the Hikurangi margin (Figure 3.15).

3.5.4 Summary of paleotsunami in New Zealand

The New Zealand paleotsunami database (Goff, 2008; Goff et al., 2010) is a valuable and comprehensive resource documenting evidence for paleotsunami in New Zealand. It is a vast improvement on the state of paleotsunami knowledge before 2004. The distribution of paleotsunami evidence around the New Zealand coast resembles the distribution of historical tsunami, and as such, it highlights the areas of the coastline most vulnerable to tsunami hazard. The age of the paleotsunami deposits requires significant improvement; most entries in the database are poorly dated or not dated at all. The apparent increase in paleotsunami around AD 1500 is unusual and deserves further investigation. If it represents a real clustering of tsunami events the cause needs to be understood. The elevation of the paleotsunami deposits can be used to estimate a minimum runup height for paleotsunami. However, some of the best evidence for paleotsunami comes from submarine cores, while some of the highest elevations are from pebble layers which have a tenuous association to paleotsunami. There are some examples where sufficient research has been undertaken to determine the source of the tsunami that deposited a paleotsunami deposit or left other evidence (e.g. erosion/oral record). However, for most entries in the database the tsunami source is only inferred, hence the sources are not reliable.

Age and runup estimates in the New Zealand paleotsunami database are still too scattered and uncertain to give accurate magnitude-frequency relationships. However, the paleotsunami database is a valuable resource for assessing tsunami hazard in New Zealand because our historical record is far too short to capture the range of tsunami that could potentially affect New Zealand shores. As paleotsunami research continues to increase beyond “reconnaissance-level” studies and into detailed multi-proxy, multi-site investigations, the reliability and quality of the database will improve substantially.

Recent paleotsunami studies in New Zealand have covered a wide range of sites, from areas of low seismicity (Otago, Northland), areas of high seismicity along the Hikurangi margin (Hawkes Bay, Wairarapa, Blenheim), areas of high exposure to South American tsunami (Chatham Islands) and regions of high onshore seismicity but with relatively few offshore tsunami sources (Westland). The studies are becoming more rigorous through the use of multi-proxy techniques and an increasing knowledge of the signatures of tsunami deposition and erosion. Increasingly, sufficient data is being gathered so that the tsunami source can be identified. A future challenge will be to bring our knowledge of paleotsunami up to a standard where source models can be reliably calibrated using the inland extent and elevation of paleotsunami deposits, thus ensuring inundation models and tsunami evacuation zones are dependable.

3.6 REFERENCES

Atwater, B.F. (1987). Evidence for great Holocene earthquakes along the outer coast of Washington State: *Science*, v. 236, p. 942-944.

Beavan, J., Samsonov, S., Denys, P., Sutherland, R., Palmer, N., and Denham, M. (2010a). Oblique slip on the Puysegur subduction interface in the July 2009 MW 7.8 Dusky Sound earthquake from GPS and InSAR observations: implications for the tectonics of southwestern New Zealand: *Geophysical Journal International*, p. doi: 10.1111/j.1365-1246X.2010.04798.x.

Beavan, J., Wang, X., Holden, C., Wilson, K., Power, W., Prasetya, G., Bevis, M., and Kautoke, R. (2010b). Near-simultaneous great earthquakes at Tongan megathrust and outer rise in September 2009: *Nature*, v. 466, p. 959-963, doi:910.1038/nature09292.

Bell, R., Wang, X., Power, W., Downes, G., and Holden, C. (2009). Hikurangi Margin tsunami earthquake generated by slip over a subducted seamount: Barrell, D.J.A.; Tulloch, A.J. (eds) Geological Society of New Zealand & New Zealand Geophysical Society Joint Annual Conference, Oamaru, 23-27 November 2009 : programme and abstracts. Wellington: Geological Society of New Zealand, v. Geological Society of New Zealand miscellaneous publication 128A., p. 18.

Berryman, K., Ota, Y., Miyauchi, T., Hull, A., Clark, K., Ishibashi, K., Iso, N., and Litchfield, N. (2011). Holocene Paleoseismic History of Upper-Plate Faults in the Southern Hikurangi Subduction Margin, New Zealand, deduced from Marine Terrace Records. *Bulletin of the Seismological Society of America*, v. 101, no. 5, p. 2064-2087.

Berryman, K. (2005). Review of tsunami hazard and risk in New Zealand: MCDEM Report No. 2005/104. Wellington. 139 pp.

Borrero, J., Bell, R., Csato, C., DeLange, W., Greer, D., Goring, D., Pickett, V. and Power, W. (2012). Observations, Effects and Real Time Assessment of the March 11, 2011 Tohoku-oki Tsunami in New Zealand, *Pure and Applied Geophysics*, DOI: 10.1007/s00024-012-0492-6.

Clark, K., Hayward, B., Cochran, U., Grenfell, H. R., Hemphill-Haley, E., Mildenhall, D., Hemphill-Haley, M., and Wallace, L. (2011a). Investigating subduction earthquake geology along the southern Hikurangi margin using paleoenvironmental histories of intertidal inlets: *New Zealand Journal of Geology and Geophysics*, v. 54, no. 3, p. 255-271.

Clark, K. J., Hancox, G. T., Forsyth, P. J., Pomdard, N., Power, W., Stong, D., and Lukovic, B. (2011b). Identification of potential tsunami and seiche sources, their size and distribution on lakes Te Anau and Manapouri: GNS Science consultancy report 2011/196. 71 p.

Clark, K. J., Johnson, P. J., Turnbull, I., and Litchfield, N. (2011c). The 2009 Mw 7.8 earthquake on the Puysegur subduction zone produced minimal geological effects around Dusky Sound, New Zealand: *New Zealand Journal of Geology and Geophysics*, v. 54, no. 2, p. 237-247.

Cochran, U., Berryman, K., Mildenhall, D., Hayward, B., Southall, K., Hollis, C., Barker, P., Wallace, L., Alloway, B., and Wilson, K. (2006). Paleoecological insights into subduction zone earthquake occurrence, eastern North Island, New Zealand.: *Geological Society of America Bulletin*, v. 118, no. 9/10, p. 1051-1074.

Cochran, U.A., Berryman, K.R., Mildenhall, D.C., Hayward, B.W., Southall, K., and Hollis, C.J. (2005). Towards a record of Holocene tsunami and storms for Northern Hawke's Bay, New Zealand: *New Zealand Journal of Geology and Geophysics*, v. 48, p. 507-515.

Doser, D.I., and Webb, T. (2003). Source parameters of large historical (1917–1961) earthquakes, North Island, New Zealand, *Geophys. J. Int.*, 152, 795–832.

Downes, G., Cochran, U., Wallace, L., Reyners, M., Berryman, K., Walters, R., Callaghan, F., Barnes, P., and Bell, R. (2005). EQC Project03/490 - Understanding local source tsunami: 1820s Southland tsunami: Institute of Geological and Nuclear Sciences Client Report 2005/153, p. 92.

Fritz, H., Petroff, C., Catalán, P., Cienfuegos, R., Winckler, P., Kalligeris, N., Weiss, R., Barrientos, S., Meneses, G., Valderas-Bermejo, C., Ebeling, C., Papadopoulos, A., Contreras, M., Almar, R., Dominguez, J., and Synolakis, C. (in press). Field Survey of the 27 February 2010 Chile Tsunami: *Pure and Applied Geophysics*, p. 1-22.

Goff, J.R., Chagué-Goff, C., Archer, M., Dominey-Howes, D. and Turney, C. (2012). The Eltanin asteroid impact: possible South Pacific palaeomegatsunami footprint and potential implications for the Pliocene–Pleistocene transition. *Journal of Quaternary Science*, v. 27, p. 660-670.DOI: 10.1002/jqs.2571

Goff, J., Nichol, S., Chagué-Goff, C., Horrocks, M., McFadgen, B., and Cisternas, M. (2010a). Predecessor to New Zealand's largest historic trans-South Pacific tsunami of 1868AD: *Marine Geology*, v. 275, no. 1-4, p. 155-165.

Goff, J., Pearce, S., Nichol, S. L., Chagué-Goff, C., Horrocks, M., and Strotz, L. (2010b). Multi-proxy records of regionally-sourced tsunamis, New Zealand: *Geomorphology*, v. 118, no. 3-4, p. 369-382.

Goff, J.R. (2008). The New Zealand Palaeotsunami Database: NIWA Technical Report, No. 131, 24 p.

Goff, J.R., Lane, E., and Arnold, J. (2009a). The tsunami geomorphology of coastal dunes: *Natural Hazards and Earth System Sciences*, v. 9, p. 847-854.

Goff, J.R., McFadgen, B.G., and Chagué-Goff, C. (2004). Sedimentary differences between the 2002 Easter Storm and the 15th-century Okoropunga tsunami, southeastern North Island, New Zealand.: *Marine Geology*, v. 204, p. 235-250.

Goff, J.R., Nichol, S.L., and Kennedy, D. (2010c). Development of a palaeotsunami database for New Zealand: *Natural Hazards*, 54, p. 193-208. DOI 10.1007/s11069-009-9461-5

Hayward, B.W., (1974). Notes on orientation of ventifacts in a coastal reg, Kawerua: *Tane*, v. 20, p. 152-155.

Integrated Tsunami Database for the World Ocean: http://tsun.sscc.ru/WinITDB.htm

Lane, E.M., Gillibrand, P.A., Wang, X., and Power, W. (2012). A Probabilistic Tsunami Hazard Study of the Auckland Region, Part II: Inundation Modelling and Hazard Assessment: *Pure and Applied Geophysics*, p. 1-12.

Lowe, D.J., and de Lange, W.P. (2000). Volcano-meteorological tsunamis, thec. AD 200 Taupo eruption (New Zealand) and the possibility of a global tsunami: *The Holocene*, v. 10, no. 3, p. 401-407.

Mori, N.,T., Takahashi, T. Yasuda, and Yanagisawa, H. (2011)., Survey of 2011 Tohoku earthquake tsunami inundation and run-up, *Geophys. Res. Lett.*, 38, L00G14, doi:10.1029/2011GL049210.

Nanayama, F., Satake, K., Furukawa, R., Shimokawa, K., Atwater, B. F., Shigeno, K., and Yamaki, S., 2003, Unusually large earthquakes inferred from tsunami deposits along the Kuril trench: *Nature*, v. 424, p. 660-663.

Nichol, S.L., Chagué-Goff, C., Goff, J. R., Horrocks, M., McFadgen, B.G., and Strotz, L.C. (2010). Geomorphology and accommodation space as limiting factors on tsunami deposition: Chatham Island, southwest Pacific Ocean: *Sedimentary Geology*, v. 229, no. 1-2, p. 41-52.

Nichol, S.L., Goff, J.R., Devoy, R.J.N., Chague-Goff, C., Hayward, B.W., and James, I. (2007a). Lagoon subsidence and tsunami on the West Coast of New Zealand: *Sedimentary Geology*, v. 200, p. 248-262.

Nichol, S.L., Lian, O.B., and Carter, C.H. (2003). Sheet-gravel evidence for a late Holocene tsunami run-up on beach dunes, Great Barrier Island, New Zealand: *Sedimentary Geology*, v. 155, no. 1-2, p. 129-145.

Nichol, S.L., Lian, O.B., Horrocks, M., and Goff, J.R. (2007b). Holocene record of gradual, catastrpohic, and human-influenced sedimentation from a backbarrier wetland, northern New Zealand: *Journal of Coastal Research*, v. 23, no. 3, p. 605-617.

Okal, E.A., and Hébert, H. (2007). Far-field simulation of the 1946 Aleutian tsunami: *Geophysical Journal International*, v. 169, no. 3, p. 1229-1238.

Okal, E.A., Plafker, G., Synolakis, C.E., and Borrero, J.C. (2003). Near-Field Survey of the 1946 Aleutian Tsunami on Unimak and Sanak Islands: *Bulletin of the Seismological Society of America*, v. 93, no. 3, p. 1226-1234.

Power, W., Wang, X., Lane, E., and Gillibrand, P. (2012). A Probabilistic Tsunami Hazard Study of the Auckland Region, Part I: Propagation Modelling and Tsunami Hazard Assessment at the Shoreline: *Pure and Applied Geophysics*, p. 1-14.

Power, W., Downes, G., McSaveney, M., Beavan, J., and Hancox, G. (2005). The Fiordland Earthquake and Tsunami, New Zealand, 21 August 2003: Tsunamis: *Advances in Natural and Technological Hazards Research*, v. 23, p. 31-42, DOI: 10.1007/1001-4020-3331-1001_1002

Prasetya, G., Beavan, J., Wang, X., Reyners, M., Power, W., Wilson, K., and Lukovic, B. (2011). Evaluation of the 15 July 2009 Fiordland, New Zealand Tsunami in the Source Region: *Pure and Applied Geophysics*, v. DOI: 10.1007/s00024-011-0282-6.

Simons, M., Minson, S.E., Sladen, A., Ortega, F., Jiang, J., Owen, S.E., Meng, L., Ampuero, J.-P., Wei, S., Chu, R., Helmberger, D.V., Kanamori, H., Hetland, E., Moore, A.W., and Webb, F.H.,(2011). The 2011 Magnitude 9.0 Tohoku-Oki Earthquake: Mosaicking the Megathrust from Seconds to Centuries: *Science*, v. 332, no. 6036, p. 1421-1425.

Vigny, C., Socquet, A., Peyrat, S., Ruegg, J.-C., Métois, M., Madariaga, R., Morvan, S., Lancieri, M., Lacassin, R., Campos, J., Carrizo, D., Bejar-Pizarro, M., Barrientos, S., Armijo, R., Aranda, C., Valderas-Bermejo, M.-C., Ortega, I., Bondoux, F., Baize, S., Lyon-Caen, H., Pavez, A., Vilotte, J. P., Bevis, M., Brooks, B., Smalley, R., Parra, H., Baez, J.-C., Blanco, M., Cimbaro, S., and Kendrick, E. (2011). The 2010 Mw 8.8 Maule Megathrust Earthquake of Central Chile, Monitored by GPS: *Science*, v. 332, no. 6036, p. 1417-1421.

Wang, X., Power, W., Bell, R., Downes, G., and Holden, C. (2009). Slow rupture of the March 1947 Gisborne earthquake suggested by tsunami modelling.: Barrell, D.J.A.; Tulloch, A.J. (eds) Geological Society of New Zealand & New Zealand Geophysical Society Joint Annual Conference, Oamaru, 23-27 November 2009 : programme and abstracts. Geological Society of New Zealand miscellaneous publication 128A., p. 221.

4.0 TSUNAMI MODELLING

Tsunami modelling usually uses a set of mathematical formulae that describe the physical characteristics of tsunami, called a tsunami model, to evaluate and predict the evolution of tsunami waves and their coastal impact. Tsunami models can be used to estimate the probable arrival times of tsunami, their amplitudes, inundation ranges, flow depths and/or current speeds. There are two main types of tsunami models: numerical models (i.e., computer-derived models) and empirical models. Numerical models (i.e., computer-derived simulation packages) use a grid system for the area of interest that contains information such as bathymetry, topography and surface roughness. Using numerical techniques, the numerical models solve the mathematical equations governing the physical process of tsunami wave evolution at each point in the grid system, passing information between surrounding grids. Therefore, a numerical model can incorporate complicated geographic variations in bathymetry, topography and land uses, and can simulate different aspects of tsunami, including their variations in wave amplitude, current speed and inundation depth.

In contrast, empirical models employ statistical relationships, usually calibrated using field observations, to evaluate tsunami properties. It is difficult to incorporate both the changing nature of tsunami waves as they travel, as well as topographical and bathymetrical complexity, in empirical models, but empirical models are very useful for rapid evaluation, particularly when detailed source information and/or high-resolution bathymetric and topographical data are not available. This section provides an overview of current techniques for modelling tsunami, and summarizes tsunami modelling results and what has been learnt from them that is applicable to the New Zealand region.

4.1 NUMERICAL MODELS

Numerical models are used to evaluate and predict the physical characteristics of tsunami. They play an important role for tsunami hazard mitigation in determining arrival times, tsunami heights, current velocities and inundation ranges in a tsunami event, and are especially useful for preparing maps showing inundation and threat levels for potential events along those coastlines vulnerable to tsunami flooding.

Numerical modelling of tsunami allows us to estimate the effects of events which may occur, and to evaluate our understanding of past tsunami. It usually involves three stages:

- Source modelling, in which the generation of the tsunami, either by earthquakes, landslides, volcanic eruptions or bolide impact, is simulated.
- Propagation modelling, in which the dispersal of the tsunami waves around the ocean, sea, or lake is simulated.
- Inundation modelling, in which the water flow over dry land is simulated.

Due to the nature of tsunami evolution, different scales are inevitably involved in tsunami simulations, for example propagation across oceans involves large-scale modelling and land inundation fine-scale modelling. Consequently, tsunami models often have the capability to deal with tsunami evolution at one or more scales.

The devastating 2004 Indian Ocean (Sumatra) tsunami spurred an increase in the development of numerical models. The latest tsunami models simulate tsunami generation, propagation and inundation together, overcoming the difficulty of abrupt changes in

conditions at the shore, which is the most dynamic and complex phase of a tsunami. Among others, COMCOT (Cornell University, USA; GNS Science, New Zealand), TSUNAMI-N1/2 (Tohoku University, Japan) and MOST (National Center for Tsunami Research, USA) have demonstrated their capability for the investigation of the three stages of tsunami evolution—generation, propagation and inundation.

Most computer-derived tsunami models, including those aforementioned, were developed by numerically solving Shallow Water Equations (Pedlosky, 1979; Imamura et al., 1988; Vreugdenhil, 1994; Liu et al., 1995; Cho and Yoon, 1998) which neglect the vertical variation of velocity over water depth due to the fact that tsunami wave lengths are usually much larger than ocean depths. Some of the models were derived on the basis of Boussineq-type Equations (Peregrine, 1967; Madsen and Sorensen, 1992; Nwogu, 1993; Kennedy et al., 2000, 2001; Lynett and Liu, 2004a,,b), which include the vertical variation of velocity to some extent, such as CoulWave (Lynett and Liu, 2004a, b) and FunWave (Kennedy et al., 2000, 2001).

At the Institute of Geological and Nuclear Sciences (GNS Science), New Zealand, COMCOT has been continuously under development since the end of 2008, based on the original version from Cornell University, USA (Liu et al., 1998). The latest development incorporates multiple mechanisms for generating tsunami, such as submarine earthquakes and landslides. The built-in fault model is able to model the transient process of rupturing along a fault with variable slip in an earthquake event, which is particularly helpful in evaluating tsunami impacts in nearby coastal areas. Using a nested grid setup, different spatial resolutions may be used for the different stages of tsunami evolution, which allows us to study the entire life-span of a tsunami simultaneously, from its generation in the source area to inundation in coastal regions. This mode has been used to evaluate the tsunami threats to New Zealand for the events of the 2009 M_W8.1 Samoa earthquake, the 2010 M_W8.8 Chilean earthquake and the 2011 M_W9.0 Tohoku earthquake in Japan (see Section 3.3 for more information on these events). It has also been used to study the tsunami hazards and coastal impacts around New Zealand, for both local and distant-source scenarios, for Gisborne District Council (Wang et al., 2009), Tiwai Point (Prasetya et al., 2010a), Riverton (Prasetya et al., 2010b), Auckland Region (Power et al., 2012; Lane et al., 2012), Bay of Plenty and Tauranga.

At National Institute of Water and Atmospheric Research (NIWA), New Zealand, RiCOM (River and Coastal Ocean Model) has been under development for over ten years (Walters et al., 2003, 2005, 2006; Lane et al., 2012) and is frequently used at NIWA, New Zealand for studies of tsunami inundation around New Zealand. It is a general-purpose hydrodynamics and transport model, used to simulate near-shore flooding processes. It uses an unstructured triangular grid with spatially variable resolution allowing high-resolution land grids to be meshed seamlessly with the open ocean for inundation modelling, without the need for nested grids. RiCOM can initialise tsunami using various methods, including static initial conditions (Okada, 1985), a moving bottom boundary (Walters, 1992/2005) and temporally and spatially variable lateral boundary conditions. It has been used to study tsunami hazard and inundations from local, regional and/or distant sources in coastal areas of New Zealand, including Northland, Auckland Region, Waikato, Bay of Plenty, Canterbury and Otago (Lane et al., 2007a/2007b; Arnold et al., 2009; Goff et al., 2006; Walters et al., 2006; Gillibrand et al., 2011; Lane et al., 2012). More recently NIWA has also adapted Gerris, a highly advanced fluid dynamics solver, to enable tsunami modelling, including modules that incorporate tsunami sources and run-up and inundation. Using efficient quad-tree methods, Gerris can adaptively refine its numerical grid where needed to ensure resolution and accuracy. Gerris

is very effective at solving for trans-ocean tsunami propagation and run-up (Popinet, 2003). The model has also been used to study potential landslide tsunami hazards in Cook Strait, New Zealand and tsunamis in the Pacific islands, including Wallis and Futuna and Tokelau.

Other numerical models have also been developed, or model applications have been expanded to study the impacts of tsunami. Most of these models are particularly focused on modelling the run-up and inundation, as well as wave propagation close to the source. These models include CoulWave (Cornell University, USA), FunWave (University of Delaware, USA), Tsunami-Claw (Washington University, USA), MIKE21 (DHI, Denmark), and 3DD (ASR Ltd., New Zealand).

4.2 TSUNAMI GENERATION

Tsunami are generated by large-area disturbances on the bottom of a water body, such as submarine earthquakes, landslides and volcanic activity, or on the water surface, for example from meteorite impacts.

4.2.1 Submarine earthquakes

Tsunami source models are well developed for submarine earthquakes, where the seafloor deformation is typically estimated by assuming that the earthquake represents a finite dislocation (i.e., slip) within an elastic body (Okada, 1985; Mansinha and Smylie, 1971). These techniques have been tested against data from numerous real events and generally demonstrate a reasonable agreement, although the 26 December 2004 Indian Ocean earthquake has highlighted some areas for improvement (Lay et al., 2005).

The simple implementation of this type of source model usually assumes a finite rupture interface with uniform dislocation (e.g., slip movement along a fault). Its size and the amount of dislocation may be estimated via empirical relationships based on the seismic magnitude of an earthquake (e.g., Wells and Coppersmith, 1994). This source model is helpful in quickly constructing faulting scenarios and tsunami simulations and generally works well for distant tsunami. However, it neglects the spatial variations in slip, which are very important for evaluating tsunami impacts in regions close to the earthquake source, as demonstrated in the 11 March 2011 Tohoku M_W9.0 earthquake and tsunami. In this event, a slip of over 40.0 metres was estimated around the epicentre and the tsunami produced tremendous damage to the coast areas in Japan from Soma to Miyako, with run-up heights observed of up to 40.0 metres (Fujii et al., 2011; Lay et al., 2011a; 2011b; Mori et al., 2011). In general, the tsunami impact in distant areas is less sensitive to variations in slip.

The Okada (1985) model for fault slip is linear and so a simple improvement is to model a group of fault segments, each with a different amount of slip. Geist (1998) showed that local tsunami run-up can vary by over a factor of 3 depending on the slip distribution. Further model improvements take into account the time of the start of the rupture and the duration of uplift. Variable rupture start time and transient rupture are most important in earthquakes that rupture slowly, such as ‘tsunami earthquakes’ that typically rupture the very shallowest part of the plate interface.

Tsunami earthquakes refer to earthquake events with moderate magnitudes that are nevertheless exceptionally capable of generating tsunami. In these events, tsunami run-up heights are usually much larger than would be expected from their earthquake magnitudes (Kanamori, 1972). This type of earthquake is characterized by a slow rupture velocity and no strong ground shaking. For example, the 15 June 1896 Sanriku Ms 7.2 earthquake in Japan

generated an anomalously larger tsunami than expected from its seismic waves. With run-up heights over 25 metres and causing over 22,000 casualties, this became one of the worst tsunami in Japanese history. In the past decades, with implementation of modern seismic detection techniques, more tsunami earthquakes have been identified. They include the 2 September 1992 Nicaragua M_W7.6 earthquake, with run-up heights of over 9.0 m (Kanamori and Kikuchi, 1993; Ide et al., 1993), the 2 June 1994 Java M_W7.6 earthquake, with run-up heights of up to 14 metres and over 250 casualties (Tsuji et al., 1995; Abercrombie et al., 2001), and the 17 July 2006 Java M_W7.8 earthquake, with run-up heights of up to 8 metres and over 600 casualties (Ammon et al., 2006; Fritz et al., 2007).

Historical records show that the east coast of North Island may also suffer from the impacts of tsunami earthquakes. In 1947, two earthquakes, the 25 March 1947 M_W7.1 event and the 17 May 1947 M_W5.9 event, struck offshore from Gisborne and both triggered exceptionally large tsunami. Tsunami heights up to 13 metres were observed along the east coast just north of Gisborne in these events (New Zealand Historical Tsunami Database, by Gaye Downes of GNS Science, in preparation for publication). However, no strong shaking had been felt by local residents (see Sections 3.2 and 5.3.1.2 for further details on these events). Wang et al. (2009) carried out a set of numerical simulations to investigate the tsunami generated by the 25 March 1947 M_W7.1 earthquake. The numerical studies reveal the importance of slip variation and suggest that this event may have been a typical tsunami earthquake (Figure 4.1 and Figure 4.2). Because ground shaking, which is often strongly felt in common earthquakes, will be far less severe in these events, it is difficult to use shaking as a warning to the public of a potential tsunami during this type of event, especially for regions near the earthquake source, such as the east coast of North Island, New Zealand.

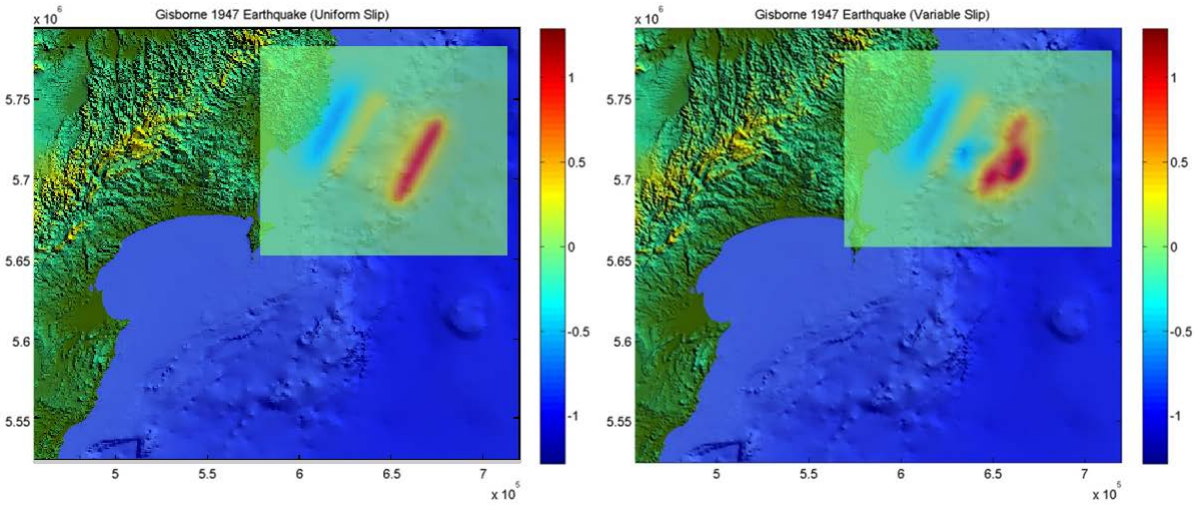

Figure 4.1 Seafloor deformation for the 27 March 1947 Gisborne earthquake (MW7.1) computed using a uniform slip model (left model) and a variable slip model (right panel). The variable slip model assumes that slip is greatest at the site of a subducting seamount (Wang et al., 2009).

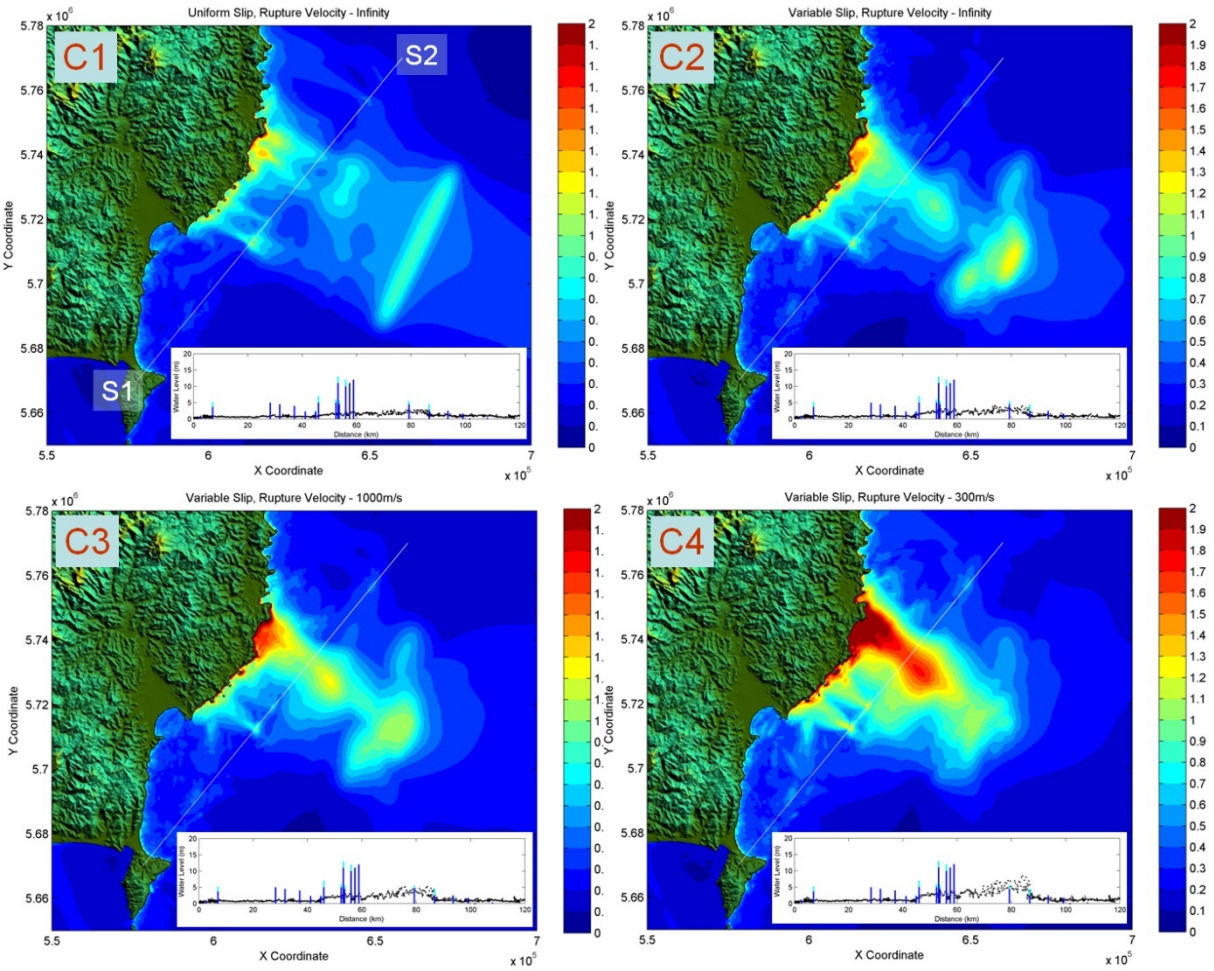

Figure 4.2 The modelled maximum tsunami elevations of the 27 March 1947 offshore Gisborne earthquake (MW7.1). The upper left panel (C1) shows the maximum tsunami elevation derived from a uniform slip model with instantaneous rupture; the upper right panel (C2) shows the maximum tsunami height from a variable slip model with infinite rupture velocity; the lower left panel (C3) shows the maximum tsunami height from a variable slip model with a rupture velocity of 1000 m/s; and the lower right panel (C4) shows the maximum tsunami height from a variable slip model with a rupture velocity of 300 m/s (Wang et al., 2009).

4.2.2 Landslides and volcanoes

Tsunami may also be triggered by landslides or volcanic eruptions. Far less frequent than the occurrences of earthquake tsunami, tsunami generated by landslides and volcanic eruptions may be catastrophic, especially in areas close to the source, but tend to be more localised in impact.

In coastal areas, landslides represent one of the most dangerous mechanisms for tsunami generation, due to their “silent” nature. Moreover, underwater landslides can be triggered by moderate earthquakes and thus the tsunami in such events will be much bigger than expected. Moreover, as they often occur on the continental slope, landslide tsunami offer little time to warn local populations and are particularly challenging for planning evacuation.

Though their role is often controversial, submarine landslides are generally considered to have contributed to the exceptionally large tsunami following several earthquakes, such as the 12 December 1992 Flores Island earthquake in Indonesia, the 17 July 1998 Papua New Guinea M_W7.0 earthquake, with a run-up height of about 15 m and over 2,200 casualties (Geist, 2000; Tappin et al., 2001; Tappin et al., 2008; Synolakis et al., 2002) and the 1 April

1946 Unimak (Aleutian) Ms7.1 earthquake, with run-up heights of up to 42 metres and 167 casualties (Fryer et al., 2004).

The wave amplitudes and characteristics of landslide-generated tsunami have been studied through three main approaches—laboratory experiments, analytical descriptions and numerical simulations (Heinrich, 1992; Watts, 1998; Liu et al., 2005; Enet et al., 2003; Enet and Grilli, 2007). These studies reveal many important aspects of tsunami generated by submarine landslides and indicate that the characteristics of landslide tsunami are related to the shape, physical properties and sliding mechanisms of landslides in a complicated way. Tsunami amplitudes are limited by the volume of mass that moves and the vertical extent of landslide motion (Watts, 1998). Watts et al. (2005) derived semi-empirical predictive equations for tsunami amplitude above the initial location for a two-dimensional rigid landslide. Using mass conservation arguments, they further derived expressions for the characteristic wave amplitude for a 3-dimensional rigid landslide. Experimental studies by Enet and Grilli (2007) validated these empirical models and also indicated that the initial acceleration of landslides is a more important factor in tsunami generation than the terminal velocity. Although empirical relationships can be established for the initial tsunami amplitude generated by simplified rigid landslides, the complexity of deformation, spreading and local bathymetry in reality usually limits their usefulness for more general studies.

Compared to earthquake and landslide tsunami, tsunami generation by volcanic events is far more complicated and often involves more than one physical process. Tsunami can be generated by a variety of volcanic mechanisms—pyroclastic flows, debris avalanches, collapse of sectors of a volcanic edifice, and even by aerial or submarine landslides, and meteo-tsunami caused by the pressure wave from the volcano. Tsunami waves generated by such complex source mechanisms usually behave quite differently to earthquake tsunami. In general, due to the small dimensions of the source areas, these waves are much shorter, with wave periods ranging up to several minutes, and they experience strong dispersion effects. Similar to many landslide-generated tsunamis, their impacts tend to be localized and do not pose a significant danger at great distances from the source (Pararas-Carayannis, 1992; 2002; 2003; 2006).

In brief, for tsunami modelling there are robust, physically based techniques to initialise tsunamis triggered by earthquakes, but none yet for landslides and volcanoes. The generation mechanisms are far more complicated than displacements in earthquake events, and the physics of these mechanisms is in some cases only partly understood. Consequently, while past events can be modelled and specific scenarios for future events can be investigated, the studies are usually on a case-by-case basis and it is harder to develop general insights.

4.3 PROPAGATION MODELLING

In a tsunami event, once the water body has been displaced from its equilibrium position in its source area, the potential energy gained during the generation process is converted to kinetic energy. Tsunami waves are thus generated and spread away from the source area to all the directions. If the tsunami is generated by an earthquake, typically most of the wave energy radiates out along the path perpendicular to the fault line. However, the propagation will be affected by the bathymetry patterns such as submarine ridges, plateaus and seamounts, diverting the propagation direction and focusing tsunami energy in a specific pattern (i.e., wave guiding effect). In ocean basins, the speed at which tsunami waves travel is usually proportional to the square root of the water depth. For example, in the Pacific basin

tsunami travel at a speed of 700-900 km per hour, comparable to that of commercial jets. Over continental shelfs, tsunami travel slower than in the deep ocean. However, their amplitude increases as the water depth drops and the propagation will be gradually diverted in a direction perpendicular to the coast line (called shoaling effects).

4.3.1 Modelling tsunami propagation numerically

Simulating tsunami waves spreading out from the source is well understood in terms of the underlying physics. Below we present two examples using COMCOT to model the propagations of the 27 February 2010 Chile M_W8.8 event and the 11 March 2011 Tohoku M_W9.0 event in Japan (see Section 3.3 for more information on these events).

In the 27 February 2010 Chile tsunami, the major energy of the tsunami was steered toward Japan and the Kuril Islands (Figure 4.3 and Figure 4.4). New Zealand was off the main track of its impact. However, the Chatham Rise, together with the Campbell Plateau, east of the South Island, served as a wave guide, focusing more energy toward the east coast of South Island (Figure 4.3). In New Zealand, the first peak of the tsunami arrived at Chatham Island about 12 hours after the earthquake, with increases in water level of up to one metre recorded at tsunami gauges in Chatham Island and Gisborne. The sea levels oscillated for over 12 hours before they attenuated.

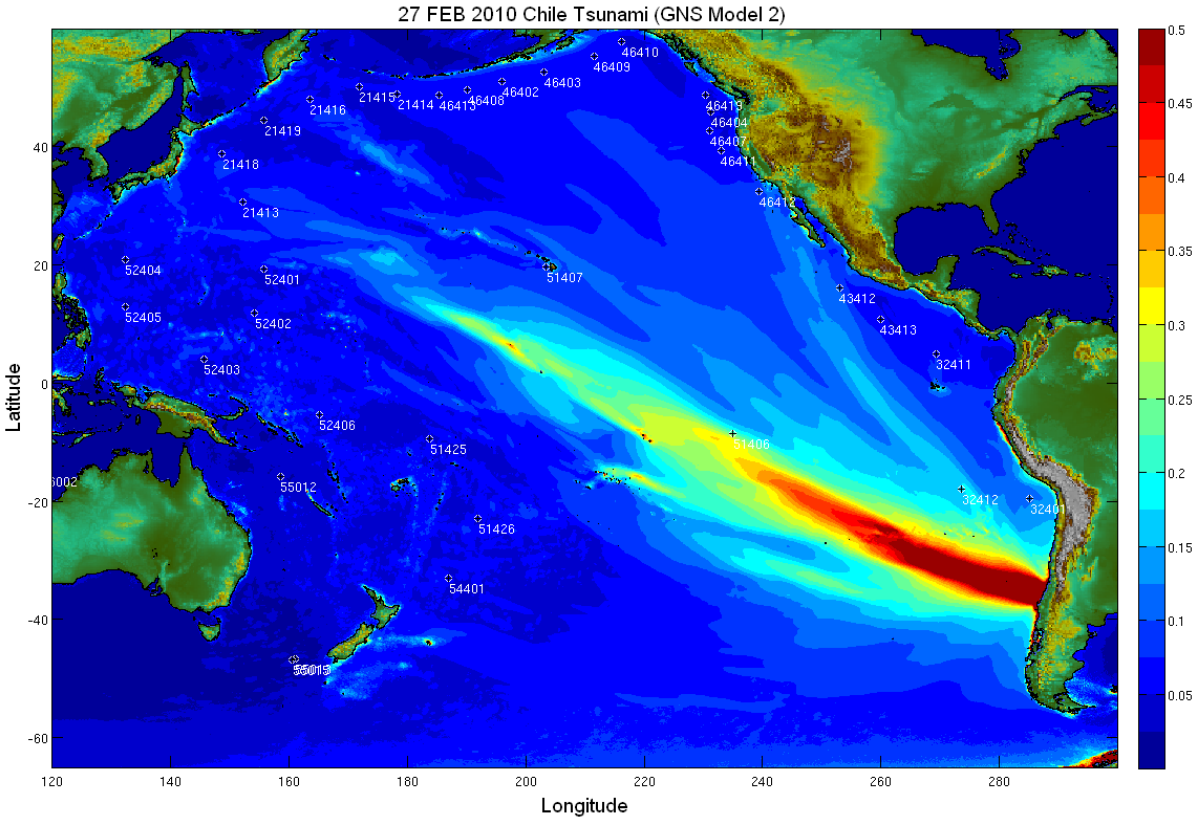

Figure 4.3 Modelled distribution of maximum tsunami elevations throughout the Pacific for the 2010 Chilean tsunami event (numerical simulations by tsunami scientists at GNS Science, New Zealand). DART buoys are indicated by white circles with a black cross inside. The colour scale presents tsunami elevations above ambient water level in metres.

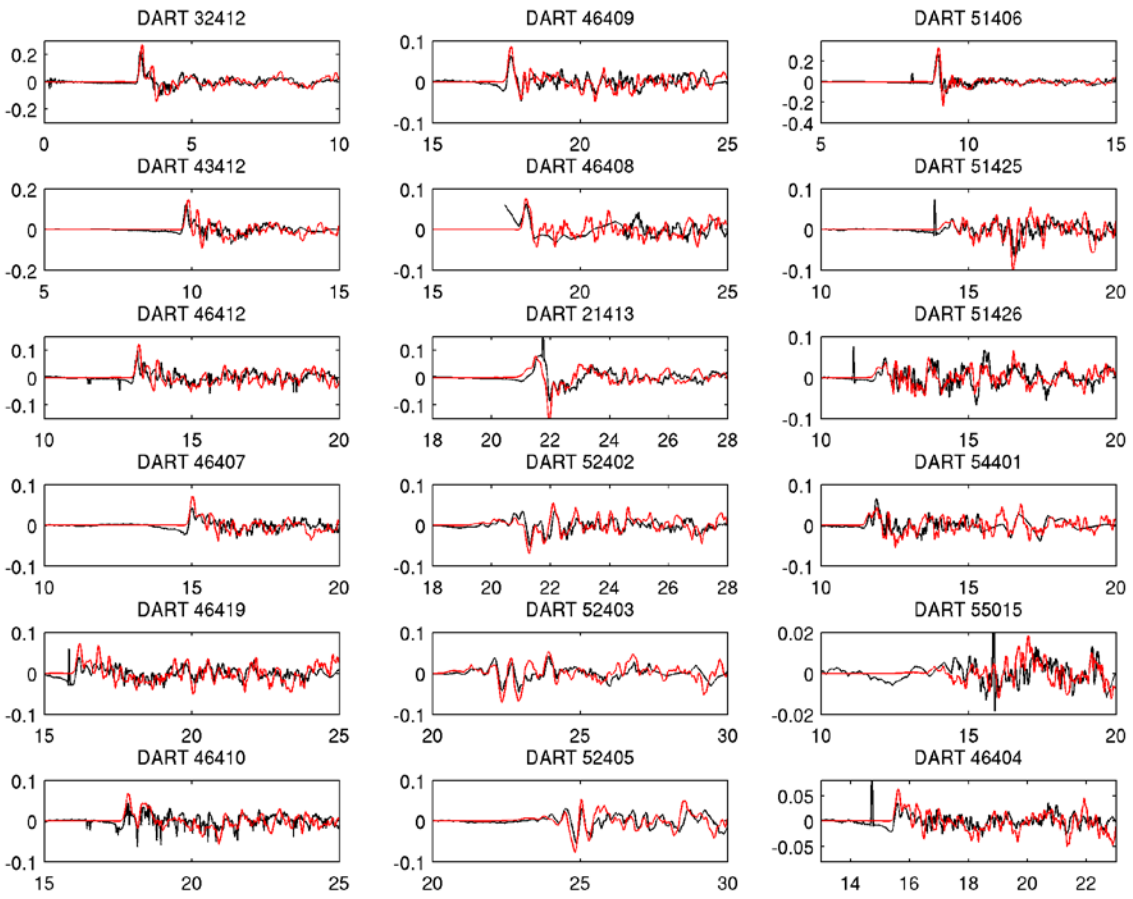

Figure 4.4 Comparisons between the modelled sea surface fluctuations and the measurements at DART buoys for the 2010 Chilean tsunami (numerical simulations by tsunami scientists at GNS Science, New Zealand). The red colour presents the modelled data and the black colour indicates the measurements. The horizontal axes show hours after the main shock and the vertical axes denote the sea-level anomaly in metres.

In the 11 March 2011 Tohoku M_W9.0 earthquake in Japan, numerical simulation shows that the major energy of the tsunami propagated toward the coast of North and South America through Hawaii (Figure 4.5 and Figure 4.6). The minor amount of tsunami energy travelling toward New Zealand was mostly blocked by Pacific islands, such as Solomon Island, Tonga, and Fiji (Figure 4.5). In New Zealand, the tsunami started to affect the North Island about 12 hours after the main shock. Figure 4.6 shows a comparison between modelled and measured sea level fluctuations during this tsunami. Tsunami amplitudes of up to 1.0 metre were recorded by several tsunami gauges at the coasts of New Zealand, however, the sea level oscillations lasted for over 30 hours before they attenuated (Figure 4.7). This indicates that people in coastal areas of New Zealand need to remain vigilant for long periods of time following tsunami from distant source locations.

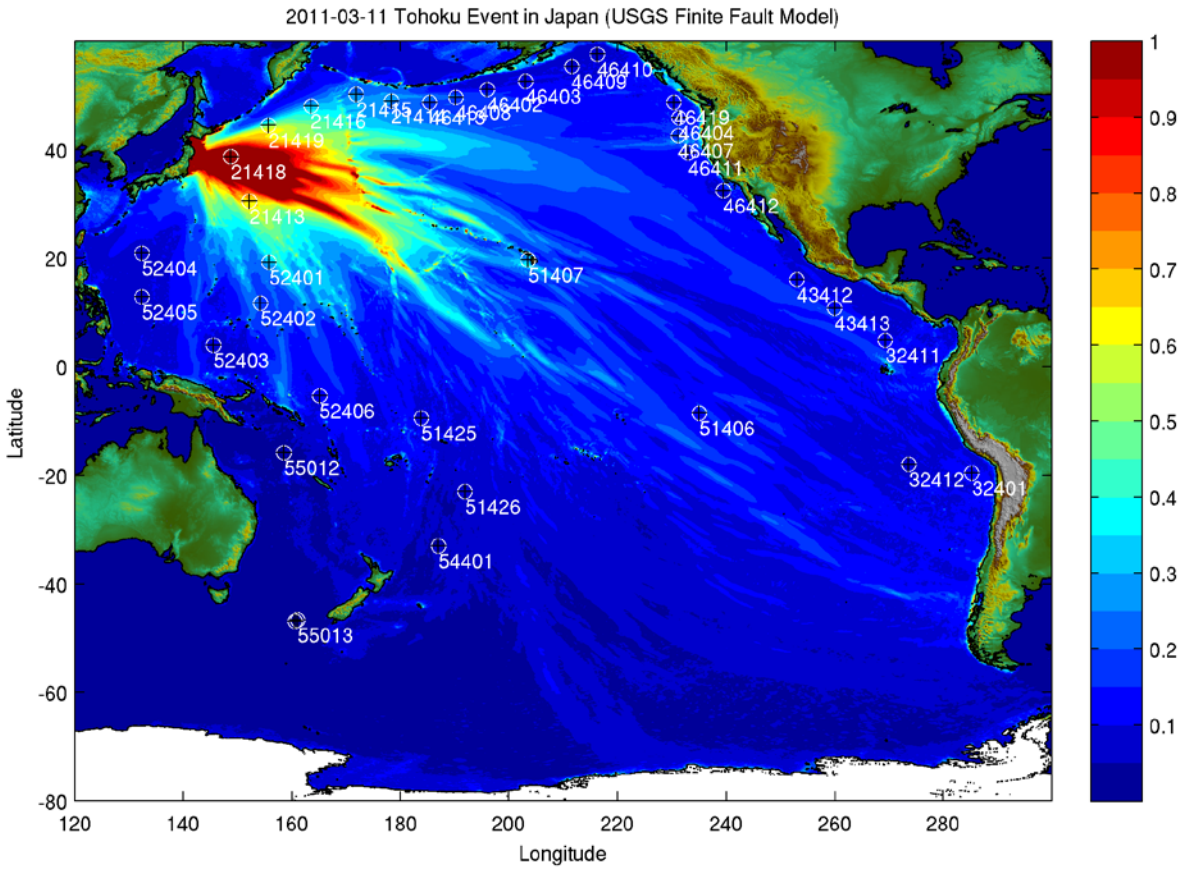

Figure 4.5 Modelled maximum tsunami elevations in the Pacific for the 11 March 2011 Tohoku earthquake in Japan (tsunami simulations were carried out by tsunami scientists at GNS Science, New Zealand, using COMCOT, with the source model of the USGS finite fault solution). DART buoys are indicated by white circles with black crosses inside. The colour scale represents maximum water level increments in metres due to this

tsunami.

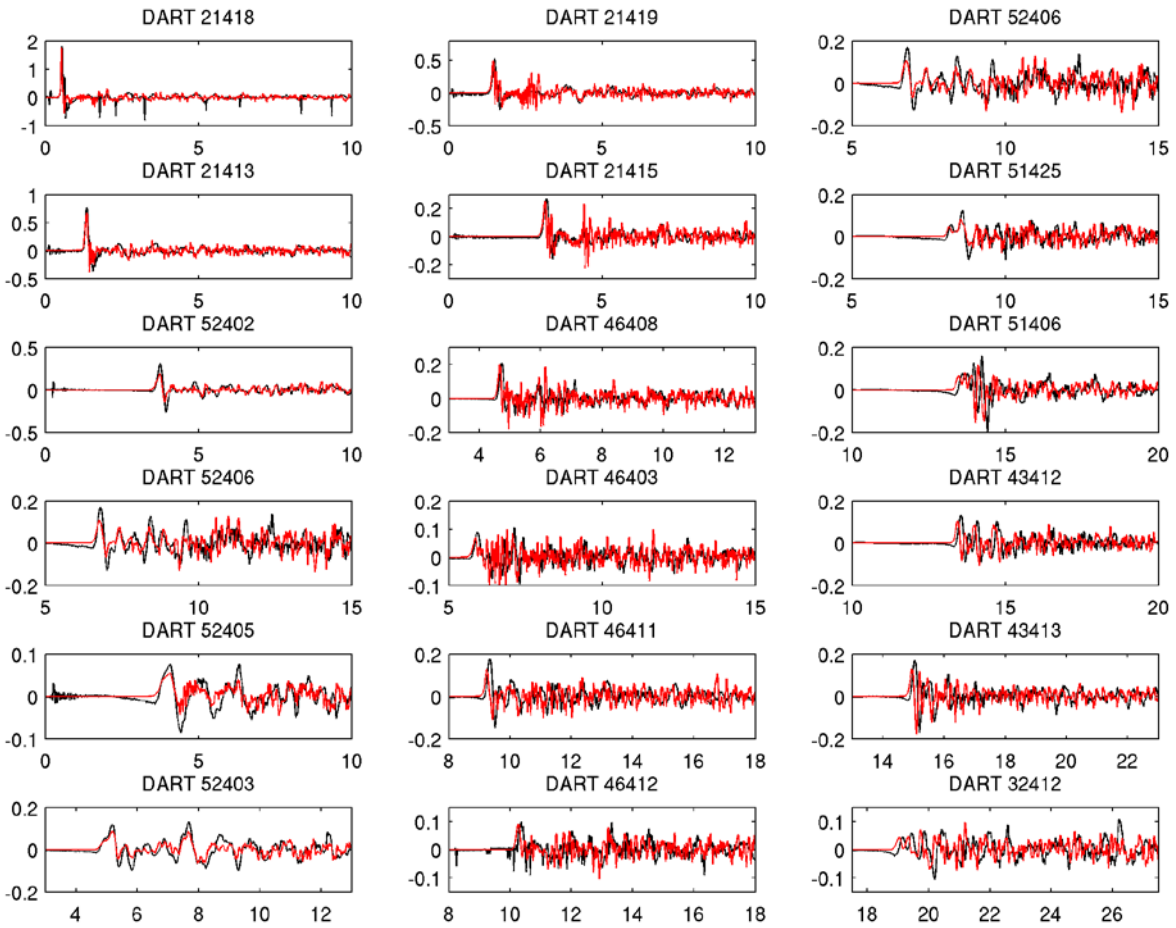

Figure 4.6 Comparison between the tsunami sea-level fluctuations over time derived from modelling and the measurements made at DART buoys (filtered) throughout the Pacific for the 2011 Tohoku event in Japan. The red colour presents the modelled data and the black colour indicates the measurements. The horizontal axes show hours after the main shock and the vertical axes denote the sea level anomaly in metres.

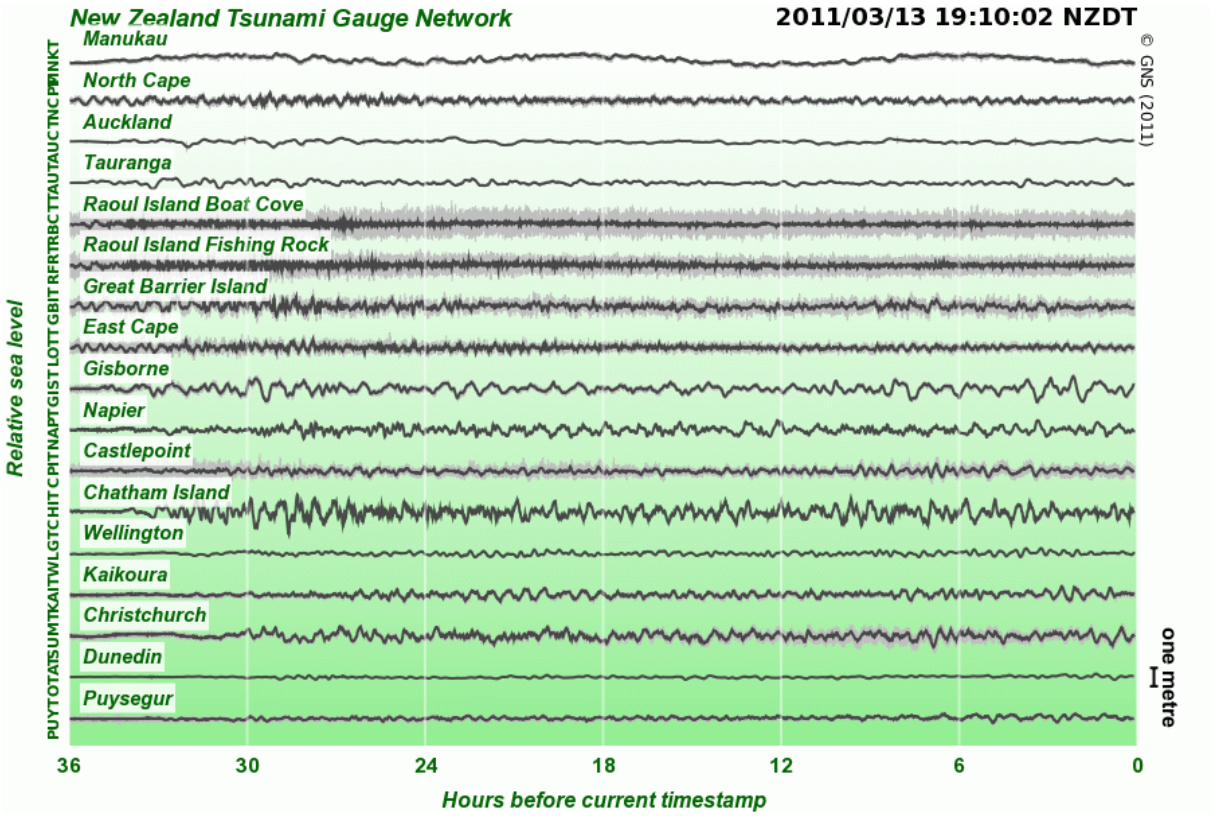

Figure 4.7 Measurements of the 11 March 2011 (UTC) Japan tsunami at coastal tsunami gauges in New Zealand. The measurements at Gisborne and Chatham Island show that significant oscillations were still being recorded over 30 hours after the leading wave arrived.

4.3.2 Insights from propagation modelling

Extensive studies and numerical modelling have been carried out to evaluate tsunami hazards in New Zealand from local, regional and distant sources (see examples in Figure 4.1 and Figure 4.2, Figure 4.8 and Figure 4.9 and studies listed in Appendix 1). Many useful insights can be gained from the propagation modelling and these are summarized below.

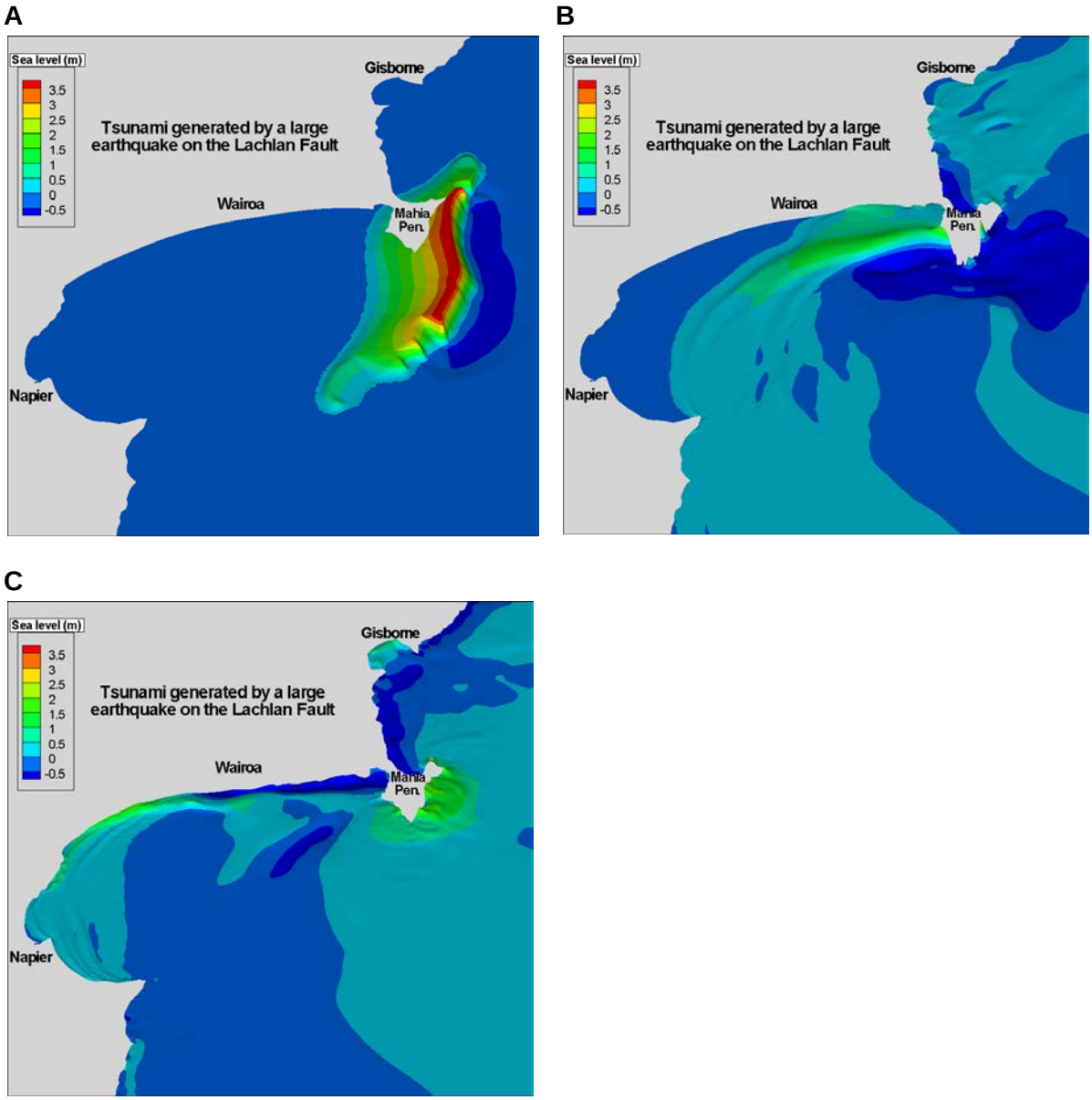

Figure 4.8 A series of images illustrating the propagation of a tsunami generated by an earthquake on the Lachlan fault (which lies offshore of Hawke's Bay, approximately at the position of the tsunami in image A), modelled by Roy Walters et al. with RiCOM model at NIWA, prepared for the Hawke's Bay Aquarium.

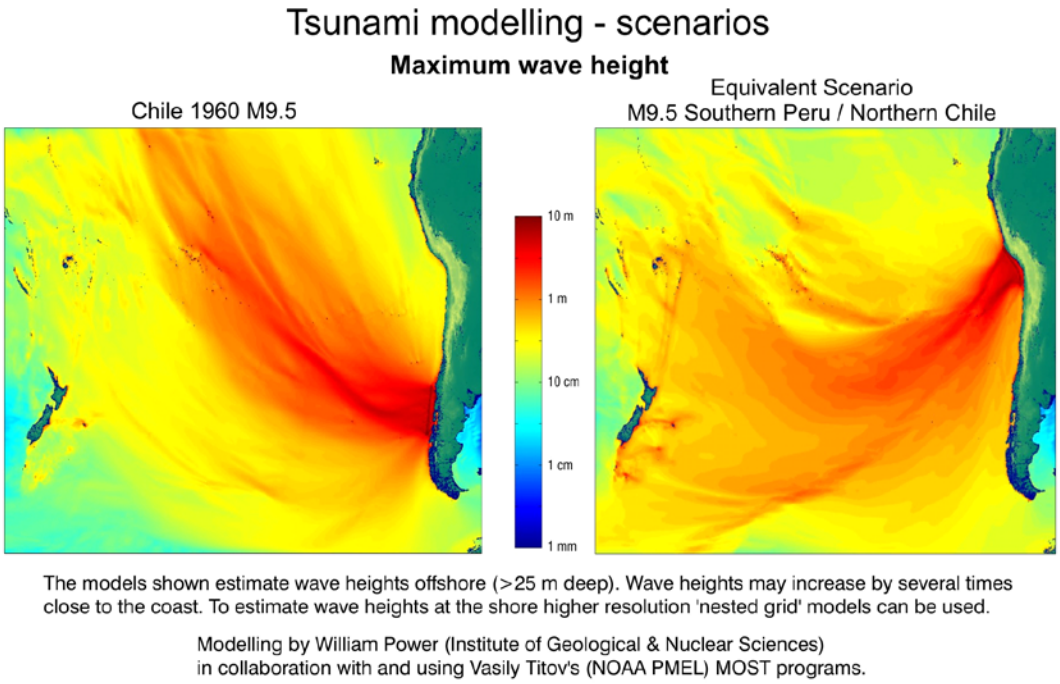

Figure 4.9 A comparison of two scenarios for South American tsunami affecting New Zealand, illustrating the effect that directivity of the source can have on distant locations. This effect explains why the ~M9 1868 Peru earthquake caused tsunami heights in New Zealand that were about as large, and in some locations larger, than those caused by the ~M9.5 1960 Chile earthquake, even though the 1960 earthquake was substantially greater in magnitude (see Section 3.2).

- Earthquake-generated tsunami typically propagate in such a way that most of the wave energy is directed perpendicular to the fault on which the earthquake occurred, and the initial wave is separated into two components travelling in opposite directions.
- Landslide sources can be highly directional, sending a fairly concentrated tsunami 'beam' perpendicular to the slope which has given way and in the direction of the landslide movement (Ward, 2001; Walters et al., 2006). Many volcano sources can also be highly directional, but more typically radiate in a circular pattern.
- Where the dimensions of the tsunami source are small, less than a few tens of kilometres, the resulting waves are subject to dispersion, in which the different frequencies present in the tsunami wave propagate at different speeds. This leads to a stretching-out of the tsunami wave train, and generally lower wave amplitudes. This is one reason why landslides and volcanoes tend not to be a tsunami risk at large distances from the source.
- Tsunami waves tend to become concentrated above undersea ridges because of refraction. In this situation the ridge acts as a 'waveguide', which can lead to enhanced tsunami wave heights at locations where these ridges lead to the shore (Koshimura et al., 2001). In New Zealand a good example is given by the Chatham Rise, an area of shallow bathymetry which lies between Banks Peninsula and the Chatham Islands. The presence of this ridge leads to larger wave heights reaching Banks Peninsula than would otherwise be the case.

- Bays and inlets around the coast have specific natural frequencies, determined by the time it takes for water to slosh into and out of the bay (e.g., Walters, 2002; Walters and Goff, 2003; Tolkova and Power, 2011). If the natural frequency of a bay matches that of the tsunami waves then the waves may be amplified. This can often explain variations in tsunami height that may at first appear random along a given section of coastline. Identifying the natural frequencies of coastal bays and comparing them with characteristic frequencies for tsunami is a useful first step towards identifying those areas most at risk.

Specific aspects of tsunami that affect New Zealand

- Of the South American tsunami sources, it is those lying between the Peru-Chile border (19°S) and the 8°S line of latitude, which are most effective at directing tsunami towards New Zealand. The tsunami of 1868, which was the worst distant-source tsunami of historical times in this country, originated from the southern half of this region (about 17.7°S). The last large tsunami from the northern half of this region (about 12.5°S) was in 1746, too early to appear in written records in New Zealand, but modelling suggests that such tsunami are likely to also have a strong impact here. Locations on the east coast of New Zealand tend to be the most vulnerable to South American tsunami, but the ability of tsunami to bend around corners in the coastline means that they can still pose a hazard to locations that are out of direct line-of-sight (Figure 4.9).
- Distant tsunami originating from locations in the Northern hemisphere, such as Cascadia, and the Aleutians, and also from areas of the southwest Pacific north of New Zealand, tend to have their greatest impact on Northland, the Coromandel, and the Bay of Plenty.
- Local tsunami generated by submarine landslides and thrust faults can have a large local impact on the east coast of New Zealand from south of Kaikoura northwards to Northland.
- The east coast of North Island may have suffered from tsunami earthquakes. Modelling studies suggest the 27 March 1947 M_W7.1 earthquake and the 17 May 1947 M_W6.9 earthquake offshore from Gisborne were tsunami earthquakes that generated far larger tsunami than expected given the magnitude of the earthquakes. This type of earthquake is usually not associated with strong ground shaking.
- As observed from the recent 2010 Chilean tsunami and the 2011 Japan tsunami, coastal oscillations tend to last for a significant duration. In the 2011 Japan tsunami, in Gisborne and Chatham Island (among others), coastal tsunami gauge records show that the coastal water levels had oscillated for over 30 hours before apparent decay occurred (Figure 4.7).

Numerical modelling studies relevant to New Zealand are tabulated in Appendix 1.

4.4 INUNDATION MODELLING

Inundation modelling is used to determine the range of flooding inland and the flow depths in a tsunami event. There are various methods by which inundation can be modelled; in order of increasing complexity and accuracy these are:

- A simple bathtub model that projects the level of the maximum tsunami height inland;
- A rule-based tsunami height attenuation model, applied inland from the coast. This approach derives a more realistic output than a simple 'bathtub' model but is still a rough estimate that cannot account for physical variations in wave behaviour.
- A computer-derived simulation model that allows for added complexities such as varying land roughness depending on land use and evaluates comprehensive dynamics of tsunami waves, but which still takes as input a single tsunami height at the coast.
- A computer simulation that takes account the physical properties affected by land use and the dynamics of the tsunami waves, but which is directly linked to a tsunami propagation model. This provides the most comprehensive inputs to the inundation modelling.

4.4.1 Numerical modelling of tsunami inundation

In a tsunami event, or scenario study with a specified source model, inundation in a specific area can be modelled numerically, provided high-resolution topography and bathymetry data are available. While a tsunami may travel thousands of kilometres across ocean basins, land inundation is confined to tens to hundreds of metres (a few kilometres in extreme cases). To accurately model this requires an inundation grid that can resolve these scales. The inundation grid covers not only the sea but also land areas of interest. The depth and velocity of the water in wet areas are modelled using standard physical equations (e.g., non-linear shallow water equations or Boussinesq-type equations) and a wetting/drying algorithm determines the instantaneous boundary of the water, allowing the wave to inundate the land areas but also for areas to become dry as the wave retreats. The inundation modelling must be linked to a propagation model, which provides sea surface fluctuations and velocity information to the inundation model as boundary conditions.

COMCOT uses a series of nested grids to increase resolution in areas where inundation modelling is required (Wang and Power, 2011), passing information from the larger scale propagation grids on the boundaries of the more refined grid. RiCOM uses an unstructured grid which can be gradually refined for areas of interest, allowing a seamless transition between propagation and inundation. Gerris uses adaptive grid-refinement techniques to increase resolution where and when inundation occurs.

Numerical models provide the inundation range, flow depth and velocity information for a tsunami simulation. Together with maps or aerial photos, these data can be used for tsunami hazard planning, such as evaluation of potential tsunami hazards, development of evacuation maps, etc. The magnitude of the forces impacting structures in the inundated areas may also be evaluated using the results of inundation modelling, to provide guidance on building tsunami-resilient communities (Wang and Liu, 2007; Wijetunge et al., 2008). Figure 4.10 and Figure 4.11 show the modelled flow depth in the Gisborne area for an M_W9.0 scenario event, involving rupture of the whole Hikurangi subduction margin off the east coast of New Zealand. In these figures, the modelled flow depth is overlaid on a Google map and on an aerial photo of the same area to illustrate the extent of inundation (Wang et al., 2009).

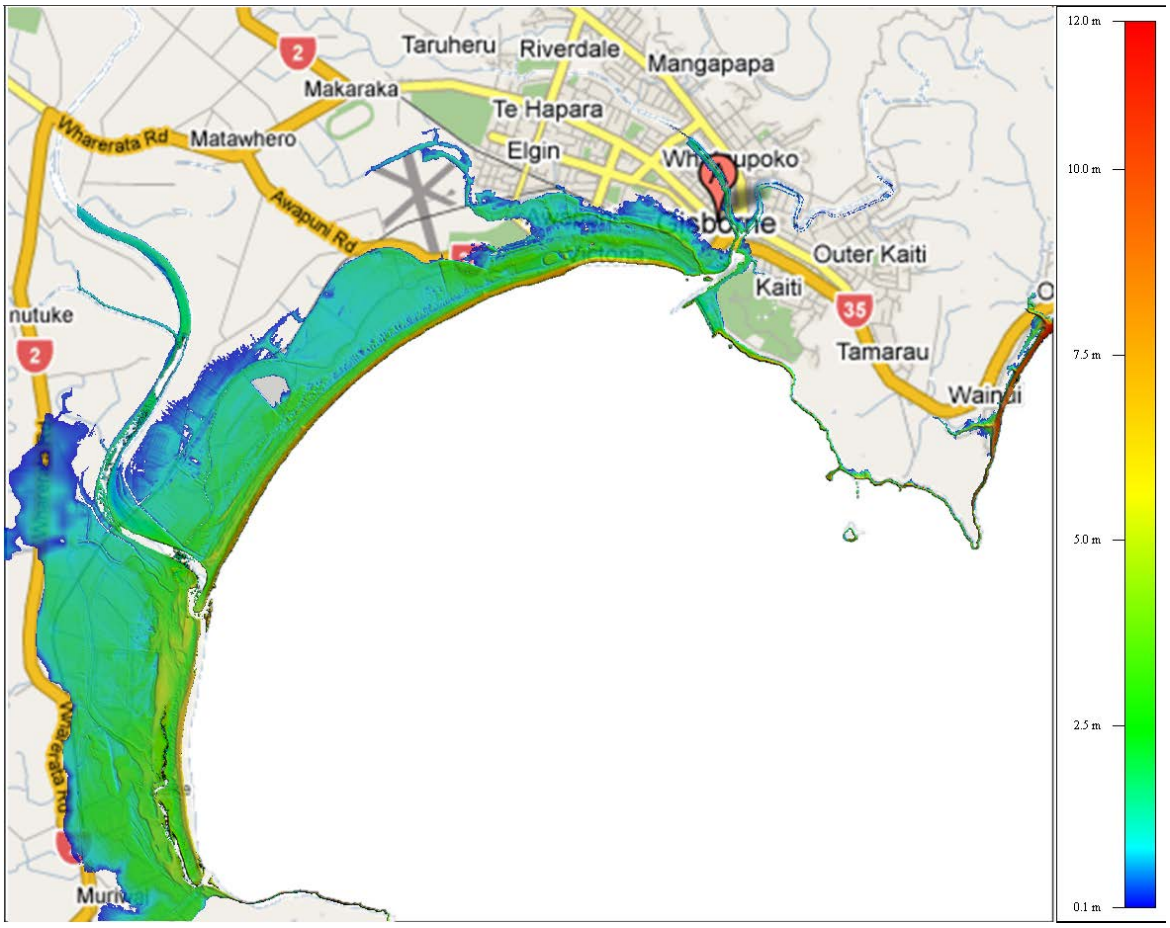

Figure 4.10 The modelled flow depth in the Gisborne area for an MW9.0 scenario event involving rupture of the whole Hikurangi margin. The numerical simulation was performed by Wang et al. (2009) using the COMCOT model and the modelled flow depth on land is overlaid on a Google map).

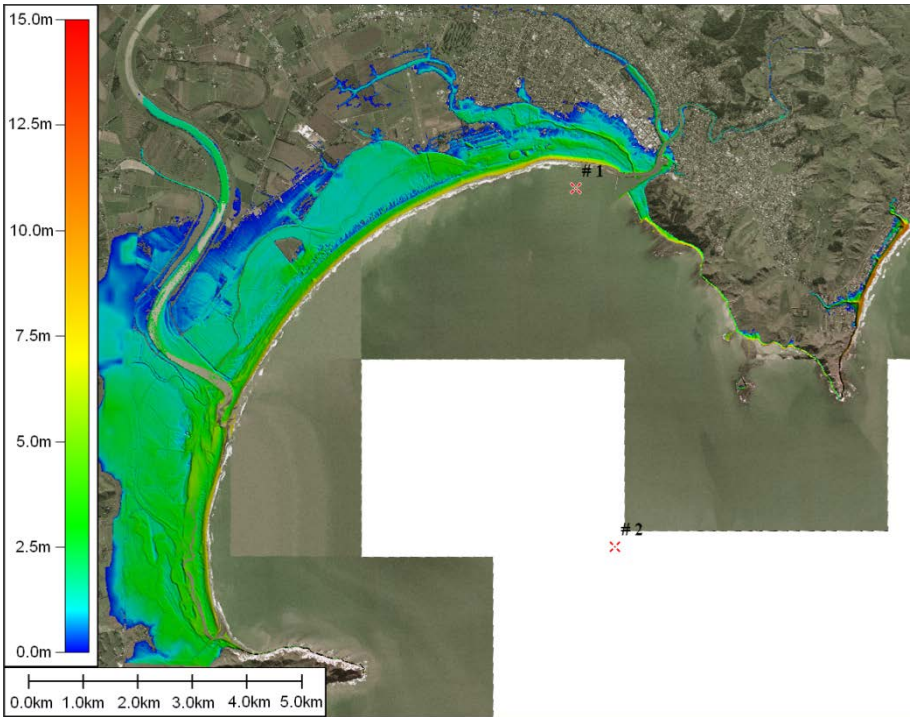

Figure 4.11 The modelled flow depth in Gisborne area for an MW9.0 scenario event involving rupture of the whole Hikurangi margin. The numerical simulation was performed by Wang et al. (2009) using the COMCOT model, and the modelled flow depth on land is overlaid on an aerial photo. The red crosses indicate the location of virtual tidal gauges for time history data output.

High-resolution data on topography is necessary to produce a satisfactory output for inundation modelling. This type of data usually comes from LiDAR or RTK surveys. LiDAR (Light Detection and Ranging) is an optical remote-sensing technology that can be used to measure the distance to the land surface from an aircraft by illuminating the target with light, e.g., a laser, and thus create high-resolution topography data with vertical accuracy usually in the 10-15 centimetre range. RTK (Real-Time Kinematic) survey is a technique used in land survey based on the use of carrier phase measurements of GPS or GLONASS signals, where a single reference station provides the real-time corrections with up to centimetre-level accuracy. RTK surveys, while very accurate, are very labour intensive and have limited spatial extent. They are useful to delineate specific features (such as stopbanks) or locate damaged buildings or indicate inundation extents in post-disaster surveys. If LiDAR or some other high-resolution DEM is not available, results from RTK surveys may be used to build up a rough topographic model.

As one of the factors that retard inundation, land-use conditions also have to be considered and are usually incorporated into the modelling process as land roughness. LiDAR information can also be used to derive roughness estimates for inundation modelling (Smart et al., 2004).

4.5 EMPIRICAL TSUNAMI MODELLING

An alternative to directly modelling the physical processes in a tsunami is to use historical data to construct a statistical model of probable tsunami characteristics (e.g., height at the coast) as a result of factors such as earthquake magnitude and distance to the epicentre. These models are very quick to compute, but because they bypass physical considerations by statistically fitting the data to a simple equation, they are limited in their ability to predict tsunami characteristics, e.g., tsunami heights and inundation extents, in a relatively simple situation.

4.5.1 Empirical modelling of tsunami heights

4.5.1.1 Estimating heights of tsunami from distant sources

Based on a compilation of historic data, largely for the Pacific Ocean, Abe (1979) proposed the following equation for estimating the tsunami height, H, of a tsunami at a distant shore due to an earthquake of magnitude M_W

$$H = 10^{(M_W - B)}$$ **Equation 4.1**

Where B is a parameter that varies for each site and earthquake source. B can be determined using either historical data, or numerical modelling, or a combination of both. The data on which Abe (1979) based this equation has considerable scatter, so the relationship has significant uncertainty which must be taken into account.

Tsunami-height information from historical observations, or from a collection of synthetic models, can be used to estimate parameter B for each site and source region. In Section 6 we apply this method using synthetic models to estimate B, an approach which is sometimes referred to as semi-empirical modelling.

4.5.1.2 Estimating heights of tsunami from local sources

For local source tsunami, the equivalent Abe relationship to that used for distant sources is given by:

$$Ht = 10^{M_W - \log R + 5.55 + C}$$ **Equation 4.2**

where H_t is the tsunami height at a local coast, *R* is the source-to-site distance and *C* is a parameter that varies for each site and earthquake source. The best available values of *C* are derived from Japanese data and have possible values of 0.0 and 0.2, depending upon location. Because Ht in Equation 4.2 becomes unrealistically large at small values of R, Abe introduced a limiting tsunami height near the source of:

$$Hr = 10^{0.5M_W - 3.30 + C}$$ **Equation 4.3**

These equations estimate the tsunami height based only on earthquake magnitude and distance, and take no account of the effects of bathymetry or source orientation, consequently it is important to take into account the uncertainty in these estimates. More details of this analysis, including the uncertainty treatment, are given in Section 6. The interpretation of Ht needs further comment—originally it was interpreted, and the equation parameters used, were in terms of peak-to-trough tide gauge measurements. However direct interpretation of these results is complicated by the limitations of tide gauges at the time the data was collected—these often tended to underestimate wave heights (Satake et al., 1988). Abe (1995) later related Ht to the average run-up height along a section of coast, and 2Ht to the maximum run-up height anywhere along a section of coast (see Kajiura, 1983 and Abe, 1995 for details); this is the interpretation used in Section 6.

4.5.2 Empirical modelling of tsunami inundation

Empirical inundation modelling is usually used for areas where numerical modelling is at a preliminary stage because resources and data are limited. There are many different processes taking place during inundation, some of which may not be well understood. Consequently, effective modelling of the combined processes remains challenging. In addition, high-resolution numerical modelling is time-consuming and requires substantial computing capacity. As an alternative, empirical models can provide rapid estimates when they are needed.

The 2005 Tsunami Hazard and Risk Report described several empirical modelling approaches to tsunami inundation. Since 2005, one approach has often been used for interim evacuation zone planning in situations where data and computing resources were not yet available for full modelling. Due to the conservative assumptions used, it is more accurate to describe this as an ‘evacuation zone estimation method’ rather than a ‘tsunami inundation model’. This method is briefly explained in the following section.

4.5.3 Deriving rules for defining tsunami evacuation zones

Field surveys following tsunami have involved collection of a lot of data on tsunami flow-heights and run-up heights for several events (e.g., the 2004 Indian Ocean tsunami). Analysis of comprehensive survey data from large tsunami shows that the largest run-up heights occur close to the coast, while the inundation extends furthest inland in areas of low, flat topography.

Field survey data from Lhok Nga and Banda Aceh (Lavigne et al., 2009) shows this relationship (Figure 4.12) in measurements of the 2004 Indian Ocean tsunami. Note that this data was collected onshore from sections of coast ~10-20km long, i.e., it does not represent just a single transect. From this data it is possible to define an 'envelope' which sets the maximum possible water level at a given distance from the coast. Assuming a linear envelope, we find that the maximum achievable water level decreases by approximately 1 metre for every 200 metres inland.

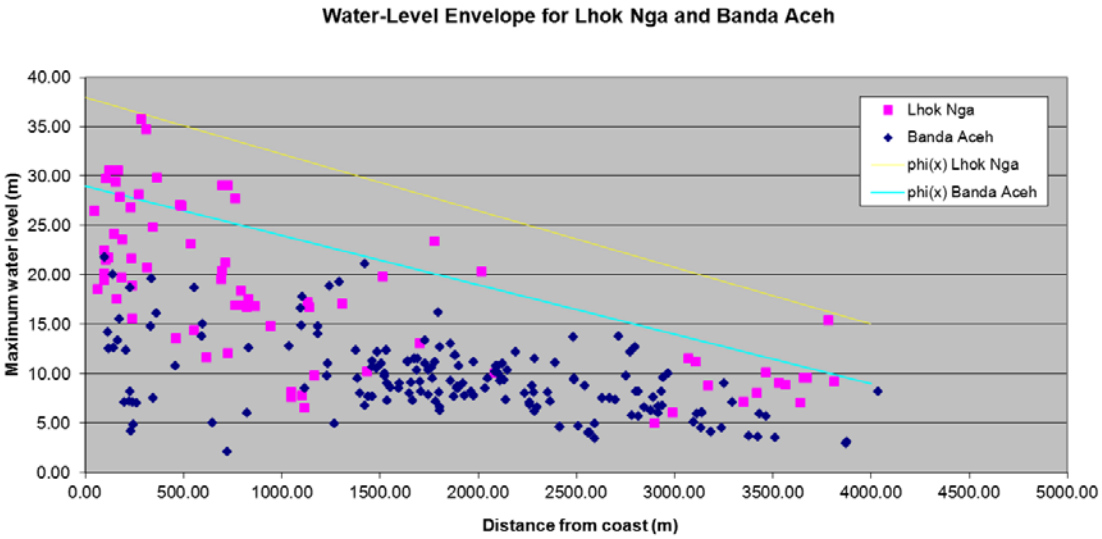

Figure 4.12 Water level plotted as a function of distance from the coast, using field survey data from the districts of Lhok Nga and Banda Aceh, as recorded by Lavigne et al. (2009) following the 2004 Indian Ocean tsunami.

This analysis of survey data is valid only if the dataset of survey points is comprehensive and if the tsunami encounters varied terrain (i.e., with various slopes and topographic forms). Unfortunately, these conditions are rarely met—of the datasets in Figure 4.12 Lhok Nga covers quite a variety of terrain, whereas in the area spanned by the Banda Aceh data the terrain is more uniform. The 2011 Japan tsunami has provided excellent datasets for more analyses of this type (Fraser and Power, 2013). Smaller tsunami are rarely field surveyed in as much detail; one exception is the 1983 Japan Sea tsunami, for which the maximum achievable water level dropped off faster, approximately 1 metre for every 100 metres inland, as might be expected from a shorter period tsunami from a smaller source.

Using the empirical rule to define evacuation zones then requires an estimate of the maximum possible water level at the coast, and then including in the zone those points that lie inside the 'wedge' defined by the 1:200 rule. The method is applied conservatively—the maximum height at the coast is usually taken to be twice the water level at the coast of a tsunami propagation model with reflecting 'wall' boundary conditions (i.e., assuming that small-scale topographic features can at most double the tsunami height), and the 1:200 decay is taken as a conservative limit on the decay rate.

Tsunami propagate further along rivers than they do across land. Data from Banda Aceh suggests they may travel about twice as far, hence a 1:400 decay (a 1 metre drop for every 400 metres upriver) is generally assumed.

Fraser and Power (2012) compared tsunami evacuation zones defined using the above rule, and assuming a 35 m maximum run-up at the coast, with actual inundation data from the 2011 Japan tsunami. They found the resulting zones to be successful in encompassing the true extent of inundation, with a degree of over-evacuation that was acceptable for a simple interim evacuation mapping technique.

4.5.3.1 Limitations of empirical inundation modelling and rule-based evacuation zoning

The rule-based approach to evacuation mapping has been applied as an interim measure where data and computing resources are limited. It has been designed conservatively, as explained above; however this conservatism comes at a cost—it may result in evacuating larger areas than necessary. It is anticipated that such rule-based evacuation zoning will be phased out as the data and computational needs for full numerical modelling become available.

4.6 REAL-TIME TSUNAMI MODELLING AND FORECASTS

Numerical models are extremely helpful for studying the tsunami impacts of historical events, and for evaluating the tsunami threat from potential events, or establishing a tsunami scenario database. However, it can be very challenging to apply them to evaluating and forecasting tsunami threats in real time, especially for tsunami from local or regional sources, due to the extensive time required for model setup, computation and data analysis.

Emergency managers and other officials are in urgent need of operational tools that will provide accurate tsunami forecasts to guide them in making rapid, critical decisions in which lives and property are at stake. In light of this, advanced tools have been developed to evaluate and forecast tsunami threats in real time. In the USA, a next-generation real-time tsunami forecast model has been developed by the National Oceanic and Atmospheric Administration (NOAA) Center of Tsunami Research (NCTR). The model, Web-based Short-term Inundation Forecast of Tsunami (WebSIFT), can provide real-time deep-ocean tsunami propagation forecast worldwide (Titov et al., 2005; Gica et al., 2008). This model uses a pre-computed propagation database of tsunami evolution based on unit earthquakes from fault planes with a size of 100 km x 50 km called unit sources. These unit sources, with a slip amount of 1.0 metres, are placed along the subduction zones around the rim of ocean basins. Then the propagation database is constructed by running a propagation model to obtain offshore scenario wave kinematics for each unit source. In a specific event, the deep-ocean tsunami propagation can be quickly obtained through the linear combination of unit sources using an inverse analysis in which real-time tsunami measurements from DART (Deep-ocean Assessment and Reporting of Tsunamis) are used to improve the tsunami forecast. The DART system is particularly designed to detect tsunami waves and provide real-time measurements of sea-level changes due to tsunami (Figure 4.13).

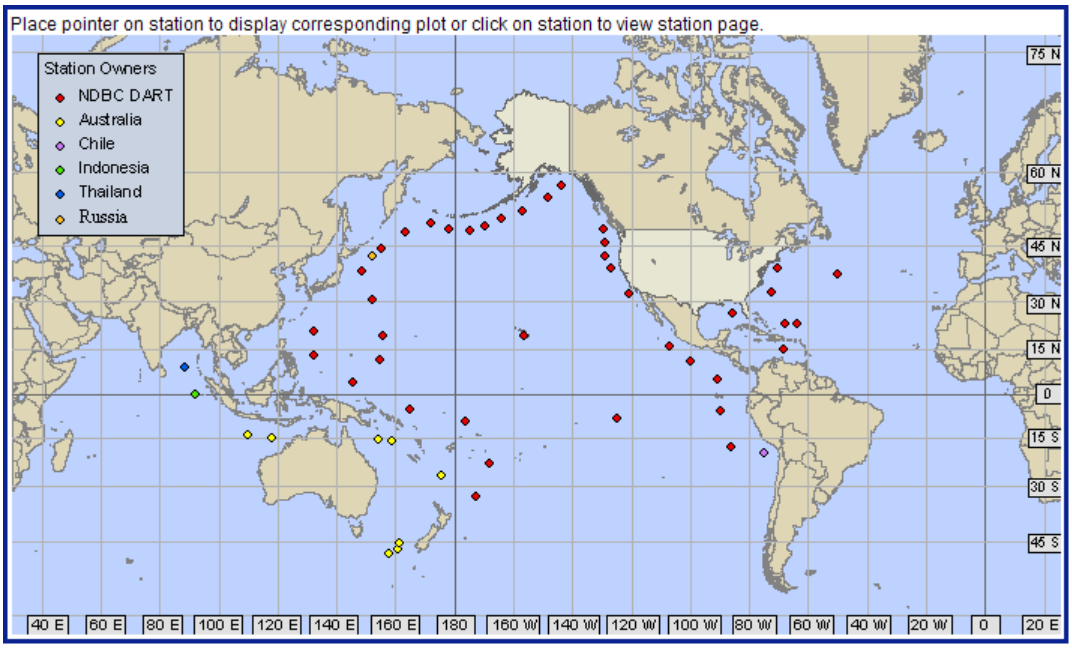

Figure 4.13 DART buoys in deep oceans (NCTR, USA). At DART buoys, sea levels are measured by bottom pressure recorders and transmitted to related data centers in real time.

Figure 4.14 shows the user interface of WebSIFT and the forecasted tsunami amplitude and arrival time for the 29 September 2009 Samoa event.

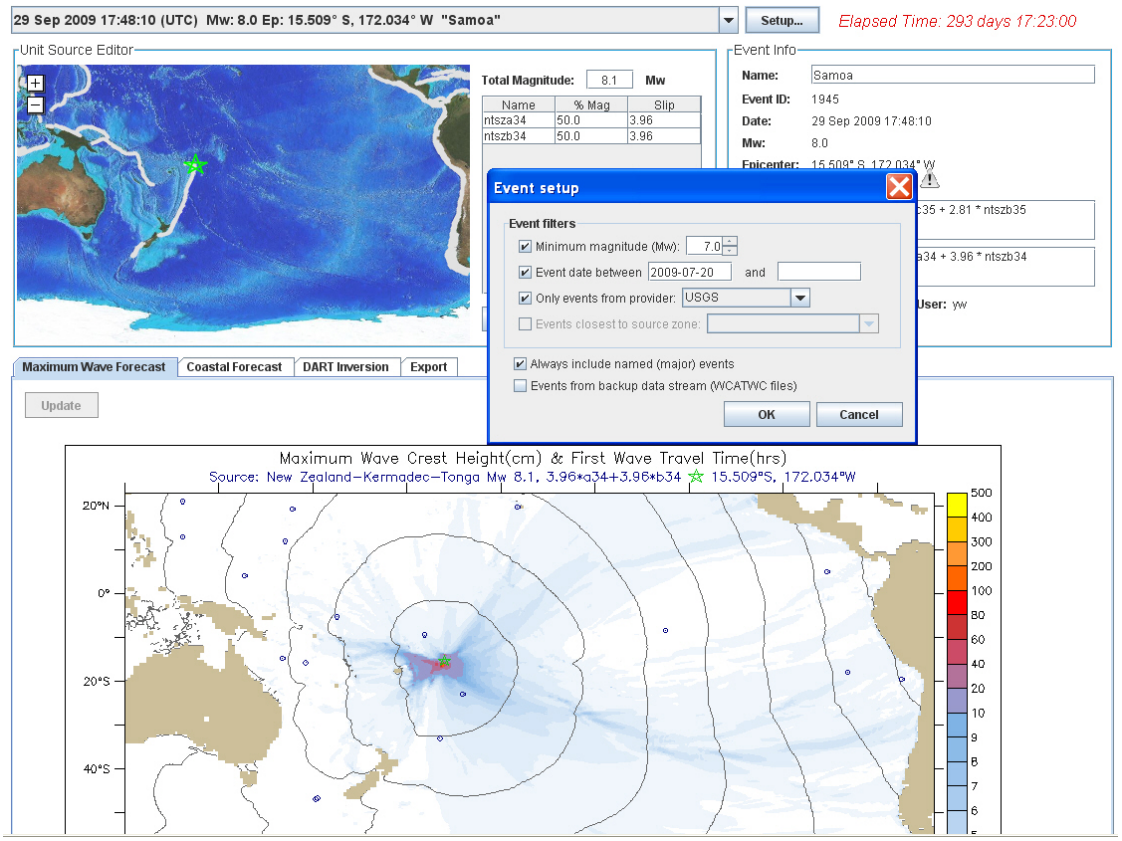

Figure 4.14 User interface of WebSIFT (NCTR, USA) and the forecasted tsunami amplitude and arrival time for the 29 September 2009 Samoa event.

The offshore tsunami wave information, provided by the real-time propagation forecast model, includes variations of wave amplitudes and velocities over time and may be used as an input to other tsunami models to evaluate the nearshore tsunami threat and calculate inundation. To facilitate this procedure, NCTR has also developed a new tool, a web-based Community Modelling Interface for Tsunamis (ComMIT), to provide site-specific inundation forecasts. ComMIT uses the output from a pre-computed tsunami propagation database, i.e., WebSIFT, as the initial condition and has a graphic user interface to output modelled results. ComMIT creates an easy interface between propagation models and inundation models (e.g., inundation modelling in MOST). However, other run-up and inundation models may also be used to simulate inundation process of tsunami with ComMIT.

GDACS (Global Disaster Alert and Coordination System, http://www.gdacs.org/) is another web-based platform for real-time disaster alert and coordination, managed by the European Commission Joint Research Center (Figure 4.15). Different from WebSIFT, GDACS is a cooperative framework that combines existing disaster information management applications. Therefore, it is a “system of systems”. Tsunami is one of the hazards being monitored and evaluated. GDACS can provide near real-time alerts about natural disasters around the world, and it provides real-time access to web-based disaster information systems and related tools to facilitate response coordination, including media monitoring, map catalogues and a Virtual On-Site Operations Coordination Centre.

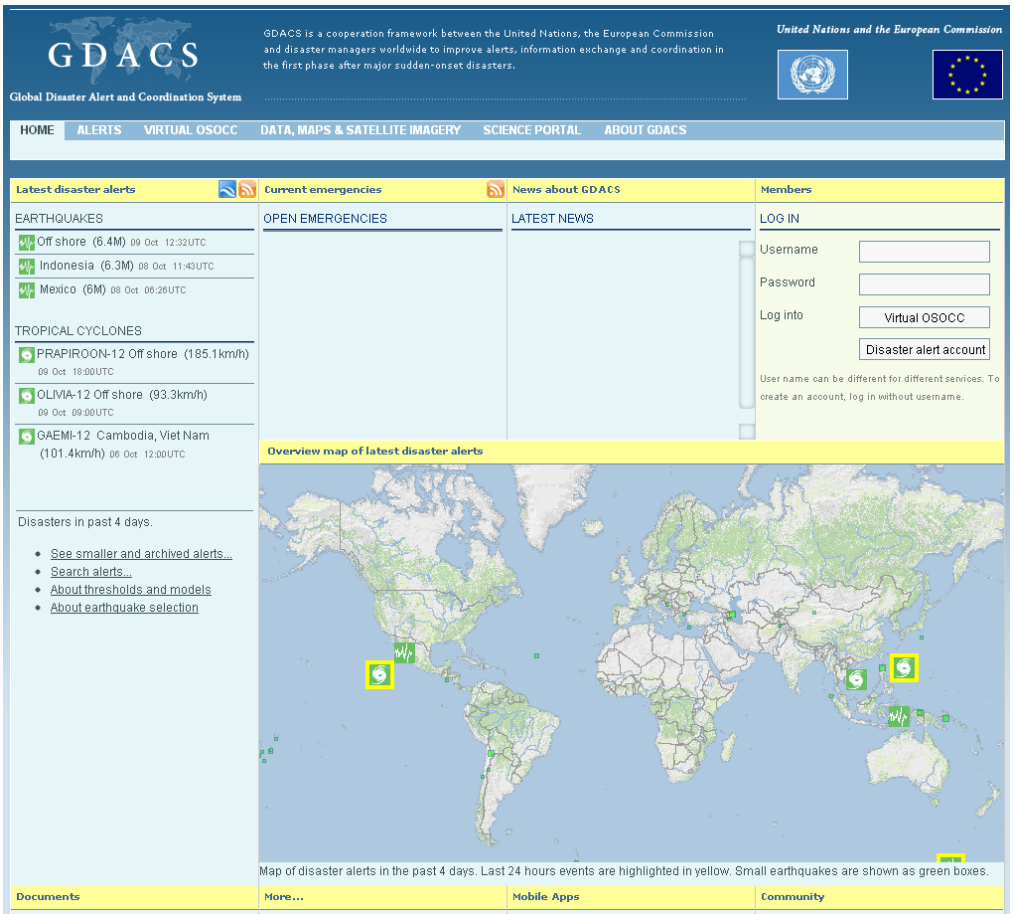

Figure 4.15 Web-based user interface of GDACS (http://www.gdacs.org/).

4.7 PROBLEMS AND LIMITATIONS OF TSUNAMI MODELLING

- In many areas of the world, including New Zealand, data from historical tsunami events, such as wave period, number of waves, inundation depths and extents, and variability along a coast, is very limited. This information is needed to validate models.
- A critical input to propagation models is the bathymetry of the seafloor, especially near-shore bathymetry, which is difficult to obtain but vital to good inundation modelling. This is because the speed, and ultimately the direction, of the tsunami are controlled by the depth of water. Model results are thus only as good as the bathymetry data allow. Much good bathymetry data exists, but combining different sources of bathymetry and processing it into the required form is one of the most labour-intensive aspects of tsunami modelling. Many bathymetry databases are proprietary, and this is also an obstacle to the preparation and use of bathymetry grids for tsunami modelling.
- Most propagation models assume that coastlines behave as perfect reflectors of tsunami waves, but this omits the natural dissipation of tsunami energy which occurs when they run-up against the shore (Dunbar et al., 1989). This leads to a gradual reduction of the accuracy of the model. This is a particular problem for modelling the effect of tsunami from distant sources, as incoming waves may arrive over the course of several hours and interact with earlier waves, especially in locations where tsunami waves may become 'trapped' within bays and inlets.
- Inundation modelling requires detailed data on the topography of the areas being considered, ideally with a vertical resolution of less than 0.25 m. Currently, very few areas of New Zealand have topography mapped to this resolution. High-resolution inundation modelling also benefits from data on the size and shape of buildings and on the nature of different land surfaces, e.g. whether forested, cultivated, urban, etc. Ideally the nearshore bathymetry and on-land topography and surface roughness can be obtained as a seamless digital elevation dataset to allow simulations using the full power of high-resolution hydraulic modelling software.
- Characterization of the tsunami source represents the biggest uncertainty for tsunami modelling. Where models are used for real-time forecasting, it is usually possible to determine only very basic information on the characteristics of the source in the time available. This problem also applies to modelling past historical tsunami where little source information may be available. Source details (e.g., slip distribution) are particularly important for local-source tsunami, as they strongly influence run-up. Deep-water wave buoys may be useful in forecasting the potential effects of distant tsunami, as they "record" the source characterization in that particular event and can be used for inverse modelling.

4.8 TSUNAMI MODELLING STUDIES RELEVANT TO NEW ZEALAND

4.8.1 Tsunami modelling studies in New Zealand

Coastal hazard analysis and detailed modelling studies such as maximum tsunami elevations and inundation modelling have been carried out for several regions in New Zealand for tsunami originating from local, regional and/or distant sources. Most of these studies are scenario-based. However, efforts have also been made recently to evaluate tsunami threats probabilistically to account for variations and uncertainties in the sources (e.g., Power et al., 2012; Lane et al., 2012).

The publicly available tsunami modelling and inundation studies are summarized in Appendix 1.

4.9 REFERENCES

Abe, K. (1979). Size of great earthquakes of 1837–1974 inferred from tsunami data. *Journal of Geophysical Research, 84*: 1561-1568.

Abe, K. (1995). Estimate of tsunami run-up heights from earthquake magnitudes. In *Tsunami: Progress in Prediction, Disaster Prevention and Warning*, Adv. Nat. Technol. Hazards Res., vol. 4, Y. Tsuchiya and N. Shuto (eds.), Kluwer Acad.: 21-35.

Abercrombie, R.E.; Antolik, M.; Felzer, K.; Elstrom, G. (2001). The 1994 Java tsunami earthquake: slip over a subducting seamount. *Journal of Geophysical Research, 106(No.B4)*: 6595-6607.

Ammon, C.J.; Kanamori, H.; Lay, T.; Velasco, A.A. (2006). The 17 July 2006 Java tsunami earthquake. *Geophysical Research Letters, 33*, L24308, doi:10.1029/2006GL028005.

Arnold, J.; Carter, J.; Dumas, J.; Gillibrand, P. (2007). Northland Regional Council Tsunami Modelling Study 3. NIWA Client Report: CHC2009-042, June 2009.

Cho, Y.-S. and Yoon, S.B. (1998). A modified leap-frog scheme for linear shallow-water equations. *Coastal Engineering Journal* 40 (2), 191–205.

Dunbar, D., LeBlond, P.H.; Murty, T.S. (1989) Maximum tsunami amplitudes and associated currents on the coast of British Columbia. *Science of Tsunami Hazards 7*: 3-44.

Enet, F.; Grilli, S.T. (2007). Experimental Study of Tsunami Generation by Three-Dimensional Rigid Underwater Landslides. *Journal of Waterway, Port, Coastal and Ocean Engineering, 133(6)*: 442-454.

Enet, F.; Grilli, S.T.; Watts, P. (2003). Laboratory experiments for tsunamis generated by underwater landslides: comparison with numerical modeling. Proc., 13th Offshore and Polar Engineering Conf., ISOPE03, Vol. 3, Honolulu, ISOPE, Cupertino, Calif., 372-379.

Fraser, S.A.; Power, W.L. (2013). Validation of a GIS-based attenuation rule for indicative tsunami evacuation zone mapping. GNS Science Report 2013/02 21 p.

Fritz, H.M. *et al.* (2007). Extreme runup from the 17 July 2006 Java tsunami. *Geophysical Research Letters, 34*, L12602, doi:10.1029/2007GL029404, 2007.

Fryer, G.J.; Watts, P.; Pratson, L.F. (2004). Source of the great tsunami of 1 April 1946: a landslide in the upper Aleutian forearc. *Marine Geology, 203*: 201-218.

Fujii, Y.; Satake, K.; Sakai, S.; Shinohara, M.; Kanazawa, T. (2011). Tsunami source of the 2011 off the Pacific coast of Tohoku Earthquake. *Earth Planets Space, 63*: 815-820.

Geist, E.L. (1998). Local tsunamis and earthquake source parameters. *Advances in Geophysics 39*: 117-209.

Geist, E.L. (2000). Origin of the 17 July 1998 Papua New Guinea Tsunami: Earthquake or Landslide? *Seismological Research Letters, 71(3)*: 344-351.

Gica, E.; Spillane, M.C.; Titov, V.V.; Chamberlin, C.D.; Newman, J.C. (2008). Development of the Forecast Propagation Database for NOAA's Short-Term Inundation Forecast for Tsunamis (SIFT), NOAA Technical Memorandum OAR PMEL-139.

Gillibrand, P.; Arnold, J.; Lane, E.; Roulson, H.; Enright, M. (2011). Modelling Coastal Inundation in Canterbury from a South American Tsunami. Environment Canterbury report number R11/08. ISBN: 978-1-927146-25-5, February 2011.

Goff, J.; Walters, R.; Callaghan, F. (2006). Tsunami source study. NIWA Client Report: CHC2006-082, August 2006.

Heinrich, P. (1992). Nonlinear water waves generated by submarine and aerial landslides. *Journal of Waterway, Port, Coastal, and Ocean Engineering, 118(3)*: 249-266.

Ide, S.; Imamura, F.; Yoshida, Y.; Abe, K. (1993). Source characteristics of the Nicaragua tsunami earthquake of September 2, 1992. *Geophysical Research Letters, 20(9)*: 863-866.

Imamura, F., Shuto, N., Goto, C. (1988). Numerical simulations of the transoceanic propagation of tsunamis. In: Proceedings of the Sixth Congress Asian and Pacific Regional Division, IAHR, Japan, pp. 265–272.

Kajiura, K. (1983). Some statistics related to observed tsunami heights along the coast of Japan, Tsunamis – Their Science and Engineering, Terra Pub., Tokyo, pp. 131-145.

Kanamori, H. (1972). Mechanism of Tsunami Earthquakes. *Physics of the Earth and Planetary Interiors 6*: 346-359.

Kanamori, H.; Kikuchi, M. (1993). The 1992 Nicaragua earthquake: a slow tsunami earthquake associated with subducted sediments. *Nature, 361*: 714-716.

Kennedy, A.B., Chen, Q., Kirby, J.T. and Dalrymple, R.A. (2000). Boussinesq modeling of wave transformation, breaking, and runup. part i: 1d. *Journal of Waterway, Port, Coastal and Ocean Engng*., 126(1):39–47.

Kennedy, A. B., Kirby, J. T., Chen, Q.; Dalrymple, R. A. (2001). Boussinesq-type equations with improved nonlinear behaviour. *Wave Motion* 33, 225–243.

Koshimura, S.; Imamura; F.; Shuto, N. (2001). Characteristics of Tsunamis Propagating over Oceanic Ridges. *Natural Hazards, 24(3)*: 213-229.

Lane, E.; Walters, R.; Arnold, J.; Roulson, H. (2007a). Northland Regional Council Tsunami Modelling Study 1. NIWA Client Report: CHC2007-109. September 2007.

Lane, E.; Walters, R.; Wild, M.; Arnold, J.; Enright, M.; Roulston, H.; Mountjoy, J. (2007b). Otago region hazards management investigation: tsunami modelling study. NIWA Client Report: CHC2007-030. September 2007.

Lane, E.M.; Gillibrand, P.A.; Wang, X.; Power, W. (2012). A Probabilistic Tsunami Hazard Study of the Auckland Region, Part II: Inundation Modelling and Hazard Assessment. *Pure and Applied Geophysics*, DOI: 10.1007/s00024-012-0538-9.

Lavigne, F.; Paris, R., Grancher, D.; Wassmer, P.; Brunstein, D.; Vautier, F.; Leone, F.; Flohic, F.; de Coster, B.; Gunawan, T.; Gomez, C..; Setiawan, A.; Cahyadi, R.; Fachrizal (2009). Reconstruction of tsunami inland propagation on December 26, 2004 in Banda Aceh, Indonesia, through field investigations. *Pure and Applied Geophysics 166(1-2)*: 259-281.

Lay *et al.* (2005). The Great Sumatra-Andaman Earthquake of 26 December 2004. *Science,* 308(5725): 1127-1133, DOI:0.1126/science.1112250

Lay, T.; Ammon, C.J.; Kanamori, H.; Kim, M.J.; Xue, L. (2011a). Outer trench-slope faulting and the 2011 Mw 9.0 off the Pacific coast of Tohoku Earthquake. *Earth Planets Space, 63*: 713-718.

Lay, T.; Yamazaki, Y.; Ammon, C.J.; Cheung, K.F.; Kanamori, H. (2011b). The 2011 Mw 9.0 off the Pacific coast of Tohoku Earthquake: Comparison of deep-water tsunami signals with finite-fault rupture model predictions. *Earth Planets Space, 63*: 797-801.

Liu,P.L.-F., Cho, Y-S., Briggs, M.J., Synolakis, C.E. and Kanoglu, U. (1995). Run-up of solitary waves on a circular island. *Journal of Fluid Mechanics*, 302: 259–285.

Liu, P.L.-F..; Woo, S.-B.; Cho, Y.-S. (1998). Computer programs for tsunami propagation and inundation. Technical report, Cornell University, 1998.

Liu, P.L.-F.; Wu, T.-R.; Raichlen, F.; Synolakis, C.E.; Borrero, J.C. (2005). eRunup and rundown generated by three-dimensional sliding masses. *Journal of Fluid Mechanics, 536*: 107-144.

Lynett, P. and Liu, P. L.-F. (2004a). A Two-Layer Approach to Water Wave Modeling. *Proc. Royal Society of London A*. v. 460, p. 2637-2669.

Lynett, P. and Liu, P. L.-F. (2004b). Linear Analysis of the Multi-Layer Model. *Coastal Engineering*, v. 51(6), p. 439-454.

Madsen, P.A., Sorensen, O.R. (1992). A new form of the Boussinesq equations with improved linear dispersion characteristics: Part II. A slowly varying bathymetry. *Coastal Engineering*, 18, 183–204.

Mansinha, L.; Smylie, D.E. (1971). The displacement fields of inclined faults. *Bulletin of the Seismological Society of America, 61*: 1433-1440.

Mori, N.; Takahashi, T.; Yasuda, T.; Yanagisawa, H. (2011). Survey of 2011 Tohoku earthquake tsunami inundation and run-up. *Geophysical Research Letters, 38*, L00G14, doi:10.1029/2011GL049210, 2011

Nwogu, O. (1993). Alternative form of Boussinesq equations for nearshore wave propagation. J. Waterw. Port Coast. *Ocean Eng.* 119 (6), 618–638.

Okada, M. (1985). Surface deformation due to shear and tensile faults in a half-space. *Bulletin of the Seismological Society of America, 75(4)*: 1135-1154.

Pararas-Carayannis, G. (1992). The tsunami generated from the eruption of the volcano of Santorin in the Bronze Age. *Natural Hazards 5(2)*:115-123.

Pararas-Carayannis, G. (2002). Volcanically Generated Tsunamis. 2nd Tsunami Symposium, Honolulu, Hawaii, USA, May 28-30, 2002.

Pararas-Carayannis, G. (2003). Near and Far-Field Effects of Tsunamis Generated by the Paroxysmal Eruptions, Explosions, Caldera Collapses and Slope Failures of the Krakatau Volcano in Indonesia, on August 26-27, 1883. Presentation for the International Seminar/Workshop on Tsunami "In Memoriam 120 Years Of Krakatau Eruption Tsunami And Lesson Learned From Large Tsunami" August 26-29 2003, Jakarta and Anyer, Indonesia. Also published in 2003 in the *Journal of Tsunami Hazards, Volume 21(4)*: 191-201.

Pararas-Carayannis, G. (2006). Risk Assessment of Tsunami Generation from Active Volcanic Sources in the Eastern Caribbean Region. In *Caribbean Tsunami Hazards* - Proceedings of National Science Foundation Caribbean Tsunami Workshop, March 30-31, 2004, Puerto Rico, Aurelio Mercado-Irizarry and Philip Liu (Eds.), World Scientific Publishing Co. Pte. Ltd., Singapore, 341 pp.

Pedlosky, J. (1979). Geophysical fluid dynamics. Springer-Verlag, 624 pp.

Peregrine, D.H. (1967). Long waves on a beach. *J. Fluid Mech*. 27, 815–827.

Popinet, S. (2003). Gerris: a tree-based adaptive solver for the incompressible Euler equations in complex geometries. *Journal of Computational Physics, 190(2)*: 572-600.

Power, W.L.; Wang, X.; Lane, E.; Gillibrand, P. (2012). A Probabilistic Tsunami Hazard Study of the Auckland Region, Part I: Propagation Modelling and Tsunami Hazard Assessment at the Shoreline. *Pure and Applied Geophysics*, DOI 10.1007/s00024-012-0543-z.

Prasetya, G.; Wang, X.; Palmer, N., Grant, G. (2010a). Tsunami inundation modelling for Tiwai Point. GNS Science consultancy report 2010/293, 75 pp.

Prasetya, G.; Wang, X.; Palmer; N.; Grant, G. (2010b). Tsunami inundation modelling for Riverton and New River Estuary Southland, GNS Science Consultancy Report CR 2011/150, 87 pp.

Satake, K.; Okada, M.; Abe, K. (1988). Tide gauge response to tsunamis: Measurements at 40 tide gauge stations in Japan. *Journal of Marine Research, 46*: 557-571.

Synolakis, C.E.; Bardet, J.-P.; Borrero, J.C.; Davies, H.L.; Okal, E.A.; Silver, E.A.; Sweet, S.; Tappin, D.R. (2002). The slump origin of the 1998 Papua New Guinea tsunami. *Proceedings of the Royal Society of London A 458*: 763-789.

Tappin, D.R.; Watts, P.; Grilli, S.T. (2008). The Papua New Guinea tsunami of 17 July 1998: anatomy of a catastrophic event. *Natural Hazards and Earth System Sciences, 8*: 243-266.

Tappin, D.R.; Watts, P.; McMurtry, G.M.; Lafoy, Y.; Matsumoto, T. (2001). The Sissano, Papua New Guinea tsunami of July 1998—Offshore evidence on the source mechanism. *Marine Geology, 175*: 1-23.

Titov, V.V.; Gonzalez, F.I.; Bernard, E.N.; Eble, M.C.; Mofjeld, H.O.; Newman, J.C.; Venturato, A.J. (2005). Real-Time Tsunami Forecasting: Challenges and Solutions. *Natural Hazards 35*: 41-58.

Tolkova, E.; Power, W.L. (2011). Obtaining natural oscillatory modes of bays and harbors via Empirical Orthogonal Function analysis of tsunami wave fields. *Ocean Dynamics, 61(6)*: 731-751; doi:10.1007/s10236-011-0388-5.

Tsuji, Y.; Imamura, F.; Matsutomi, H.; Synolakis, C.E.; Nanang, P.T.; Jumadi; Harada, S.; Han, S.S.; Arai, K.; Cook, B. (1995). Field survey of the east Java earthquake and tsunami of June 3, 1994. *Pure and Applied Geophysics, 144(3/4)*: 839-854.

Vreugdenhil, C. B. (1994). Numerical Methods for Shallow Water Flow, Boston: Kluwer Academic Publishers, 1994.

Walters, R.A. (1992). A three-dimensional, finite element model for coastal and estuarine circulation. *Continental Shelf Research*, Volume 12, Issue 1, p. 83-102.

Walters, R.A. (2005). Coastal ocean models: Two useful finite element methods. *Continental Shelf Research*, 25:775-793.

Walters, R.A.; Barnes, P.; Lewis, K.; Goff, J.R. (2006). Locally generated tsunami along the Kaikoura coastal margin: Part 2. Submarine landslides. *New Zealand Journal of Marine and Freshwater Research, 40(1)*: 17-28.

Walters, R.A.; Goff, J. (2003). Assessing tsunami hazard along the New Zealand coast. *Science of Tsunami Hazards 21(3)*: 137.

Wang, X.; Liu, P.L.-F. (2007). Numerical simulation of the 2004 Indian Ocean tsunami – Coastal Effects. *Journal of Earthquake and Tsunami, 1(3)*: 273-297.

Wang, X.; Power, W. (2011). COMCOT: a Tsunami Generation Propagation and Run-up Model, GNS Science Report 2011/43, 127 pp., in press.

Wang, X.; Power, W.L.; Bell, R.E.; Downes, G.L.; Holden, C. (2009). Slow rupture of the March 1947 Gisborne earthquake suggested by tsunami modelling. P. 221 In: Barrell, D.J.A.; Tulloch, A.J. (Eds.) Geological Society of New Zealand & New Zealand Geophysical Society Joint Annual Conference, Oamaru, 23-27 November 2009: programme and abstracts. Wellington: Geological Society of New Zealand. Geological Society of New Zealand miscellaneous publication 128A.

Wang, X.; Prasetya, G.; Power, W.L.; Lukovic, B.; Brackley, H.L.; Berryman, K.R. (2009). Gisborne District Council tsunami inundation study. GNS Science consultancy report 2009/233, GNS Science, New Zealand.

Watts, P. (1998). Wavemaker curves for tsunamis generated by underwater landslides. *Journal of Waterway, Port, Coastal, and Ocean Engineering, 124(3)*: 127-137.

Watts, P.; Grilli, S.T.; Tappin, D.R.; Fryer, G.J. (2005). Tsunami generation by submarine mass failure. II: Predictive equations and case studies. *Journal of Waterway, Port, Coastal, and Ocean Engineering, 131(6)*: 298-310.

Wells, D.L.; Coppersmith, K.J. (1994). New Empirical Relationships among Magnitude, Rupture Length, Rupture Width, Rupture Area, and Surface Displacement. *Bulletin of the Seismological Society of America, 84(4)*: 974-1002.

Wijetunge, J.J.; Wang, X.; Liu, P.L.-F. (2008). Indian Ocean tsunami on 26 December 2004: numerical modelling of inundation in three cities on the south coast of Sri Lanka. *Journal of Earthquake and Tsunami, 2(2)*: 133-155.

5.0 DEFINING TSUNAMI SOURCES

This section summarises known information about the possible sources of tsunami that could cause damage in New Zealand. For the purposes of emergency management and the time needed to respond and act on warnings, tsunami may be categorised as distant, regional or local source, depending on the shortest travel time of the tsunami from its source to the closest part of the New Zealand coastline. The travel time is generally consistent with the location of the sources, in that distant sources for New Zealand are mainly around the Pacific rim, while local sources relate to the New Zealand 'continent'. The categories that we adopt for this report are:

- Distant source – more than 3 hours travel time from New Zealand
- Regional source – 1–3 hours travel time from New Zealand
- Local source – 0–60 minutes travel time to the nearest New Zealand coast (most sources are <30 minutes travel time)

It should be noted that a local source tsunami, which may strike the nearest shore within 60 minutes, may take more than sixty minutes to travel to other New Zealand locations. This affects the time available for Emergency Management to issue a warning and so needs to be kept in mind when warning systems are being considered.

The definition of a regional source in terms of travel time sometimes causes confusion when discussing tsunami sources occurring in the southwest Pacific 'region', as a tsunami from for example, the Solomon Islands, may take more than three hours to reach New Zealand. To minimise confusion we recommend explicitly using the words 'SW Pacific region' if classifying tsunami sources according to their location rather than their travel time.

5.1 DISTANT SOURCES

5.1.1 Earthquakes

Large to Great (M>8) earthquakes are the most frequently-occurring source of damaging tsunami worldwide, and 80% of these earthquakes occur around the margins of the Pacific Ocean. At many of the plate boundaries in the circum-Pacific one tectonic plate is diving down beneath another tectonic plate, in a process called subduction (Figure 5.1). Often, the subducting and overriding plates can become stuck together due to friction on the boundary between the plates. Eventually the stored energy due to this "locking" process overcomes the strength of the plate boundary, and the two plates suddenly slip past each other in a large earthquake. The 2004 Indian Ocean tsunami was generated by this process in the Indian Ocean, where the Australian plate is subducted beneath the Eurasian plate along the Sumatran subduction zone. The Tohoku (Japan) 2011 tsunami was similarly generated on a plate boundary where the Pacific plate is subducted beneath northern Japan.

The potential of subduction zones to produce tsunami at the New Zealand coast has been assessed from the available data, including historical occurrences, numerical modelling and literature on earthquake recurrence and magnitude. The evaluation revealed that only sources in the circum-Pacific region (including New Zealand's subduction zones and some offshore faults) are likely to generate tsunami with heights of > 2 m (Figure 5.1). Tsunami have been recorded along the New Zealand coast from other sources (for example the 2004 Indian Ocean tsunami from the Indian Ocean), but these are not expected to exceed 2 m in

the maximum 2500 year return period considered in this study. The characteristics of the tsunami source areas used in the probabilistic model in Chapter 6 have been based on up-to-date review literature of the Pacific Rim regions, and include input from Global Earthquake Model (GEM) workshops and consultation with international experts. A complete compilation of the literature is beyond the scope of this review.

The 2011 Tohoku earthquake demonstrated that there may be very long intervals of time between the largest earthquakes on a subduction zone (the most recent earthquake of similar size in Tohoku was in 869 AD). Consequently, the ability to infer a maximum potential earthquake size from historical data is very limited in the Pacific where, apart from Japan, records of historical events are typically only a few hundred years long. Attempts to infer maximum earthquake sizes from geophysical properties of the converging plates have also been hampered by the short span of records, and several factors that have previously been proposed as controlling maximum earthquake size have been contradicted by recent events. From a civil defence standpoint it is should be assumed that any subduction zone could produce a magnitude 9 earthquake, unless there are strongly convincing counter-arguments. For hazard and risk assessments, the uncertainty in estimates of maximum magnitude should be reflected in the hazard modelling inputs (i.e., logic-tree weights, or epistemic uncertainty distributions) for the source regions.

5.1.1.1 South America

The west coast of South America (Figure 5.1) is one of the most frequent sources of tsunami in the Pacific, resulting from great earthquakes on the boundary where the Nazca, Cocos, and Antarctic plates subduct beneath the South American tectonic plate. Earthquakes along this coastline produce tsunami that are often directed towards New Zealand, due to both the orientation of the plate boundary on which the earthquakes occur, and to a lesser degree from refraction of tsunami waves by undersea ridges and other bathymetric features between South America and New Zealand. There are also very few island chains between New Zealand and South America to block or scatter the tsunami waves.

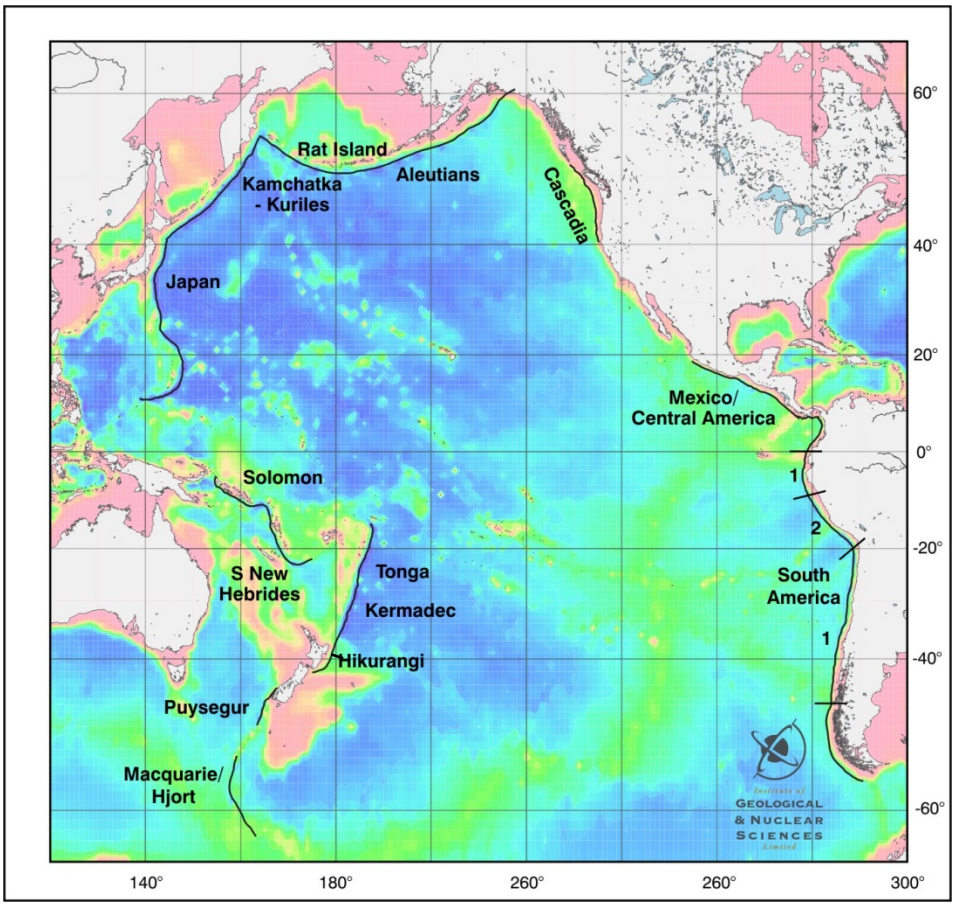

Figure 5.1 Subduction margins in the circum-Pacific region. The South American coastal margin can be partitioned into regions that propagate tsunami either south-westward toward eastern New Zealand (region 2), or direct tsunami further northward, thus more strongly affecting the north Pacific (region 1). The 1868 tsunami was generated in region 2, while the larger but less damaging (in New Zealand) 1960 tsunami originated in region 1.

For example, the distant-source tsunami that caused the most damage to New Zealand in historical times was caused by an earthquake on the southern coast of Peru in 1868 (region 2 of Figure 5.1; see also Section 3.2); the magnitude of this earthquake is estimated to be about M_W9.1. This area of South America's coastline is oriented in such a way that the tsunami energy is more effectively directed towards New Zealand than it is for other sections of the South America coast, where the majority of the energy tends to be directed further north. Should a larger earthquake than the 1868 event occur along this part of the coast, the effects in New Zealand could be considerably greater than occurred in 1868.

In contrast, the 1960 tsunami, although caused by a much larger earthquake (M_W9.4, possibly M_W9.5; see Section 3.2), occurred on a part of the South American plate boundary that is not as well oriented to New Zealand as the 1868 location (southernmost region 1 of Figure 5.1). It produced a smaller tsunami in New Zealand than would have occurred had the source location been better oriented. Nevertheless, the 1960 tsunami caused run-ups of up to 4 m in parts of the North and South Islands. The 2010 Chilean tsunami, caused by an earthquake of magnitude M_W8.8 that occurred to the north of the location of the 1960 earthquake, had run-up heights of up to 1 m in parts of the North and South Islands.

The magnitude of the 1960 earthquake, at M_W9.4-9.5, is probably close to the upper limit for earthquakes for the whole South American coastline (and worldwide). It is uncertain whether other portions of the South American subduction margin are capable of producing earthquakes of this size, or whether most segments have more frequent but relatively smaller earthquakes of M_W8–9.When the earthquake catalogue for the whole South American

margin is analysed, the frequency of large earthquakes appears to decrease with increasing magnitude—for every unit increase in magnitude the frequency of earthquakes drops by about a factor of ten.

Computer models (Power et al., 2004), combined with historical observations, suggest that there is minimal risk of a damaging tsunami in New Zealand generated by South American earthquakes with magnitudes of less than 8.5.

The historical records of Peru and Chile, which are hundreds of years longer than New Zealand's, indicates that large earthquakes and tsunami have occurred relatively frequently in the last 450 years (Table 5.1). From the table it can be seen that over 450 years there were nine earthquakes with magnitudes of $M_W > 8.5$ that caused run-up heights near the earthquake source that were similar to or greater than those produced by the 1868event. Those earthquakes prior to 1868 probably produced significant tsunami in New Zealand prior to European settlement. The average return period (50 years) is about the same as has occurred in the last 160 years, and indicates the frequency of potentially damaging tsunami from South American sources in New Zealand.

Paleotsunami work conducted by Cisternas et al. (2005) suggests that tsunami comparable in size to the 1960 event occur in southern Chile with an average interval of slightly less than 300 years.

As tsunami from South America approach New Zealand from the east, the east coast will be more affected than the west coast. However, waves do propagate around New Zealand, as well as through Cook Strait, and the west coast will have significant waves in some cases.

Table 5.1 Large South American earthquakes that have produced tsunami with maximum tsunami heights greater than 8 m locally (extracted from Gusiakov, 2001; additional information on the 2001 and 2010 earthquakes from the NGDC tsunami database). Events shown in bold are either known to have caused, or had the potential to have caused a significant impact in New Zealand comparable to the 1868, 1877 and 1960 tsunami. The magnitudes for early events (shown by grey shading) may have large errors. Note: M_b or M_s – body wave or surface magnitude; M_W –moment magnitude; M_t –tsunami magnitude [Abbreviations: S = south; N = north;].

Year	Mth	Day	Lat. (°N)	Long. (°E)	M_b or M_s	M_w	M_t	Max. run-up at source (m)	Source	Max run-up in NZ (m)
1562	**10**	**28**	**-38.70**	**-73.20**	**8.0**			**16**	**S. Central Chile**	
1586	**7**	**9**	**-12.20**	**-77.70**	**8.5**			**26**	**Off Lima, Peru**	
1604	**11**	**24**	**-18.50**	**-70.35**	**8.4**			**16**	**Africa, N. Chile**	
1657	3	15	-36.80	-73.00	8.0			8	Conception, S. Chile	
1687	10	20	-13.50	-76.50	8.5			8	Callao, Lima, Peru	
1730	**7**	**8**	**-32.50**	**-71.50**	**8.7**			**16**	**Valparaiso, Chile**	
1746	**10**	**29**	**-12.50**	**-77.00**	**8.0**	**8.6**	**9.2**	**24**	**Callao, Lima, Peru**	
1806	12	1	-12.10	-77.10	7.5			6	Peru	
1835	**2**	**20**	**-36.50**	**-72.60**	**8.5**			**14**	**Conception, S. Chile**	
1837	11	7	-42.50	-74.00	8.5		9.2	8	Corral, S Chile	
1859	10	5	-27.00	-70.40	7.7			6	Caldera, Chile	
1868	**8**	**13**	**-17.70**	**-71.60**	**8.8**	**9.1**	**9.0**	**18**	**Arica, S. Peru**	**4; (10 Chatham Islands)**
1877	**5**	**10**	**-21.06**	**-70.25**	**8.8**	**9.0**		**21**	**Iquique, N. Chile**	**~3.5**
1922	11	11	-28.31	-70.28	8.3	8.7		9	Caldera, Chile	~1
1929	8	9	-23.60	-70.40				8	N. Chile	
1960	**5**	**22**	**-38.31**	**-72.65**	**8.6**	**9.5**	**9.4**	**25**	**S. Chile**	**~4**
1960	11	20	-6.64	-80.55	6.9	7.7	7.7	9	N. Peru	
1996	2	21	-9.71	-79.86	6.6/7.5	7.8	7.8	5	Peru	
2001	6	23	-16.26	-73.64	6.7/8.2	8.4	8.2	7.0	Camana, S. Peru	
2010	2	27	-36.122	-72.898	7.2/8.5	8.8	8.8	29.0	Conception, S. Chile	~1

5.1.1.2 Mexico and Central America

The largest well-recorded historical earthquakes in the Mexico and Central America area (Figure 5.1) have magnitudes of less than M_W 8.5, too small generally to produce a damaging Pacific-wide tsunami. However an earthquake in 1787 is estimated at ~M_W 8.6 (Suarez and Albini, 2009), and the possibility of still larger earthquakes cannot be excluded (Hjorleifsdottir et al., 2012).The coastline of this region is well oriented for directing tsunami towards New Zealand, and the possibility of earthquakes that produce tsunami large enough to be damaging in New Zealand cannot be ruled out.

5.1.1.3 Cascadia

The Cascadia margin refers to the boundary between the Juan De Fuca and North American tectonic plates between northern California and Vancouver Island (Figure 5.1). The Cascadia plate interface has an extensive paleoseismic record based on analysis of turbidites (Goldfinger et al., 2012). The turbidite record suggests 40 large earthquakes in the past 10,000 years, 19 of which are thought to have been whole-region ruptures of about magnitude 9.0, and the remainder are thought to be segmented ruptures with typical magnitudes of 8.2-8.6. Between these large events the Cascadia plate interface appears to be relatively seismically inactive.

The last great Cascadia earthquake occurred in 1700 AD; it was identified from historical tsunami records in Japan, and is consistent with geological evidence from the United States and Canada (Atwater et al., 2005). This date is earlier than written records in New Zealand, as it is in the United States and Canada, and the only means to estimate likely impact in New Zealand is by using numerical modelling. Japanese researchers have estimated the magnitude of the 1700 AD event at M_W 9.0. An earthquake of this magnitude is expected to produce a tsunami with amplitudes up to about 1 m in many parts of New Zealand, and possibly 1–3 m in Banks Peninsula and the Chatham Islands. The dimensions of the Cascadia subduction zone appear to set an upper limit on the magnitude of possible earthquakes at about M_W 9.2; at this magnitude many areas of New Zealand would be expected to experience waves with amplitudes between 1–3 m.

5.1.1.4 Alaska and the Aleutians

The plate boundary between Alaska and the Aleutians (Figure 5.1) is a highly active source of great (M_W> 8.0) earthquakes and tsunami in the Pacific. Historically, three earthquakes—the 1964 M_W 9.4 Alaska, the 1957 M_W 8.7–9.1 Rat Island, and the 1946 M_W 7.9 Aleutian earthquakes—have caused run-ups of up to 2 m along the north and east coasts of New Zealand, but not at any of the urban centres.

The historical record here is too short to reflect the full range of tsunami that New Zealand might experience from the Alaskan and Aleutians region. However, most parts of the coastline produce tsunami that are not particularly well directed to New Zealand, with exception of the area around the source zone of the 1957 Rat Island earthquake.

5.1.1.5 Kurile Islands, Kamchatka

The largest earthquake in the Kurile Islands-Kamchatka area (Figure 5.1) to produce a tsunami recorded in New Zealand is an M_W 9 earthquake south of Kamchatka Peninsula in 1952. Near the earthquake source this event produced a maximum run-up of nearly 19 m,

with a maximum run-up in New Zealand of over 1 m in Gisborne. A larger tsunami, with a maximum run-up of 63 m locally and 15 m at a distance of over 1000 km away, was recorded in 1737 from an earthquake with an estimated magnitude of M8.3. Its effects in the larger Pacific area are unknown. The capacity of the area to produce earthquakes with magnitudes greater than the M9.0 in the historical record is unknown.

5.1.1.6 Japan

The subduction zones off Japan (Figure 5.1) are some of the most active in the Pacific. The region also has one of the longest historical records of large earthquakes and tsunami, spanning over a thousand years. Until recently, no earthquakes offshore Japan were thought to have reached magnitude 9, although there are many historical events over magnitude 8. In New Zealand's historical record prior to 2011, only very small waves with amplitudes of less than a metre were recorded from Japanese earthquakes. The largest historical subduction thrust earthquake in Japan was of M_W 9.0 rupturing much of the northern Japan Trench in March 2011 (see also Section 3.3). This event produced tsunami with runup heights of as much as 35 m at locations along the northeast Japan coastline, with inundation of areas up to about 5 km inland from the coast on the Sendai plain, and significantly further along the banks of rivers. In New Zealand wave amplitudes of up to about 1 m were recorded at various tide gauges (Borrero et al., 2012). A marine threat warning was issued throughout New Zealand for this event, and anomalous waves and currents related to the tsunami were observed for several days after the earthquake. There was some flooding of residential houses at the head of the bay at Port Charles in the Coromandel. We expect that earthquakes on Japan's subduction boundaries much larger than the March 2011 event are rare (i.e. with recurrence intervals of several thousands of years, if they occur at all), although events up to M_W 9.5 cannot be entirely ruled out. The worst case M_W 9.5 scenario would lead to wave heights in New Zealand approximately 2–3 times the ones observed from the March 2011 event. Fortunately, the propagation path from Japan to New Zealand is studded with islands that are thought to protect New Zealand from wave amplitudes of more than 2–3 m, even in this worst case.

5.1.1.7 Solomon Islands, Papua New Guinea

Historically, the Solomon Islands and Papua New Guinea (Figure 5.1) have produced few earthquakes over magnitude 8.5, although we cannot rule out this possibility. In Papua New Guinea, the primary source that could affect New Zealand would be the New Britain Trench. However, the PNG mainland and numerous islands located between the New Britain Trench and New Zealand would scatter the waves. However, great earthquakes on the San Cristobal Trench just to the southwest of the Solomon Islands could pose a significant tsunami hazard to New Zealand. Modelling has shown that the Lord Howe Rise behaves as a waveguide, steering tsunami waves from the Coral Sea region towards New Zealand. Historically, few tsunami from this region have produced tsunami heights exceeding 1–2 m at a large distance from the source. The M_W8.1 earthquake in the Solomon Islands on 2 April 2007 produced a tsunami with a maximum reported run-up height of 12 m in the Solomons and killed 52 people; the largest recorded waves in New Zealand from this event were just over half a metre in amplitude.

5.1.1.8 Northern New Hebrides

The northern part of the New Hebrides subduction zone is a distant source, while the central and southern parts (see Section 5.2.1.1) are regional sources, using our criteria based on travel-time. The possibility exists that a very large earthquake could rupture multiple fault

segments. Near Vanuatu in the central part of the New Hebrides region, large earthquakes with magnitudes of 8.5 or less have created tsunami with run-ups of 12 m locally. The northern part of the New Hebrides subduction zone is not well oriented to direct tsunami towards New Zealand, although modelling suggests that undersea ridges in the Tasman Sea will direct some of the tsunami energy towards New Zealand.

At the New Hebrides Trench, the Australian plate is moving northeast and being subducted beneath Vanuatu and the adjacent area containing a complex series of rifts and transforms in the North Fiji Basin. Plate movement velocities determined by GPS indicate the plates are converging at the New Hebrides Trench at rates of 4–16 cm/year (Calmant et al, 2003; Power et al, 2012), The GPS data in Vanuatu suggest that a large portion of the plate interface of the New Hebrides subduction zone is strongly locked together between earthquakes (Power et al., 2012), which will presumably result in a major subduction thrust earthquake in that region when the accumulated plate boundary strain is eventually released.

There have been dozens of earthquakes (> M_W 7.5) in the New Hebrides Trench region over the last century, including two estimated M_W 8.0 events in 1878 and 1920. However, we cannot rule out the possibility of rupture of the northern New Hebrides Trench over a larger area, causing an M_W 9 or larger earthquake (Wright et al., 2011).

5.1.1.9 Summary comments

Few areas can, with certainty, be excluded as a source of damaging tsunami until all earthquake sources are considered and numerical modelling has revealed the extent, or lack, of a threat. For global distances, there are significant uncertainties about the potential for tsunami from sources in northern South America, Cascadia (western USA), Mexico, Central America, Alaska and the Aleutians. The 2004 Sumatra and 2011 Tohoku (Japan) tsunami have, however, changed the perspective regarding the potential for earthquakes of magnitude 9 or above on many subduction zones. It has become apparent that many conclusions were incorrectly drawn because they were based on historical records that were in fact too short to include the largest earthquakes which occur infrequently. At this time the main plausible way to determine a limit on the maximum size of earthquake that a subduction zone could experience is from the total length of the subduction zone, i.e., subduction zones cannot experience earthquakes larger than a cut-off magnitude determined by their length (McCaffrey, 2007); this cut-off is lower for shorter subduction zones.

5.1.2 Landslides

The role of submarine landslides and their potential to produce local, regional and Pacific-wide tsunamihas undergone critical international scientific review and debate in recent years, particularly as a result of a devastating tsunami in 1998 in Papua New Guinea. Some scientists have attributed this larger-than-expected tsunami to the magnitude and seismic characteristics of the generating earthquake, others to the occurrence of an offshore landslide a few minutes after the earthquake (Geist, 2000; Tappin et al., 2001). This has led many tsunami researchers to recognise that submarine landslides may play a greater part in generating local tsunami than previously thought. Submarine landslides have also been argued to have added substantially to the trans-Pacific tsunami resulting from a 1946 earthquake in the Aleutians (Fryer et al., 2004). They argue that the narrow “beam” of devastating tsunami that swept Hawaii and the Marquesas Islands, and had a run-up of 4 m in Antarctica, was the result of a 200 km^3 landslide triggered by the M_W 7.9 subduction earthquake. Others (e.g.,Tanioka and Seno, 2001) have suggested the earthquake had very

large slip for its apparent magnitude, such that it would fall into the category of so-called "tsunami earthquakes".

Modelling indicates that huge sector collapses (1000–5000 km^3) of the flanks of the Hawaiian volcano chain could produce Pacific-wide tsunami, as well as very large local tsunami of hundreds of metres (McMurtry et al., 2004). While it is likely that flank collapses of this scale would produce large tsunami in New Zealand, their return periods from any one source are well in excess of the 2500-year return period covered in this study. Therefore, no landslides at global distances are considered viable tsunami sources within the 2500 year period.

5.1.3 Volcanoes

Other than the potential for flank collapse on the slopes of volcanoes, no volcanoes in the historical record are known to have directly produced significant tsunami at great distances. The great 1883 eruption of Krakatau, Indonesia, produced huge local tsunami with some run-up heights exceeding 40 m, but tsunami-like water level oscillations observed at great distances from the volcano have been attributed to a coupling of an atmospheric pressure wave with the ocean. These waves, given the name *rissaga*, or atmospheric tsunami, are outside the scope of this review. Not enough is known about their mechanisms to include them as a tsunami source for this review. Nevertheless, oscillations in New Zealand following the Krakatau eruption included 1.8 m (measured peak to trough) waves at Whitianga and in the anchorage area at Auckland (although only 0.9–1.2 m at the Auckland docks) (de Lange and Healy, 1986).

5.1.4 Bolide impact

As an island nation surrounded by a large deep sea, New Zealand has a tsunami hazard from impacts of asteroids and comets. This hazard is real, finite and determinable, but the probability of a damaging tsunami from bolide impact is low. One such large event is known to have occurred on Earth within recorded human history—a meteor exploded over Constantinople on a clear afternoon in 472 AD, hitting the city with a wave that knocked sailboats flat in the water.

Asteroids and comets are collectively known as Near Earth Objects (NEOs) when they approach close to Earth, especially if their closest approach is less than the distance to the moon. If they enter the Earth's atmosphere, they are collectively called bolides. The visible track of a bolide across the sky is a meteor, or shooting star. The solid objects that sometimes are recovered later are meteorites. A meteorite survives its passage through the atmosphere and hits Earth about once every two hours.

Current technology allows us to detect and track the larger NEOs (larger than a few metres in diameter) and calculate their probability of hitting Earth, days, weeks, and sometimes months in advance of their closest approach. The larger the body, the further out it can be identified and tracked. At any time, there are always some NEOs, and many approaching. (A current list of NEOs can be viewed at http://neo.jpl.nasa.gov, and is updated at least daily). If a NEO large enough to be of concern were likely to hit the Earth, substantial advance warning would be given; in fact several warnings have been made public before very near misses. All significant objects on a collision course can be tracked, and their likely impact site on Earth predicted, with known uncertainty, some substantial time in advance of impact. Large bolides, however, have never been so common that they have featured prominently in human history.

Numerical estimates of the frequency of impact of a meteorite of sufficient size within a distance range of New Zealand that could cause a damaging tsunami appear to have a recurrence interval many times longer than the 2500 years considered in this project (see Appendix 2 for details of the calculation). This estimate of long recurrence intervals for meteorite generation of damaging tsunami is consistent with their scarcity in human records. Because of the apparent long return period for a damaging tsunami generated by meteorite to affect New Zealand we do not consider this source further in our tsunami source descriptions.

While most bolide impacts occur as distant sources of tsunami to New Zealand, they may also occur at regional or local distances.

5.2 REGIONAL SOURCES

The warning time for tsunami from regional sources is about 1–3 hours, and presents a real challenge to monitoring and warning agencies. To locate an event, evaluate its tsunami potential and issue a warning in so short a time is problematic, requiring pre-planning and scenario development. Self-evacuation of residents will be required at short notice. As outlined in the following sections, regional source tsunami may represent a significant hazard and risk, and these may be catastrophic on rare occasions.

Regional sources include earthquakes and volcanoes (eruption and flank collapse) from tectonically active regions to the north of New Zealand, and south of New Zealand from about 50-60°S. Regional sources of tsunami to the east and west are highly unlikely (but note that the Solomon Islands subduction zone is a *distant* source that primarily affects the west coast of New Zealand, even though it occurs in the 'SW Pacific region'). Hence, the coasts most at risk from regional source tsunami are the northern half of the North Island and the southern half of the South Island.

The following sections outline what is known about the historical impact of regional source tsunami, about the sources of potentially damaging tsunami, and what has been learnt and can be learnt from numerical modelling, and from geological studies of pre-historical tsunami. They form the basis for what is known about the frequency and magnitude of events that New Zealand might expect to experience.

5.2.1 Earthquakes

In New Zealand's historical record, the largest earthquakes along the arc between New Hebrides (Vanuatu), Kermadec Islands and Tonga have been less than magnitude 8.5. Only two of these are known to have caused tsunami with run-ups in New Zealand approaching 1 m. Although the record of run-ups in New Zealand may be incomplete, we would expect a large event in historical times to have been noted.

To the south of New Zealand, only a few large earthquakes have occurred since the 1960s, when the installation of a worldwide seismic network allowed large earthquakes to be identified and located. The only three large earthquakes in the last 40 years had magnitudes between 7.8 and 8.4, and all were in areas of the plate boundary where earthquakes with predominantly horizontal (strike-slip) movement along the fault occur. These earthquakes do not usually generate large tsunami and none had run-up of > 1 m in New Zealand (along the south and west coasts of the South Island).

In this section we address the potential of each subduction zone at regional distances, to generate tsunami that could produce tsunami heights of 2 m or more in New Zealand, and within the 2500 year return period considered in this project.

The 2011 Tohoku earthquake demonstrated that there may be very long intervals of time between the largest earthquakes on a subduction zone (the most recent earthquake of similar size in Tohoku was in 869 AD). Consequently the ability to infer a maximum potential earthquake size from 100–200 years of historical data is very limited.

5.2.1.1 Southern New Hebrides

The central and southern parts of the New Hebrides subduction zone are regional sources according to our criteria based on travel-time, while the northern part is a distant source (see 5.1.1.8). Large earthquakes with magnitude up to 8.5, causing tsunami with run-ups of 12 m locally, have occurred near Vanuatu in the central part of the New Hebrides region. The central part of the New Hebrides subduction zone is not well oriented to direct tsunami towards New Zealand. The southern part is well oriented, but here the record of earthquakes is probably complete only from 1960 onward.

The historical record of earthquakes in the Southern New Hebrides is short, and complete for major earthquakes (M_W >~7.5) only over the past century. This is primarily a consequence of their remote location, the largely uninhabited nature of the few islands in the eastern part of the arc, and the lack of surviving oral history accounts from the pre-colonisation cultures on the islands. The largest historical event occurred in August 1901, with an estimated magnitude of 7.9–8.4, and several lives were lost on islands close to the earthquake due to the tsunami (see summary in Power et al., 2012). The observed maximum water heights in Hawaii from this tsunami were up to 1.2 metres, and were significantly larger than those of the 2009 M_W 8.1 Samoa earthquake. On this basis, Power et al. (2012) favour the interpretation of a moment magnitude for this event of around 8.4.

Power et al. (2012) show that earthquakes larger than an M_W 8.0 on the southern section of the New Hebrides trench (Figure 5.1) could present a significant hazard for Northland. An under-sea ridge (the Three Kings Ridge) extends north from Cape Reinga and acts as a waveguide (see the discussion of waveguide effects in Section 4.2.2.2), leading to potentially hazardous wave heights in the northern North Island. Numerical models show that earthquake scenarios ranging from M_W 8.15 to M_W 8.8 on the southern New Hebrides Trench could lead to maximum tsunami heights of 2 to 15 m respectively at highly amplifying sites in the far north, such as the Aupouri Peninsula. Along the eastern and western coastlines of Northland, maximum expected tsunami heights range from less than 1 to ~5 metres as the magnitude ranges from M_W 8.15 to M_W 8.8.

5.2.1.2 Tonga Trench

Historically, earthquakes have not exceeded magnitude 8.5 in the Tonga Trench (between 14–26°S), and the tsunami have not significantly affected New Zealand, principally because of the orientation of the subduction margin. It has been thought that the potential for regional scale tsunami was limited, as the plate interface appears to be uncoupled, so the plates slide past each other relatively freely (Bevis et al., 1995), but the September 2009 Samoa tsunami (also called the ‘South Pacific tsunami’; see Section 3.3) was found to be caused by two near simultaneous earthquakes—one on the subduction interface and the other on an outer rise normal fault (Beaven et al., 2010; Lay et al., 2010), so this assumption is open to question. If the magnitude of earthquakes on the Tonga Trench were to be limited only by subduction

zone length, then earthquakes with magnitudes up to the low 9s would be possible; yet this still appears to be unlikely based on the lack of coupling revealed by current geodetic measurements (though these measurements are not sufficient to fully reveal the extent of coupling, especially close to the trench).

5.2.1.3 Kermadec Trench

The Kermadec Trench is both a regional tsunami source and a local source. Earthquakes caused by rupture along only the northern half of the Kermadec Trench could produce tsunami that take more than an hour to reach New Zealand (excluding the Kermadec Islands), while rupture of the Kermadec Trench south of ~33°S could produce tsunami that reach some parts of New Zealand in less than an hour. Because of the orientation of the Kermadec Trench, even for tsunami originating on the southern part of the trench, the most strongly affected coasts are usually more than one hour travel time away.

The c. 1400 km long Kermadec Trench has a moderate level of historical seismic activity, In the 33 years from 1976 to 2009, 544earthquakeswith a magnitude greater than 5 originated on the shallow part (≤ 40 km depth) of the plate interface (based on thrust mechanisms) (Power et al., 2012). Power et al. (2012) used the seismicity data, and the available geodetic data, to assess the potential for large tsunamigenic earthquakes, and modelled the consequences of such events.

There have been three significant earthquakes on the southern half of the Kermadec Trench (e.g., south of 29°S) since the beginning of the 20th century, namely the earthquakes of 2 May 1917 (M8–8.6), 14 Jan 1976 (M7.8–8), and 20 October 1986 (M 7.9). The 1976 earthquake occurred near Raoul Island and was likely a low-angle thrust earthquake along the main subduction plate interface. This earthquake caused a tsunami that was widely observed in the Pacific, primarily on tide gauges, but also as observed run-ups. Several yachts were damaged in Tutukaka harbour near Whangarei in New Zealand (Bay of Plenty Times, 15 January 1976; Downes, pers. comm.). The 1986 earthquake is consistent with normal faulting within the subducting Pacific Plate (see summary in Power et al., 2012), and only very small (< 10 cm) water height changes were observed at tide gauges in Hawaii, French Polynesia and Samoa.

The ability of the Kermadec Trench to produce earthquakes larger than about M_W 8.5 is not well known. Comparisons with other subduction margins similar to the Kermadecs (Mariana, for example) would lead us to suspect that the plate interface is relatively weakly coupled, i.e., the plates are sliding past each other relatively freely and without building up elastic energy that is then released as earthquakes. However, analysis of GPS data from Raoul Island (the only existing GPS site on the Trench) indicates that the plate interface is probably strongly coupled or locked, at least in that part of the Trench (Power et al., 2012).

Power et al. (2012) conducted numerical modelling of four plausible scenarios for Kermadec Trench rupture, ranging from earthquakes of M_W 8.5 (restricted to the far southern Kermadec Trench) to M_W 9.4 (rupture of the entire Kermadec Trench). The M_W 9.4 scenario was included, as the possibility of rupture of the entire trench cannot be ruled out empirically (McCaffrey, 2007), although if such an event occurs it is likely to be very rare (i.e., with a recurrence interval of several thousand years). The numerical results show that tsunami generated from the southern and/or middle sections of the Kermadec subduction zone pose a greater hazard to the coast of New Zealand than tsunami generated along the northern Kermadec Trench. For tsunami generated on the northern Kermadec Trench, the majority of energy travels towards the open Pacific, as well as through the South Fiji Basin to the

northwest toward Norfolk Island and New Caledonia. In contrast, if the southern and/or middle sections of Kermadec plate interface are ruptured, refraction effects due to the sloping continental shelf of North Island will gradually bend tsunami waves onshore, and thus much more energy will be directed toward the coasts of the Northland and Auckland regions.

The largest event modelled by Power et al. (2012) was an M_W 9.4 earthquake rupturing the plate interface along the entire Kermadec Trench. Numerical models show that such an event could produce tsunami causing tremendous damage throughout the coastal areas between Gisborne and Northland. Along the coasts of the Raukumara Peninsula and the Bay of Plenty, tsunami wave amplitudes around 5–10 m would be expected. On many parts of the northeastern coasts of Great Barrier Island and Northland, calculated tsunami run-up heights would be about 15–20 m above the normal level. Tsunami waves of over 10 m amplitude also would strike the southwestern coast of the Aupouri Peninsula and Ahipara Bay on the west coast of northern Northland. However, if such giant events do occur, they would be very rare indeed.

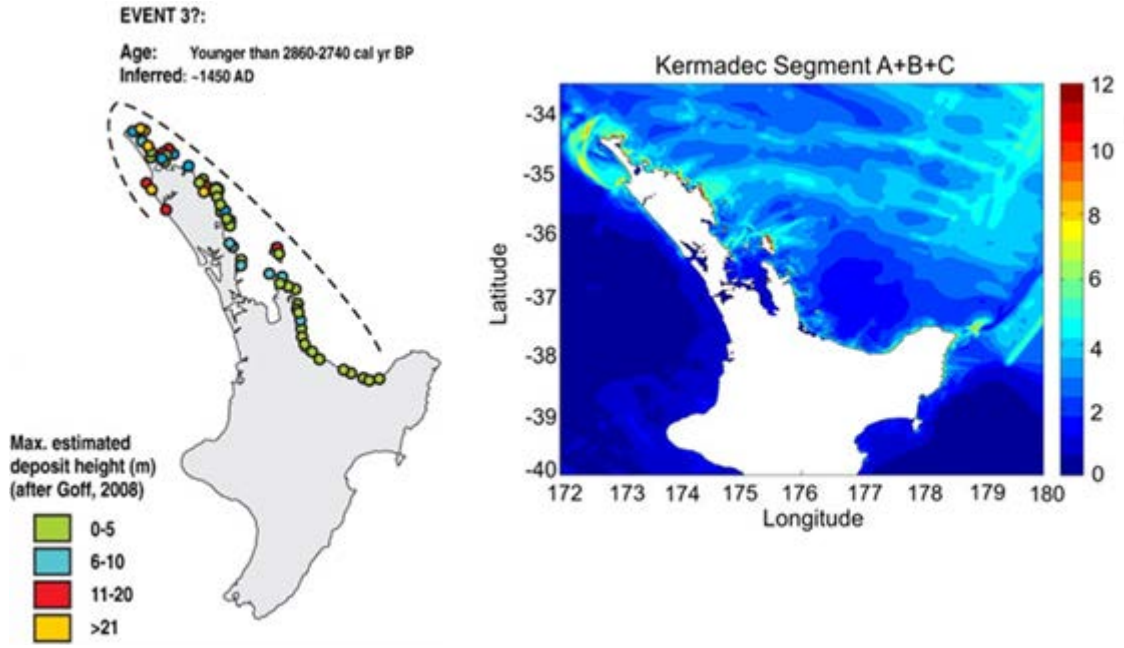

Figure 5.2 (Left) Paleotsunami deposits and their height distribution for the event with an inferred date of ~1450AD (Goff, 2008; Goff et al., 2010); (Right) maximum water level distribution (offshore) in modeled MW 9.4 Kermadec Trench scenario (Power et al., 2012).

There is a remarkable similarity in the distribution of estimated tsunami heights caused by the hypothetical M_W 9.4 event and the distribution of paleotsunami deposits assigned to a tsunami in approximately 1450 AD by Goff et al. (2010) (Figure 5.2). As most of the tsunami energy originating on the northern half of the Kermadec Trench passes to the north of New Zealand, an earthquake on just the southern part of the trench could achieve a similar distribution of run-up heights at a lower magnitude, though this would probably still need to be at least M_W 9. Unless a more plausible explanation for the paleotsunami data can be made, the possibility of such events needs to be taken seriously.

For the scenario in which a 300 km long section of the southern Kermadec Trench (between ~36°S to ~38°S) ruptures in an M_W 8.5 event, water levels 3–5 m above mean sea level would occur along the northeastern coasts of Northland and the Auckland region, as well as the coasts of Gisborne and the Bay of Plenty. Waves with amplitudes of over 10.0 m would strike the northeastern coasts of Great Barrier Island. Water level increases of 1.0–3.0 metres would occur along the southwestern coast of Northland.

5.2.1.4 South of New Zealand (including Macquarie Ridge)

Most plate boundary zones in the Southern Ocean have horizontal (strike-slip) movement and large earthquakes in these zones are unlikely to produce large tsunami. There are no highly active subduction zones in the Southern Ocean. The Hjort Trench (56°S–60°S) and subduction zone is the only part of the margin where significant vertical deformation could be expected in a large earthquake, and the orientation of the zone plate boundary there would partially direct tsunami towards New Zealand. However, recent studies of the Hjort trench area (Meckel et al., 2003) suggest subduction in this region is immature with little significant down-dip movement, so large thrust earthquakes are unlikely to occur.

Historically, large earthquakes along the Macquarie Ridge (M_W8.1 earthquakes in 1989 and 2004), and further south near the Balleny Islands (M_W8.1 in 1998) have involved strike-slip (horizontal) movement, producing small tsunami (less than 50 cm) in southern New Zealand. The effects of an M8.3 earthquake on the Macquarie Ridge in 1924 have not yet been well researched.

The Puysegur subduction zone, immediately to the south of New Zealand, is a local source and described in Section 5.3.1.7.

5.2.2 Volcanoes

There are 26 volcanoes (>10 km in diameter) along the active Taupo - Kermadec arc that lie between 300 km and 1000 km from mainland New Zealand (Figure 5.3), we will refer to these as the Kermedec Volcanoes. Three “scenarios” of how these volcanoes represent possible regional tsunami sources are:

- catastrophic submarine silicic eruption and caldera collapse,
- large catastrophic sector collapse,
- frequent small avalanches on edifice flanks.

5.2.2.1 Catastrophic submarine silicic eruption and caldera collapse

Submarine eruptions of silicic-type magma can occur in a series of explosive pulses, each of which can generate tsunami. Associated caldera collapse, such as occurred at Kratatau in 1883, is another possible tsunami source.

South of 30°S, four silicic caldera complexes with explosive styles of eruption have been surveyed—Macauley, Havre, Brothers and Healy (see Figure 5.3). A fifth caldera (Rumble II West) has a partial silicic composition, and thus may generate tsunami on occasion. Macauley is the largest caldera and the source of the Sandy Bay Tephra pyroclastic eruption 6300 years ago. Estimates of the eruption volume vary; Latter et al. (1992) estimated 100 km^3, Lloyd et al. (1996) estimated a lower limit of 1–5 km^3.Recent sea floor mapping reveals an unfilled caldera ~10.8 km long and ~8.2 km wide (Wright et al., 2006)—that can be interpreted to represent the eruption of 35-58 km^3 of material. Havre is a silicic caldera volcano mantled in pumice of unknown age, but the pumice is interpreted to be older than the Sandy Bay Tephra eruption. Havre erupted in July 2012, producing an ash plume and a pumice raft estimated to cover circa 20,000 km^2 (volume ~1 km^3) but no tsunami was observed. Brothers and Healy volcanoes have <3.5 km wide calderas, and consist of explosive-type lavas (Wright and Gamble, 1999). Healy was probably formed by catastrophic submarine rock and ash flow eruptions, with the destruction of a 2.4—3.6 km^3 volcanic cone and formation of a caldera. The eruption is tentatively correlated with part of the Loisels

Pumice of c. 600 years ago, which is found along much of the eastern North Island coastline (Wright et al., 2003).

5.2.2.2 Large catastrophic sector collapse

Seafloor mapping reveals that many of the southern Kermadec volcanoes have undergone large-scale mass-wasting or sector collapse. The volumes of material involved in each sector collapse are currently undocumented. However, an upper limit to any individual sector collapse is probably 4–5 km^3, as evinced by the collapse of the western flank of Rumble III (Wright et al., 2004). Both the age of the Rumble III collapse in particular, and the frequency of large sector collapse in general are unknown, but possibly have recurrence intervals of >10,000 years for any one volcano.

5.2.2.3 Frequent small landslides and debris avalanches

All Kermadec volcanoes, to varying degrees, show evidence of small and frequent landslides and debris avalanches (Wright et al., 2006). Typically these collapses are <1 km^3. The timing and frequency of such failures is almost entirely unknown, but the one example based on repeat multi-beam surveys of Monowai volcano reveals the collapse of 0.03 km^3 of material between 1998 and 2004 (Wright unpublished data). Similar shallow failures, typically 10–300 m thick, occur on all southern Kermadec volcanoes. The recurrence interval of such events is unknown but could be 10 years for any one volcano.

5.2.2.4 Summary of Kermadec volcanoes as tsunami sources in New Zealand

No historical records exist of volcanic activity in the Kermadec chain producing tsunami in New Zealand or elsewhere. Therefore we have little basis for modelling possible tsunami from activity in the Kermadec volcanoes (Table 5.2, Figure 5.4). In general, the volumes of the eruptions associated caldera collapses and the scale of sector collapse features so far identified are significantly (at least an order of magnitude) smaller than has been proposed in the literature for damaging tsunami effects at distances of 1000 km or so. Additionally, a numerical model of a 1 km^3 rock and ash avalanche entering the sea from Mayor Island in the Bay of Plenty indicated only a 0.5 m tsunami on the coast about 30 km distant (de Lange and Prasetya, 1997) so we expect that events with volumes typically 10 times larger but at 10–30 times the distance will have effects no larger than indicated by the modelling of the Mayor Island event. However, significant doubts remain about the source characteristics, and about the effectiveness of rock and ash flows/avalanches and collapsing high altitude eruption columns in producing tsunami that could be damaging at the 300–1000 km distances between the volcanoes and New Zealand. Volcanic unrest in the Kermadec volcanoes leading to a major eruption is expected to have a long lead time, so an extended period of preparation prior to any tsunami should be possible.

5.2.3 Landslides

No landslide sources, at regional distances, have been thus far identified that are sufficiently large or frequent enough to justify the inclusion of regional distance landslides in the tsunami source model for this study. However, further consideration of this potential source, by searching for giant landslides such as the Matakaoa and Ruatoria features of eastern North Island (section 5.3.2.1) along the Tonga-Kermadec and Puysegur-Macquarie margins is warranted.

Table 5.2 Summary of available data from Kermadec chain volcanoes. * = local sources < 100 km from New Zealand.

Volcano	Edifice/Caldera Volume (km^3)	Eruptive Volume (km^3)	Collapse Volume (km^3)	Age of Last Event (yrs before present)	Frequency (yrs)
Macauley	17.4	100 <5 35-58		6,300	?
Havre	6.8	1-10		<1	?
Brothers	2.8	~5		>~5,000	?
Healy	2.4-3.6	10-15		600	?
Rumble III			4.4	Unknown	?10,000
Generic volcano			0.03	<1	?100
Mayor Is.*		~1		6,300	~10,000
White Is.*			0.01	?100	?100

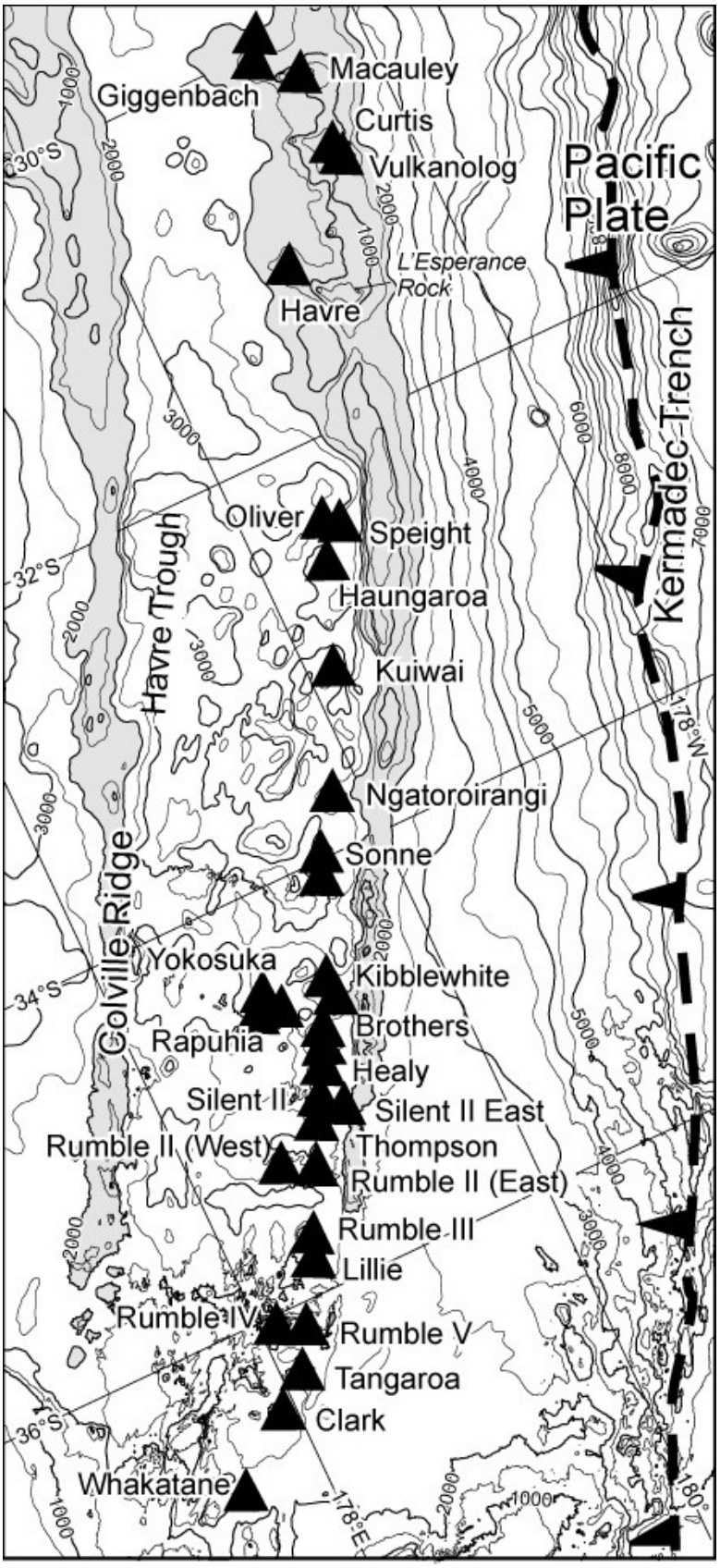

Figure 5.3 Distribution of submarine volcanoes along the southern Kermadec arc between 30°S and 36°30'S (after Wright et al., 2006).

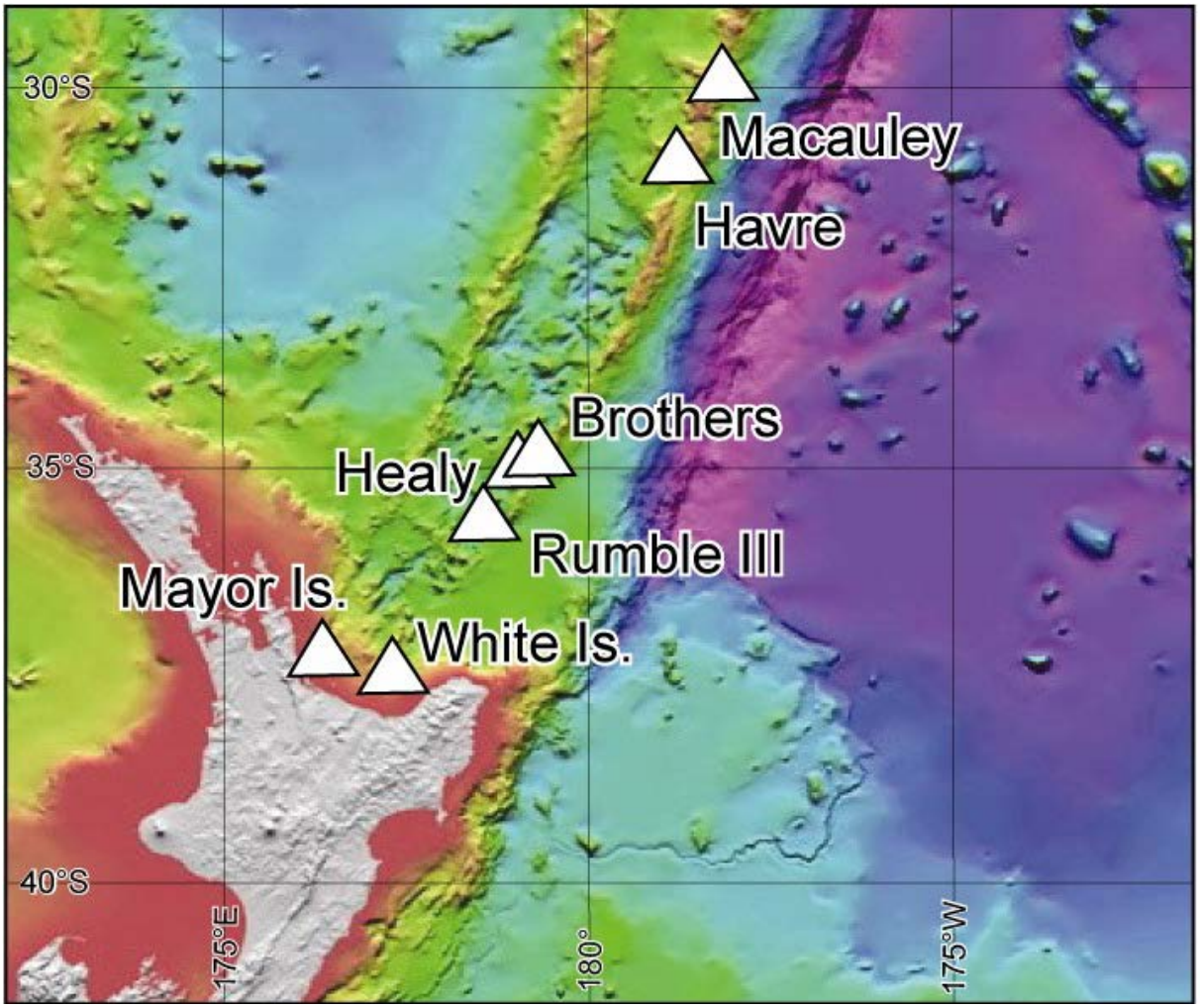

Figure 5.4 Location of possible volcano sources for tsunami along the southern Kermadec arc.

5.3 LOCAL SOURCES

By definition, tsunami generated by local sources arrive at the nearest coastline within an hour, and many can arrive within minutes. New Zealand's location astride a plate boundary means that it experiences many large earthquakes, some of which cause local-source tsunami. It is also exposed to local-source tsunami from submarine and coastal landslides, and island and submarine volcanoes.

5.3.1 Earthquakes

Local earthquakes have the potential to produce catastrophic tsunami, with 10 m or more run-up, over a short length of coast (local impact, i.e., tens of kilometres of coast) or over a longer length of coast (regional impact, i.e. hundreds of kilometres of coast). The impact depends on the extent of fault rupture and seafloor deformation, which in turn depends on the magnitude of the earthquake. The tsunami resulting from a very large, 200–300 km long rupture of the Hikurangi Trough plate-interface on the east coast of the North Island could affect 200–300 km or more of the nearby coast, with large run-ups. Such an event could cause significant to severely damaging waves along much of the east coast and in the Chatham Islands.

Some coasts are more at risk from tsunami than others because of their proximity to areas of high local seismic activity, but no part of New Zealand coastline can be considered completely free from local source tsunami hazards. The tsunami hazard is also present around the shores of our larger freshwater lakes, although consideration of this hazard is not within the scope of this study.

The probabilistic tsunami hazard model described in Chapter 6 uses earthquake magnitude-frequency distributions for the subduction zones around New Zealand that have been derived for use in the preliminary Global Earthquake Model (GEM) from the various studies described below.

Information on crustal faults comes from historical earthquakes and from the mapping of active faults in the offshore areas around New Zealand—these have been the primary methods for determining the local potential sources for earthquakes producing tsunami. The model for these faults used for the present probabilistic study is based on the offshore faults in the New Zealand Hazard Model (NZSHM; Stirling et al., 2012) and removing those too small, or with the wrong fault mechanisms, to produce significant tsunami. Some additional faults were tentatively added to the model following group discussions, in particular faults along the Hikurangi Outer Rise, the west coast of the South Island, and in the Tasman Bight (see Appendix 5 for further details).

Stirling et al. (2012) produced a series of maps showing the locations of the faults in the NZSHM, and this reference may be used to locate the faults described in the following sections.

5.3.1.1 Kermadec Trench

The Kermadec Trench is both a regional and a local source for tsunami. Earthquakes that rupture only on the northern half of the Kermadec Trench produce tsunami that take more than an hour to reach New Zealand (excluding the Kermadec Islands), while those whose ruptures include portions of the trench south of ~33°S produce tsunami that reach parts of New Zealand in less than an hour. Because of the orientation of the trench, even for tsunami originating on the southern part of the trench, the most strongly affected coasts are usually more than one hour travel time away. The main description of the Kermadec Trench as a tsunami source is in Section 5.2.1.3.

5.3.1.2 Tsunami sources in offshore eastern North Island

We recognise that a significant source of large vertical seafloor displacements during earthquakes is in conjunction with the Hikurangi subduction margin off the eastern North Island. Tsunami could be generated by large to great earthquakes (M7.5–9.0) on the plate interface itself from slip between the two opposing plates (Wallace et al., 2009), or by rupture of steeper faults that extend upward through the Australian plate (see Figure 5.5).

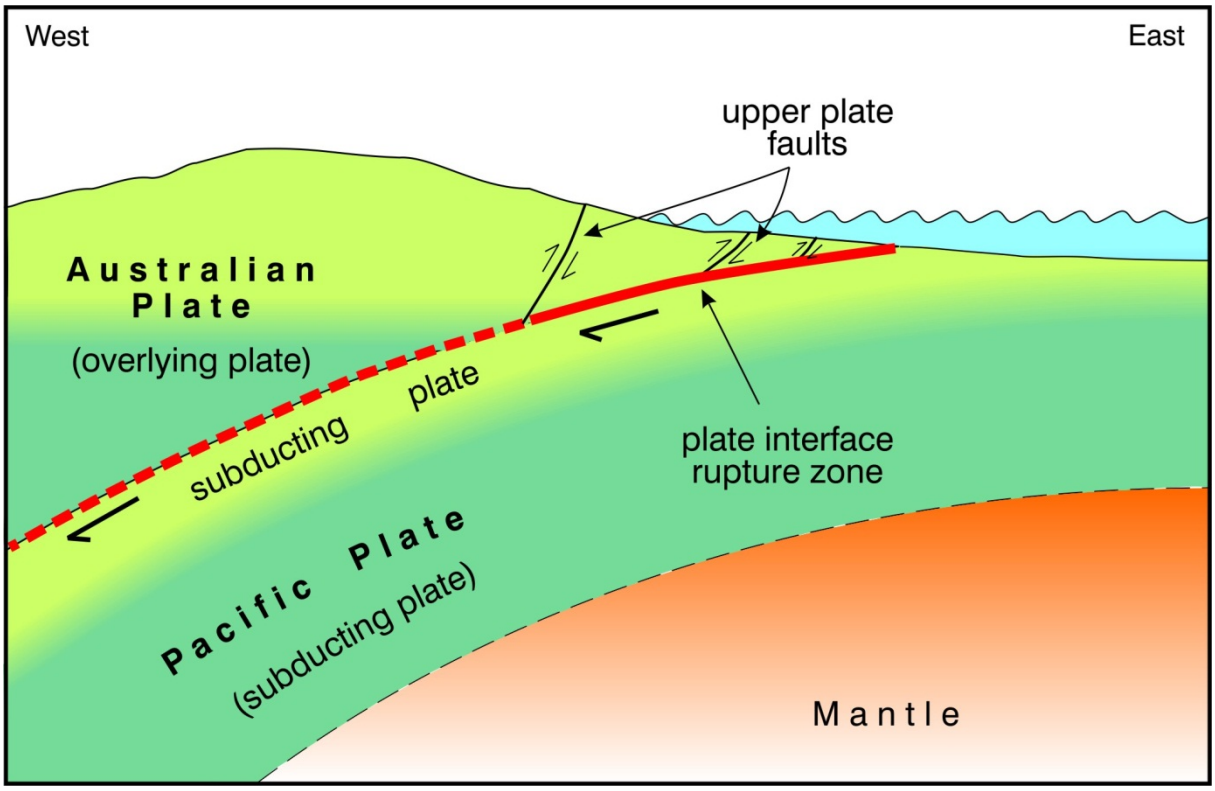

Figure 5.5 Schematic cross-section through the Hikurangi subduction zone.

NIWA scientists have mapped many faults in the offshore area from the inner shelf (~ 50 m water depth) to the deep ocean (>2000 m water depth) of the Hikurangi subduction margin (e.g., Barnes et al., 1998). This mapping has defined the subduction front and structural features on the shelf and slope. Many of these structures mimic onshore faults and folds, having lengths of tens of kilometres and heights of up to 500 m.

Some information on fault slip rates comes from studies of specific faults such as the Lachlan Fault, offshore of Mahia Peninsula (Barnes et al., 2002) and from the presence of uplifted marine terraces of Holocene age (c. <10,000 years) along the east coast (Berryman et al., 1989; Berryman, 1993; Berryman et al., 2011). Data from these linked studies provide a basis for assigning fault parameters to other structures when location and fault length are the only data available. For example, studies of the uplifted marine terraces on Mahia Peninsula and the offshore seismic stratigraphy of the Lachlan Fault show that this fault is capable of generating a large surface earthquake that ruptures the sea bed every 615–2333 years (Barnes et al., 2002). This is confirmed by the evidence for five uplift events on the peninsula in the last c. 5000 years (Berryman, 1993). Other data that provide tie-points for assigning fault parameters include the source dimensions and magnitude of the M 7.8 Hawkes Bay earthquake of 1931.

Research summarised in the New Zealand Seismic Hazard Model indicates more than 80 faults in the continental shelf and slope part of offshore eastern North Island occur in bedrock that is interpreted to be strong. Further offshore the fault structures have developed in softer, weaker rocks and it is unclear whether these are strong enough to break independently in large earthquakes. It may be that these “outer margin” faults only rupture in association with major subduction thrust earthquakes. Currently faults are treated as independent tsunami sources in our tsunami hazard model if they are represented as independent seismic sources in the national seismic hazard model (Stirling, 2012); however the assumptions regarding these outer margin faults warrant further work. Earthquake magnitudes and recurrence

intervals have been estimated. based on the length of the faults (as they are expressed on the sea floor) and estimated slip rates, Outer Rise earthquakes, occurring in the Pacific plate where it bends prior to subduction, are a potentially important tsunami source that has so far received little attention. A major component of the Samoa 2009 tsunami was caused by an Outer Rise earthquake, as have some major historical tsunami in Japan. This type of tsunami source is discussed in Appendix 5.

The Hikurangi subduction zone is arguably the most important local-source tsunami hazard posed to New Zealand (and a comparable hazard to the Kermadec Trench subduction zone, which we regard primarily as a regional source). However few data are available on the timing and size of large-to-great earthquakes from the Hikurangi subduction zone. We have developed the source model with a range of possible earthquake sizes and recurrence intervals, based on historical earthquakes, plate motion rates from GPS, and GPS measurements of the accumulation of elastic strain. Elastic strain accumulation measurements help to assess which portions of the plate interface are currently locked or "stuck" and building up strain for future earthquakes.

GPS measurements show that the southern Hikurangi subduction interface (beneath Wellington and the Wairarapa) is currently "locked" and that strain is building up that will probably eventually be released in a great (M_W > 8.0) subduction megathrust event. This is in contrast to the northern part of the Hikurangi margin (adjacent to Hawke's Bay, Gisborne and Raukumara peninsula) which appears to be a region of more moderate subduction interface earthquakes (M_W <7.1) and steady creep rather than extremely large earthquakes. However, this does not mean that there is no tsunami hazard posed to the Gisborne region by the Hikurangi subduction zone. On the contrary, in 1947, two historic M_W 7.0–7.1 earthquakes offshore of Gisborne led to much larger than expected tsunami with run-ups of up to 10 and 6 m. These earthquakes had classic characteristics of "tsunami earthquakes". They were located close to the trench where the interface is at very shallow depths, rupture velocities were slow (assumed to be <1 km/s), and rupture durations were long (at least 40 and 25 seconds for the March and May 1947 events, respectively). A low energy release at high frequencies resulted in low $M_L$values (5.9; 5.6) compared to M_S values (both 7.2) and M_W values (7.0–7.1; 6.9–7.1), and larger than expected tsunami, with run-ups of 10m and 6m respectively (Downes et al., 2000; Doser and Webb, 2003). Power et al. (2008) suggested that earthquakes might recur in the source area of the 1947 tsunami earthquakes as frequently as every ~70–80 years.

Overall, we expect that the southern Hikurangi margin experiences less frequent (i.e., at ~300-900 year intervals) but extremely large to great (M_W > 8.0) subduction earthquakes. The northern Hikurangi margin, on the other hand, probably experiences more frequent, moderately sized earthquakes that are located at very shallow levels along the Hikurangi trench; these could also produce significant tsunami (e.g., the 1947 earthquakes near Gisborne, see Sections 3.2 and 4.2.1 for further details). We also cannot rule out very infrequent subduction thrust events that rupture the entire Hikurangi margin in M_W ~ 9.0 earthquakes. If such events occur, they would produce devastating tsunami similar to those observed in Japan in the M_W 9.0 Tohoku event in March 2011. We account for these variations in our assigned parameters for the subduction zone as a whole (Appendix 3), but uncertainties in both the distribution of earthquake magnitudes and their recurrence intervals are large, and the properties determining these characteristics are likely to vary along the length of the subduction zone. Further work is needed to incorporate such varying factors into a tsunami hazard model.

5.3.1.3 Tsunami sources from faults in the Bay of Plenty

There are many active faults in the offshore area of the Ruapehu-White Island volcanic zone. These faults typically have smaller dimensions than the faults offshore of the eastern North Island, and the maximum earthquake that these faults can produce is believed to be about M 7, with 2–3 m of potential seabed displacement on a fault up to ~30 km long. These relatively small sources are not thought to be capable of producing large tsunami.

5.3.1.4 Tsunami sources from faults near Auckland

The active Kerepehi Fault probably extends into the Hauraki Gulf about 40 km east of Auckland, and is the only offshore active fault known in the Auckland region. The fault can produce earthquakes up to about M 7, similar to those in the Bay of Plenty. At 40 km distance, we consider it unlikely that the fault poses a significant tsunami hazard to Auckland. In addition, de Lange and Healy (2001) and Chick et al. (2001) completed some numerical modelling of a tsunami generated by the Kerepehi Fault source, and found it would not produce a run-up of 2 m or more in Auckland.

5.3.1.5 Tsunami sources from faults in the Cook Strait and offshore Marlborough

Numerous active faults occur in the Cook Strait area and offshore Marlborough (Barnes et al., 1998; Barnes et al., 2008; Pondard and Barnes, 2010), including the offshore southern part of the Wairarapa Fault that in 1855 generated a tsunami with 10 m of local run-up (and up to a 5 m run-up in Wellington). The potential of the active faults for producing tsunami are based on their length and by assigning earthquake magnitudes based on their onshore continuations in Marlborough and southern North Island. The southern section of the Wairarapa fault ruptured into Cook Strait, with at least 6 m of vertical movement, and this produced the tsunami mentioned above. Using the Abe local source equation (see section 4.2 for details) we calculated that the offshore section of the fault, to produce the tsunami run-up observed in the Wairarapa, Wellington, and Kapiti Coast, would be approximately equivalent to a M_W7.7 earthquake. This approximation appears to be reasonable, based on recent numerical propagation models of this source (Rob Bell, pers. comm., 2005; Cousins et al., 2007). Other Marlborough and Wellington region faults include the Boo Boo, Needles, Chancet, Campbell Banks, Cloudy, Te Rapa, Kekerengu Bank, Palliser-Kaiwhata, Wellington, Ohariu, Awatere and Wairau Faults. For this study we have excluded strike-slip faults such as the Boo-Boo Fault from the hazard model, though the possibility of uplift along the small step-overs in such faults remains, as does the possibility for some residual vertical component to the fault motion (Cousins et al., 2007). Apart from the Wairarapa Fault, the largest earthquakes assigned to offshore faults in this region are M 7.5–7.8.

5.3.1.6 Tsunami sources from faults in the western Cook Strait and offshore Manawatu

An extensive marine survey of the region offshore from the Manawatu-Kapiti area has recently been completed (Lamarche et al., 2005), and has provided valuable new insight into the location and characteristics of offshore faults in the region. These structures have a modest potential to generate tsunami (maximum earthquake magnitudes of up to M_W ~7.7), but they may be important as they are located at short distances from urban areas on the Kapiti coast, Porirua and northern South Island. Additional faults extending from the Tasman and Golden Bay area towards Taranaki were tentatively identified for this study; details are given in Appendix 5.

5.3.1.7 Tsunami sources from faults in southern South Island

In the offshore Fiordland region, plate boundary structures that include the Alpine Fault and the Puysegur subduction zone are capable of producing large-to-great earthquakes of >M 8, similar to or larger than, the M_W 7.8 Dusky sound earthquake in July 2009.This, coupled with early historical records of drownings on the south Fiordland coast, probably by a tsunami in the 1820s, has led to recent numerical simulations of tsunami generation and propagation from these sources (Downes et al., 2005; Prasetya et al., 2011a). Because the Alpine Fault is predominantly a strike-slip fault, the structure is not considered likely to generate significant tsunami except at localised areas where the fault steps from one strand to another and large vertical movements are possible. Thus, the tsunami source tends to be very localised, which could generate a large run-up locally, but is unlikely to travel as far as Invercargill.

The Puysegur subduction interface has the potential to generate major tsunami. The plate interface here is the mirror image of the Hikurangi subduction zone, in that the Australian plate is here subducted beneath the Pacific plate. The relative motion of the plates is highly oblique, though the implications of this for tsunami generation are unclear. The subduction zone has been studied by Hayes and Furlong (2010), and models have been constructed by Downes et al. (2005), Goff et al. (2009), and Prasetya et al. (2011b).The bathymetry off the southern South Island appears to offer some natural protection to southern shores. This is because the water shallows at a substantial distance from the coast and some of the energy is dissipated at the shelf edge.

5.3.2 Landslides

New Zealand is vulnerable to tsunami hazard from both coastal and submarine landslides. In historical times, several earthquake-triggered coastal landslides have resulted in documented localised tsunami. These include a tsunami north of Westport associated with coastal landslides triggered by the 1929 M_W 7.8 Buller (Murchison) earthquake, a tsunami near Napier associated with coastal cliff failure triggered by the 1931 M_W 7.6 Hawke's Bay earthquake, and a tsunami in Charles Sound during the 2003 M_W 7.2 Fiordland earthquake that had a run-up of 4–5 m (Hancox et al., 2003). In addition to earthquakes, wave action and coastal processes, heavy rain and human activities can trigger coastal landslides.

There are no confirmed historical instances of tsunami triggered by submarine landslides in New Zealand. Some reported tsunami do bear characteristics of landslide-source tsunami however, e.g. at Goose Bay south of Kaikoura (Du Bois 2012). Marine geophysical data demonstrate the widespread occurrence of submarine landslide deposits on the sea floor around New Zealand's submerged continent.

5.3.2.1 Submarine landslides

The number of published studies on New Zealand submarine landslides has increased significantly since 2005 (Lewis and Barnes, 1999; Carter, 2001; Collot et al., 2001; Faure et al., 2006; Crutchley et al., 2007; Lamarche et al., 2008; Mountjoy et al., 2009; Mountjoy et al., 2009; Barnes et al., 2010; Joanne et al., 2010; Kukowski et al., 2010; Pedley et al., 2010; Micallef et al., 2012; Mountjoy and Micallef, 2012). In addition to published studies, numerous un-published high-resolution multibeam data sets have been collected by NIWA and other agencies, resolving large areas of New Zealand's seafloor. The combination of published and unpublished data indicate widespread slope failure off the Bay of Plenty, the length of the eastern coast of the South and North islands, Fiordland, and the West Coast of

the South Island. Mapped landslide source areas occur from 2 to >50 km distance from the coastline, and in water depths ranging from 100 to 3000 m.

The size of known landslide source areas varies from the smallest failures resolvable using high-resolution ship-board multibeam data (several tens of metres across) to continental margin scale failures (several tens of kilometres across). The size range is poorly distributed, however, with the majority of source volumes estimated at 10^{-3}–1 km^3(e.g., Micallef et al., 2012), a few failures at 10km^3 scale (Mountjoy and Micallef, 2012; NIWA unpublished data); and two landslides near East Cape at the extreme end of the volume scale (>100km^3) (Collot et al., 2001; Lamarche et al., 2008).

While the magnitude of submarine landslides can be relatively easily measured in geophysical data, determining the age of submarine landslides is significantly harder and more costly. Typically only the largest landslides justify individual case studies and thus have known ages. A summary of the details of the largest landslides documented on the New Zealand margin is provided in Table 5.3.

Table 5.3 Summary parameters of the largest submarine landslides documented on the New Zealand margin.

Landslide Name	**Volume (km^3)**	**Upper water depth (m)**	**Age (kyr)**	**reference**
Matakaoa Debris Avalanche	~430	~200	600±150	(Lamarche et al., 2008)
Ruatoria Avalanche	3150±630	~140	170±40	(Collot et al., 2001)
Paritu Debris Avalanche	~30	~800	7.6±0.6	(Mountjoy and Micallef, 2012; Pouderoux et al., 2012a)

As the low number and older ages of the very large-scale mass failures indicates, we expect that such events occur very rarely, and are outside the time frame relevant to risk assessment. To complete a risk assessment, a key piece of information needed is the recurrence interval (return time) for hazardous events. It is generally not possible to gain recurrence-type information from individual mass failure complexes, however, slope-failure-recurrence is being used as a proxy for seismic activity on the Hikurangi and Fiordland margins (c.f. Goldfinger, 2011). The method is based on the assumption that significant earthquakes will trigger widespread slope failure across a large area of a margin. Detailed work by Pouderoux et al. (2012b) across three locations on the Hikurangi margin indicates mean return times for turbidite deposits of 270–430 years. This data is very useful for understanding the frequency of slope disturbance on active margins, however it does not indicate the magnitude of the slope failure at the source, and thus is not directly applicable to assessing the tsunami hazard from submarine landslides.

The best studied and most widely publicised landslide tsunami scenario in New Zealand is for the head of Kaikoura Canyon. An unstable accumulation of 0.25 km^3 of sediment there has been inferred, based on local sedimentary processes (Lewis and Barnes, 1999). The shallowest area of the sediment is in only 35 m water depth. Dated sedimentary events within Kaikoura Canyon and further down-slope suggest that sediment failure occurs every 200–300 years. Based on this scenario, Walters et al. (2006) carried out a tsunami simulation and found that for the average-case scenario, the inferred landslide is capable of generating waves up to 13 m above tide level in adjacent Goose Bay, and 2 m at Kaikoura. The arrival time for these waves is very short, at 1 minute and 15 minutes respectively. Large local tsunami in this region are supported by historical records and paleo-tsunami data (Du Bois, 2012).

Very little other research has been carried out to model landslide-tsunami for specific scenarios around New Zealand. Joanne (2008) modelled the potential of smaller failures on the flanks of the Matakaoa Submarine Instability Complex for producing tsunami, and demonstrated a potential for significant inundation at Te Araroa on the East Cape. Kukowski et al.(2010) infer a potential for large-scale failure of a frontal ridge of the Hikurangi Margin. The inferred worst-case scenario is for complete failure of the "Rock Garden" ridge offshore of Hawke's Bay involving 150–170 km^3 material, initiating in ~700 m water depth. Modelling the tsunami potential for this worst case generates a sea-surface disturbance of 40 m, however no wave runout was modelled to assess the effect at the coast for this event.

While it is definitely useful to undertake tsunami assessments for individual landslides based on specific scenarios, in order to determine the hazard and risk to coastal populations it is necessary to consider multiple landslide sources across a broad area. As with earthquake hazards, the uncertainty inherent in magnitude and frequency of submarine landslides best lends itself to probabilistic hazard assessment (Grilli et al., 2009).

5.3.2.2 Coastal landslides

Sub-aerial landslides entering the sea (or lakes), especially into deep water, can generate major but local tsunami. Some historical examples were noted in Section 5.3.2. There is no systematic monitoring of coastal cliff stability around New Zealand. At any time, there are always coastal cliffs with marginal stability, requiring only a minor trigger to collapse them.

We have carried out a qualitative assessment of this hazard in the vicinity of each of the urban centres considered in this project. Criteria for assessing tsunami-inducing coastal-landslide hazard have included:

- topography (steep, high slopes close to water)
- geology (the relevant strength and structure of the rock)
- known landslides (presence and types that can be identified as reaching the water)
- historical evidence – e.g. 1931 Napier, 1855 Wellington, 1929 Murchison (note – all of these landslides are associated with large earthquakes. There is a much lower risk of similar landslides without earthquakes).

Whangarei	Whangarei Heads could pose a small threat. Landslides at Onerahi are too small to cause significant waves.
North Shore	No risk - no steep, large slopes at coast.
Waitakere	Little risk (apart from west coast beaches and north side of Manukau Heads, which have significant landslide potential – possibly waves of a few metres over a distance of up to 1 km).
Auckland	Some risk at St Heliers - Achilles Point - Karaka Bay. Coastal-cliff collapses in the order of 100 m wide, but into shallow water.
Manukau	Probably has greatest risk in Auckland region, especially the north side of the harbour from Green Bay to Manukau Heads.
Tauranga	Although there are many landslides, none seem capable of generating more than small waves, except for a small chance of large failures of Mount Maunganui.

Whakatane	Possibly greatest risk is from Moutohora Island just offshore. It has collapsed to the north pre-historically, and there may be a risk of collapse to the south. Whakatane headland collapse could pose a danger, although the rock strength is good
Gisborne	Low hazard, almost no risk. Possible nearshore uplift caused by landslides, but very rare. Hill at Titirangi has greatest potential to cause waves, but very small – only 100m high and not steep enough.
New Plymouth	Collapse of Paritutu cliffs could cause modest waves, but Whitecliffs is too far away.
Napier	Local risk on east side of Bluff Hill – small rockfalls (but none into sea in the 1931 earthquake). Greater risk is presented by landslides between Napier and Wairoa, as in 1931, but likely to affect only a limited area (<10 km).
Wanganui	Landslides at Castlecliff are unlikely to cause any waves. Greatest risk of wave generation from landslide is from Shakespeare Bluff into the river. The effects are likely to be small.
Kapiti	Some risk between Pukerua Bay and Paekakariki. Brendan's Beach and the restaurant south of Paekakariki are at greatest risk.
Porirua	A small risk at Titahi Bay, but little risk elsewhere.
Lower Hutt	Eastbourne/Gracefield/Seaview is at some risk. Some risk from Wellington fault scarp earthquakes affecting Petone, but this is only likely to occur in association with large earthquakes.
Wellington	Coastal collapse between Ohiro Bay and Sinclair Head is a hazard for south coast bays. Some risk from fault scarp collapse into harbour. Some risk in larger landslides such as at Worser Bay, but effects likely to be limited, and only likely in the event of large earthquakes.
Nelson	Possible but low likelihood of large-scale movement at Tahunanui causing heave at the toe of the slide out to sea.
Christchurch	A small risk from rockfalls into Lyttelton and Akaroa harbours. No very large-scale landslides are apparent, and most slope instability is shallow failures in loess and regolith.
Timaru	Low cliffs at Caroline Bay/Dashing Rocks pose a negligible risk (high quality rock).
Dunedin	No large landslides, capable of causing large waves, are known adjacent to Otago Harbour. The outer coast cliffs both east and west of the city (Highcliff, Lawyers Head, St Clair cliffs, Tunnel Beach) have potential for landslides large enough to cause waves at coastal suburbs. At least one large prehistoric landslide (Lovers Leap) is known, but in general the rock appears solid.
Invercargill	May be affected by tsunami from very large landslides in Fiordland, but only as a result of a very large earthquake. Otherwise the risk is very low. No apparent risk at Bluff Harbour.

5.3.2.3 Conclusions

The likelihood of coastal landslides inducing tsunami is low except during large earthquakes, in which case other tsunami-generating phenomena are likely to be more important, apart from in the immediate vicinity of the landslides.

The greatest potential for very large landslides is in relatively uninhabited areas of very high relief such as Fiordland, but the risk of such events must be orders of magnitude lower under undisturbed conditions than during earthquakes.

5.3.3 Volcanoes

5.3.3.1 Mayor Island and White Islands

Mayor and White island volcanoes are very close potential source for tsunami. Mayor Island has produced both explosive and lava flow eruptions, and includes three phases of caldera collapse. The last caldera collapse, associated with the largest eruption, occurred 6,300 years ago (Houghton et al., 1992) and included the movement of rock and ash flows into the sea.; this event is probably the only recorded instance of rock and ash flows entering the sea within the New Zealand region. Numerical modelling of a credible 1 km^3 ("Mt St Helens scale") rock and ash flow from Mayor Island, that enters the sea, would produce a 0.5 m high tsunami on the adjacent coast around Whakatane (de Lange and Healy, 1986; de Lange, 1997).

White Island is the emergent summit of a larger submarine volcano. Eruptions have included both lava flow and small explosive eruptions of mostly andesite (of typically moderately explosive style), but including dacite (associated with a more energetic eruptive style), though the eruption history of the volcano is poorly known. A small collapse of the inner crater wall in 1914 produced a debris avalanche that may have entered the sea. The active hydrothermal system weakens the volcano structure and enhances the potential for sector collapse on both the outer subaerial and submarine flanks.

The probability of generation of a significant tsunami from White Island is considered low (de Lange and Healy, 1986; de Lange and Prasetya, 1997), not least because the most likely sector collapse direction is toward the east, and thus any tsunami generated would be directed offshore. Other small caldera volcanoes and associated pumice deposits occur on the outer Bay of Plenty continental slope (Gamble et al., 1993; NIWA unpublished data). Based on the low likelihood of damaging tsunami indicated by these specific modelling studies, we find no reason to add these volcano or landslide sources to the tsunami source model in this project.

5.4 REFERENCES

Atwater, B.F., Musumi-Rokkaku, S., Satake, K., Tsuji, Y., Ueda, K.and Yamaguchi, D.K. (2005). The orphan tsunami of 1700–Japanese clues to a parent earthquake in North America, U.S. Geological Survey Professional Paper 1707, 133pp.

Barnes, P.M., Lamarche, G., Bialas, J., Henrys, S., Pecher, I., Netzeband, G.L., Greinert, J., Mountjoy, J.J., Pedley, K., Crutchley, G. (2010). Tectonic and Geological Framework for Gas hydrates and Cold Seeps on the Hikurangi Subduction Margin, New Zealand. *Marine Geology* 272(1-4): 26-48.

Barnes, P.M., Mercier de Lépinay, B., Collot, J-Y., Delteil, J., Audru, J-C. (1998). Strain partitioning in the transition area between oblique subduction and continental collision: Hikurangi margin, New Zealand. *Tectonics*17, 534-557.

Barnes, P.M., Nicol, A., Harrison, T. (2002). Neogene deformation history and seismic potential of Lachlan Ridge: a major active thrust complex, Hikurangi subduction margin, New Zealand. *Geological Society of America Bulletin* 114,1379-1405.

Barnes, P.M., Pondard, N., Lamarche, G., Mountjoy, J., Van Dissen, R., Litchfield, N. (2008). It's Our Fault: active faults and earthquake sources in Cook Strait. NIWA Client Report WLG2008-56: 36 p.

Beavan, J., Wang, X., Holden, C., Wilson, K., Power, W., Prasetya, G., Bevis, M., Kautoke, R. (2010). Near-simultaneous great earthquakes at Tongan megathrust and outer rise in September 2009. *Nature*, 466: 959–963

Berryman, K.R. (1993). Age, height, and deformation of Holocene marine terraces at Mahia Peninsula, Hikurangi subduction margin, New Zealand. *Tectonics 12::* 1347-1364

Berryman, K.R., Ota, Y., Hull, A.G. (1989). Holocene paleoseismicity in the fold and thrust belt of the Hikurangi subduction zone, eastern North Island, New Zealand. *Tectonophysics* 163, 185-195.

Berryman, K., Ota,Y., Miyauchi, T., Hull ,A., Clark, K., Ishibashi,K., Iso, N., and Litchfield, N. (2011). Holocene Paleoseismic History of Upper-Plate Faults in the Southern Hikurangi Subduction Margin, New Zealand, Deduced from Marine Terrace Records. *Bulletin of the Seismological Society of America*, Vol. 101(5): 2064–2087, doi: 10.1785/0120100282

Bevis, M., Taylor, F.W., Schutz, B.E., Recy, J., Isacks, B.L., Helu, S., Singh, R., Kendrick, E., Stowell, J., Taylor, B., and Calmant, S. (1995). Geodetic observations of very rapid con- vergence and back-arc extension at the Tonga arc: *Nature*, v. 374, p. 249-251.

Borrero, J., Bell, R., Csato, C., DeLange, W., Greer, D., Goring, D., Pickett, V. and Power, W. (2012). Observations, Effects and Real Time Assessment of the March 11, 2011 Tohoku-oki Tsunami in New Zealand, *Pure and Applied Geophysics*, DOI: 10.1007/s00024-012-0492-6.

Calmant, S., Pelletier, B., Lebellegard, P., Bevis, M., Taylor, F.W., Phillips, D.A. (2003). New insights on the tectonics along the New Hebrides subduction zone based on GPS results: *J. Geophys. Res*., v. 108(18), doi:10.1029/2001J1200644.

Carter, L. (2001). A large submarine debris flow in the path of the Pacific deep western boundary current off New Zealand. *Geo-Marine Letters* 21: 42-50.

Chick, L.M., De Lange, W.P., Healy, T.R., (2001). Potential Tsunami hazard associated with the Kerepechi Fault, Firth of Thames, New Zealand. *Nat. Hazards* 24, 309–318.

Cisternas, M., Atwater, B.F., Torrejón, F., Sawai, Y., Machuca, G., Lagos, M., Eipert, A., Youlton, C., Salgado, I., Kamataki, T., Shishikura, M., Rajendran, C.P., Malik, J.K., Rizal, Y., Husni, M. (2005). Predecessors of the giant 1960 Chile earthquake, *Nature*, 437: 404-407.

Clague, J. J. (1997). Evidence for large earthquakes at the Cascadia subduction zone.*Reviews of Geophysics* 35, 439-460.

Collot, J.-Y., Lewis, K.B., Lamarche, G.; Lallemand, S.(2001). The giant Ruatoria debris avalanche on the northern Hikurangi Margin, New Zealand: Result of oblique seamount subduction. *Journal of Geophysical Research* 106(B9): 19,271 - 219,297.

Cousins, W.J., Power, W.L., Destegul, U., King, A.B. (2007). Combined earthquake and tsunami losses from major earthquakes affecting the Wellington Region. GNS Science Consultancy Report 2007/280.

Crutchley, G. J., Gorman, A.R., Fohrmann, M.(2007). Investigation of the role of gas hydrates in continental slope stability west of Fiordland, New Zealand. *New Zealand Journal of Geology and Geophysics* 50(4): 357-364.

de Lange, W.P., Healy, T.R. (1986). Tsunami hazards in the Bay of Plenty, New Zealand: an example of hazard analysis using numerical models. *Journal of Shoreline Management* **2***,* 177-197.

de Lange, W.P. (1997). Tsunami and storm surge scenarios for the Auckland Region. Carson Group and Auckland Regional Council, July 1997. Auckland

de Lange, W.P., Prasetya, G. (1997). Volcanoes and tsunami hazard – implications for New Zealand. *Tephra* 17, 30-35.

de Lange, W.P.; Healy, T.R. (2001). Tsunami Hazard for the Auckland Region and Hauraki Gulf, New Zealand. *Natural Hazards* 24: 267-284.

Doser, D. I., and T. Webb (2003), Source parameters of large historical (1917–1961) earthquakes, North Island, New Zealand, *Geophys. J. Int.*, 152, 795–832.

Downes G, Cochran U, Wallace L, Reyners M, Berryman K, Walters R, Callaghan F, Barnes P, Bell R (2005). EQC Project03/490-Understanding local source tsunami: 1820s Southland tsunami. Institute of Geological and Nuclear Sciences Client Report 2005/153.p. 92.

Downes, G.L., Webb, T.H., McSaveney, M.J., Darby, D.J., Doser, D., Chague-Goff, C., Barnett, A. (2000). The 26 March and 17 May 1947 Gisborne earthquakes and tsunami : implication for tsunami hazard for East Coast, North Island, New Zealand. p. 21 In: The International Workshop : tsunami risk assessment beyond 2000 : theory, practice and plans : in memory of Professor Sergey L. Soloviev, June 14-16, 2000, Russia, Moscow.

Du Bois, J. (2012). Hazard assessment for a submarine landslide generated local-source tsunami from Kaikoura Canyon. *Geophysical Research Abstracts* Vol. 14, EGU2012-3906, 2012 (EGU General Assembly 2012).

Faure, K., Greinert, J.; Pecher, I.A.; Graham, I.J.; Massoth, G.J.; de Ronde, C.E.J.; Wright, I.C.; Baker, E.T.; Olson, E.J. (2006). Methane seepage and its relation to slumping and gas hydrate at the Hikurangi margin, New Zealand. *New Zealand Journal of Geology and Geophysics* 49(4): 503-516.

Fryer G.J., Watts, P., Pratson, L.F. (2004). Source of the great tsunami of 1 April 1946: a landslide in the upper Aleutian forearc. *Marine Geology* 203: 201-218

Gamble, J.A., Wright, I.C., Baker, J.A. (1993). Seafloor geology and petrology of the oceanic to continental transition zone of the Kermadec - Havre - Taupo Volcanic Zone arc system, New Zealand. *New Zealand Journal of Geology and Geophysics* 36*,* 417-435.

Geist, E.L. (2000). Origin of the 17 July 1998 Papua New Guinea Tsunami: Earthquake or Landslide? *Seismol. Res. Lett.* 71 (3): 344–351.

Goff, J.R. (2008). The New Zealand Palaeotsunami Database. NIWA Technical Report 131,ISSN 1174–2631, 24 pp+Appendix.

Goff, J.R., Lane, E.; Arnold, J. (2009).The tsunami geomorphology of coastal dunes. *Natural Hazards and Earth System Sciences*, 9(3), 847-854.

Goff, J.R., Pearce, S., Nichol, S.L., Chagué-Goff, C., Horrocks, M., Strotz, L., (2010). Multiproxy records of regionally-sourced tsunamis, New Zealand. *Geomorphology* 118, 369–382. doi:10.1016/j.geomorph.2010.02.005.

Goldfinger, C. (2011). Submarine Paleoseismology Based on Turbidite Records. *Annual Review of Marine Science*, Vol 3 3: 35-66.

Goldfinger, C., Nelson, C.H., Morey, A.E., Johnson, J.E., Patton, J.R., Karabanov, E., Gutiérrez-Pastor, J., Eriksson, A.T., Gràcia, E., Dunhill, G., Enkin, R.J., Dallimore, A., and Vallier, T. (2012). Turbidite event history—Methods and implications for Holocene paleoseismicity of the Cascadia subduction zone: U.S. Geological Survey Professional Paper 1661–F, 170 p. (Available at http://pubs.usgs.gov/pp/pp1661f/).

Grilli, S.T., Taylor, O.-D.S., Baxter, C.D., Maretzki, S. (2009). A probabilistic approach for determining submarine landslide tsunami hazard along the upper east coast of the United States. *Marine Geology* 264(1-2): 74-97.

Gusiakov, V.K. (2001). Basic Pacific tsunami catalog and database 47 BC–2000 AD: Results of the first stage of the project. *ITS 2001 Proceedings* 263–272.

Hancox, G.T., Cox, S.C., Turnbull, I.M., Crozier, M.J. (2003). Reconnaissance studies of landslides and other ground damage caused by the M_w7.2 Fiordland earthquake of 22 August 2003. Institute of Geological & Nuclear Sciences science report 2003/30.32 p.

Hayes, G.P. and Furlong, K.P. (2010). Quantifying potential tsunami hazard in the Puysegur subduction zone, south of New Zealand, *Geophysical Journal International,* 183(3): 1512–1524

Hjorleifsdottir, V., Sánchez-Reyes, H.S., Singh, S.K., Ji, C., Iglesias, A., Perez-Campos, X. (2012). Areas of slip of recent earthquakes in the Mexican subduction zone, Abstract T13F-2680 presented at 2012 Fall Meeting, AGU, San Francisco, Calif., 3-7 Dec.

Houghton, B.F., Weaver, S.D., Wilson, C.J.N., Lanphere, M.A. (1992). Evolution of a Quaternary peralkaline volcano: Mayor Island, New Zealand. *Journal of Volcanology and Geothermal Research* 51, 217-236.

Joanne, C. (2008). The Matakaoa Submarine Instability Complex, offshore East Cape, New Zealand: Mass-transport processes and impact of mega-instabilities on architecture and evolution of the continental margin. Geology, Geosciences Azur/NIWA.PhD Thesis.

Joanne, C., Collot, J-Y., Lamarche, G., Migeon, S. (2010). Continental slope reconstruction after a giant mass failure, the example of the Matakaoa Margin, New Zealand. *Marine Geology* 268: 67-84.

Kukowski, N., Greinert, J.; Henrys, S. (2010). Morphometric and critical taper analysis of the Rock Garden region, Hikurangi Margin, New Zealand: Implications for slope stability and potential tsunami generation. *Marine Geology* 272: 141-153.

Lamarche, G., Joanne, C., Collot, J-Y. (2008). Successive, large mass-transport deposits in the south Kermadec fore-arc basin, New Zealand: The Matakaoa Submarine Instability Complex. *Geochemistry, Geophysics, Geosystems* 9(4).

Lamarche, G., Proust, J-N., Nodder, S.D. (2005). Long-term slip rates and fault interactions under low contractional strain, Wanganui Basin, New Zealand. *Tectonics* 24.

Latter, J.H., Lloyd, E.F., Smith, I.E.M., Nathan, S. (1992). Volcanic hazards in the Kermadec Islands, and at submarine volcanoes between southern Tonga and New Zealand. Hazards Information Series No. 4, Ministry of Civil Defence. 44p.

Lay, T., Ammon, C.J., Kanamori, H. Rivera, L., Koper, K.D. and Hutko, A.R. (2010). The 2009 Samoa-Tonga great earthquake triggered doublet, *Nature*, 466, pp. 964–968.

Lewis, K.B. and Barnes, P.M. (1999). Kaikoura Canyon, New Zealand: active conduit from near-shore sediment zones to trench-axis channel. *Marine Geology* 162(1): 39-69.

Lloyd, E.F., Nathan, S., Smith, I.E.M., Stewart, R.B. (1996). Volcanic history of Macauley Island, Kermadec Ridge, New Zealand. *New Zealand Journal of Geology and Geophysics* 39, 295-308.

McCaffrey, R. (2007). The Next Great Earthquake, *Science* 315: 1675-1676.

McMurtry, G.M., Watts, P., Fryer, G.J., Smith, J.R., Imamura, F. (2004). Giant landslides, mega-tsunamis, and paleo-sea level in the Hawaiian Islands. *Marine Geology* 203*,* 219-233.

Meckel, T.A., Coffin, M.F., Mosher, S., Symonds, P., Bernadel, G., Mann, P. (2003). Underthrusting at the Hjort Trench, Australian-Pacific plate boundary: Incipient subduction? *Geochemistry, Geophysics Geosystems* 4(12): 1099.

Micallef, A., Mountjoy, J.J., Canals, M., Lastras, G. (2012). Deep-Seated Bedrock Landslides and Submarine Canyon Evolution in an Active Tectonic Margin: Cook Strait, New Zealand. In Submarine Mass Movements and Their Consequences. Advances in Natural and Technological Hazards Research Volume 31: 201-212.

Mountjoy, J.J., Barnes, P.M., Pettinga, J.R. (2009). Morphostructure and evolution of submarine canyons across an active margin: Cook Strait sector of the Hikurangi Margin, New Zealand. *Marine Geology* 260(1-4): 45-68.

Mountjoy, J.J., McKean, J.; Barnes, P.M., Pettinga, J.R. (2009). Terrestrial-style slow-moving earthflow kinematics in a submarine landslide complex. *Marine Geology* 267(3-4): 114-127.

Mountjoy, J.J., A. Micallef (2012). Polyphase Emplacement of a 30 km^3 Blocky Debris Avalanche and Its Role in Slope-Gully Development. Submarine Mass Movements and Their Consequences. Y. Yamada, K. Kawamura, K. Ikehara et al., Springer Netherlands. 31: 213-222.

Pedley, K.L., Barnes, P.M., Pettinga, J.R., Lewis, K.B. (2010). Seafloor structural geomorphic evolution of the accretionary frontal wedge in response to seamount subduction, Poverty Indentation, New Zealand. *Marine Geology* 270(1-4): 119-138.

Pondard, N., Barnes, P.M. (2010). Structure and paleoearthquake records of active submarine faults, Cook Strait, New Zealand: Implications for fault interactions, stress loading, and seismic hazard. *Journal of Geophysical Research* 115, B12320.doi:10.1029/2010JB007781

Pouderoux, H., Lamarche, G., Proust,.J-N. (2012a). Building an 18 000-year-long paleo-earthquake record from detailed deep-sea turbidite characterisation in Poverty Bay, New Zealand. *Natural Hazards and Earth System Sciences* 12(6): 2077-2101.

Pouderoux, H., Proust J.-N., Lamarche G., Orpin A., Neil H. (2012b). Postglacial (after 18 ka) deep-sea sedimentation along the Hikurangi subduction margin (New Zealand): Characterisation, timing and origin of turbidites. *Marine Geology* 295: 51-76.

Power, W., Wallace, L., and Reyners, M. (2008). Tsunami hazard posed by earthquakes on the Hikurangi subduction zone interface, GNS Science Consultancy report 2008/40

Power, W.L., Wallace, L.M., Wang, X., Reyners, M. (2012). Tsunami Hazard Posed to New Zealand by the Kermadec and Southern New Hebrides Subduction Margins: An Assessment Based on Plate Boundary Kinematics, *Pure and Applied Geophysics*, *169*, p 1-36.

Power, W.L., Downes, G.L., Stirling, M.W. (2004). Progress towards a probabilistic tsunami hazard map for New Zealand. *Eos Transactions AGU* 85(47), Fall Meeting Supplement, Abstract OS22B-07

Prasetya G, Beavan J, Wang X, Reyners M, Power W, Wilson KJ, Lukovich B (2011a). Evaluation ofthe July 15, 2009 Fiordland, New Zealand tsunami in the source region. *Pure and Applied Geophysics* doi: 10.1007/s00024-011-0282-6.

Prasetya,G, Wang, X, Palmer, N, and Grant, G. (2011b). Tsunami inundation modelling for Riverton and New River Estuary Southland, GNS Science Consultancy Report 2011/150.

Stirling, M., McVerry, G., Gerstenberger, M., Litchfield, N., Van Dissen, R., Berryman, K., Barnes, P., Beavan, J., Bradley, B., Clark, K., Jacobs, K., Lamarche, G., Langridge, R., Nicol, A., Nodder, S., Pettinga, J., Reyners, M., Rhoades, D., Smith, W., Villamor, P., and Wallace, L. (2012). National seismic hazard model for New Zealand: 2010 update, *Bulletin of the Seismological Society of America*, August 2012 vol. 102 no. 4 1514-1542.

Suarez, G., Albini, P. (2009). Evidence for Great Tsunamigenic Earthquakes (M 8.6) along the Mexican Subduction Zone. *Seism. Soc. Amer. Bull.* 99(2A): 892-896.

Tanioka Y., Seno, T. (2001). Detailed analysis of tsunami waveforms generated by the 1946 Aleutian tsunami earthquake. *Natural Hazards & Earth System Science* **1,** 171-175.

Tappin, D.R., Matsumoto, T., Watts, P., Satake, K., McMurty, G.M., Matsuyama, Y., Lafoy, Y., Tsuji, Y., Kanamatsu, T., Lus, W., Iwabuchi, Y., Yeh, H., Matsumotu, Y., Nakamura, M.,Mahoi, M., Hill, P., Crook, K., Anton, L., and Walsh, J.P. (1999). Sediment Slump Likely Caused1998 Papua New Guinea Tsunami, *EOS, Trans. Am. Geophys. U.* 80, 329–340.

Wallace, L.M., Reyners, M.E., Cochran, U.A., Bannister, S.C., Barnes, P.M., Berryman, K.R., Downes, G.L., Eberhart-Phillips, D., Fagereng, A., Ellis, S.M., Nicol, A., McCaffrey, R., Beavan, R.J., Henrys, S.A., Sutherland, R., Barker, D.H.N., Litchfield, N.J., Townend, J., Robinson, R., Bell, R.E., Wilson, K.J.,and Power, W.L. (2009). Characterizing the seismogenic zone of a major plate boundarysubduction thrust: Hikurangi Margin, New Zealand: *Geochemistry, Geophysics, Geosystems*,v. 10, Q10006, doi: 10.1029/2009GC002610.

Walters, R., Barnes, P., Lewis, K., Goff, J.R., Fleming, J. (2006). Locally generated tsunami along the Kaikoura coastal margin: Part 2.Submarine landslides. *New Zealand journal of marine and freshwater research* 40(1): 17-28.

Witter, R.C., Kelsey, H.M., Hemphill-Haley, E. (2003). Great Cascadia earthquakes and tsunamis of the past 6700 years, Coquille River estuary, southern coastal Oregon. *Geological Society of America Bulletin* 115, 1289-1306.

Wright, K.C. (compiler), Beaven, J., Daly, M., Gale, N., Leonard, G.S., Lukovic, B., Palmer, N., Power, W., Reyners, M., Rosser, B., Wallace, L. and Wang, X. (2011). Filling a critical gap in end-to-end tsunami warning in the Southwest Pacific: a pilot project in Samoa to create scientifically robust, community-based evacuation maps, GNS Science Report 2011/53. 140p.

Wright, I.C., Gamble, J.A. (1999). Southern Kermadec submarine caldera arc volcanoes (SW Pacific): caldera formation by effusive and pyroclastic eruption. *Marine Geology* 161*,* 207-227.

Wright, I.C., Gamble, J.A., Shane, P.A.R. (2003). Submarine silicic volcanism of the Healy caldera, southern Kermadec arc (SW Pacific): I - volcanology and eruptive mechanisms. *Bulletin of Volcanology* 65*,* 15-29.

Wright, I.C., Garlick, R.D., Rowden, A., Mackay, E. (2004). New Zealand's Undersea Volcanoes*. NIWA Chart, Miscellaneous Series No.81*, Wellington, NIWA.

Wright, I.C., Worthington, T.J., Gamble, J.A. (2006). New multibeam mapping and geochemistry of the 30°–35°S sector, and overview, of southern Kermadec arc volcanism, *J. Volcanol. Geotherm. Res*., 149, 263–296.

This page is intentionally left blank.

6.0 PROBABILISTIC MODELLING

This chapter outlines the probabilistic hazard model included in this report, and presents the main results. It is intended to provide a general overview of the hazard model, suitable for non-specialists. Additional technical details of the hazard model are presented in Appendix 7.

6.1 INTRODUCTION AND MOTIVATION

There are many ways in which the risks caused by natural hazards can be mitigated; in the case of tsunami these include early-warning systems, evacuation mapping, public education in self-evacuation, land-use zoning, and engineered sea defences. However these techniques must be used appropriately to ensure that mitigation measures are effective in their operation and are suitably prioritised relative to mitigation of other natural and man-made hazards.

A probabilistic assessment of risk, defined as an estimate of the probable economic losses or human casualties in a period of time, is generally considered the best way to make comparisons across multiple hazards.

The relationship between risk, hazard, exposure and vulnerability is, in general terms, defined as:

Risk = Hazard x Exposure x Vulnerability

See section 2.2 for a more complete explanation of these terms. Mitigation measures reduce the exposure or the vulnerability to the hazard. The reduction in risk is then a measure of the effectiveness of mitigation.

The purpose of this report is to quantitatively estimate the tsunami hazard around the New Zealand coast, so the results may be applied to the estimation of risk and to the development of appropriate mitigation measures.

6.2 METHODOLOGY OUTLINE

The approach used for estimating tsunami hazard in this report is based on a Monte-Carlo modelling process. The method aims to estimate the maximum tsunami height that can be expected over a specified interval of time within sections of the New Zealand coast that are approximately 20 km long. As is the case in most areas of science, an estimate of tsunami hazard is of little value without an assessment of the uncertainty in that estimate, and consequently the estimation of uncertainties plays a major role in the methods used for this report.

To understand the methodology, it is first useful to clearly distinguish between variability and uncertainty. Variability refers to the natural variations that occur between different events. For instance the magnitude of earthquakes on a fault naturally varies from one earthquake to the next. Uncertainty, on the other hand, is a measure of our lack of knowledge about things which are constant in time. For example while the shape of a fault is fixed (at least within the timeframes we are interested in), its shape is not known exactly, and the uncertainty is a measure of how well it is known.

Our Monte-Carlo analysis operates on two levels (Figure 6.1). On the inner level we assume that we have perfect knowledge of the uncertain parameters that do not vary over time, and carry out a hazard assessment using Monte-Carlo sampling of those properties that naturally vary between events. On the outer level we perform Monte-Carlo sampling of the uncertain parameters, and use this to build up a set of hazard estimates that differ from those calculated for the inner level. The spread of these estimates represents the uncertainty in the hazard.

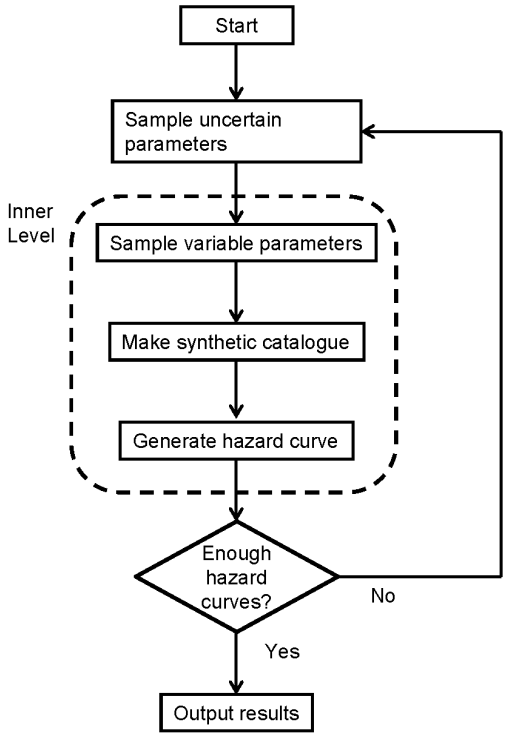

Figure 6.1 Simplified flow-chart representation of the Monte-Carlo modelling scheme.

A more detailed representation of the method is shown in Figure 6.2; in this figure each row going across the chart describes the steps used to construct one tsunami hazard curve. These steps are repeated many times using different samples of the uncertain parameters, and from these it is possible to assign 'error bars' to the tsunami hazard curves.

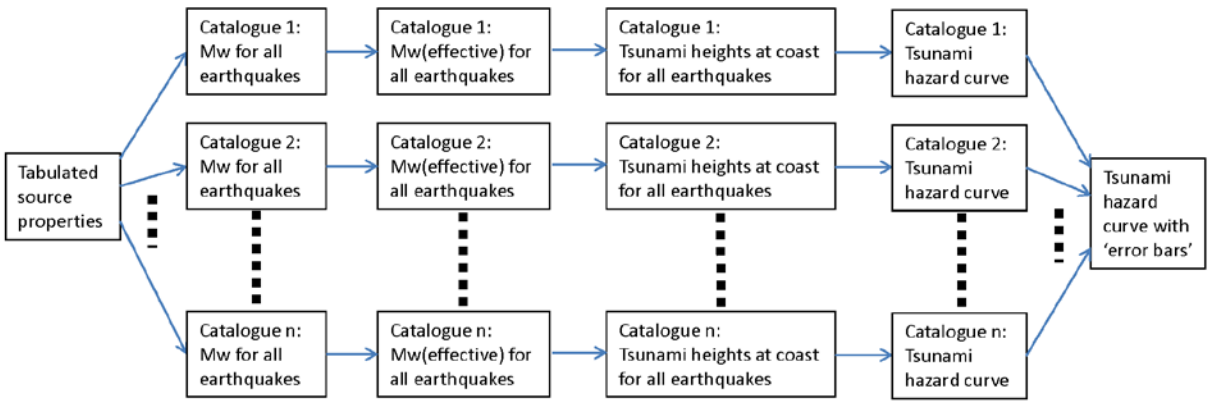

Figure 6.2 Representation of the Monte-Carlo modelling scheme.

Each hazard curve describes the maximum tsunami height reached within a coastal section, as a function of return period (see Section 6.6 and Appendix 7.4 for more details). By sampling from the uncertain parameters, and creating multiple hazard curves, it is possible to estimate the uncertainty in the tsunami hazard (Figure 6.3).

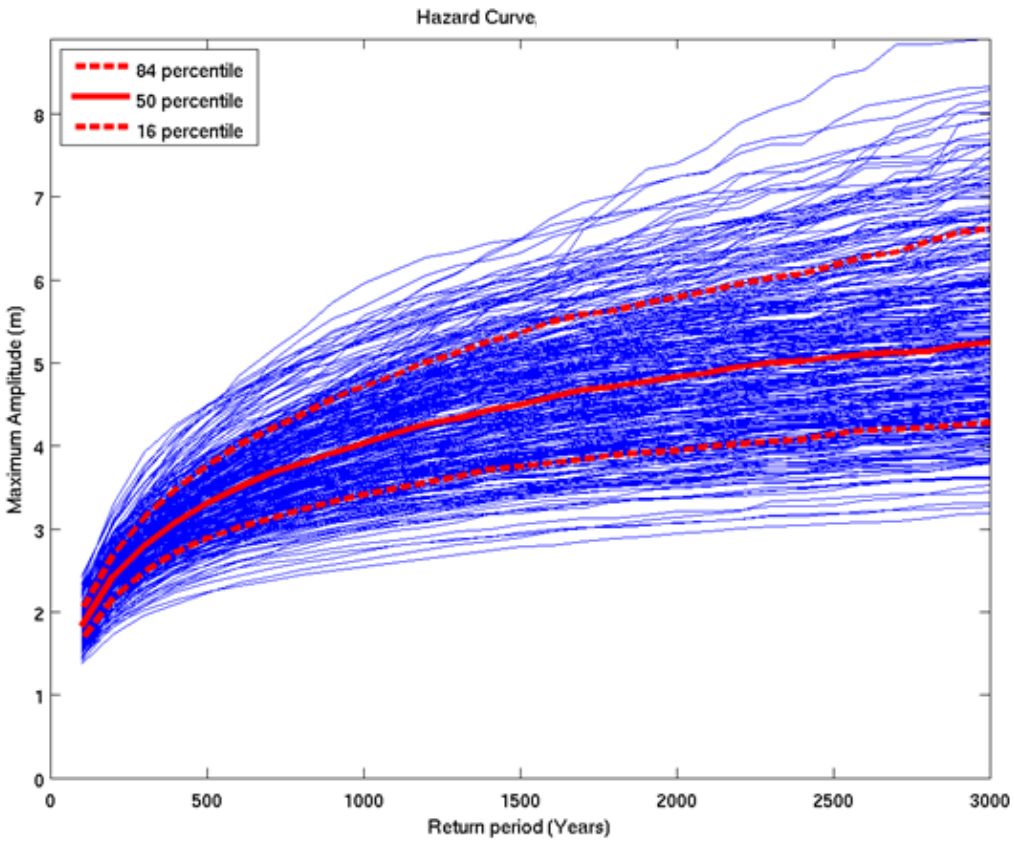

Figure 6.3 Hazard curves for 300 samples of the uncertain parameters, illustrating how the 16th, 50th and 84th percentiles of uncertainty are calculated for one coastal section.

6.3 TYPES OF UNCERTAINTY AND VARIABILITY

The uncertainties and variabilities fall into two broad categories—those associated with the source earthquake, and those associated with the modelling process. For earthquakes, the primary uncertainty is the true form of the magnitude-frequency distribution of the faults (i.e., knowing how often earthquakes of varying magnitude occur along a fault), though it also encompasses such things as uncertainty in the geometry of the faults. The earthquake variabilities represent the variation in magnitude from event to event on a particular fault, and also the variation in the distribution of slip (even among earthquakes of the same magnitude). Modelling uncertainty, on the other hand, reflects the inability of the model to fully capture the physics of tsunami generation and propagation, and uncertainties in bathymetric data. A table summarising the different types of uncertainty and variability, with pointers for further information, is presented in Appendix 7.1.

6.4 SOURCE DEFINITION

An essential input to our probabilistic hazard model is a definition of the physical and statistical properties of the various tsunami sources.

The scope of this report is to define the tsunami hazard within timeframes of up to 2500 years. On these timescales the major contribution to tsunami hazard comes from both distant and local earthquakes, and these are the sources considered here (See 'Tsunami Sources' Chapter 5). For some regions of the country, submarine landslides may contribute to the tsunami hazard in these timeframes as well, and initial steps towards estimating potential landslide contributions are described in Appendix 6.

The definition of tsunami sources from subduction-zone earthquakes, which constitute all distant earthquake sources and the most important local ones, drew heavily on work that has been done for the Global Earthquake Model (GEM). The assumed parameters for subduction-zone earthquakes used for this report are shown in Appendix 3.

The starting point for defining tsunami sources for local non-subduction zone earthquakes was the New Zealand Seismic Hazard Model (NZSHM; Stirling et al., 2012). The faults in the seismic hazard model were filtered to exclude those with characteristic magnitudes below 6.5 (which are too small to generate enough displacement to cause a tsunami), those with strike-slip mechanisms, and those that are entirely on-shore. The remaining faults are summarised in Appendix 4. Additional fault sources were added in the Outer Rise, the Taranaki Basin, and along the west coast of the South Island; these fault sources are only tentatively identified in geophysical data, and are summarised in Appendix 5.

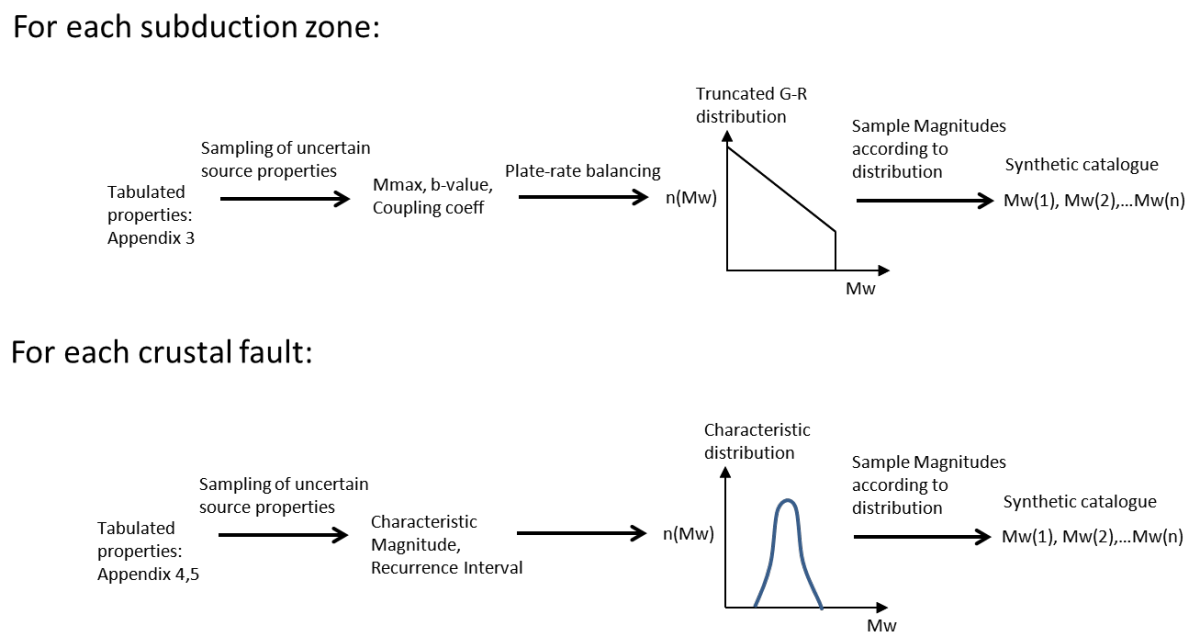

Figure 6.4 Illustration of the steps by which the tabulated fault properties are used to create synthetic earthquake catalogues. This process corresponds to the leftmost set of arrows in Figure 6.2.

The creation of synthetic earthquake catalogues from the tabulated fault and subduction zone properties is illustrated in Figure 6.4. Additional details regarding the construction of the synthetic catalogues are presented in Appendix 7.2.

6.5 TREATMENT OF VARIABLE SLIP AND MODELLING UNCERTAINTY

Magnitude alone is not enough to determine the size of tsunami that will be produced by an earthquake. It has been shown that the distribution of slip on a fault also plays an important role. Geist (2002) found that the peak amplitude of nearshore tsunami varied by over a factor of 3 depending on the slip distribution. Preliminary work by Mueller et al. (2012) has demonstrated great variation in the extent of inundation as a result of variable slip. It was found that in order to encompass the union of the inundation from 60 variable slip models of a M_W 8.4 earthquake (i.e., the area of land inundated in at least one of the 60 models), a uniform slip model would need to be of M_W 8.9 (a difference of 0.5 magnitude units). This suggests that locally the effect of variable slip may be approximately equivalent to a change in the effective magnitude of the event.

Within our model we treat the effect of non-uniform slip as if it has the effect of altering the effective magnitude of the earthquake. By adding a normally distributed variation to the magnitudes in the synthetic earthquake catalogue, we create a new catalogue of 'effective magnitudes' that represent the consequences of the variable slip. It may be argued that this is not a true representation of the effects of variable slip, since variable slip may enhance the tsunami at some locations while reducing it at others, whereas our approach sees the effective magnitude of the earthquake increase (or decrease) in the same way at all locations. This would be a problem if we were to look at correlated hazards across multiple locations, however as long as we view the hazard on a 'one site at a time' basis, this approximation appears valid.

This approach, of creating a catalogue of 'effective magnitudes', also provides a convenient way to incorporate the effects of modelling uncertainties. We regard the effects of modelling approximations and of limited data on source geometry and ocean bathymetry, as having a similar effect to (usually small) increases or decreases in the magnitude of the source earthquake. Table 6.1 summarises the parameters used for this purpose:

Table 6.1 Standard deviations associated with random adjustments to the synthetic catalogue to create a catalogue of 'effective magnitudes'. The fault-specific uncertainty covers uncertainties that are specific to the modelling of each fault, while the method bias covers uncertainties that cause a systematic bias across all faults. Units are in the M_W scale.

	Local Crust Fault (empirical model)	**Local Subduction Zone (numerical model)**	**Distant Subduction Zone (numerical model)**
Variability (e.g. non-uniform slip): σ_v	0.25	0.25	0.1
Modelling uncertainty (fault specific): σ_u	0.2	0.1	0.1
Modelling uncertainty (method bias): σ_b	0.14	0.05	0.05

An 'effective magnitude' is calculated by applying the parameters that describe the uncertainties and variabilities that affect tsunami heights, using the following equation:

$$Mw_{ijk}(effective) = Mw_{ijk} + \sigma_v N(0,1)_{ijk} + \sigma_u N(0,1)_{jk} + \sigma_b N(0,1)_k \qquad \textbf{Equation 6.1}$$

where i represents individual earthquakes on fault j, described in synthetic catalogue k. N(0,1) represents a number sampled from the normal distribution with a mean of zero and a standard deviation of 1. The subscript to N(0,1) describes the set over which individual samples are made, e.g., $N(0,1)_{jk}$ is sampled for each fault in each catalogue, but has the same value for all earthquakes on a particular fault in a particular catalogue. This calculation of an 'effective magnitude' corresponds to the second step (going left to right) in Figure 6.2.

The reasoning behind the choice of values for the parameters in Table 6.1 is explained in Appendix 7.3.

6.6 ESTIMATION OF TSUNAMI HEIGHTS

The Monte-Carlo method requires us to estimate the maximum tsunami height for each section of the coast following every event in a synthetic catalogue of earthquakes. Various techniques can be used to estimate the tsunami heights, but it is important that the calculation can be performed quickly, since it is necessary to model many events to produce robust statistics.

Three different methods are used here:

- Finding the closest available model (in terms of location and magnitude) in a pre-computed catalogue, and then applying scaling to the model results to match the synthetic catalogue magnitude.
- Using a collection of pre-calculated models of tsunami from a particular source region to estimate coefficients in a semi-empirical scaling relationship.
- Using an empirically-determined scaling-relationship based only on the magnitude and distance of historical earthquakes that have caused tsunami.

Broadly speaking, the quality of results diminishes down this list of methods, as does the work required to implement them for any particular source. The first method has been applied to subduction zone sources close to New Zealand, specifically the Hikurangi, Kermadec and Puysegur Trenches, where the location of the earthquake within the source region plays a very major role in determining the consequences for particular sections of the New Zealand coast (see Appendix 7.4 for more details). The second method has been applied to all other Pacific subduction zones, i.e., those at regional or distant locations from New Zealand; the tsunami consequences of earthquakes at these distances are less sensitive to the precise location of the source. This method uses the empirical approach of Abe (1979), except that numerical results from the New Zealand forecast database were used instead of historical catalogue data (see Appendix 7.4 and Section 4.5.1.1 for more details). The third method applies the empirical modelling approach developed by Abe (1995), and is applied to estimating the tsunami caused by local faults other than the subduction zones (see Appendix 7.4 and Section 4.5.1.2 for more details).

Tsunami height is defined here as the maximum height that the tsunami would reach against an imaginary vertical wall at the coast, relative to the background sea level at the time of the tsunami. This choice of criteria permits us to re-use the modelling used for the New Zealand forecast database. In many situations where the tsunami does not penetrate far inland (i.e., less than several kilometres) this represents a reasonable approximation to the expected run-up height, although in a small number of locations where a tsunami is focussed by small-scale topographic features, the run-up may locally reach up to about twice this height. For most practical mitigation measures it is expected that the tsunami heights derived from this study will not be used directly, but will be deaggregated (see Section 6.8) to determine the extent to which different sources contribute to the hazard, and this will be used to decide upon specific scenarios for detailed inundation modelling.

In the case of the empirical equation used for local crustal faults, Abe (1995) relates the predicted tsunami height to the average run-up height measurement, rather than to the maximum height against an imaginary vertical wall at the shore[20]. We have treated these two quantities as being equivalent, but there is considerable uncertainty about this relationship; this uncertainty contributes to the corresponding bias parameter in Table 6.1.

The numerical models used for this study were developed using the COMCOT code (Wang and Liu, 2006; Wang and Liu, 2007). A series of nested bathymetric grids were developed, ranging in size from the entire Pacific Ocean to small regions of New Zealand. Models from the New Zealand tsunami forecast database were used for the distant subduction zone sources. The local subduction zones were modelled using the same nested grid configuration in order to maintain consistency. In this grid setup the non-linear shallow water wave equations were used to model the grids closest to New Zealand, where the water depths are such that the non-linear effects may be significant, and the linear shallow water equations were used for all of the outer grids.

6.7 CALCULATION

The Monte-Carlo analysis of epistemic uncertainty was made using 300 samples of the uncertain parameters. For each of these 300 samples a 100,000 year synthetic catalogue of earthquakes was constructed. Re-running the analysis using these same parameters and a different set of random numbers demonstrated good repeatability of the results, with variations in the hazard curves that were small compared to the cumulative effect of other sources of uncertainty. The probabilistic tsunami hazard model in this report does not include modelling of tides.

6.8 DEAGGREGATION OF TSUNAMI SOURCES

The process described in the preceding sections allows the construction of tsunami hazard curves for individual sections of coast. These curves, which will be described in detail in section 6.9, indicate the height of tsunami that may be expected in a given time frame. On their own these curves do not provide a measure of the extent of inundation, only the maximum height at the coast.

Deaggregation is a process for establishing the extent to which different tsunami sources contribute to the probabilistic tsunami hazard. The main purpose for the deaggregation used in this report is to establish a particular set of scenarios whose inundation can be modelled to give an approximation of the onshore tsunami hazard at a particular level of probability (i.e., return period) and confidence.

The probabilistic hazard analysis described in Sections 6.2 to 6.7 involves the generation of a large number N (typically 300) of synthetic catalogues of effective earthquake magnitude. Each catalogue represents a sequence of earthquakes generated assuming a particular sampling of the uncertain parameters. For a selected return period R (500 years and 2500 years have been used) the median tsunami height H(R) was found from the corresponding hazard curve for the site of interest. Each synthetic catalogue was searched to find the three

[20] In earlier work Abe (1981; 1985) calibrated the tsunami height in his empirical equations using the amplitudes measured by tide gauges, however it was shown that the Japanese tide gauges of this era were often likely to underestimate tsunami amplitude because of slow instrument response (Satake et al., 1988), so we regard this interpretation as unreliable.

earthquakes that produced tsunamis at the site which were closest in height to H(R). The proportion of these 3xN events coming from particular faults was calculated, and this was used to generate the pie charts described in section 6.9. In addition, an estimate was made of the median effective magnitude of the selected earthquakes from each of the identified faults.

This deaggregation procedure can probably be improved upon with further research. In particular it may not be ideal for use in situations involving both long return periods and high levels of confidence (e.g., 2500 year RP and 95% confidence) as it is possible that some catalogues may not then contain events that reach the H(R) of a given coastal section.

6.9 RESULTS

The coast of New Zealand was divided into 268 sections, each approximately 20 km long as measured along the open coast[21]. Within each section the model produces a hazard curve that illustrates the expected maximum tsunami height (as defined in Section 6.6) as a function of return period. A series of hazard curves for several major cities are shown in Figure 6.2 to Figure 6.33: the solid line indicates the best-estimate hazard curve and the dashed lines are 'error bars' indicating the 16th and 84th percentile of uncertainty. During a tsunami the peak water levels will vary considerably even across a 20 km section of coast; in the curves shown here the 'maximum amplitude' should be interpreted as the tsunami height measured at the location within the section where it is highest; the median tsunami height within the section may be significantly lower (see, e.g., Power et al., 2010).

Opposite the hazard curves are two pie charts; these show the breakdown of the relative contribution of different fault sources to the median hazard (i.e., the 50th percentile of uncertainty in the hazard curves) at 500 years and 2500 years. The area of each slice of the pie indicates the proportion of the hazard for which a particular fault is responsible—the larger the area the more frequently that source is expected to produce tsunami of the size corresponding to the return period.

The pie charts indicate the six tsunami sources that most frequently generate tsunami at the median height (in terms of confidence) for the 500 year and 2500 year return periods. The pie charts also show the effective magnitude of earthquakes on these faults that are necessary to generate a tsunami of this height. While these events are estimated to produce tsunami of the same height at the coast, the extent of inundation is expected to vary with the number and period of waves.

In order to make an estimate of the extent of inundation at the 500 year and 2500 year return period, we suggest that the six sources making the greatest contribution are all modelled through to inundation, assuming earthquakes at the effective magnitudes given on the pie charts. The modelling should assume uniform slip at the specified effective magnitude, and if the source is one of the local subduction zone sources (Hikurangi, Kermadec or Puysegur) the earthquake should be assumed to occur on the part of the interface that the site is most sensitive to (usually the nearest). The union of the six inundations (i.e., the area inundated in

[21] This is primarily an open coast tsunami hazard model. While the modelling did include harbours, they may not be well resolved at the resolution used. Hence all coastal sections included ~20 km of open coast.

one or more of the scenarios) can then be used as a conservative approximation[22] to the extent of inundation at the chosen return period.

The fault labels on the pie charts indicate the estimated magnitude that an earthquake on each source would need to be to produce a tsunami that would reach this height according to our deaggregation. The labelling convention is as follows: first there is a code indicating the general source region (NZ=New Zealand, AK=Alaska, CA=Central America, CD=Cascadia, CL=Chile, CO=Colombia, JP=Japan, MX=Mexico, PE=Peru, PH=Philippines, PNG=Papua New Guinea, SPAC=South Pacific); then comes the fault or subduction zone name (see Appendices 3 and 4); followed by the magnitude from the deaggregation. Sometimes the effective magnitudes may be greater than those considered possible for the fault—this is a consequence of our approximations used to represent the effects of non-uniform slip and other uncertainties. In other words, a uniform slip event of this magnitude is used to approximate a non-uniform slip earthquake of lower magnitude.

In order to compare the hazard at different sites, the hazard at various return periods can be illustrated in a map view. Examples of these maps for return periods of 100, 500 and 2500 years are shown in Figure 6.34 to Figure 6.36.

[22] Tsunami of the same height at the coast will still differ in the extent of inundation as a consequence of other properties such as the number and duration of waves; this is why taking the union of the six inundations is a conservative approximation. It may be possible to remove this bias by using a combination of the individual inundations that are weighted according to their relative frequency, further research is needed to see if this is feasible.

Auckland East Coast

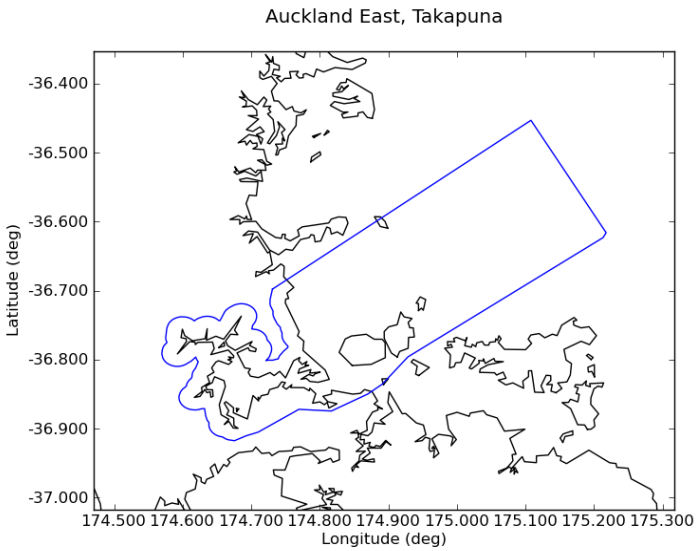

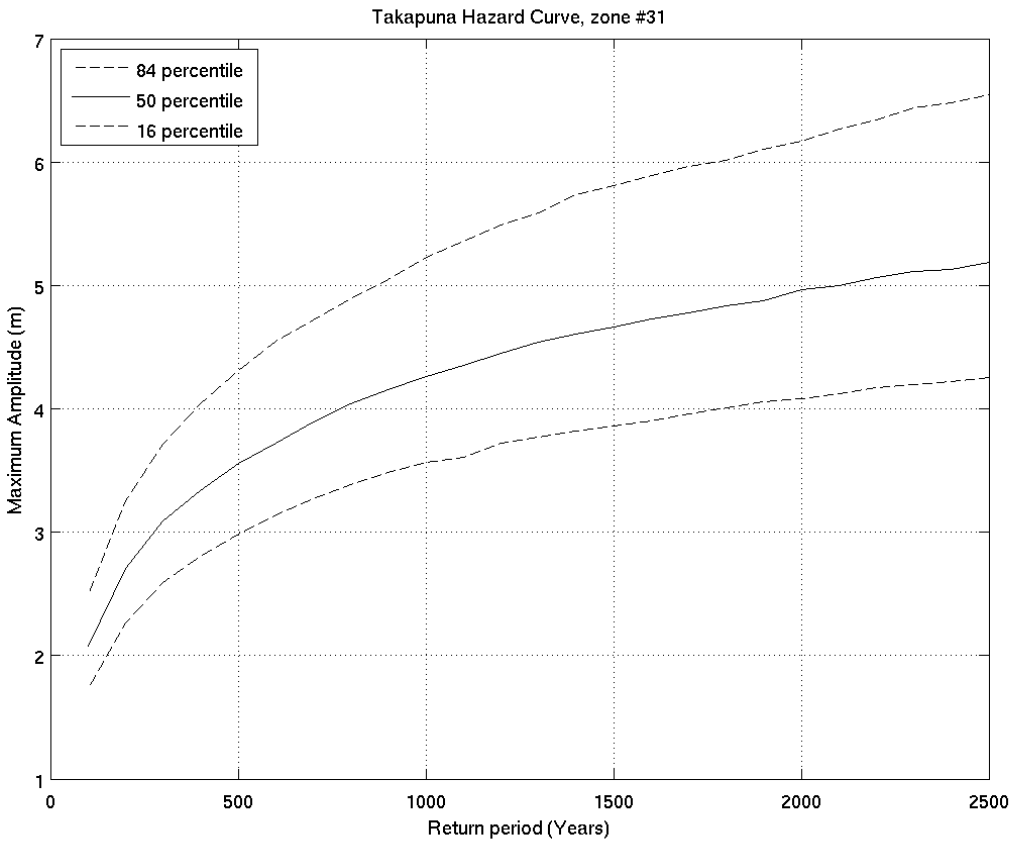

Figure 6.5 Area map and tsunami hazard curve for Auckland East.

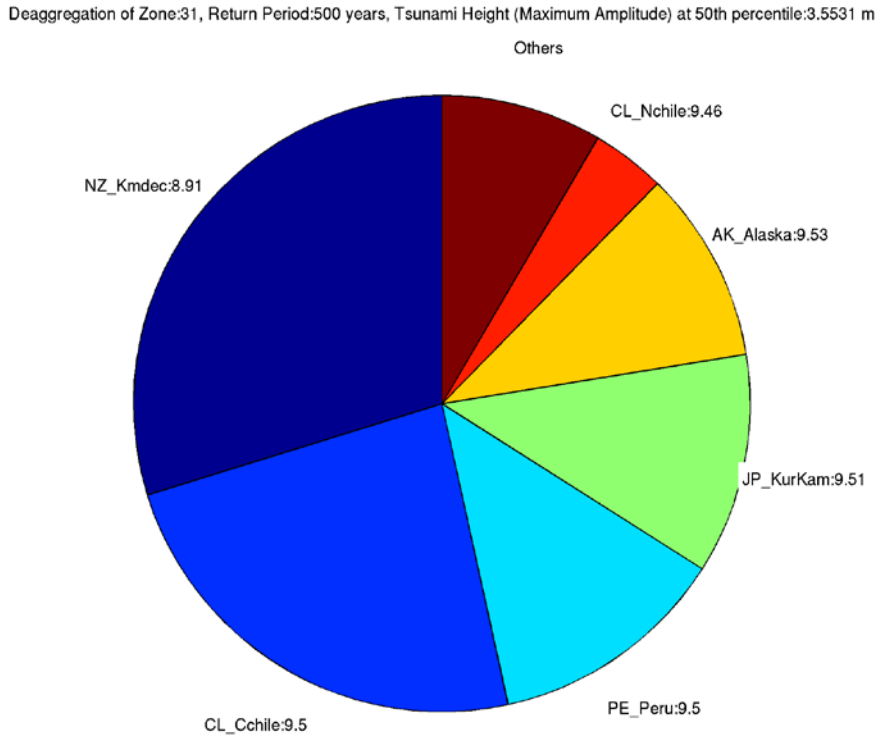

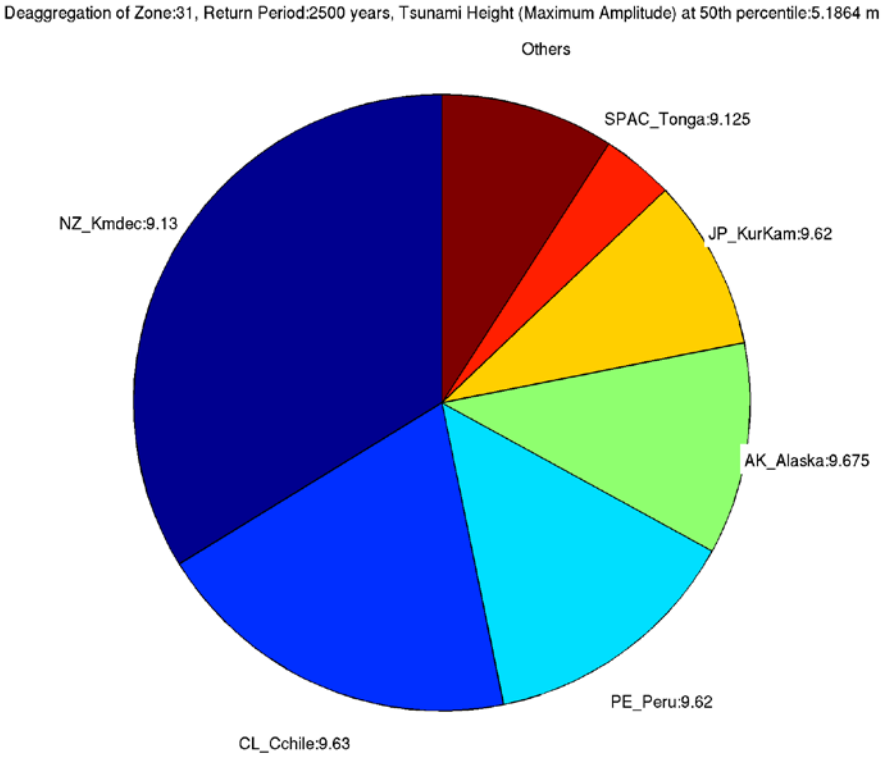

Figure 6.6 Deaggregation of tsunami sources for Auckland East Coast at 500 yr (top) and 2500 yr (bottom) return periods.

Auckland West Coast

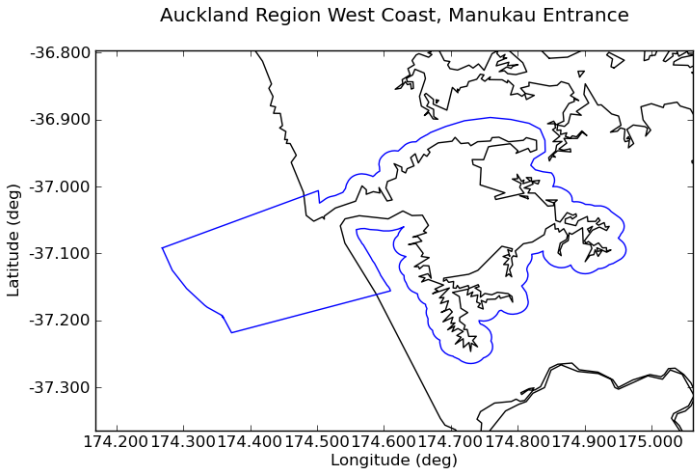

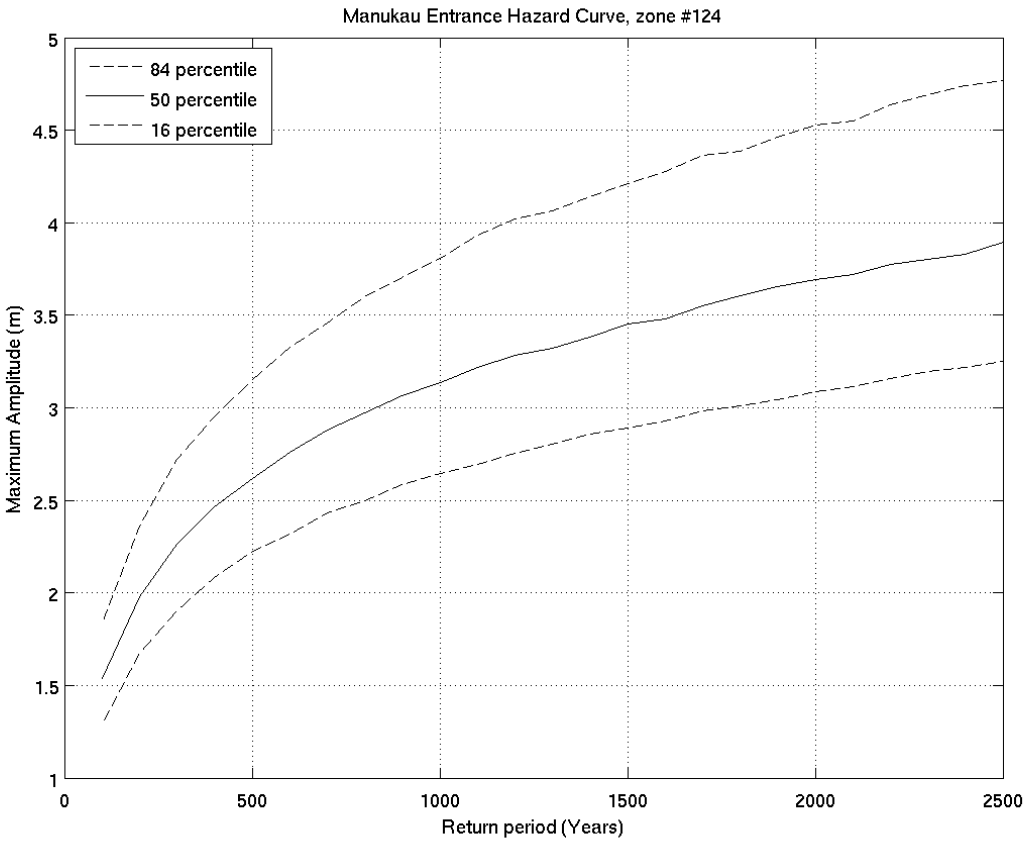

Figure 6.7 Area map and tsunami hazard curve for Auckland West Coast.

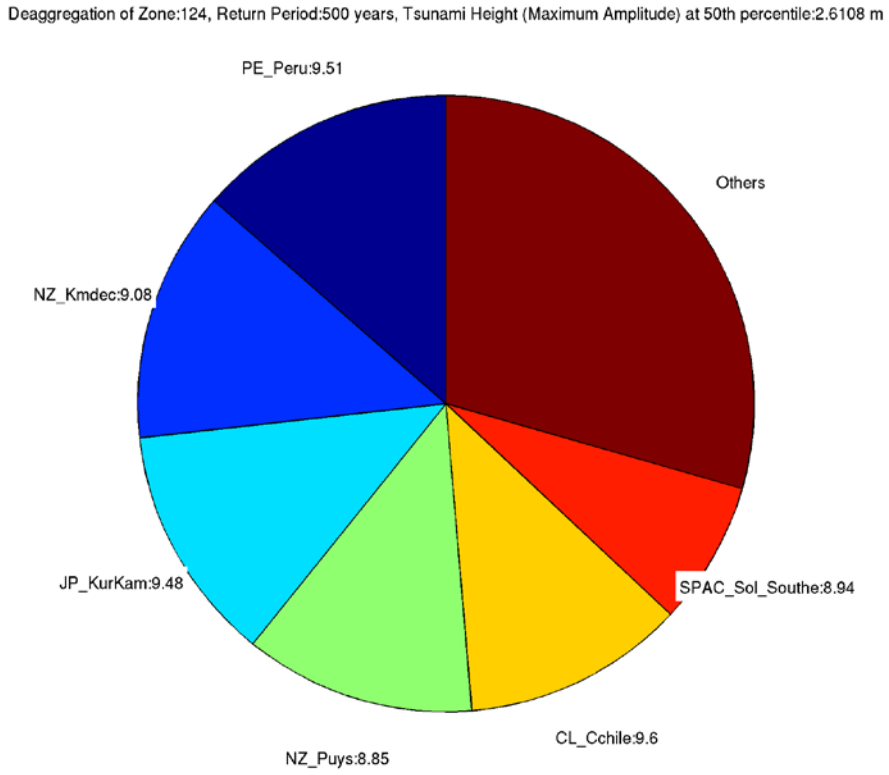

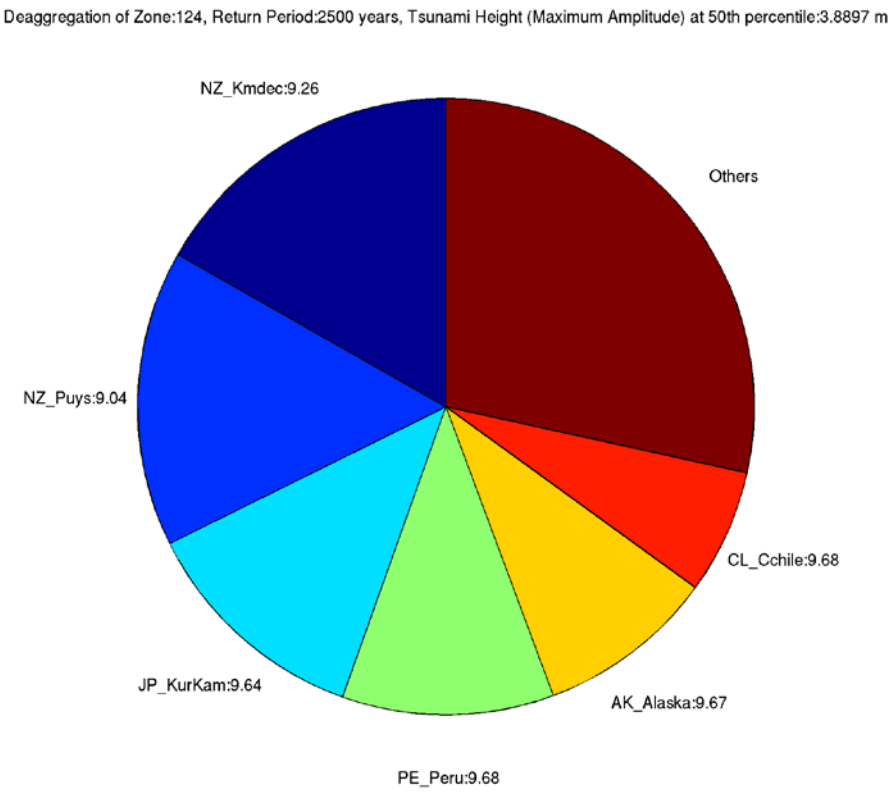

Figure 6.8 Deaggregation of tsunami sources for Auckland West Coast at 500 yr (top) and 2500 yr (bottom) return periods.

Christchurch

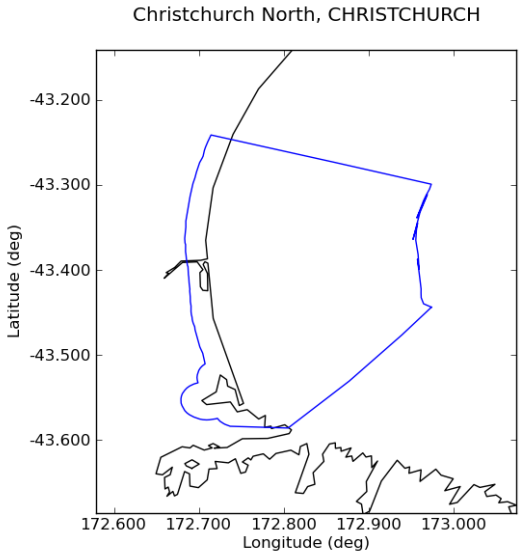

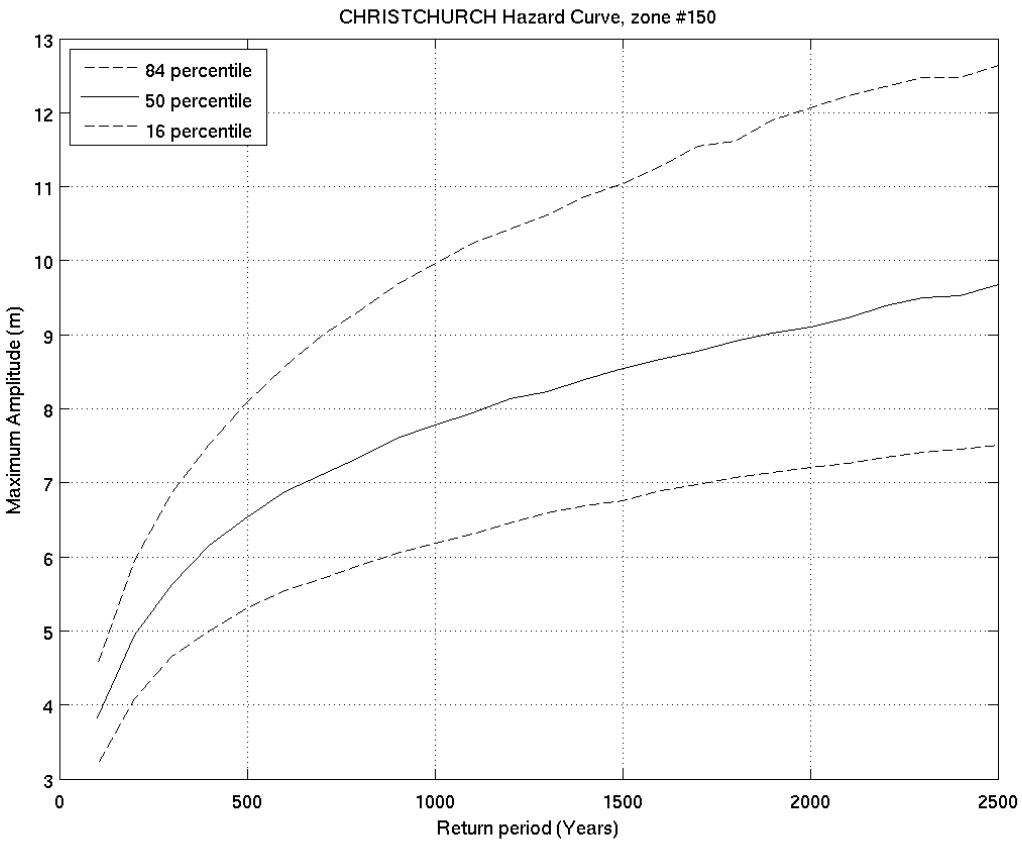

Figure 6.9 Area map and tsunami hazard curve for Christchurch.

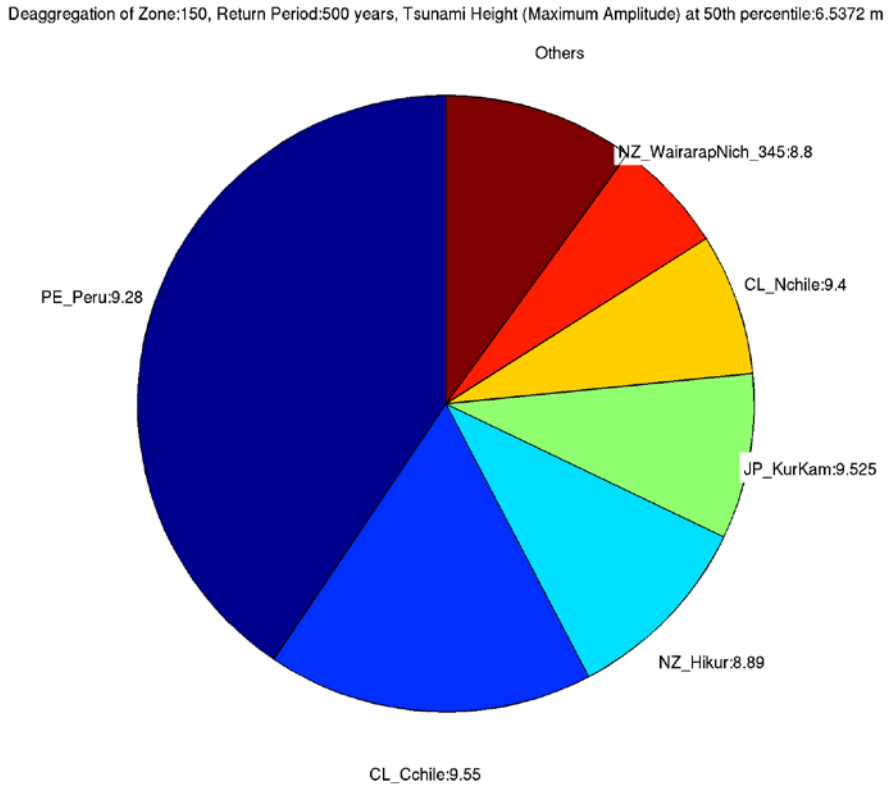

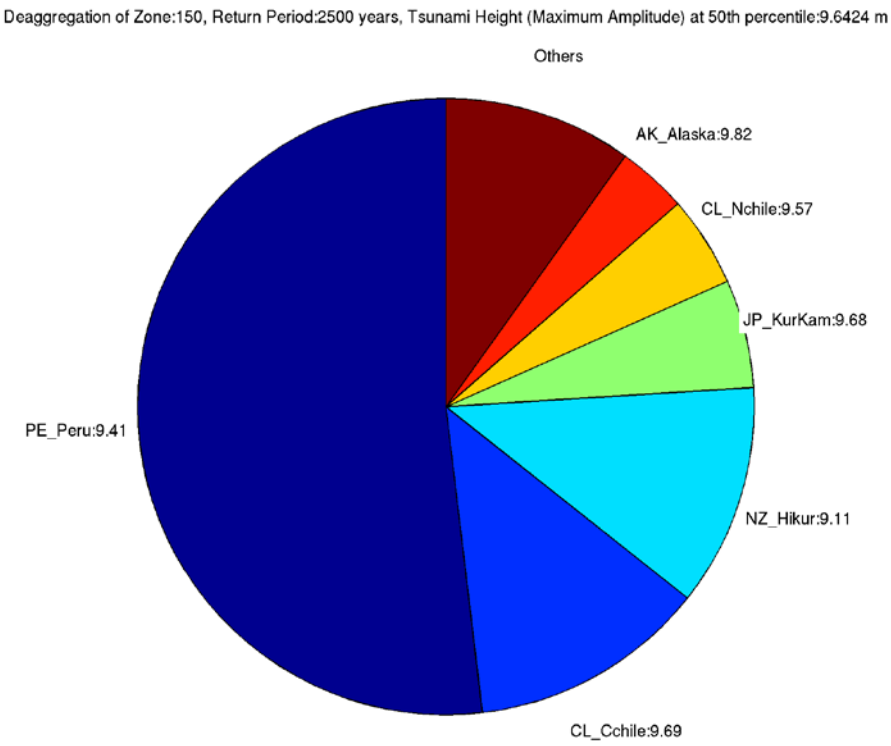

Figure 6.10 Deaggregation of tsunami sources for Christchurch at 500 yr (top) and 2500 yr (bottom) return periods.

Dunedin

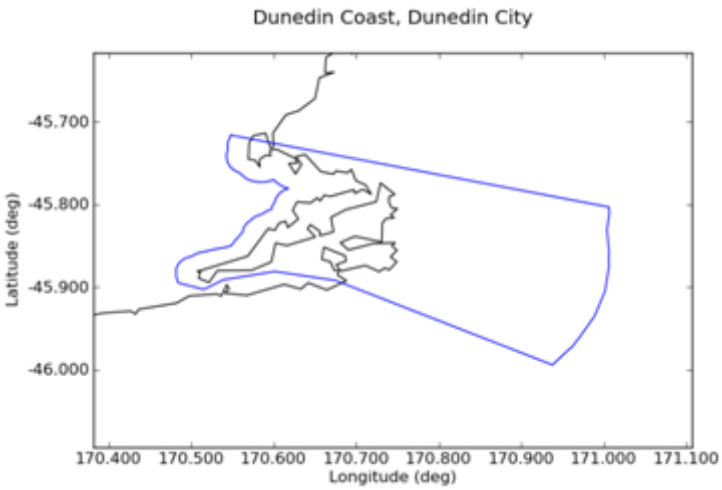

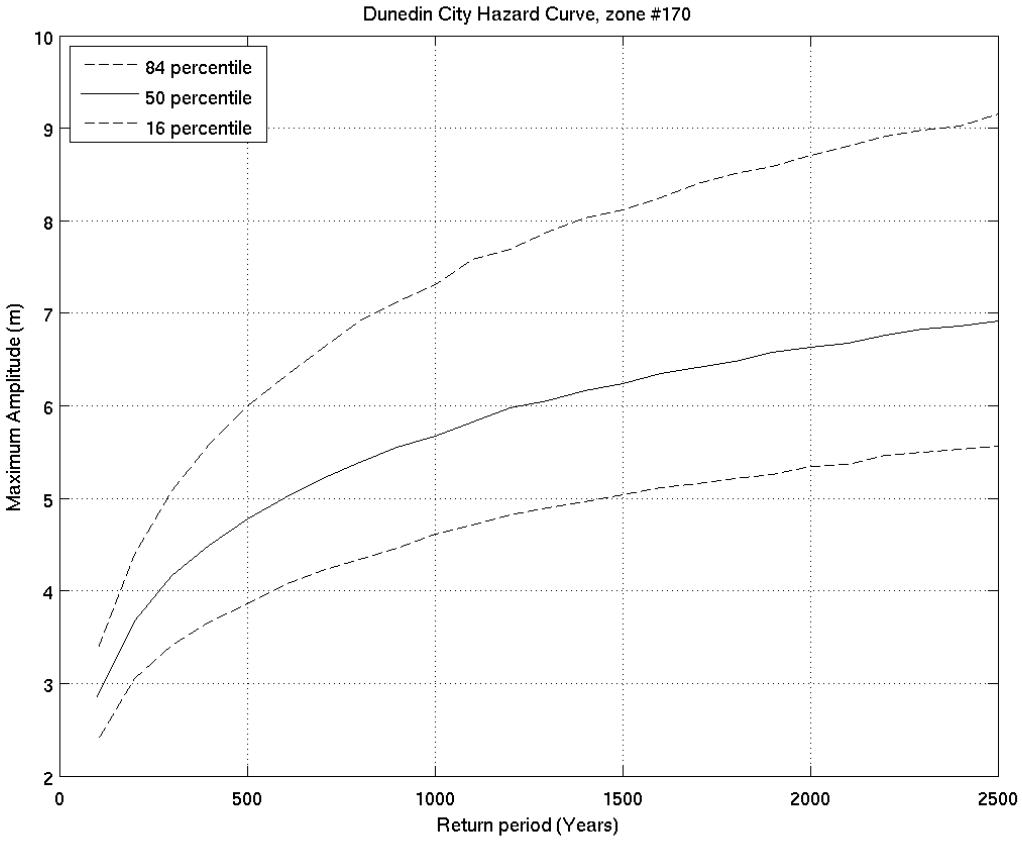

Figure 6.11 Area map and tsunami hazard curve for Dunedin.

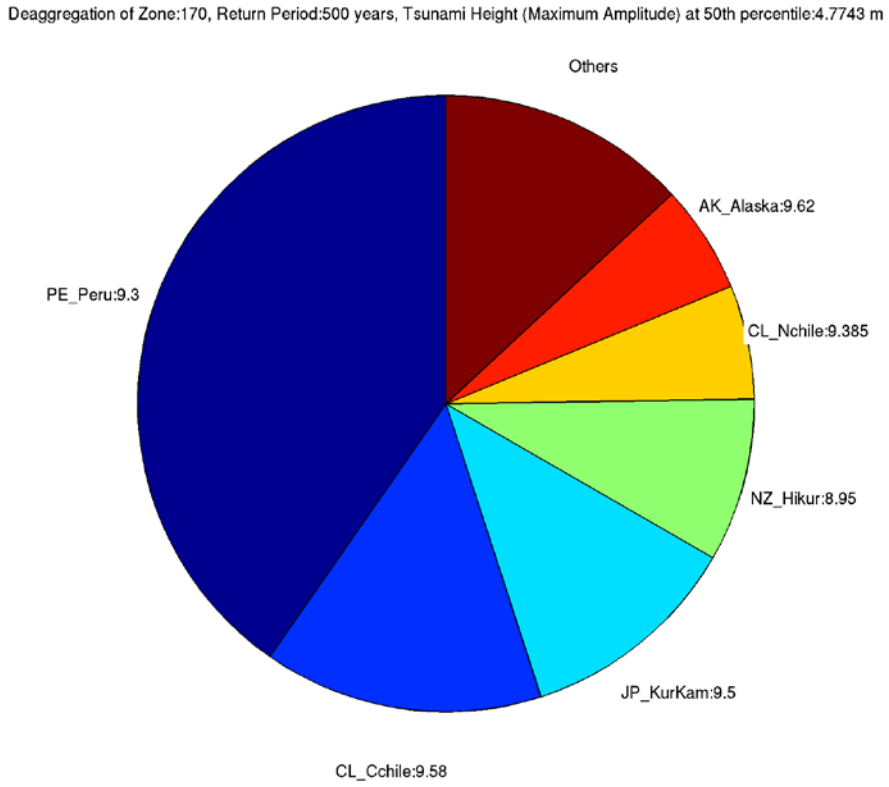

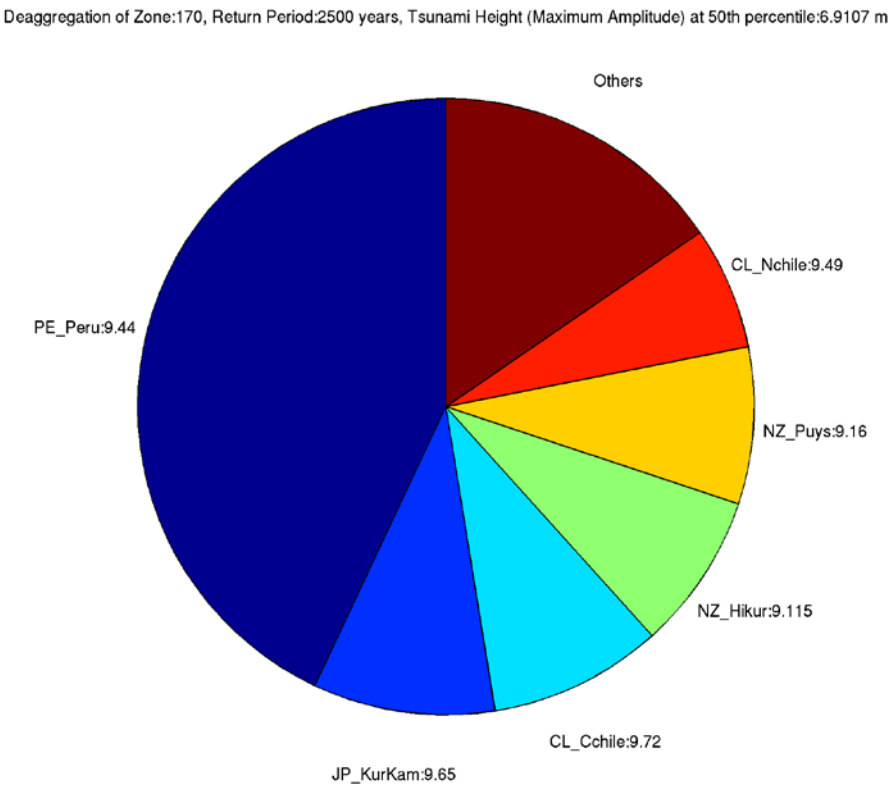

Figure 6.12 Deaggregation of tsunami sources for Dunedin at 500 yr (top) and 2500 yr (bottom) return periods.

Gisborne

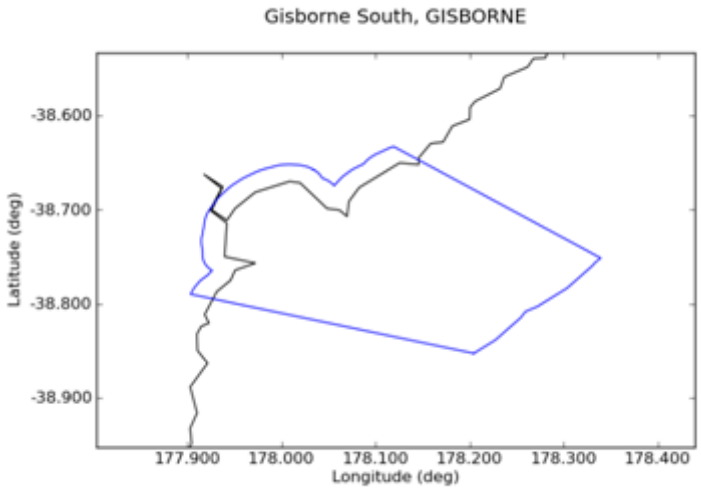

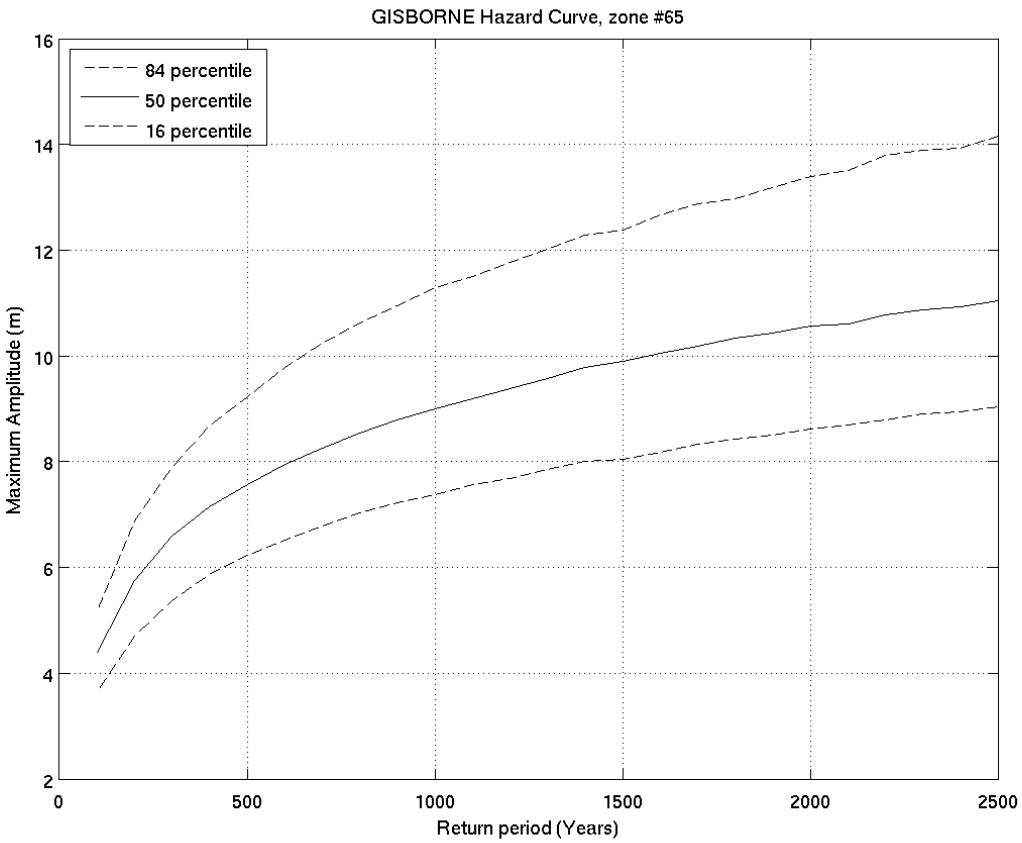

Figure 6.13 Area map and tsunami hazard curve for Gisborne.

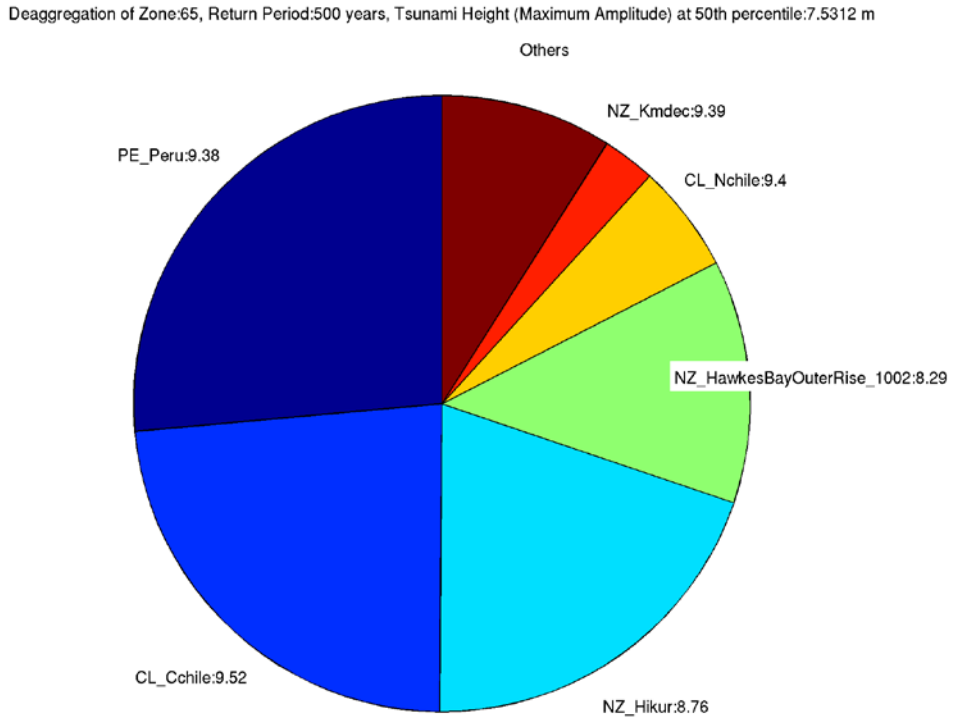

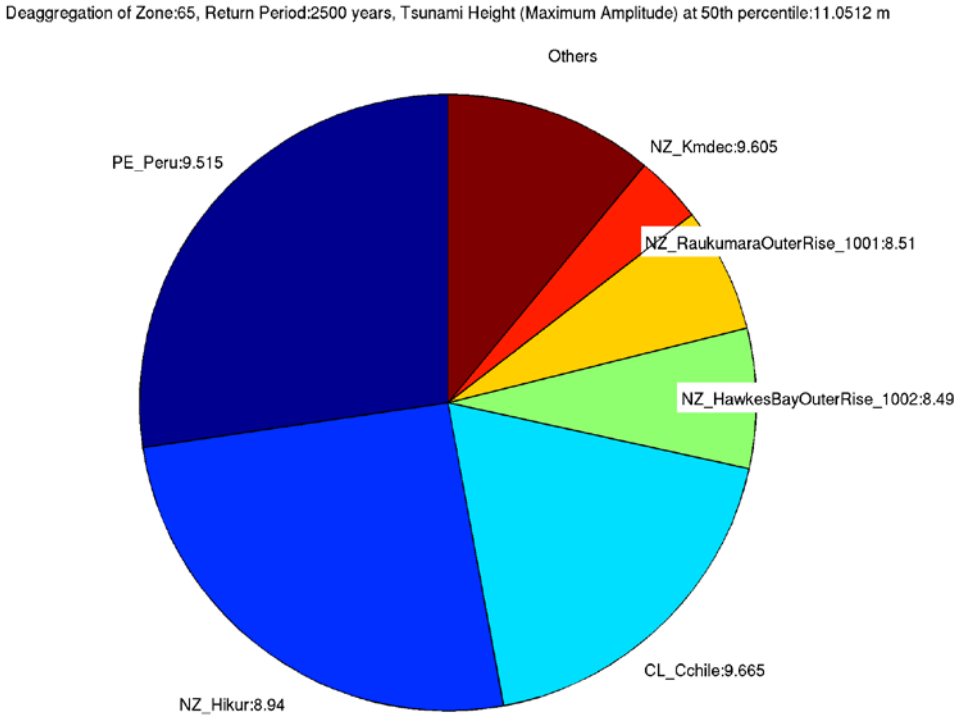

Figure 6.14 Deaggregation of tsunami sources for Gisborne at 500 yr (top) and 2500 yr (bottom) return periods.

Invercargill

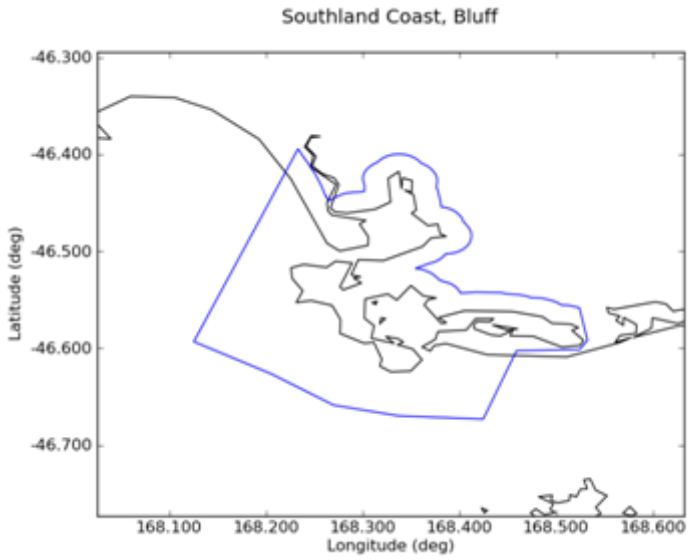

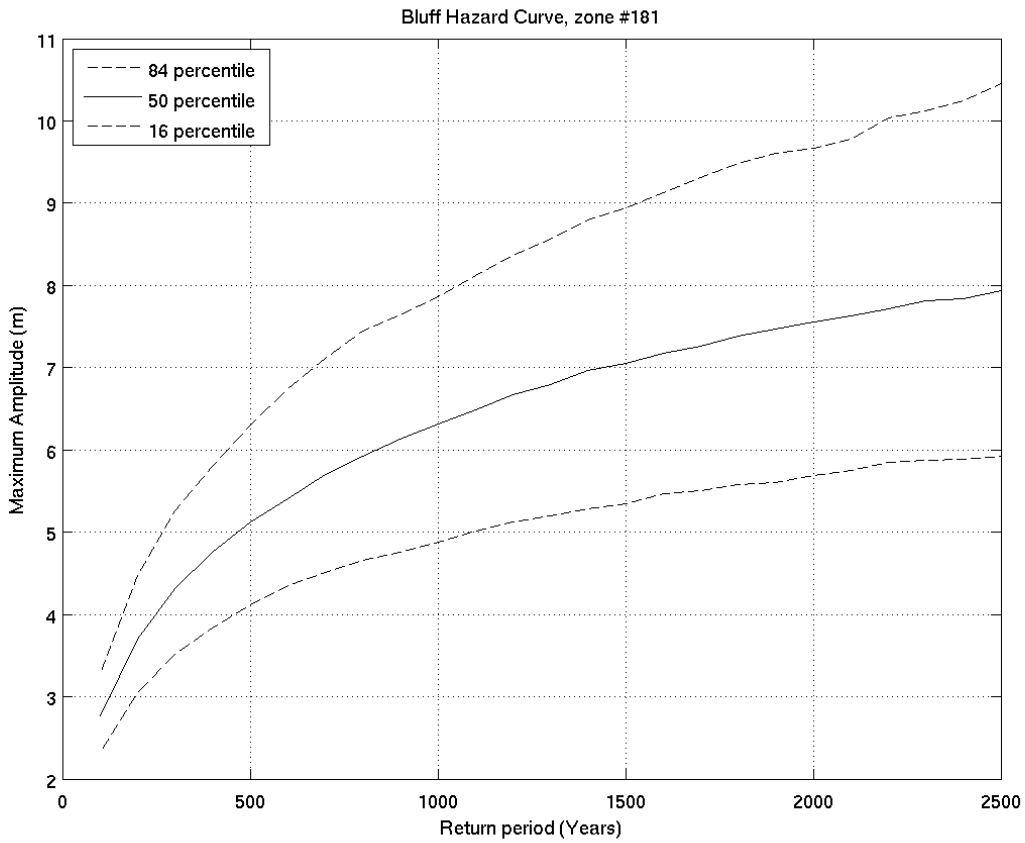

Figure 6.15 Area map and tsunami hazard curve for Invercargill.

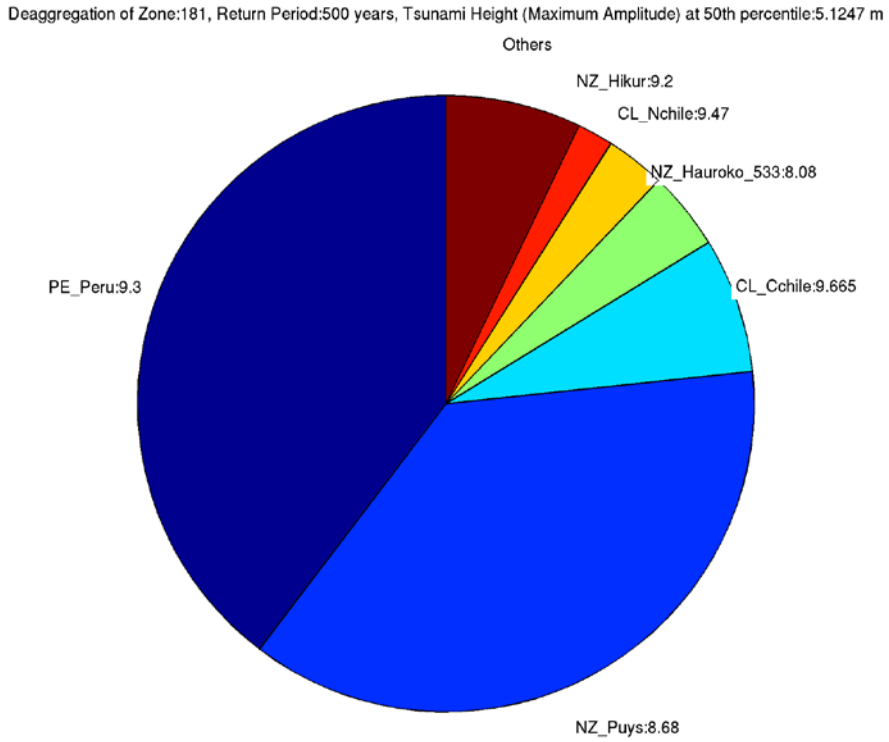

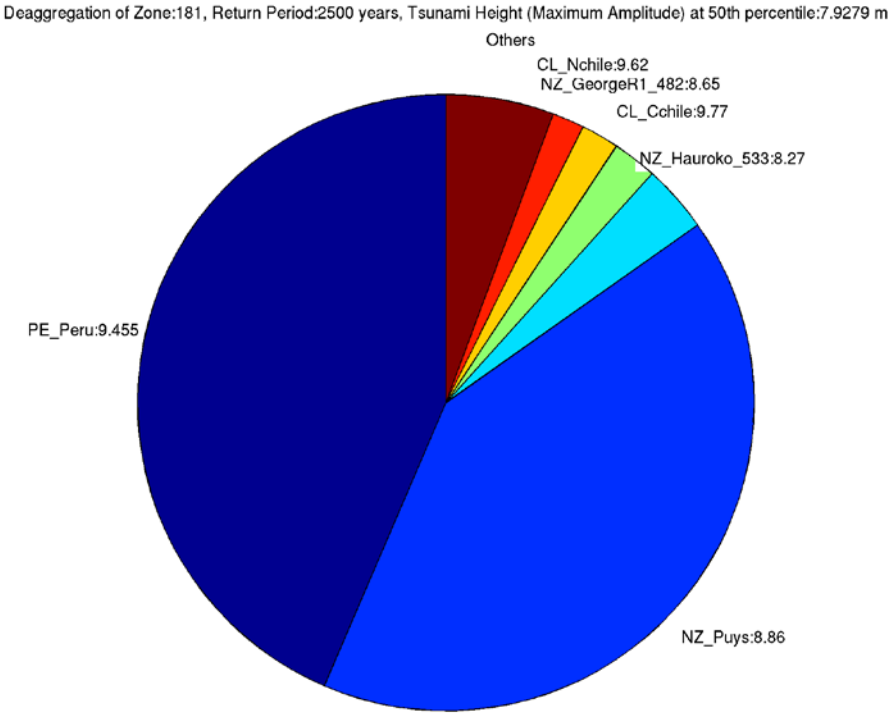

Figure 6.16 Deaggregation of tsunami sources for Invercargill at 500 yr (top) and 2500 yr (bottom) return periods.

Kapiti Coast

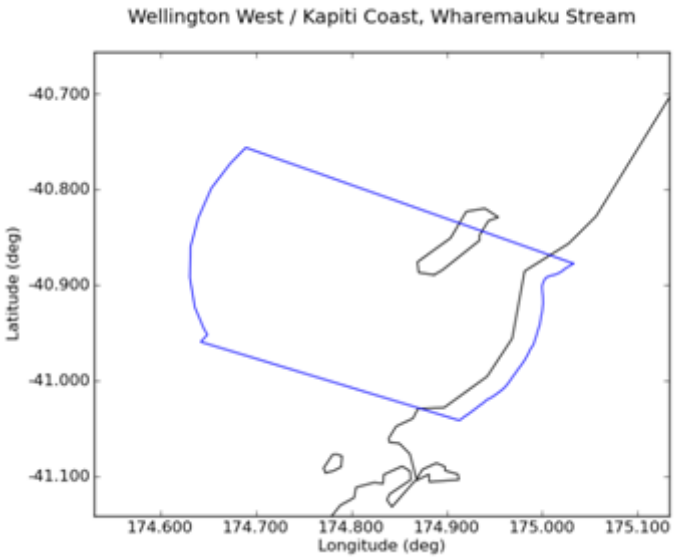

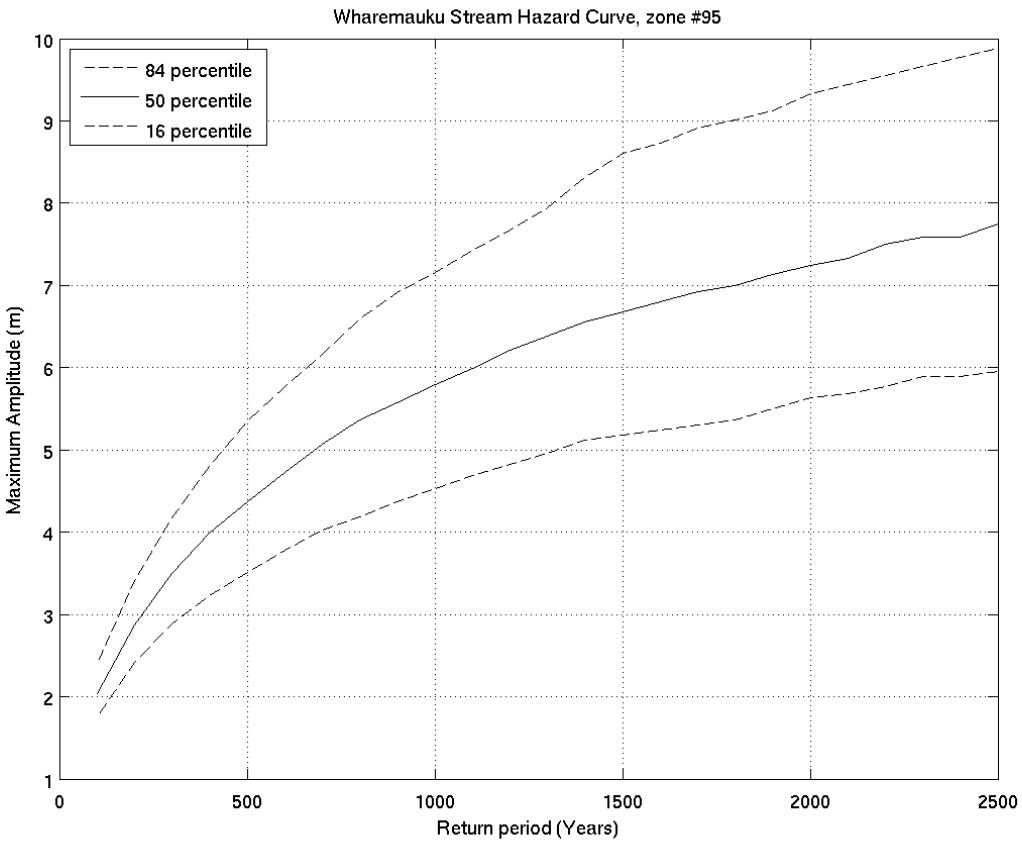

Figure 6.17 Area map and tsunami hazard curve for Kapiti Coast.

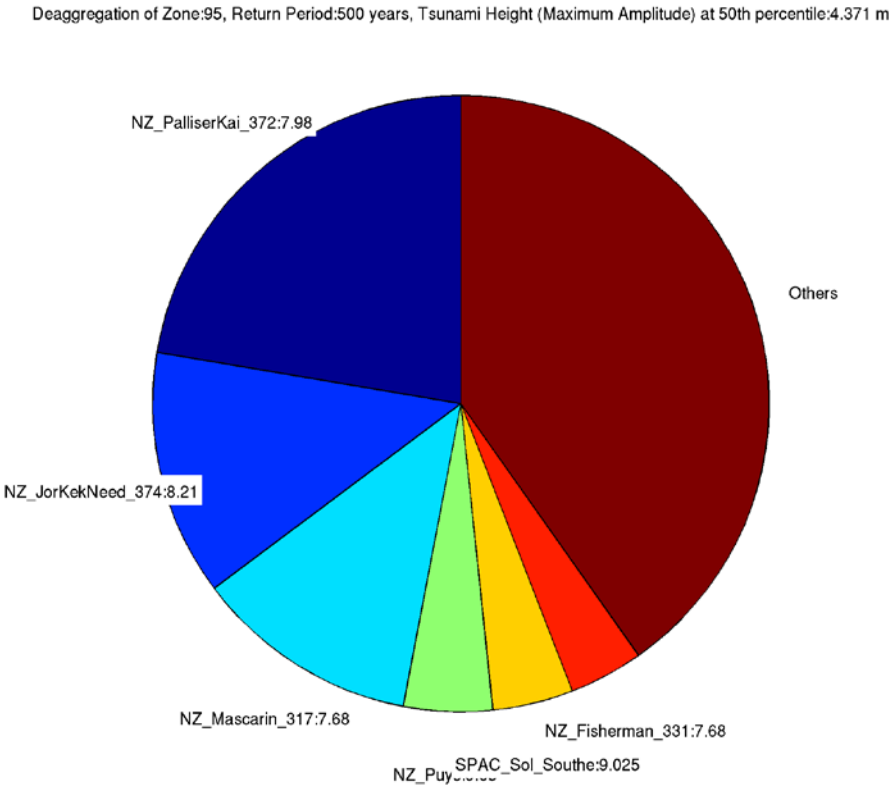

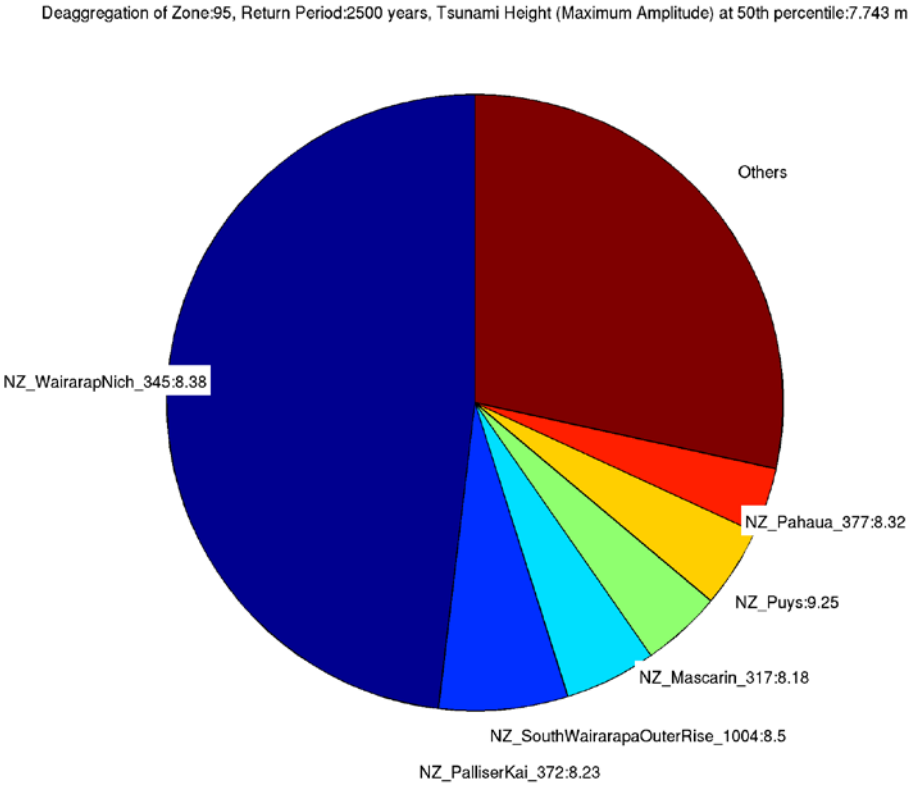

Figure 6.18 Deaggregation of tsunami sources for Kapiti Coast at 500 yr (top) and 2500 yr (bottom) return periods.

Napier

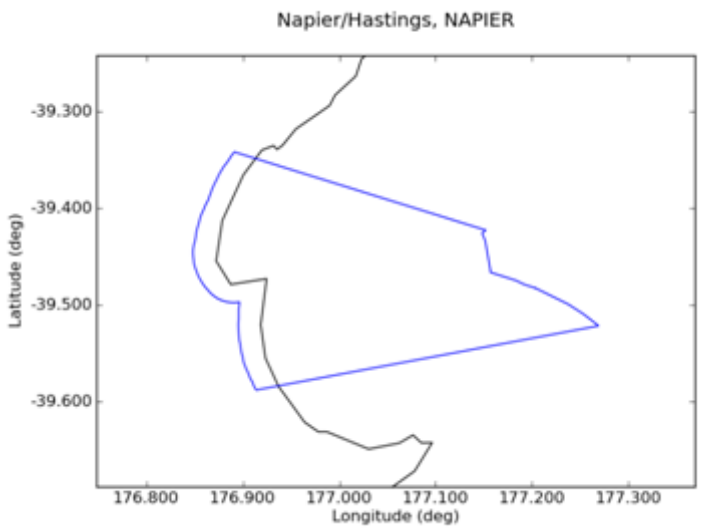

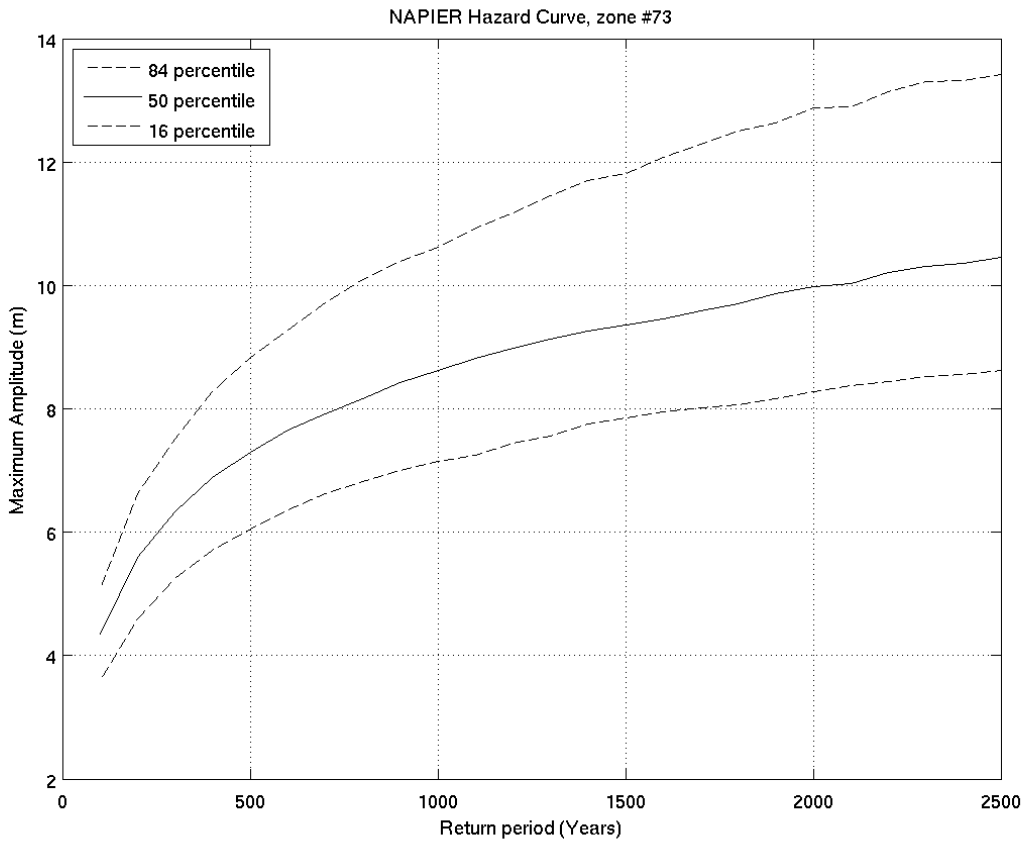

Figure 6.19 Area map and tsunami hazard curve for Napier.

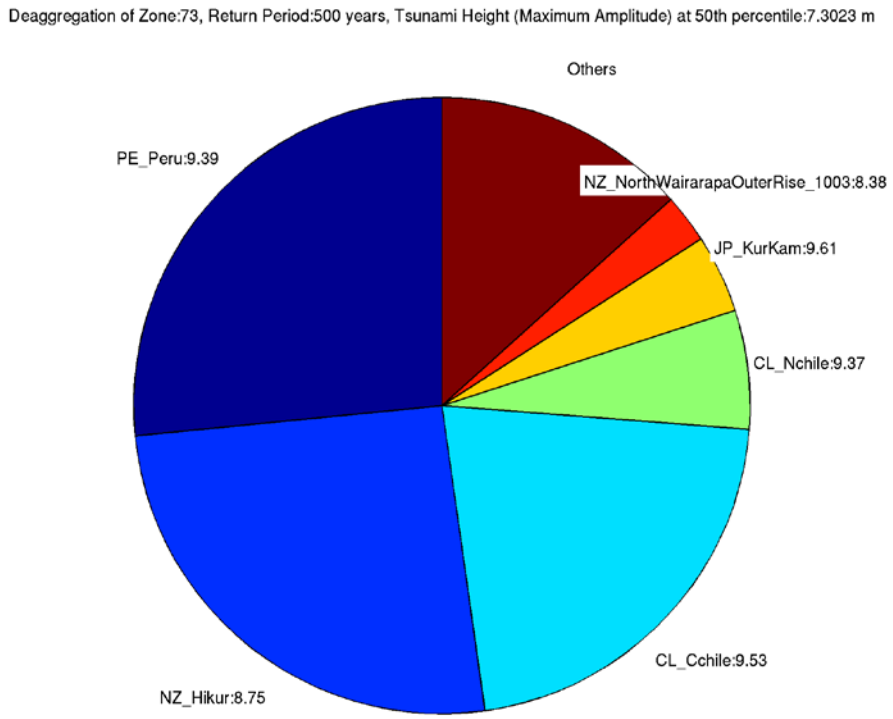

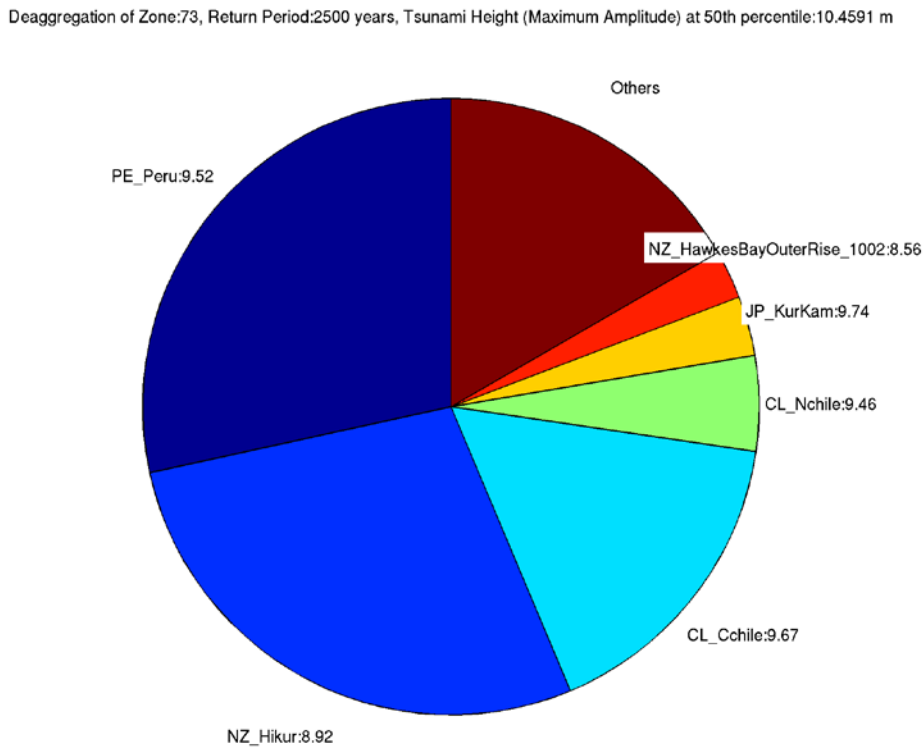

Figure 6.20 Deaggregation of tsunami sources for Napier at 500 yr (top) and 2500 yr (bottom) return periods.

Nelson

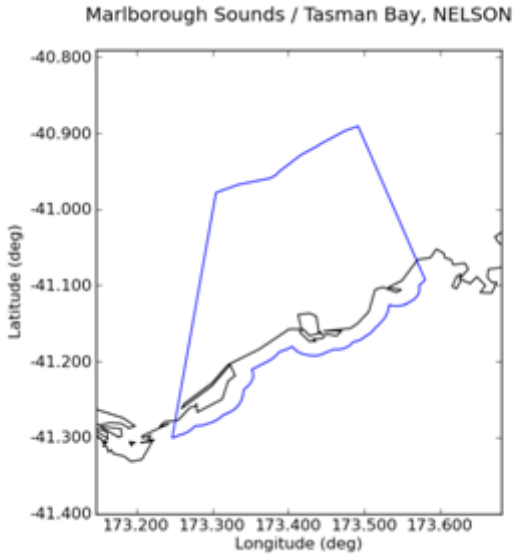

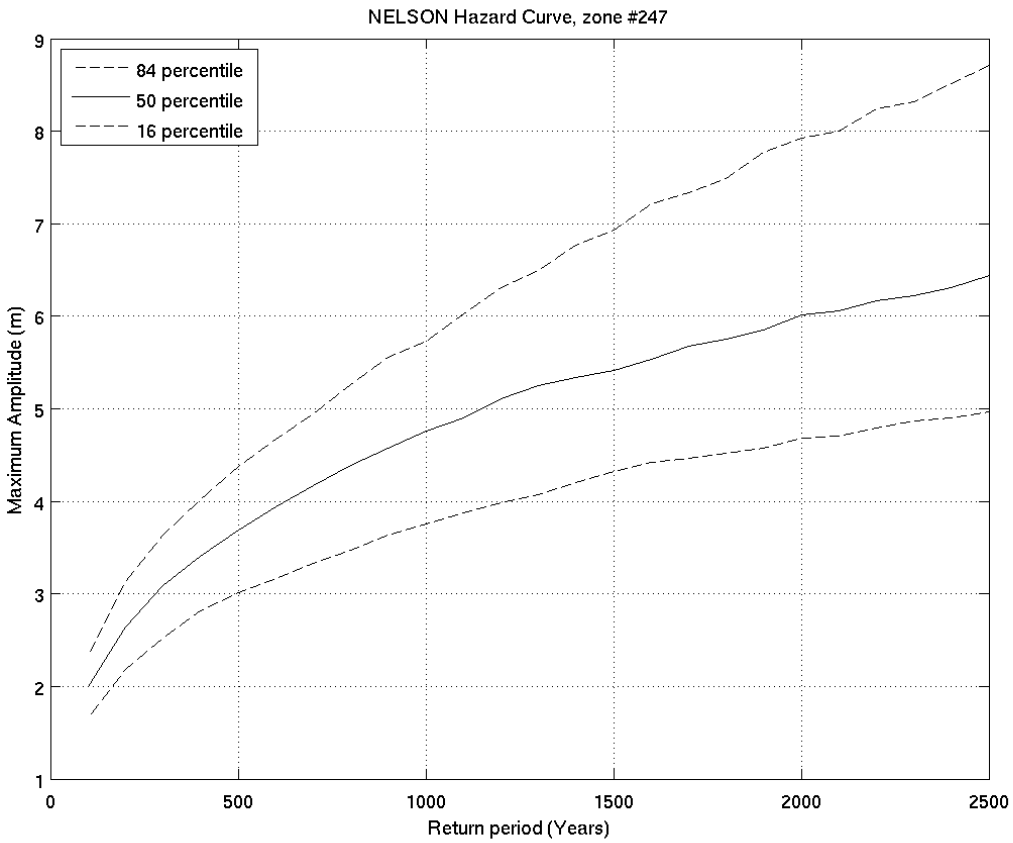

Figure 6.21 Area map and tsunami hazard curve for Nelson.

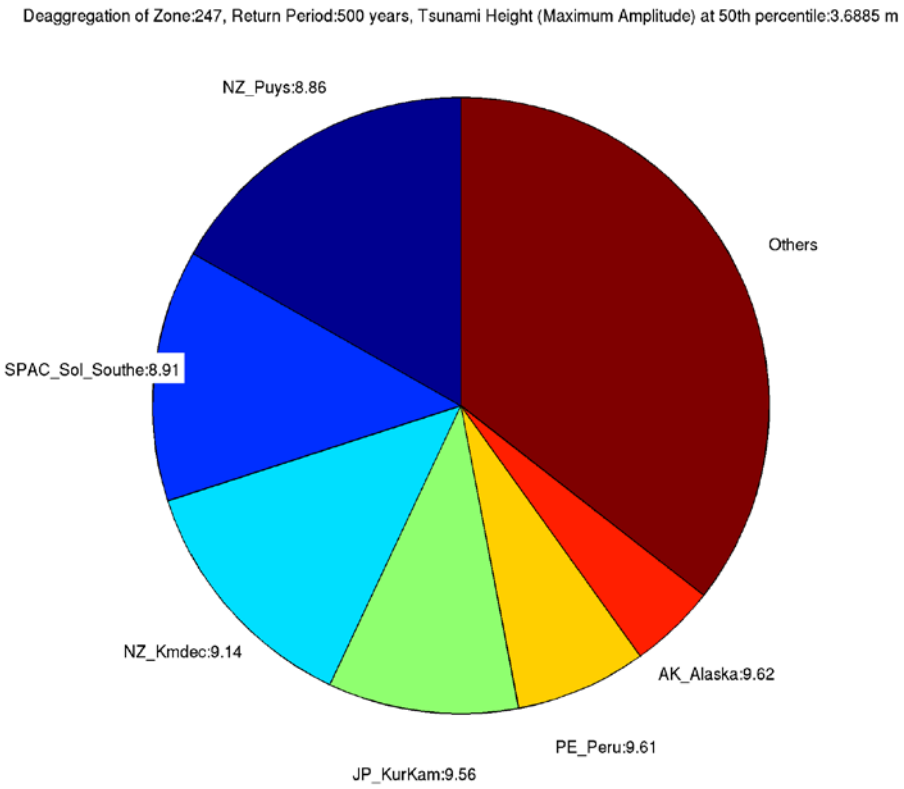

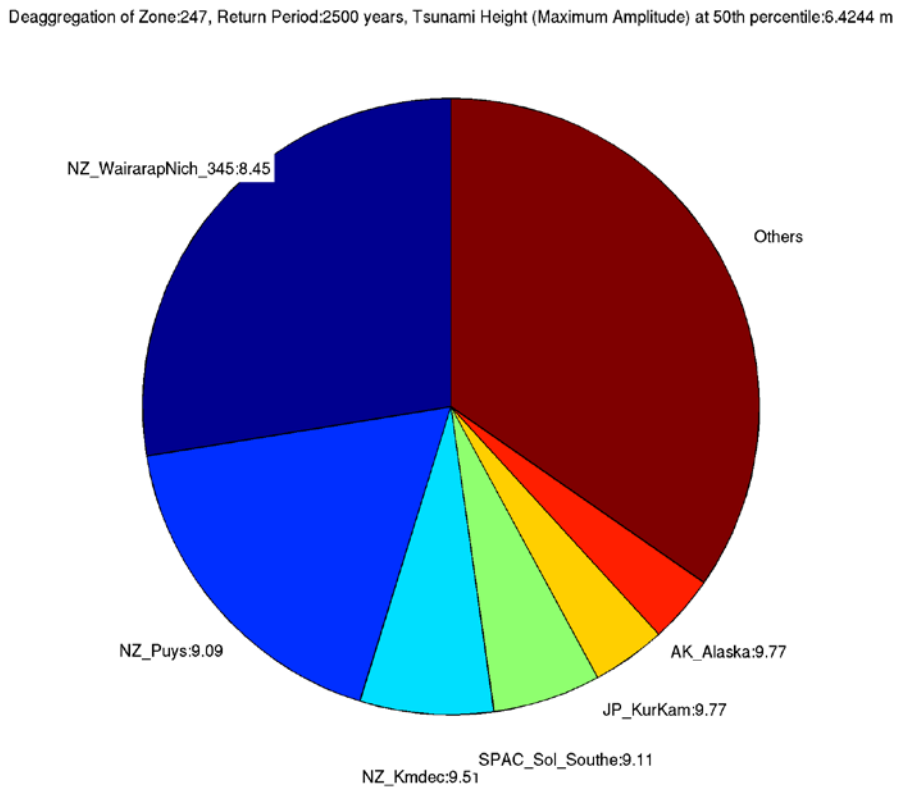

Figure 6.22 Deaggregation of tsunami sources for Nelson at 500 yr (top) and 2500 yr (bottom) return periods.

New Plymouth

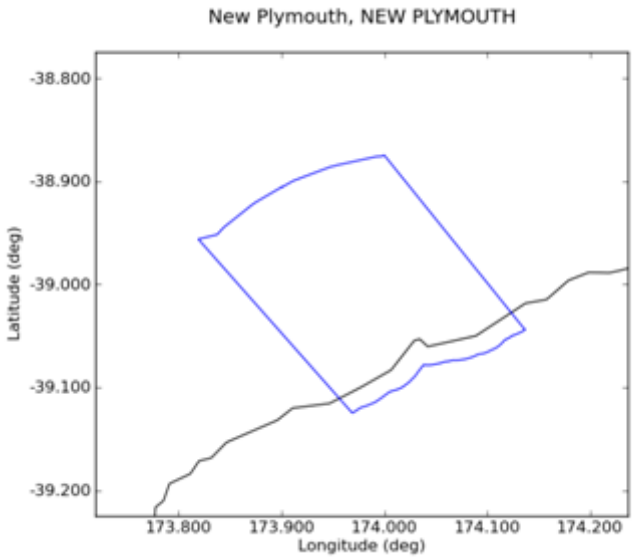

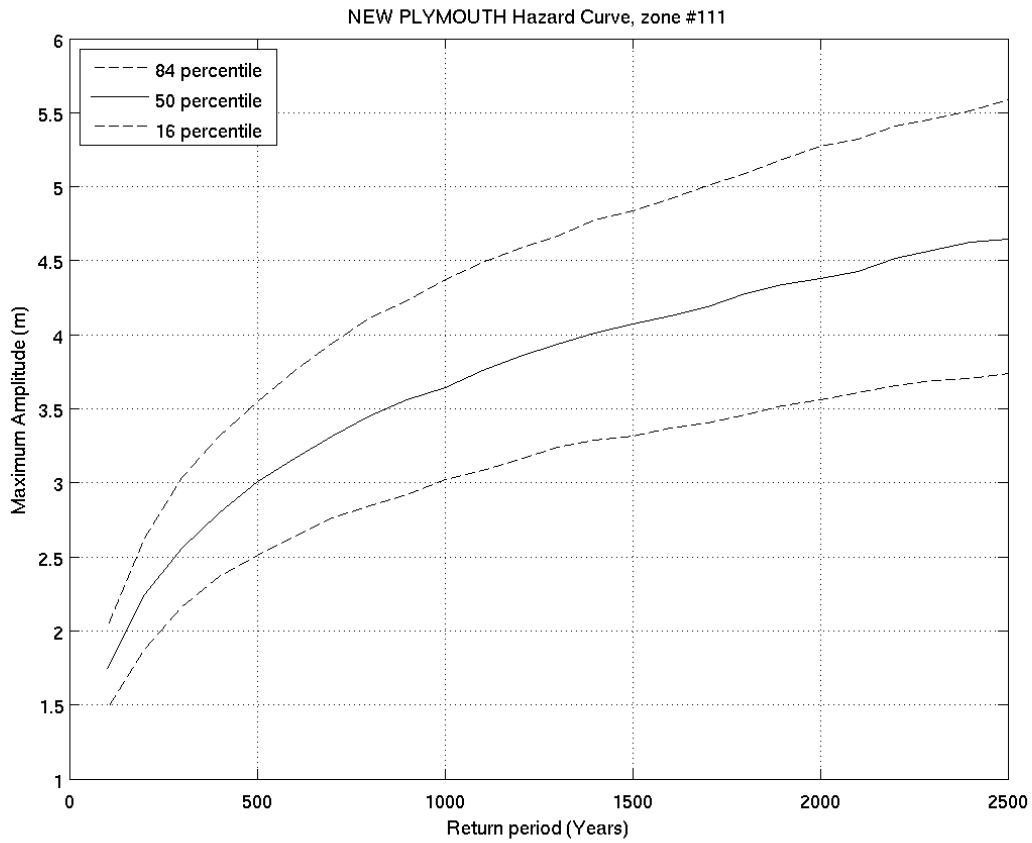

Figure 6.23 Area map and tsunami hazard curve for New Plymouth.

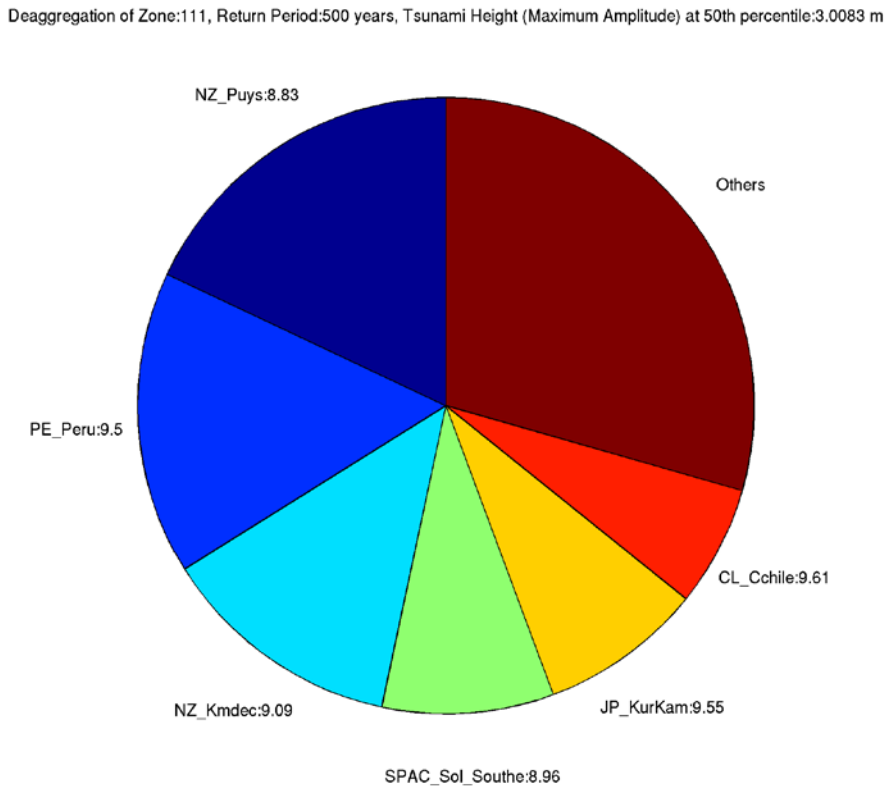

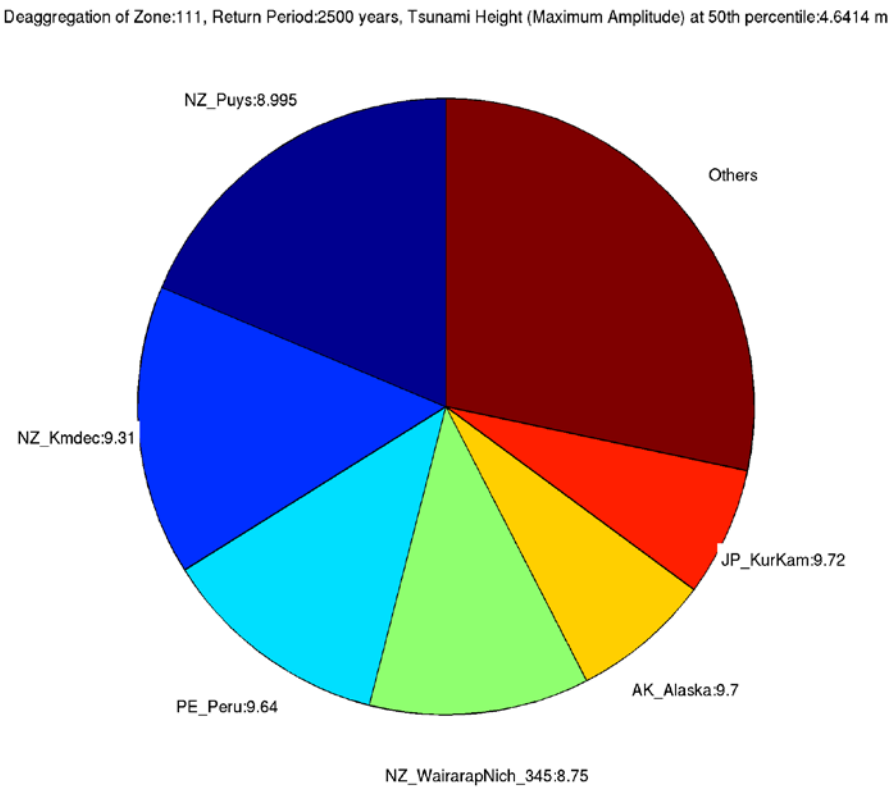

Figure 6.24 Deaggregation of tsunami sources for New Plymouth at 500 yr (top) and 2500 yr (bottom) return periods.

Porirua

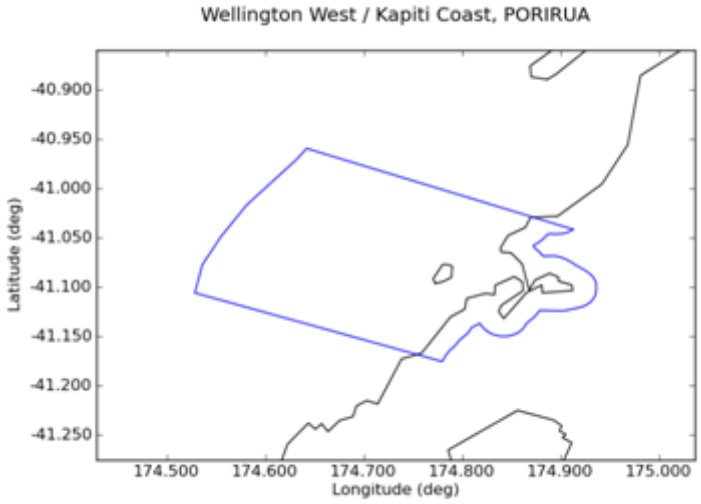

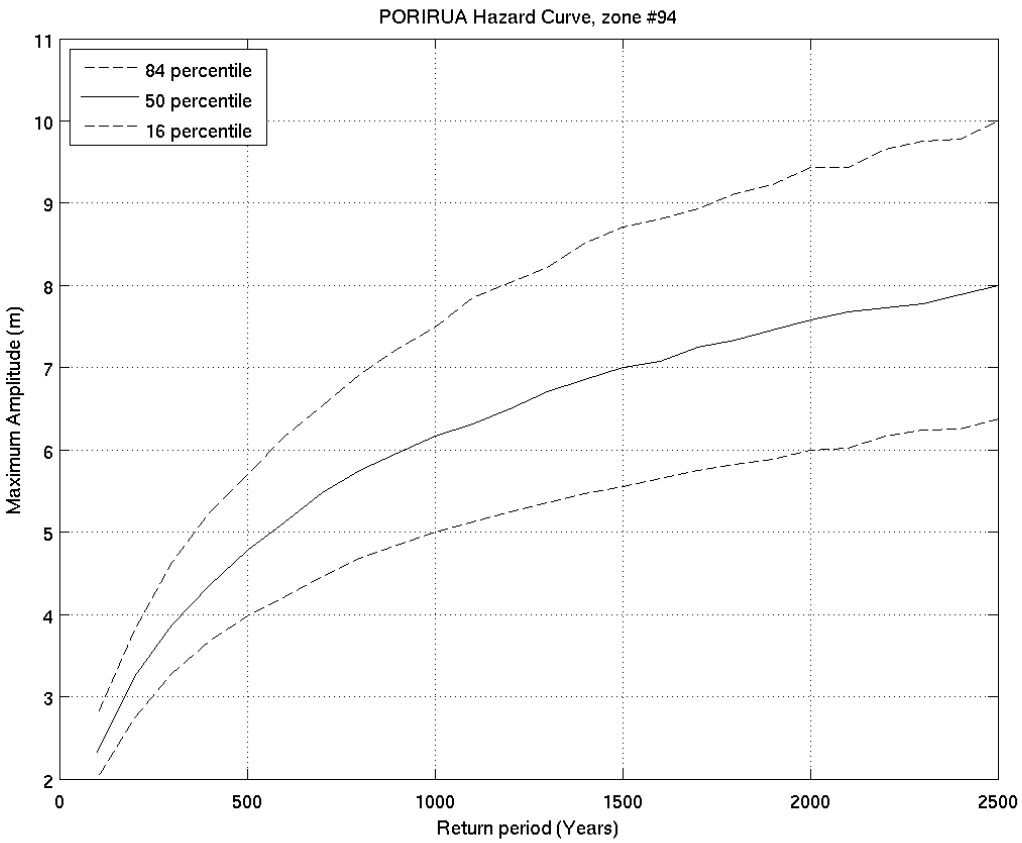

Figure 6.25 Area map and tsunami hazard curve for Porirua.

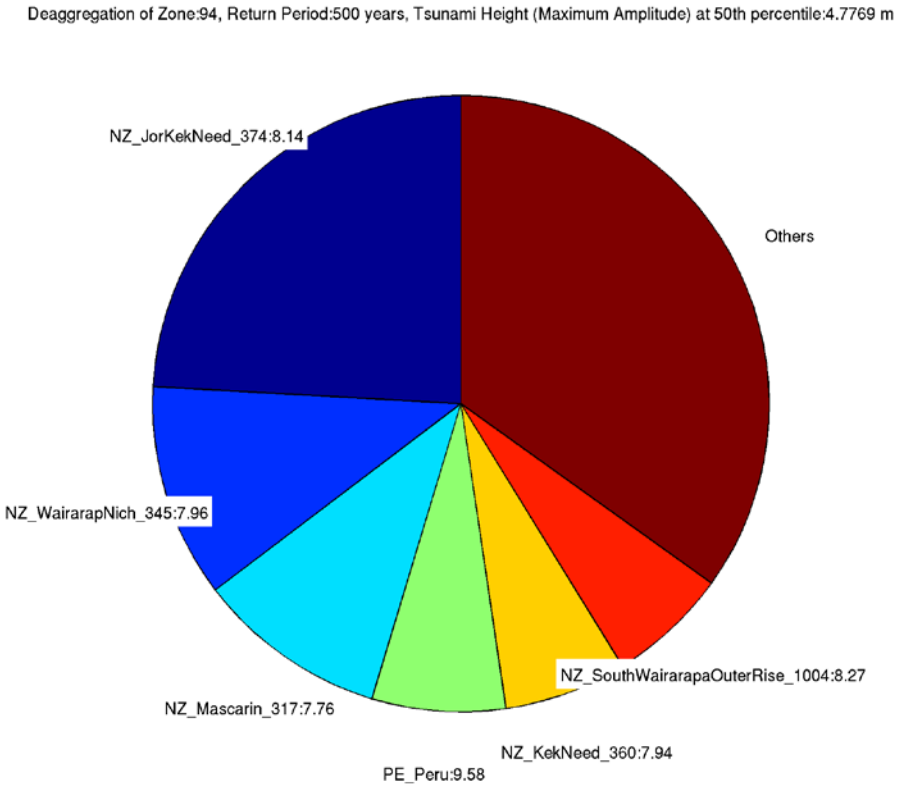

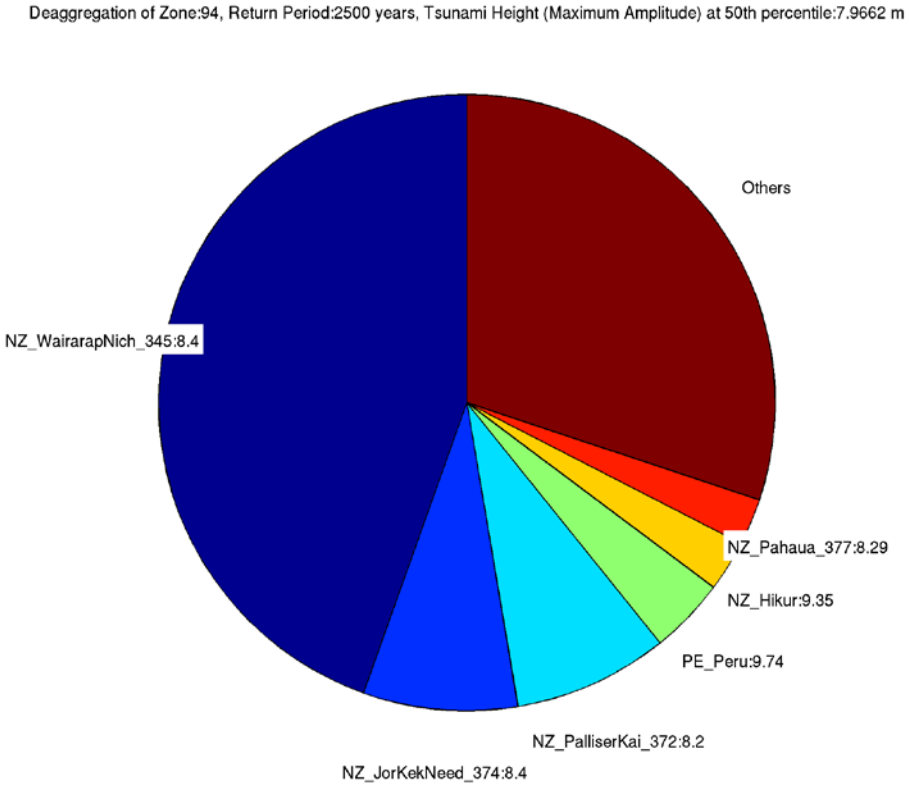

Figure 6.26 Deaggregation of tsunami sources for Porirua at 500 yr (top) and 2500 yr (bottom) return periods.

Tauranga

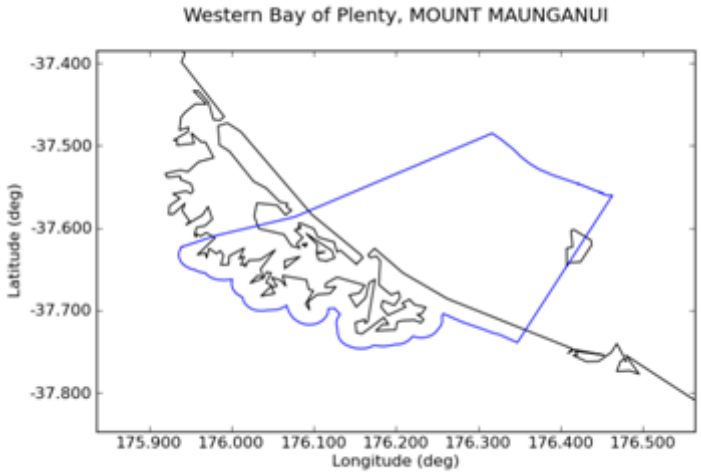

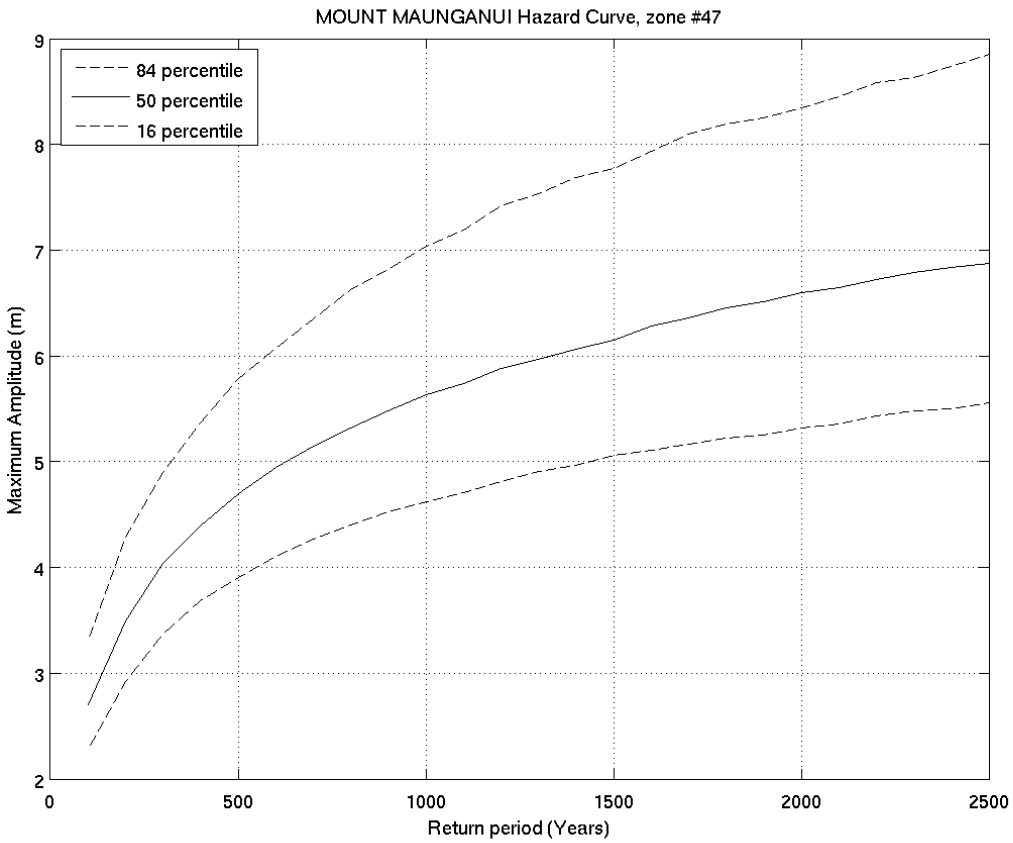

Figure 6.27 Area map and tsunami hazard curve for Tauranga.

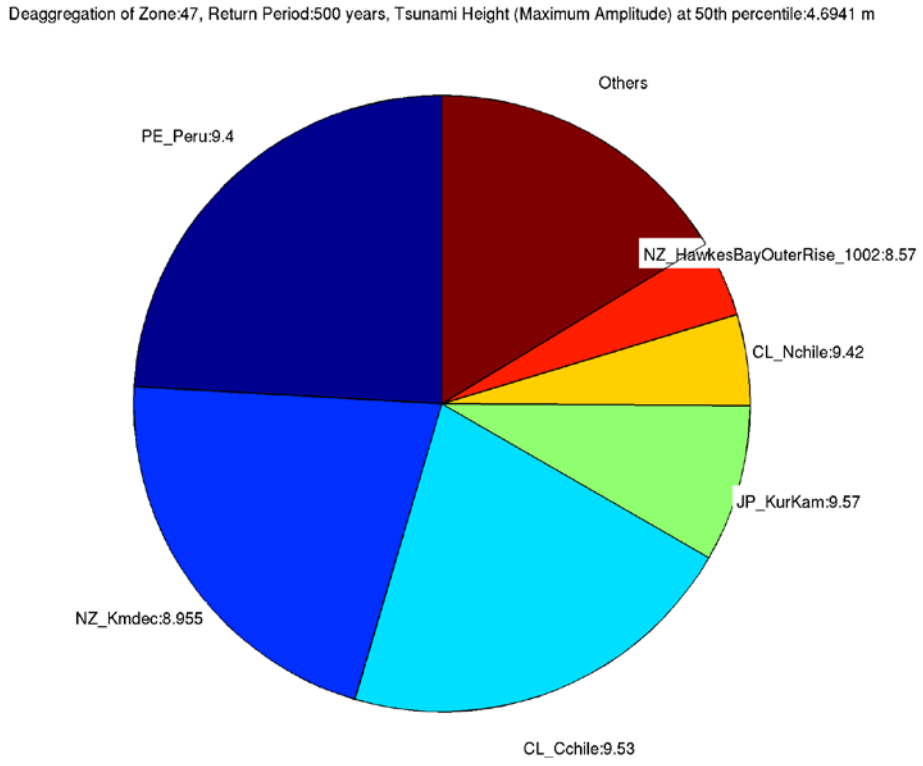

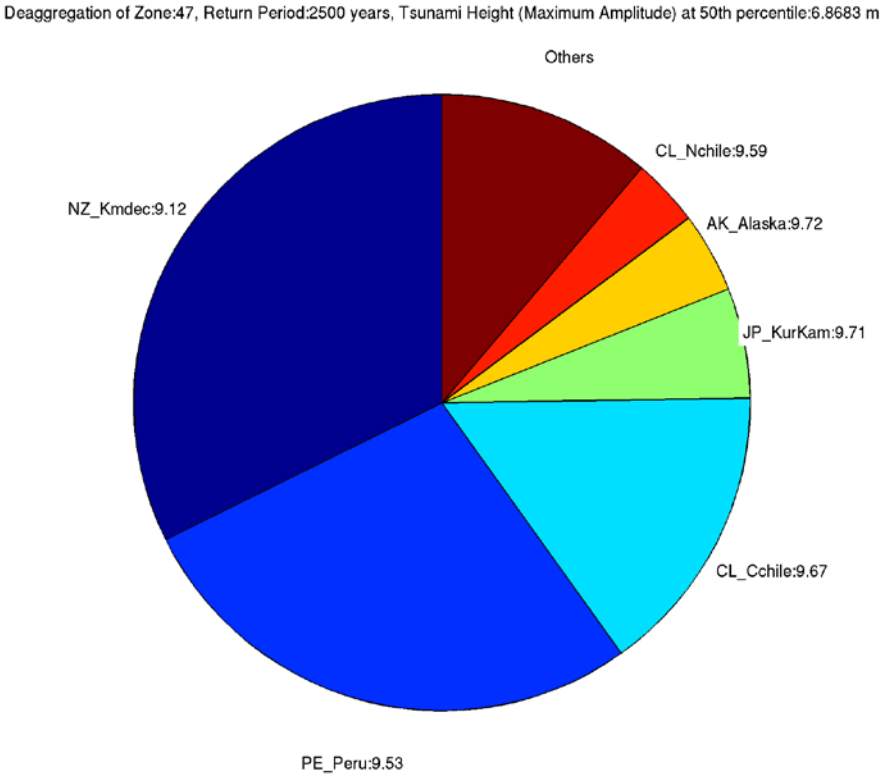

Figure 6.28 Deaggregation of tsunami sources for Tauranga at 500 yr (top) and 2500 yr (bottom) return periods.

Timaru

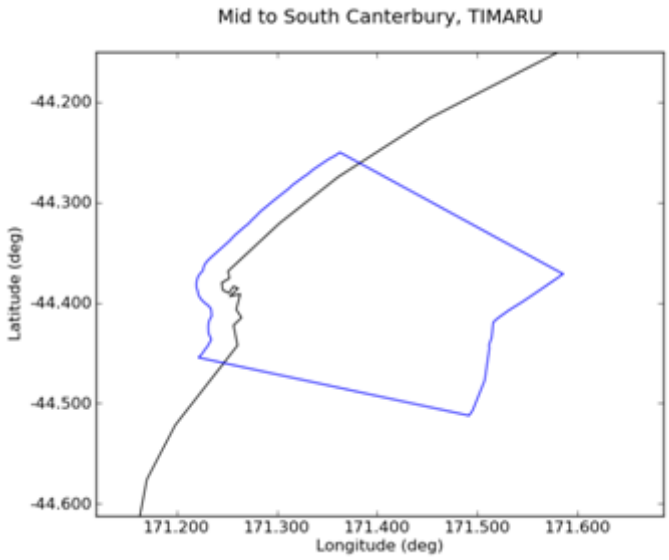

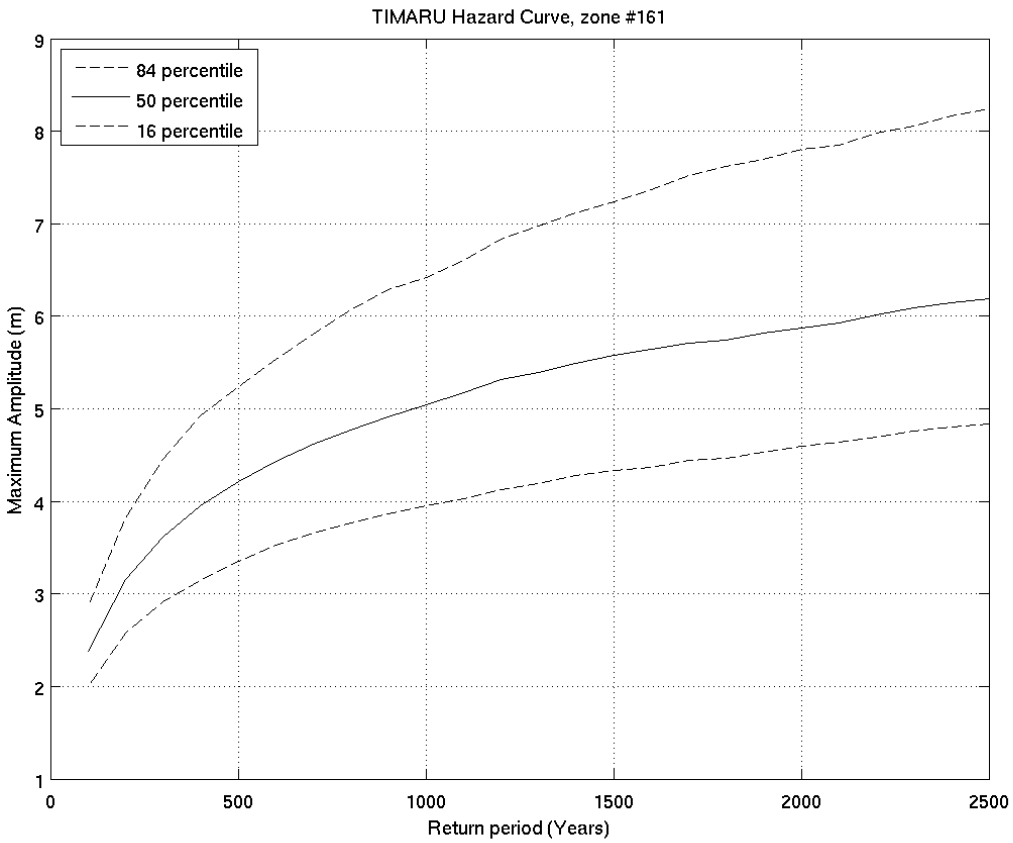

Figure 6.29 Area map and tsunami hazard curve for Timaru.

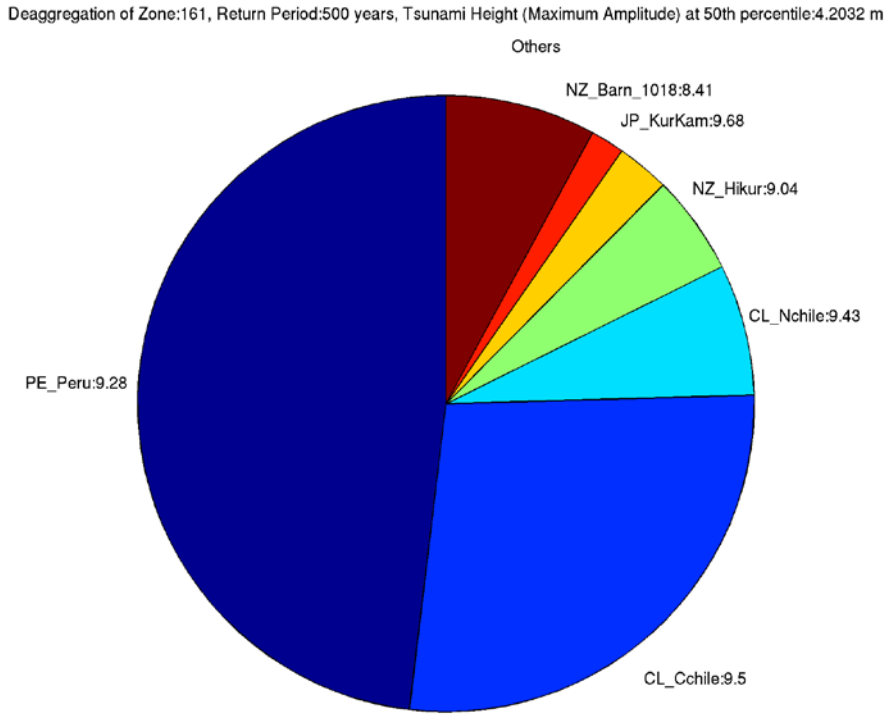

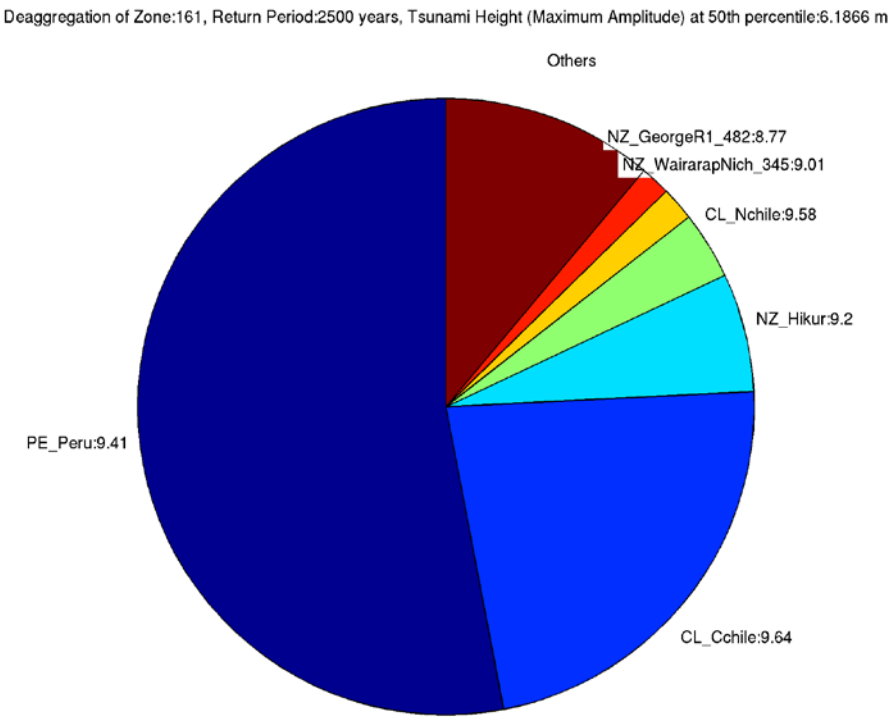

Figure 6.30 Deaggregation of tsunami sources for Timaru at 500 yr (top) and 2500 yr (bottom) return periods.

Wellington

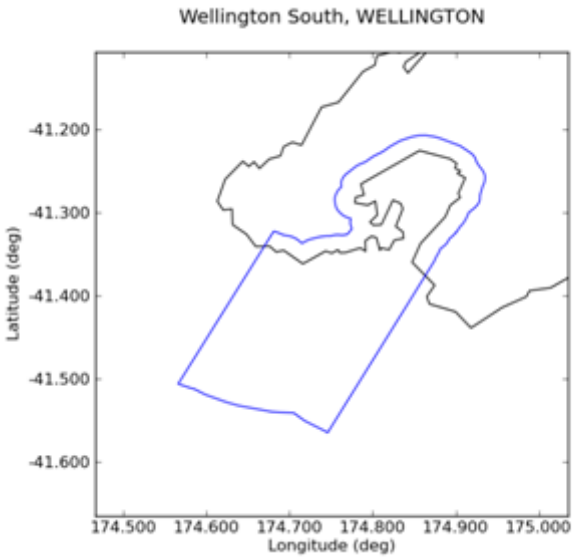

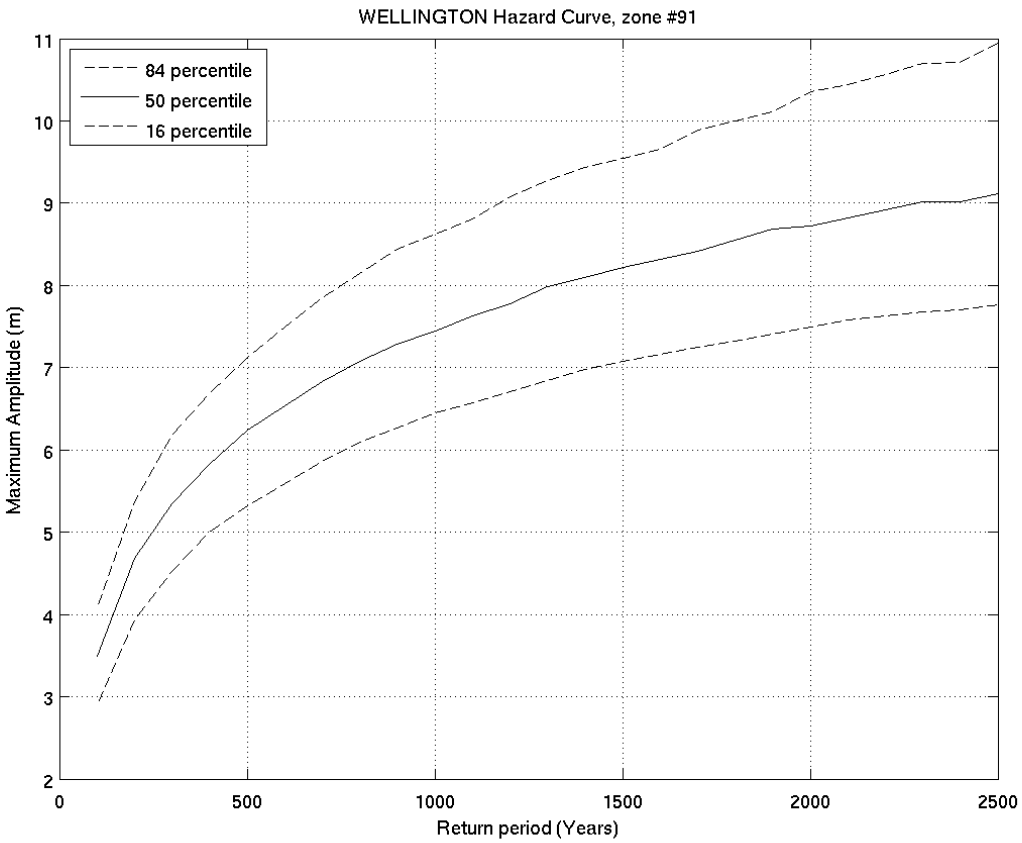

Figure 6.31 Area map and tsunami hazard curve for Wellington.

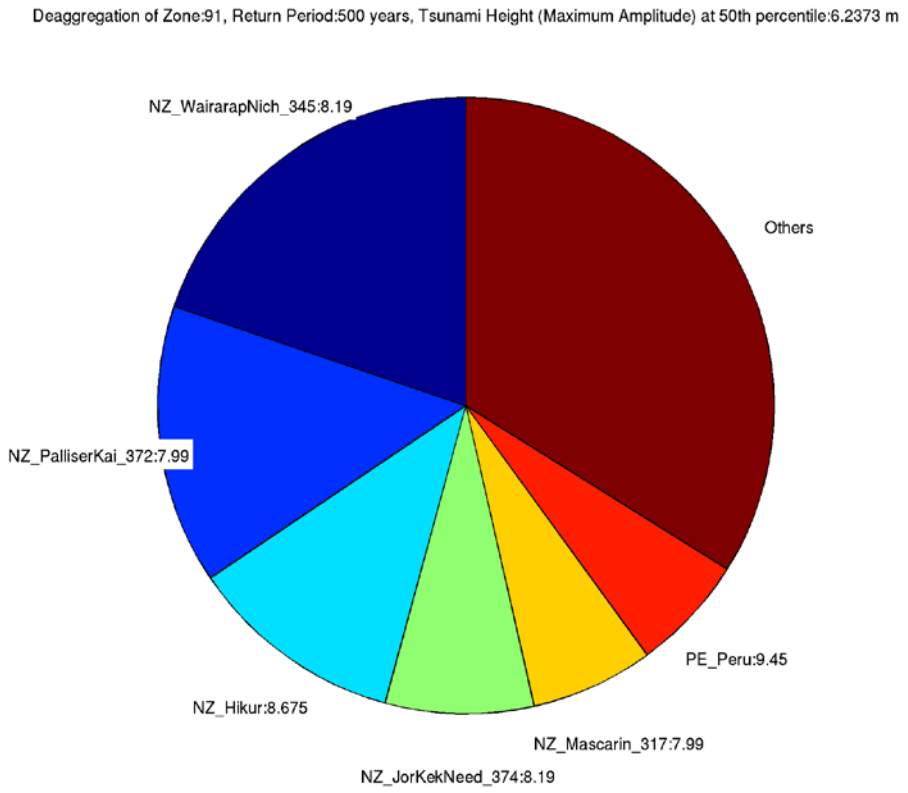

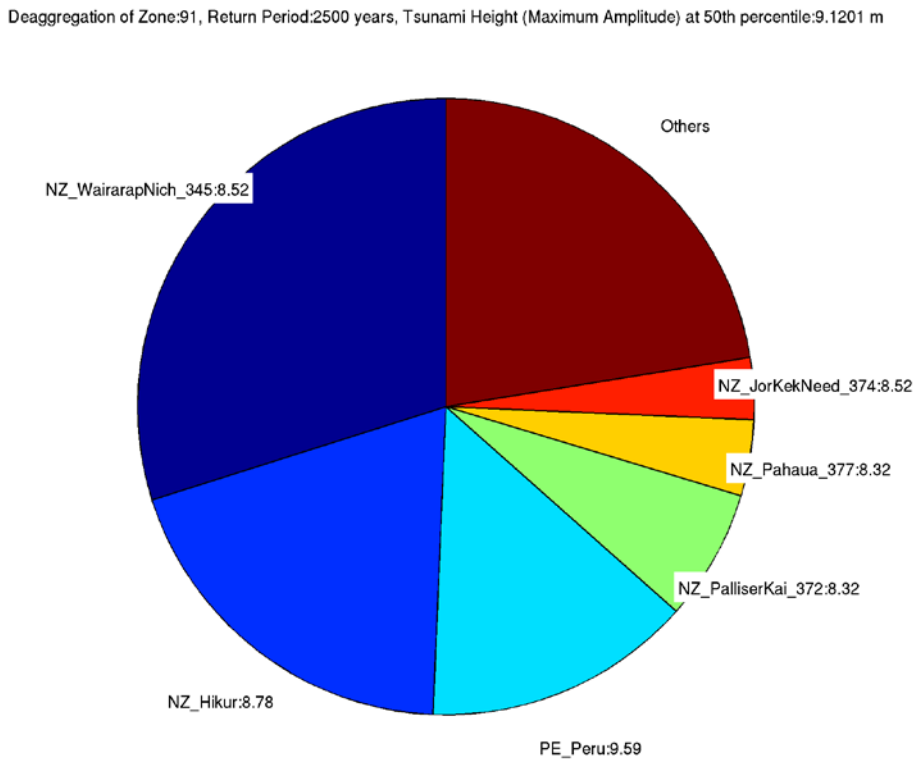

Figure 6.32 Deaggregation of tsunami sources for Wellington at 500 yr (top) and 2500 yr (bottom) return periods.

Whakatane

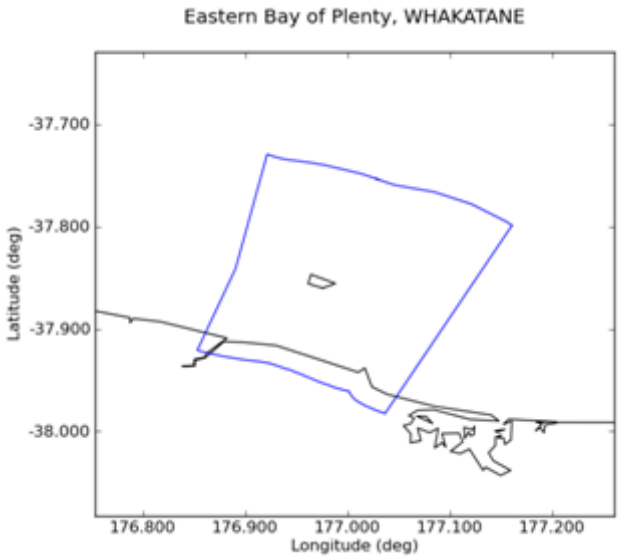

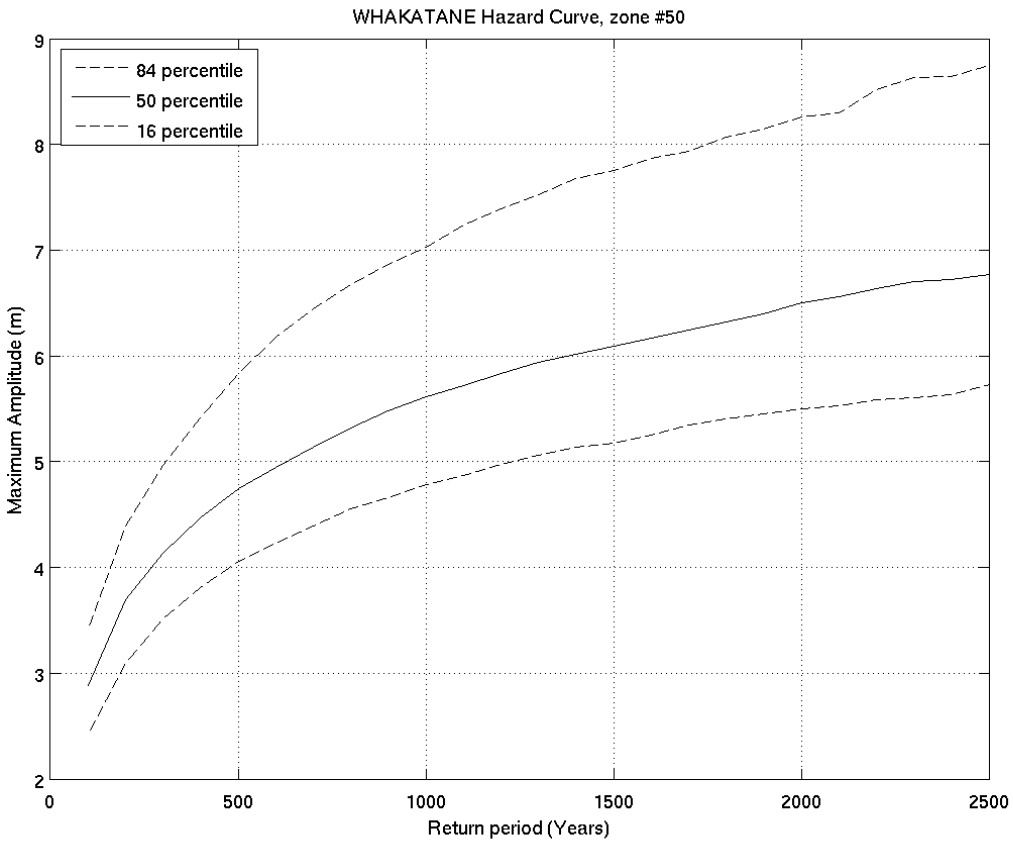

Figure 6.33 Area map and tsunami hazard curve for Whakatane.

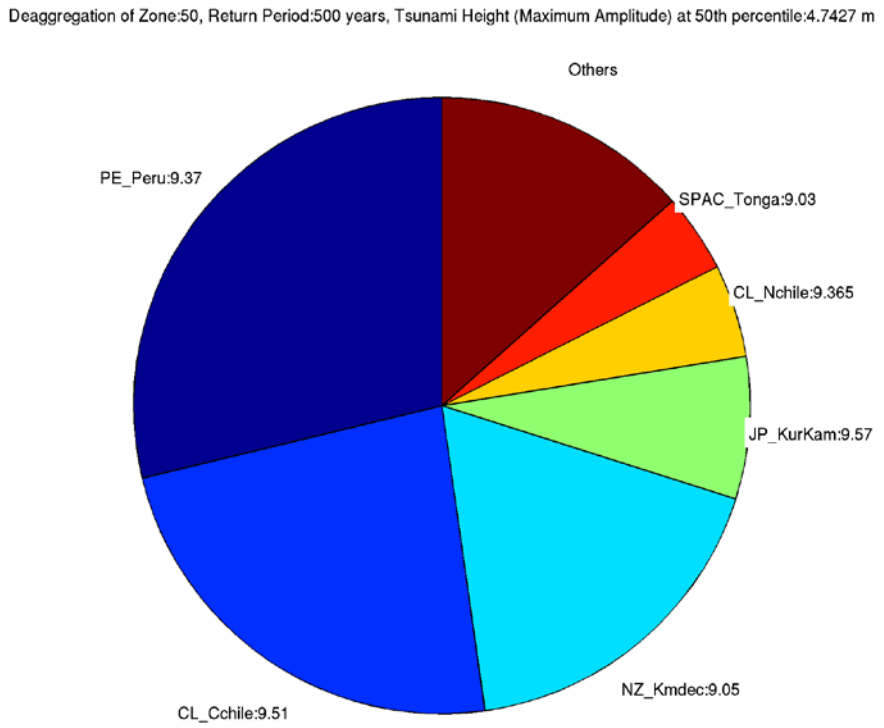

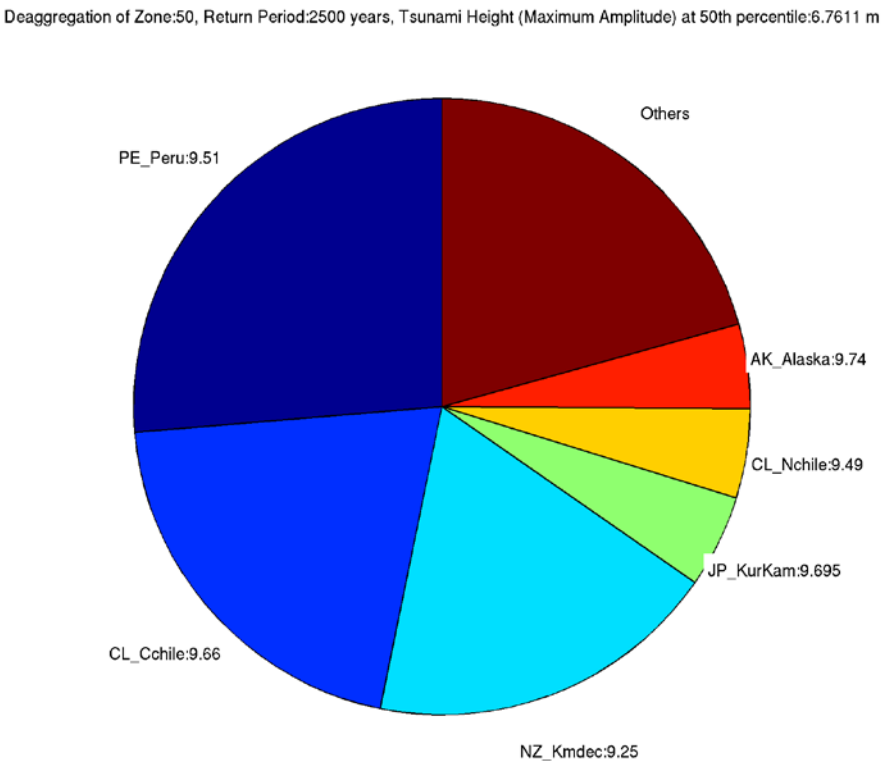

Figure 6.34 Deaggregation of tsunami sources for Whakatane at 500 yr (top) and 2500 yr (bottom) return periods.

Whangarei

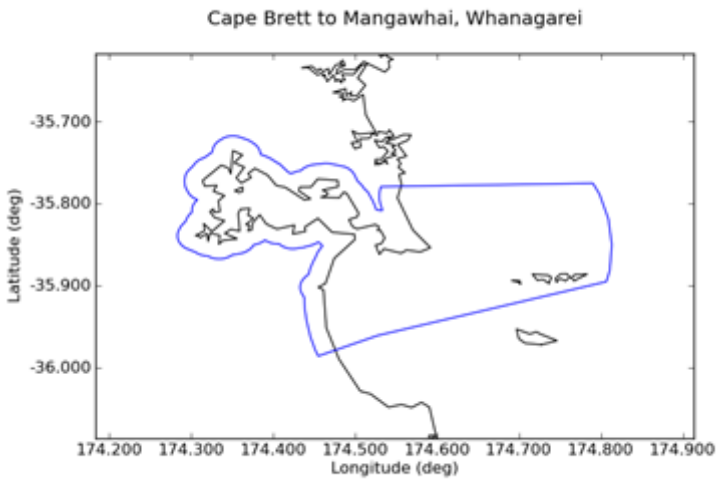

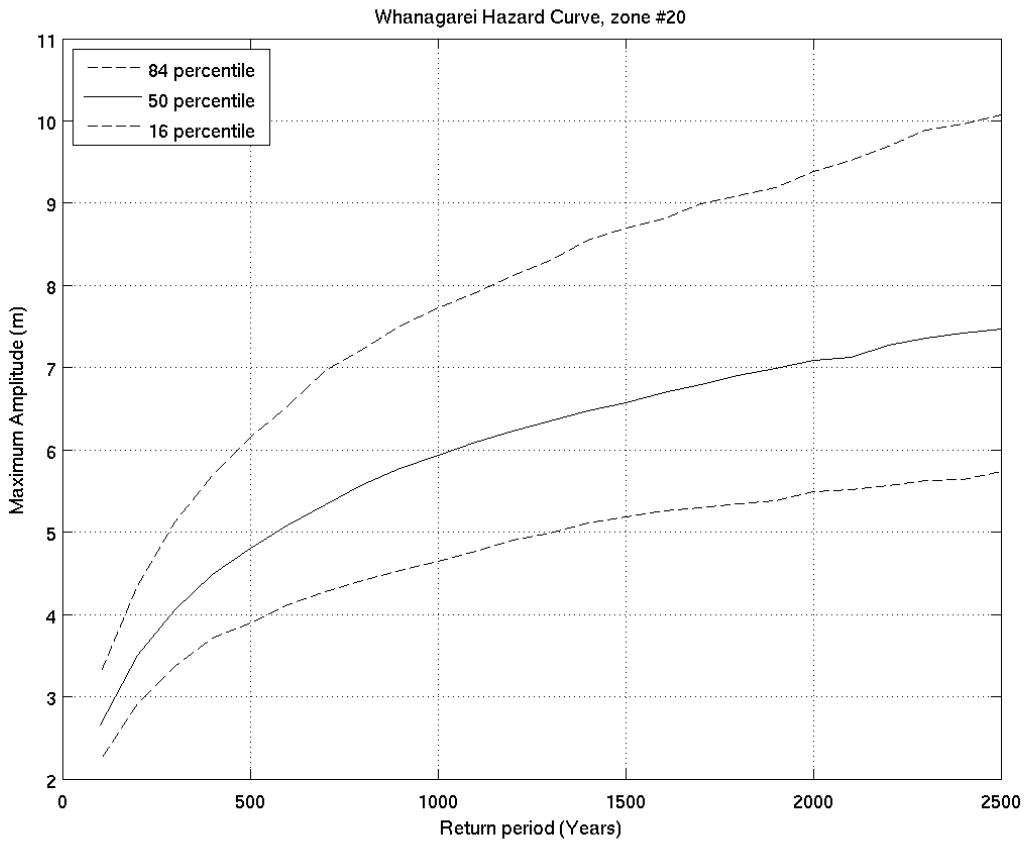

Figure 6.35 Area map and tsunami hazard curve for Whangarei.

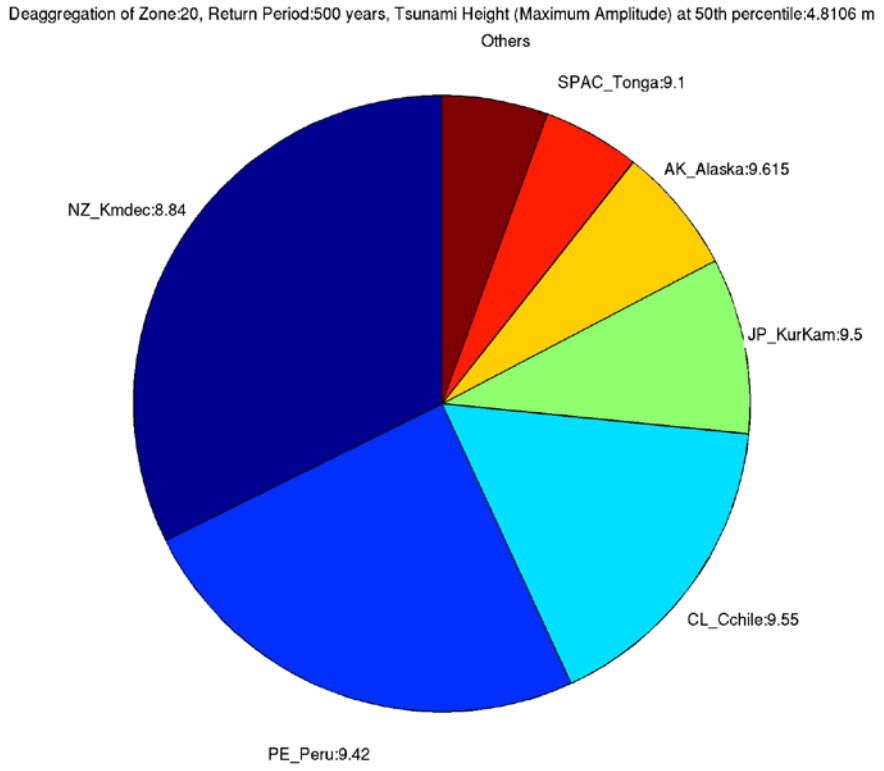

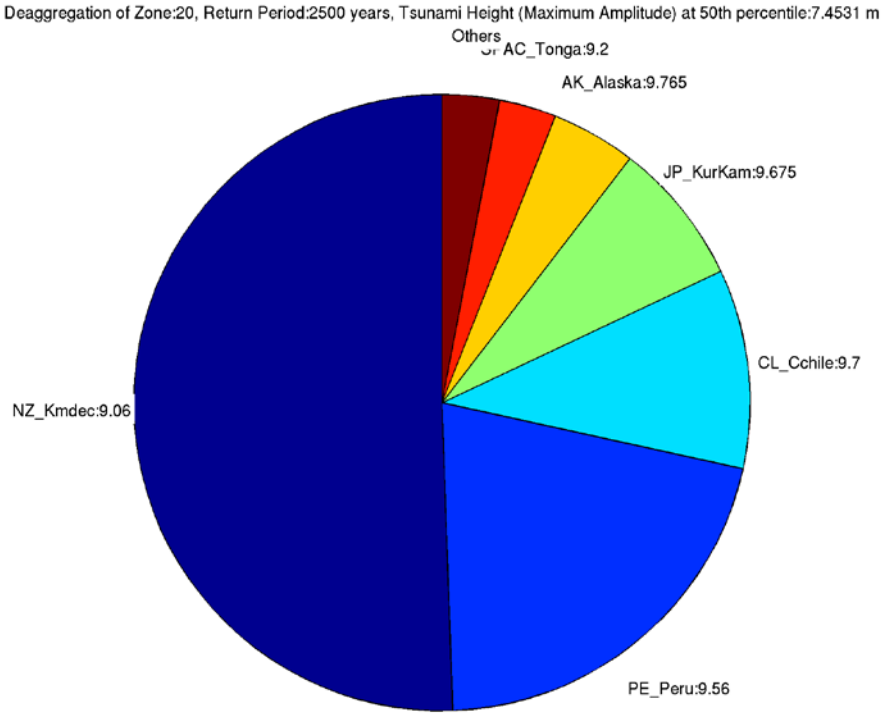

Figure 6.36 Deaggregation of tsunami sources for Whangarei at 500 yr (top) and 2500 yr (bottom) return periods.

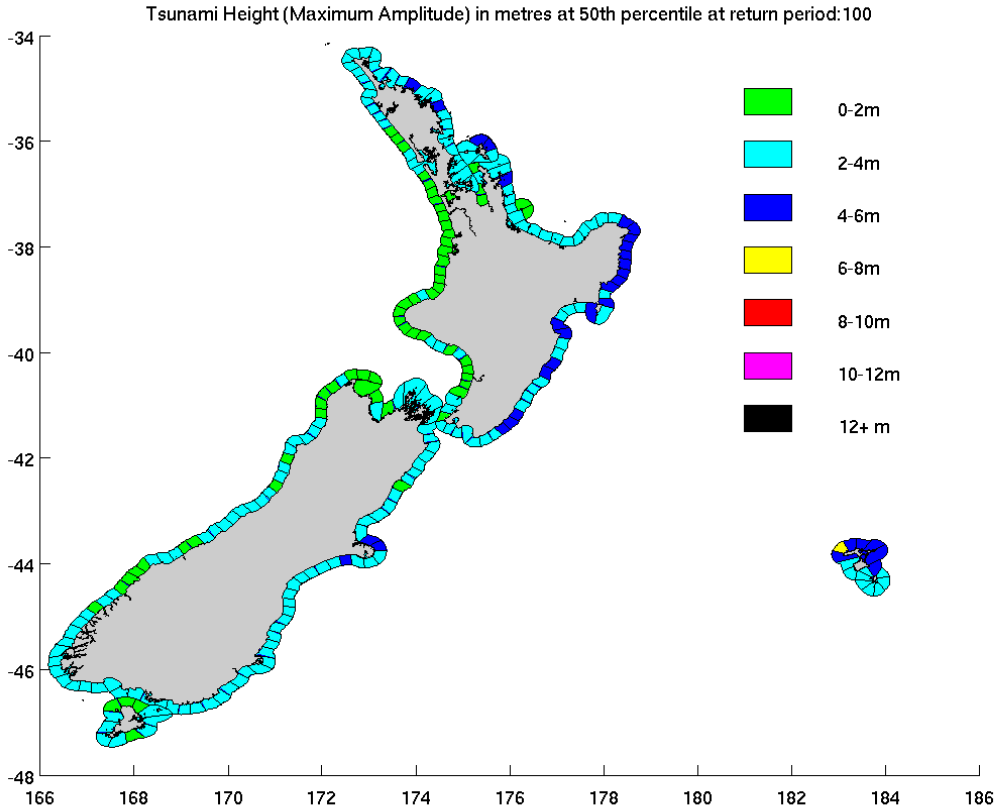

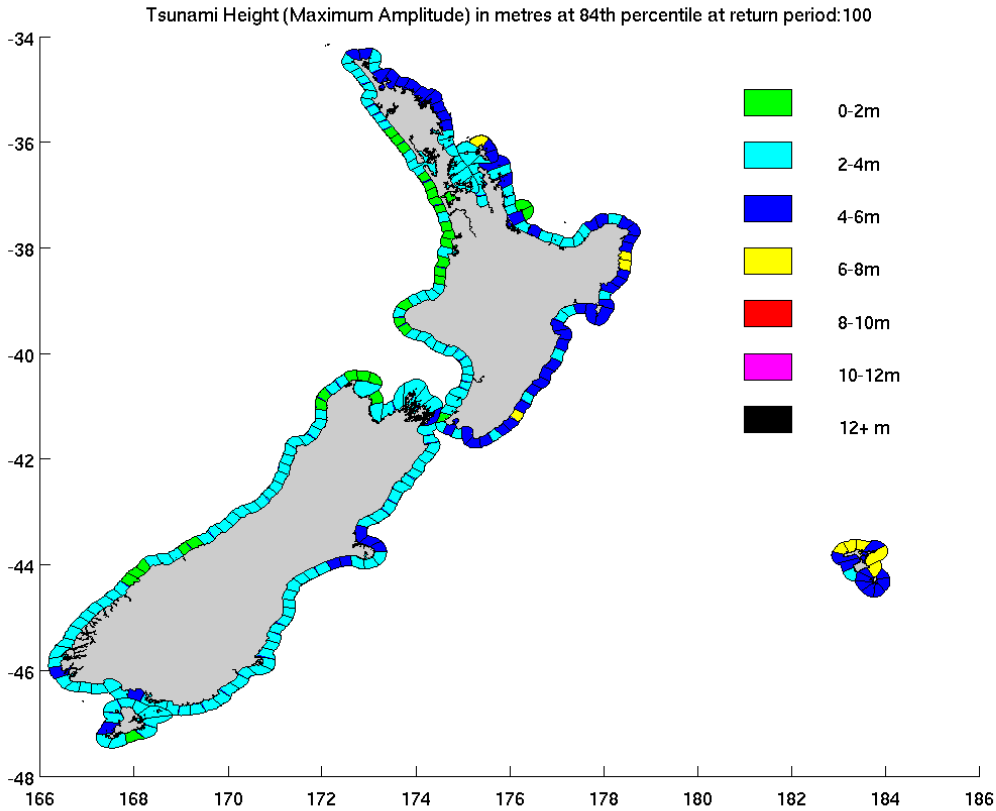

Figure 6.37 Expected maximum tsunami height in metres at 100 year return period, shown at median (50th percentile) and 84th percentile of epistemic uncertainty. See comment on the Wairarapa coast in Section 6.10.

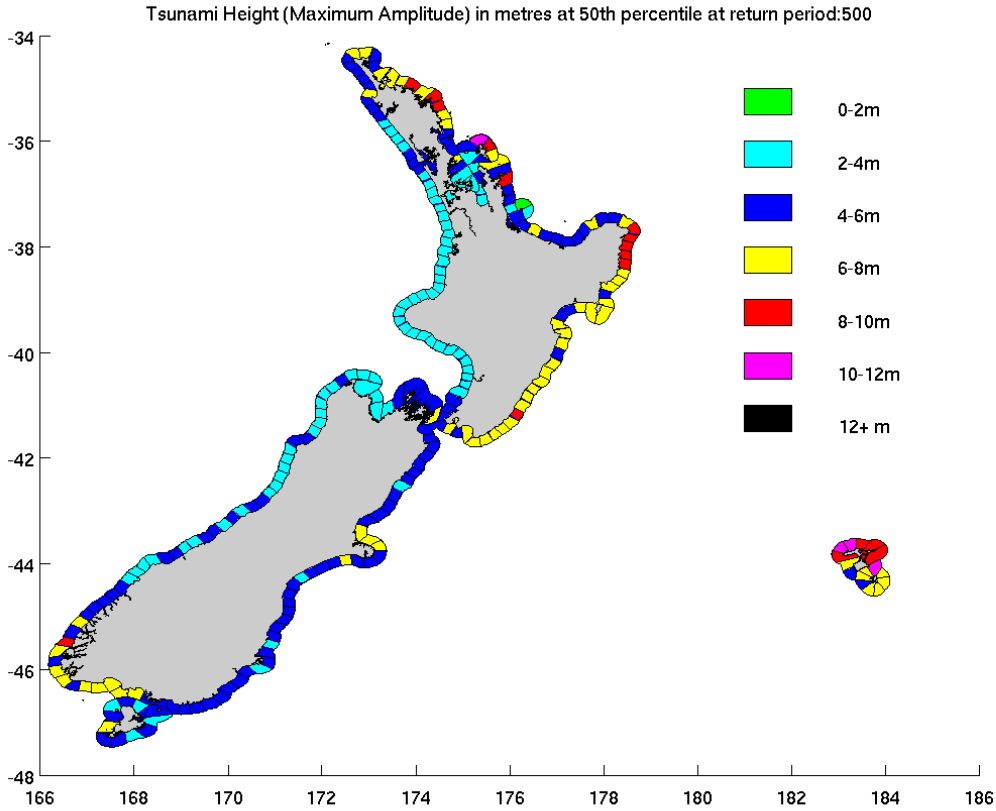

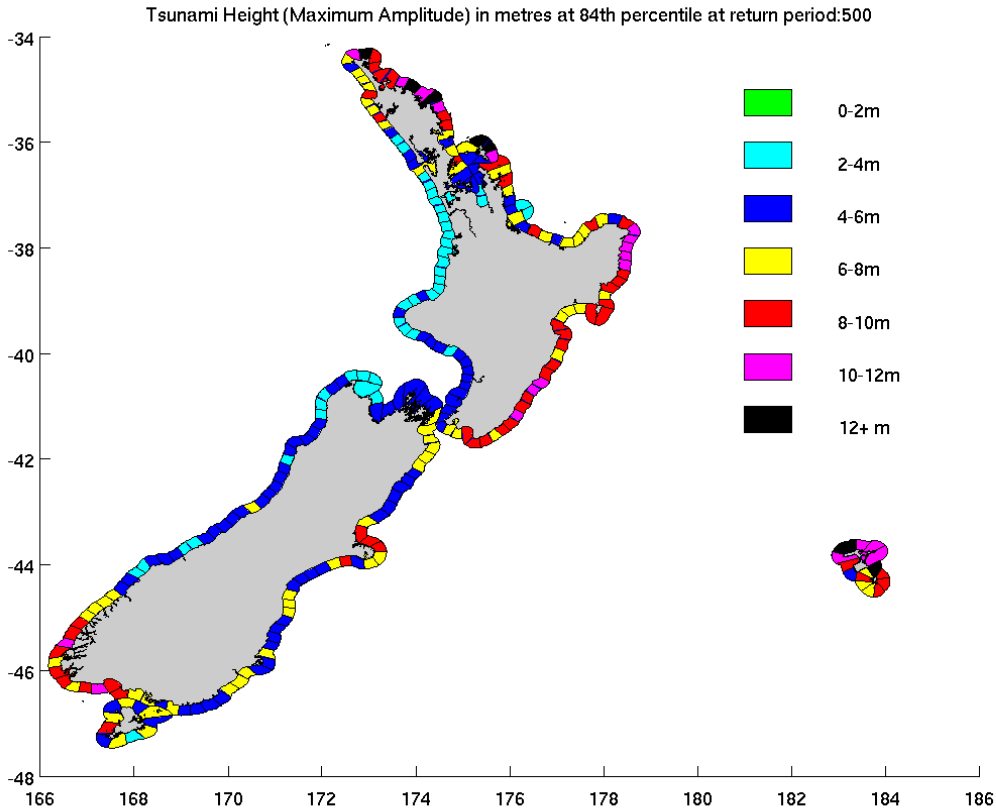

Figure 6.38 Expected maximum tsunami height in metres at 500 year return period, shown at median (50th percentile) and 84th percentile of epistemic uncertainty.

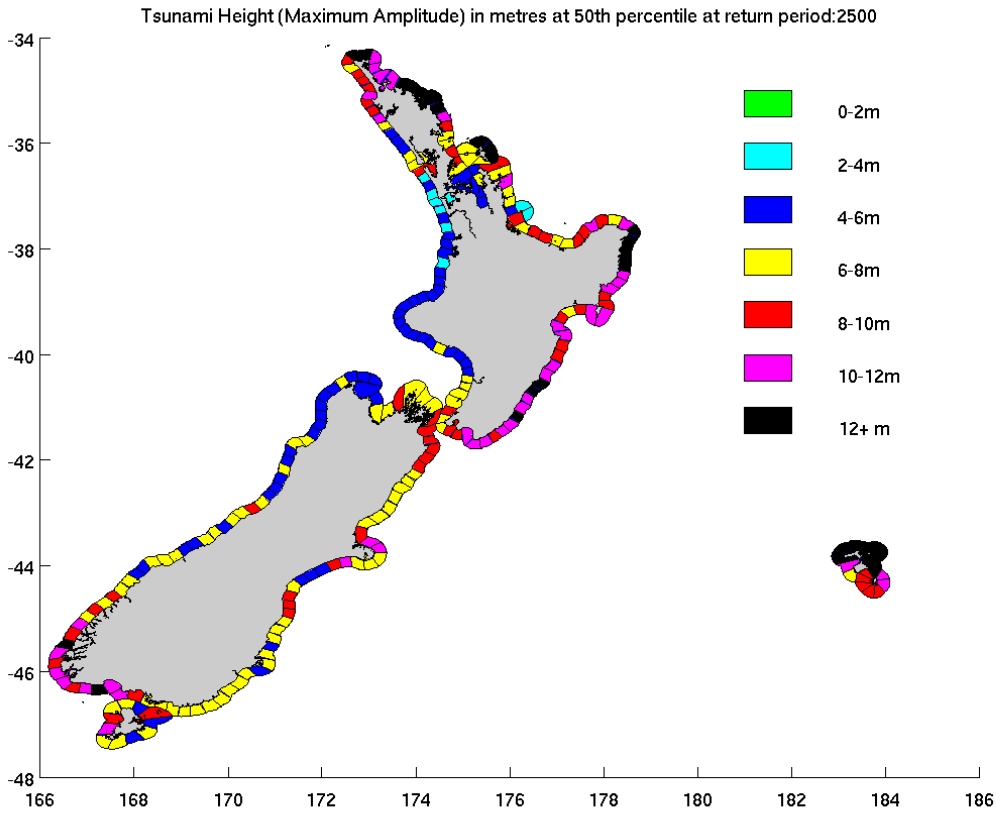

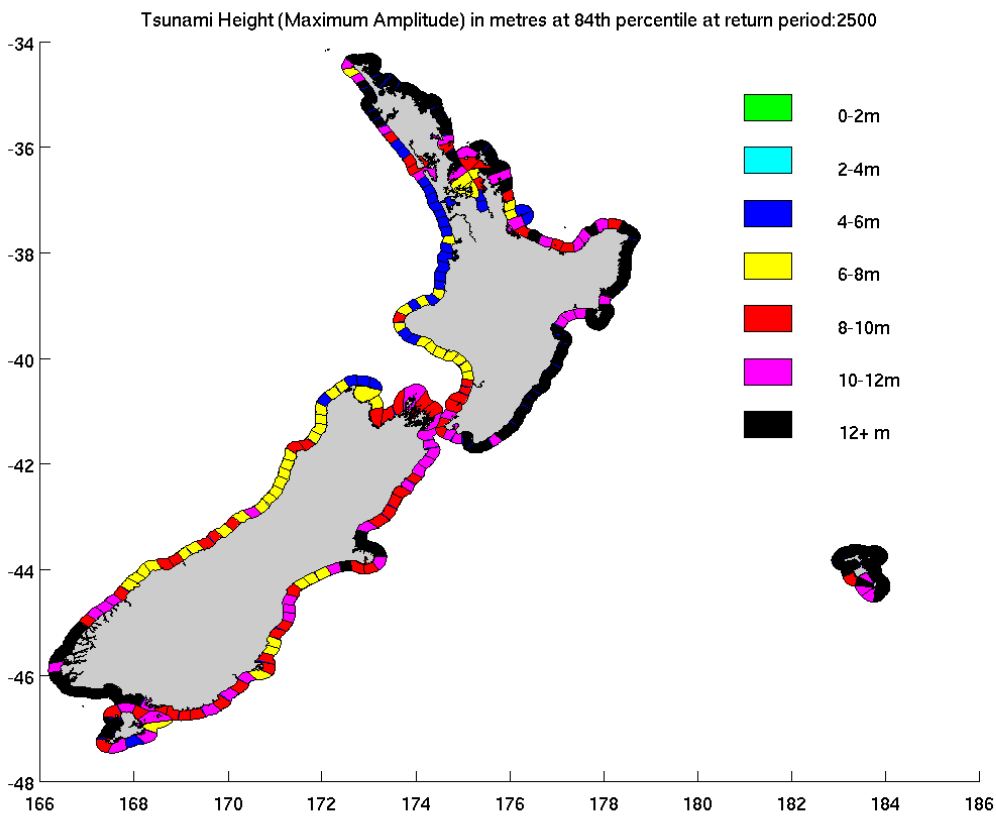

Figure 6.39 Expected maximum tsunami height in metres at 2500 year return period, shown at median (50th percentile) and 84th percentile of epistemic uncertainty.

6.10 COMMENTS AND DISCUSSION OF RESULTS

- The nationwide distribution of tsunami hazard is generally consistent with expectations, showing a higher hazard in those areas of the coast directly exposed to local subduction zones and an overall trend for the east coast to be exposed to a higher tsunami hazard than the west coast.
- For most parts of New Zealand, the distribution of tsunami hazard is quite similar to that in the 2005 report to the Ministry of Civil Defence & Emergency Management, *Review of Tsunami Hazard and Risk in New Zealand* (IGNS client report 2005/104). However the coasts that are most exposed to local subduction zones, notably the east-facing coasts of the North Island and the southwest corner of the South Island, are now typically assessed as having a higher tsunami hazard than was estimated in 2005.
- The probabilistic model does not currently take into account variations in geophysical properties within subduction zones. This is an important issue for the Hikurangi Trench, where the northern portions experience weaker coupling and faster convergence than the southern portions.
- The probabilistic model currently does not treat 'tsunami earthquakes' (see Section 5.3.1.2) on the shallowest parts of subduction interfaces as being distinct from other subduction interface earthquakes.
- The estimated tsunami hazard around the Kapiti/Manawatu coast and the north coast of the South Island may be overstated because the method used to model tsunami caused by crustal faults in the Wairarapa/Marlborough area does not take into account the dampening effect due to the constriction in Cook Strait (see Appendix 7.4, under 'Estimation of tsunami heights – Local crustal and outer rise faults').
- The division of the Pacific Rim into distinct subduction zones (Appendix 3) is in some cases based on distinct geophysical changes, but in some locations the boundaries between subduction zones are more artificial. In some regions subduction earthquakes may have ruptures that span more than one zone, a situation not represented in the current model.

The probabilistic tsunami hazard model represents the best endeavours of the report authors at the time it was created. Scientific understanding of input parameters will continue to evolve, and improved methods for calculating the hazard will be developed. The programs used to perform the calculations are complicated, and programming errors may be found and corrected. Hence the results in this report represent only a snapshot of the estimated tsunami hazard, as determined at the time of its construction.

6.11 FUTURE WORK

The method used for estimating tsunami heights for the local non-subduction zone faults is of low accuracy (high uncertainty), and in the long term it would be better to replace this with scaled-numerical modelling results. As the development of such models is difficult, it is useful to prioritise, so that the most important sources are developed first. Ranking our sources by the annualised moment release, i.e., the average seismic moment release per year, gives the following priority list:

Table 6.2 New Zealand local faults ranked by rate of moment release. See Appendix 4 for fault details. Location of faults can be identified using the NZSHM code and figures in Stirling et al. (2012).

Rank	Name and NZSHM code	M_W	Recurrence Interval (yrs)	Seismic moment/year
1	WairarapNich_345	8.2	1199	2.10E+18
2	JorKekNeed_374	7.6	389	8.13E+17
3	RaukumaraOuterRise_1001	7.8	1300	4.85E+17
4	HawkesBayOuterRise_1002	7.8	1460	4.32E+17
5	NorthWairarapaOuterRise_1003	7.8	1640	3.85E+17
6	SouthWairarapaOuterRise_1004	7.8	1900	3.32E+17
7	PalliserKai_372	7.6	1114	2.84E+17
8	Swedge5_492	7.7	1695	2.64E+17
9	GeorgeR1_482	8.1	7104	2.50E+17
10	MilfordB1_469	7.6	1416	2.23E+17
11	ArielBank_202	7.4	723	2.19E+17
12	Lachlan3_231	7.5	1068	2.10E+17
13	Cw4Swedge411_497	7.5	1254	1.79E+17
14	CBalleny_536	7.4	932	1.70E+17
15	JorKekCha_373	7.6	2089	1.51E+17
16	Swedge2_499	7.4	1068	1.48E+17
17	Madden_316	7.6	2396	1.32E+17
18	Barn_1018	7.6	2400	1.32E+17
19	Mataikona_335	7.3	853	1.32E+17
20	Pahaua_377	7.9	6779	1.32E+17

Addition of landslide sources to the probabilistic model is a goal which is discussed in Appendix 6.

Improving the source model definitions, and improving and calibrating the numerical tsunami models, is an on-going task. This is particularly important for the Hikurangi subduction zone, due to the significance of its contribution to the New Zealand tsunami hazard.

Obtaining more detail by further reduction in the length of the coastal sections used, currently 20 km, would be beneficial, as tsunami impacts may vary considerably even on this scale. It would be particularly helpful to be able to scale the hazard analysis to define separate coastal sections for the interior of the Waitemata and Wellington harbours. This would require refining of the associated numerical modelling grids in order to more accurately represent the harbour entrances.

6.12 REFERENCES

Abe, K. (1979). Size of great earthquakes of 1837–1974 inferred from tsunami data, *Journal of Geophysical Research*, 84, 1561-1568.

Abe, K (1981). Physical size of tsunamigenic earthquakes of the northwestern Pacific, *Physics of the Earth and Planetary Interiors* 27, 194-205.

Abe, K. (1985). Quantification of major earthquake tsunamis of the Japan Sea, *Physics of the Earth and Planetary Interiors*, 38, 214-223.

Abe, K. (1995). Estimate of tsunami run-up heights from earthquake magnitudes, In *Tsunami: Progress in Prediction, Disaster Prevention and Warning*, Y. Tsuchiya and N. Shuto (eds.), Kluwer Academic Publishers, 21-35.

Geist, E.L. (2002). Complex earthquake rupture and local tsunamis, *Journal of Geophysical Research*, 107(B5), 2086, doi:10.1029/2000JB000139.

Mueller, C.;, Power, W.; Fraser, S.; Wang, X. (2012). Towards a Robust Framework for Probabilistic Tsunami Hazard Assessment (PTHA) for Local and Regional Tsunami in New Zealand. Abstract volume of the Geosciences 2012 conference, Hamilton, New Zealand.p. 64.

Power, W.L.; Gale, N.H.; Lukovic, B.; Gledhill, K.R.; Clitheroe, G.; Berryman, K.R.; Prasetya, G. (2010) Use of numerical models to inform distant-source tsunami warnings. Lower Hutt: GNS Science. GNS Science report 2010/11. 22 p.

Satake, K.; Okada, M.; Abe, K. (1988). Tide gauge response to tsunamis: Measurements at 40 tide gauge stations in Japan, *Journal of Marine Research* 46, 557-571.

Stirling, M.; McVerry, G.; Gerstenberger, M.; Litchfield, N.; Van Dissen, R.; Berryman, K.; Barnes, P.; Beavan, J.; Bradley, B.; Clark, K.; Jacobs, K.; Lamarche, G.; Langridge, R.; Nicol, A.; Nodder, S.; Pettinga, J.; Reyners, M.; Rhoades, D.; Smith, W.; Villamor, P.; Wallace, L. (2012). National seismic hazard model for New Zealand: 2010 update, *Bulletin of the Seismological Society of America*, 102(4), 1514-1542.

Wang, X. ; Liu, P.L.-F. (2006). An analysis of 2004 Sumatra earthquake fault plane mechanisms and Indian Ocean tsunami. *Journal of Hydraulic Research*, 44(2), 147-154.

Wang, X.; Liu, P.L.-F.(2007). Numerical simulations of the 2004 Indian Ocean tsunamis - coastal effects. *Journal of Earthquake and Tsunami*, 1(3), 273-297.

This page is intentionally left blank.

7.0 DISCUSSION AND CONCLUSIONS

7.1 SUMMARY

7.1.1 Subduction earthquakes

The massive tsunami in 2004 in the Indian Ocean, in 2009 in the South Pacific and in 2011 in Japan have overturned many assumptions regarding the potential for severe tsunami to be generated on subduction zones throughout the Pacific. We cannot rely on a 200-year historical record to draw firm conclusions regarding the subduction zones around New Zealand. Instead, research on paleotsunami, as well as geodetic and geophysical studies, are needed to understand the potential for tsunami. New research into New Zealand's subduction tsunami sources will take time, and in the interim, in matters of public safety, it is best to assume that all subduction zones around New Zealand could generate severe tsunami from earthquakes of M_W 8-9.

7.1.2 Probabilistic tsunami hazard model

The probabilistic tsunami hazard model in this report covers all parts of the New Zealand coastline and all known seismic sources. It takes into account the changed picture regarding subduction zones, and incorporates several new crustal faults, many from the New Zealand Seismic Hazard Model. For most parts of New Zealand, the overall levels of hazard are quite similar to the assessed hazard levels in the 2005 report, but the estimated hazard has generally increased in those areas most exposed to tsunami from local subduction zones – notably the east-facing coasts of the North Island, and the southwest corner of the South Island.

The hazard model can be deaggregated, based on the contributions of various tsunami sources, and used for inundation modelling. This provides a basis for a simple form of probabilistic inundation modelling that could be used as a starting point for land-use planning (see Appendix 7.2). The hazard model and its deaggregation incorporate effects such as non-uniform slip and modelling uncertainty, at least to a first level of approximation.

7.2 DISCUSSION

7.2.1 Self-evacuation

Currently mitigation of local tsunami hazard is by self-evacuation in the event of strongly felt earthquakes. This is because local tsunami have very short travel times, which necessitate immediate evacuation before there has been adequate time and data available to issue official warnings.

Two circumstances have been identified in which a local tsunami may be generated but the earthquake that caused it is not strongly felt. One is if the earthquake is a "tsunami earthquake"—a special class of very shallow earthquake on the subduction interface that does not cause strong shaking; two earthquakes near Gisborne in 1947 were probably of this type and both caused tsunami. The other is of a subduction earthquake on the southern Kermadec Trench; in this case the shaking may not be strongly felt along the Coromandel and Northland coasts because of seismic attenuation in the offshore Taupo Volcanic Zone.

These are in addition to the possibility of a landslide-caused tsunami that is not triggered by a major earthquake.

Reliance on self-evacuation in big cities is problematic. The majority of strongly felt earthquakes will probably not cause severe tsunami, however the public needs to be educated to evacuate from every strongly felt earthquake as if it were generating the worst-case tsunami. Mass evacuation of cities in the aftermath of a major earthquake is likely to result in many problems, and this will often appear to be unnecessary in hindsight. Yet at present self-evacuation still appears to be the best option in terms of public safety.

As the technology for assessing large local earthquakes improves, and more instruments for tsunami monitoring become available, there will be a problem of public expectations. Without continuing education the public may come to expect to receive a tsunami warning for local events, and may therefore not self-evacuate if no official warning is issued. To some extent the installation of tsunami warning sirens, useful for warning of events too far away for the earthquake to be strongly felt, already contributes to this problem.

7.3 RECOMMENDATIONS

- The following actions are recommended:
- Seismic modelling should be used to evaluate how a large subduction zone earthquake on the southern Kermadec Trench will be felt at coasts on the opposite side of the offshore Taupo volcanic zone (principally the Coromandel and Northland coasts).
- Risk factors for "tsunami earthquakes" should be determined and their presence around the New Zealand coast evaluated.
- Geophysical and geological research to understand the relationship between earthquakes on upper plate faults close to the trench and earthquakes on the subduction interface would be helpful for improving the hazard model. In particular, it would be useful to discover which faults tend to rupture simultaneously with plate interface movement during subduction earthquakes.
- The potential for outer-rise earthquakes to generate tsunami close to New Zealand warrants further investigation.
- Planning and exercises to make mass self-evacuation of vulnerable urban areas as safe and easy as possible in the aftermath of an earthquake should be undertaken.
- Education regarding self-evacuation after a strongly felt earthquake, without waiting for an official warning, needs to continue.
- Geonet’s capability to identify and quantify large subduction zone earthquakes should be maintained and enhanced.
- Real-time inundation models for major cities should be trialled and evaluated.
- The national probabilistic tsunami hazard model developed for this report should be periodically updated with new information. Integration with a probabilistic model for landslide-caused tsunami should take place. Further research to develop probabilistic inundation modelling should be supported.

APPENDICES

This page is intentionally left blank.

APPENDIX 1: REFERENCES TO TSUNAMI-RELATED PUBLICATIONS RELEVANT TO NEW ZEALAND

Table A 1.1 lists tsunami modelling studies organised on the basis of study location. Table A 1.2 lists research and modelling studies, not necessarily location specific, but with relevance to New Zealand.

Table A 1.1 A brief summary of tsunami modelling and inundation studies in New Zealand.

District	Communities/Suburbs	Tsunami Sources	References
Northland	Maximum tsunami elevations along Northland coastlines	M_W8.5, 8.8, 8.9, 9.4 scenario events in Kermadec subduction zone and 3 M_W8.15 scenarios in Southern New Hebrides subduction zone	William Power, Laura Wallace, Xiaoming Wang and Martin Reyners (2012) Tsunami hazard posed to New Zealand by the Kermadec and Southern New Hebrides subduction margins: an assessment based on plate boundary kinematics, interseismic coupling and historical seismicity. Pure Appl. Geophys. 169: 1-35.
	Maximum tsunami elevations along most of Northland coastlines	M_W9.0 in South America, M_W9.2 in Solomon Sea, M_W9.2 in New Hebrides, M_W9.0 in Tonga-Kermadec trench	James Goff, Roy Walters and Fraser Callaghan (2006) Tsunami source study, NIWA Client Report CHC2006-082 (Environment Waikato Technical Report 2006/49)
	Inundation modelling in many coastal communities in the Northland region. Ahipara, Bream Bay, Bay of Islands, Doubtless Bay, East Beach, Dargaville, Mangawhai, Omapere, Whangarei, Whangarei East Coast North, Whangaeri East coast south, Whangaroa, Whangaruru	South America scenario similar to the 1868 event, M_W8.5 and M_W9.0 scenario events in Tonga-Kermadec subduction trench	Emily Lane, Roy Walters, Jade Arnold and Helen Roulston (2007) Northland Regional Council tsunami modelling study 1, NIWA Client Report CHC2007-109. Philip Gillibrand, Emily Lane, Jade Arnold, John Carter, Jen Dumas, Matt Enright and James Goff (2008) Northland Regional Council tsunami modelling study 2, NIWA Client Report CHC2008-115. Jade Arnold, John Carter, Jen Dumas and Philip Gillibrand (2009) Northland Regional Council tsunami modelling study 3, NIWA Client Report CHC2009-042.
	Whangarei Harbour and environs, including Marsden Bay, Takahiwai, Oakleigh, Otaika, Whangarei and Bream Head;	South America scenario similar to the 1868 event, M_W8.5 and M_W9.0 scenario events in Tonga-Kermadec subduction trench	Jade Arnold, Philip Gillibrand and Julian Sykes (2010) Numerical modelling of tsunami inundation for Whangarei Harbour and environs, NIWA Client Report CHC2010-133

District	Communities/Suburbs	Tsunami Sources	References
Auckland	Maximum tsunami elevations along most of Auckland coastlines	M_W9.0 in South America, M_W9.2 in Solomon Sea, M_W9.2 in New Hebrides, M_W9.0 in Tonga-Kermadec trench	James Goff, Roy Walters and Fraser Callaghan (2006) Tsunami source study, NIWA Client Report CHC2006-082 (Environment Waikato Technical Report 2006/49)
	Maximum tsunami elevations along most of Auckland coastlines	M_W8.5, 8.8, 8.9, 9.4 scenarios events in Kermadec subduction zone and 3 M_W8.15 scenarios in Southern New Hebrides subduction zone	William Power, Laura Wallace, Xiaoming Wang and Martin Reyners(2012) Tsunami hazard posed to New Zealand by the Kermadec and Southern New Hebrides subduction margins: an assessment based on plate boundary kinematics, interseismic coupling and historical seismicity. Pure Appl. Geophys. 169: 1-35.
	Inundation modelling in many coastal communities in the Auckland region, including Omaha and Snell Beach, Waiwera to Whangaparoa Peninsula, North Shore, CBD, Te Atatu to Mission Bay, Kaiaua and Waiheke Island;	M_W9.5 scenario in South America (a variation to the 1868 event)	Emily Lane, Roy Walters, Jade Arnold, Matt Enright and Helen Roulston (2009) Auckland Regional Council inundation study, Prepared by National Institute of Water & Atmospheric Research Ltd for Auckland Regional Council. Auckland Regional Council Technical Report 2009/113
	Probabilistic tsunami hazard study of Auckland region for a 2500-year return period	Kermadec subduction interface, southern New Hebrides	William Power, Xiaoming Wang, Emily Lane and Philip Gillibrand (2012). A Probabilistic Tsunami Hazard Study of the Auckland Region, Part I: Propagation Modelling and Tsunami Hazard Assessment at the Shoreline. Pure Appl. Geophys., DOI 10.1007/s00024-012-0543-z. Emily Lane, Philip Gillibrand, Xiaoming Wang and William Power (2012). A Probabilistic Tsunami Hazard Study of the Auckland Region, Part II: Inundation Modelling and Hazard Assessment. Pure Appl. Geophys, DOI: 10.1007/s00024-012-0538-9.

District	Communities/Suburbs	Tsunami Sources	References
Waikato	Maximum tsunami elevations on most of Waikato coastlines	M_W9.0 in South America, M_W9.2 in Solomon Sea, M_W9.2 in New Hebrides, M_W9.0 in Tonga-Kermadec trench	James Goff, Roy Walters and Fraser Callaghan (2006) Tsunami source study, NIWA Client Report CHC2006-082 (Environment Waikato Technical Report 2006/49)
	Maximum tsunami elevations on most of Waikato coastlines	M_W8.5, 8.8, 8.9, 9.4 scenarios events in Kermadec subduction zone and 3 M_W8.15 scenarios in Southern New Hebrides subduction zone	William Power, Laura Wallace, Xiaoming Wang and Martin Reyners(2012) Tsunami hazard posed to New Zealand by the Kermadec and Southern New Hebrides subduction margins: an assessment based on plate boundary kinematics, interseismic coupling and historical seismicity. Pure Appl. Geophys. 169: 1-35.
Bay of Plenty	Maximum tsunami elevations on most Bay of Plenty coastlines	M_W9.0 in South America, M_W9.2 in Solomon Sea, M_W9.2 in New Hebrides, M_W9.0 in Tonga-Kermadec trench	James Goff, Roy Walters and Fraser Callaghan (2006) Tsunami source study, NIWA Client Report CHC2006-082 (Environment Waikato Technical Report 2006/49)
	Maximum tsunami elevations on most of Bay of Plenty coastlines	M_W8.5, 8.8, 8.9, 9.4 scenarios events in Kermadec subduction zone and 3 M_W8.15 scenarios in Southern New Hebrides subduction zone	William Power et al. (2012) Tsunami hazard posed to New Zealand by the Kermadec and Southern New Hebrides subduction margins: an assessment based on plate boundary kinematics, interseismic coupling and historical seismicity. Pure Appl. Geophys. 169; 1-35.
	Inundation modelling for Wairakei, Te Tumu,	Tonga-Kermadec-Hikurangi M_W8.5 scenario; local faults (White Island faults, composite Volkner faults, composite Astolabe faults); complex combination of subduction zone earthquake and landslide; sector collapse of seamount/submarine volcano	Roy Walters, Fraser Callaghan and James Goff (2006) Wairakei/Te Tumu tsunami inundation study. Prepared by National Institute of Water & Atmospheric Research Ltd for Environment Bay of Plenty. NIWA Client Report CHC2006-020.

District	Communities/Suburbs	Tsunami Sources	References
Gisborne	Maximum tsunami elevations on most of Bay of Plenty coastlines	M_W8.5, 8.8, 8.9, 9.4 scenarios events in Kermadec subduction zone and 3 M_W8.15 scenarios in Southern New Hebrides subduction zone	William Power, Laura Wallace, Xiaoming Wang and Martin Reyners (2012) Tsunami hazard posed to New Zealand by the Kermadec and Southern New Hebrides subduction margins: an assessment based on plate boundary kinematics, inter-seismic coupling and historical seismicity. Pure Appl. Geophys. 169: 1-35.
	Inundation modelling around Poverty Bay, including Gisborne City center, Muriwai and Wainui;	M_W9.1 and M_W9.4 distant source scenarios from South America; M_W8.8 and M_W9.0 Whole Hikurangi subduction interface rupture	Xiaoming Wang, Gegar Prasetya, William Power, Biljana. Lukovic, Hannah Brackley and Kelvin Berryman (2009). Gisborne District Council Tsunami Inundation Study, GNS Science Consultancy Report 2009/233 130 p.
Wellington	Empirical model of inundation in Wellington and Horizon regions; the rule has been used to develop tsunami evacuation zone maps (red, orange and yellow zones) around New Zealand;	Probabilistic tsunami height with a 500 year return period from regional and distant sources; Probabilistic tsunami height with a 2500 year return period from all sources	Graham Leonard (compiler), (2009).Interim tsunami evacuation planning zone boundary mapping for the Wellington and horizons regions defined by a GIS-calculated attenuation rule. GNS Science Report SR2008/30, Lower Hutt, 18p.
Canterbury	Inundation modelling in Motunau, Waikuku Beach, The Pines/Kairaki/Kaiapoi and Woodend Beach, Lyttelton Harbour, Akaroa harbour, Taumutu village and the margins of Lake Ellesmere, Rakaia River mouth, Rangitata River mouth, Browns Beach, Seaforth to Scarborough, Pareora River mouth;	South America (1868 Scenario)	Philip Gillibrand, Jade Arnold, Emily Lane, Helen Roulston and Matthew Enright (2011) Modelling coastal inundation in Canterbury form a South American tsunami. Prepared by National Institute of Water & Atmospheric Research Ltd for Environmental Canterbury. Environmental Canterbury Report R11/08.
	Inundation modelling in coastal areas of Christchurch and Kaiapoi, taking into account of the topography variation from the 2011 February earthquake;	South America (1868 Scenario)	Emily Lane, Jade Arnold, Julian Sykes and Helen Roulston (2012) Modelling coastal inundation in in Christchurch and Kaiapoi from a South America tsunami using topography from after the 2011 February earthquake. Prepared by National Institute of Water & Atmospheric Research Ltd

District	Communities/Suburbs	Tsunami Sources	References
			for Environmental Canterbury. Environmental Canterbury Report R12/38.
	Tsunami impact along Kaikoura coast	Local faults offshore Kaikoura coast (North Canterbury shelf fault, Conway Ridge fault, Kekerengu Bank thrust), submarine landslide in Kaikoura Canyon	Roy Walters, Philip Barnes and James Goff (2006): Locally generated tsunami along the Kaikoura coastal margin: Part 1. Fault ruptures, New Zealand Journal of Marine and Freshwater Research, 40(1): 1-15. Roy Walters, Philip Barnes, Keith Lewis, James Goff and Jason Fleming (2006): Locally generated tsunami along the Kaikoura coastal margin: Part 2. Submarine landslides, New Zealand Journal of Marine and Freshwater Research, 40(1): 17-28
Otago	Clutha District: Papatowai, Catlins River Mouth (including Pounawea, New Haven, Jack's Bay), Kaka Point, Lower Clutha, Toko Mouth, Taieri Mouth; Dunedin City: Brighton, St Kilda/St Clair, Otago Harbour, Long Beach, Aramoana, Purakanui, Harwood, Warrington, Blueskin Bay, Karitane, Waikouaiti; Waitaki District: Taranui, Kakanui, Oamaru;	1:600-year near-source scenarios in Puysegur trench, 1:500-year distant source scenarios in South American Scenarios, offshore landslide scenarios	Emily Lane, Roy Walters, Michelle Wild, Jade Arnold, Matt Enright, Helen Roulston and Joshu Mountjoy (2007). Otago region hazards management investigation: tsunami modelling study. NIWA Client Report: CHC2007-030. Michael Goldsmith (2012). Community vulnerable to elevated sea level and coastal tsunami events in Otago, Prepared by Michael Goldsmith, Manager Natural Hazards, Otago Regional Council. ISBN 978 0 478 37630 2 Michael Goldsmith (2012). Community vulnerability to elevated sea level and coastal tsunami events in Otago – Map Book, Prepared by Michael Goldsmith, Manager Natural Hazards, Otago Regional Council. ISBN 978 0 478 37631-9.

District	Communities/Suburbs	Tsunami Sources	References
Southland		Local sources	Walters, R. A., & Callaghan, F. (2005). Understanding local source tsunamis: 1820s Southland tsunami EQC04201 (Vol. CHC2005-035, pp. 27 leaves : 16 figs, 14 refs). Christchurch: NIWA. Downes, G., Cochran, U., Wallace, L., Reyners, M., Berryman, K., Walters, R., . . . Bell, R. (2005). EQC Project 03/490 - Understanding local source tsunami: 1820s Southland tsunami EQC04201 (Vol. HAM2005-135, pp. 92 p.). Hamilton: NIWA and IGNS.

Table A 1.2 Tsunami research and modelling studies relevant to New Zealand.

Author(s)	Location	Reference	Source
Walters, R.A. Goff, J.	All New Zealand	(2003) *Assessing Tsunami Hazard Along the New Zealand Coast,* Science of Tsunami Hazards, 21(3): 137-153. (2002) R.A. Walters, *Long wave resonance on the New Zealand coast.* NIWA Technical Report 109, 32 pp.	Amplification estimates for distant source tsunami approaching from the east.
Power, W. Downes, G. Stirling, M.	All New Zealand	(2004) *Progress towards a probabilistic tsunami hazard map for New Zealand.* Eos Trans. AGU, 85(47), Fall Meet. Suppl., Abstract OS22B-07.	South American earthquakes
Power, W.	All New Zealand	(2005) Display for Te Papa, Wellington.	26 December 2004 Indian Ocean (Sumatra) earthquake
Power, W.	All New Zealand	(2004) Display for the National Aquarium, Hawkes Bay.	1868 Peru earthquake
Gilmour, A.E.	All New Zealand	(1964) *Tsunami travel times to New Zealand.* New Zealand Oceanographic Institute Chart Misc. Series 7, *1:37,090,000.* Wellington (1967) *Tsunami travel times to New Zealand.* New Zealand Journal of Marine and Freshwater Research, 1(2): 139-142.	Locations around the Pacific Ocean
de Lange, W.P. Healy, T.	Auckland	(2001) *Tsunami hazard for the Auckland region and Hauraki Gulf, New Zealand.* Natural Hazards, 24(3): 267-284.	Kerepehi fault, South America, Auckland Volcanic Field
Prasetya, G.S.	Auckland area	(1998) *Modelling volcanic tsunamis*. MSc Thesis, The University of Waikato, Hamilton, 299 pp.	Volcanic events in the Auckland Volcanic Field
Chittleborough, J.	Australia (Southeast)	(2004) *Tsunami waves caused by Fiordland, NZ earthquake of August 2003*: National Tidal Facility Australia, 7 pp.	2003 Fiordland earthquake
de Lange, W.P.	Bay of Plenty, East Cape	(1983) *Tsunami hazard: an investigation into the potential tsunami hazards of the Bay of Plenty Region using numerical models*. M.Sc. Thesis, University of Waikato, Hamilton, 250 pp.	Earthquakes and pyroclastic flows at Mayor Island and White Island
de Lange, W.P. Healy, T.	Bay of Plenty	*Tsunami hazards in the Bay of Plenty, New Zealand: an example of hazard analysis using numerical models.* Journal of Shoreline Management, 2: 177-197	South America

Author(s)	Location	Reference	Source
de Lange, W.P. Prasetya, G.S. Healy, T.	Bay of Plenty	(2001) *Modelling of Tsunamis Generated by Pyroclastic Flows (Ignimbrites).* Natural Hazards, 24: 251-266.	Mayor Island
McKenzie, D.D.J.	Bay of Plenty	(1993) *Numerical modelling of tsunamis in the Bay of Plenty.* MSc Thesis, University of Waikato, Hamilton, 88 pp.	Earthquakes associated with Whakatane graben, and Taupo volcanic zone faults
Weir, G.J. White, S.P.	Bay of Plenty	(1982) *Mathematical modelling of volcanic tsunamis,* New Zealand Journal of Marine and Freshwater Research, 16(3/4): 373-382.	White Island volcanic events
Todd, D.	Canterbury and Otago	(1999) *Regional tsunami studies: Canterbury and Otago,* Tephra, October: 56-58.	South America
Walters, R.A. Barnes, P. Lewis, K. Goff, J., Fleming, J.	Kaikoura	(2006) Locally generated tsunami along the Kaikoura coastal margin: Part 2. Submarine landslides. New Zealand Journal of Marine and Freshwater Research 40(1): 17-28 (2004) R.A. Walters, *Tsunami generation, propagation, and runup.* Estuarine and Coastal Modelling: Proc. of the 8th International Conference, edited by M.L. Spaulding, ASCE: 423-438. (2005) R.A. Walters, *Coastal Ocean models: Two useful finite element methods.* Continental Shelf Research 25: 775-793.	Submarine landslides, landslide in Kaikoura Canyon
Walters, R.A. Barnes, P. Goff, J.	Kaikoura	(2006) Locally generated tsunami along the Kaikoura coastal margin: Part 1. Fault ruptures. New Zealand Journal of Marine and Freshwater Research, 40(1) 1-16.. (2005) R.A. Walters, *A semi-implicit finite element model for non-hydrostatic (dispersive) surface waves*. International Journal for Numerical Methods in Fluids 49(7): 721-737.	Kaikoura thrust fault
Walters, R.A.	Hawkes Bay	(2004) Display for the National Aquarium, Hawkes Bay.	Earthquakes on the Lachlan fault
de Lange, W.P.	Poverty Bay	(1997) *Tsunami hazard associated with marl diapirism off Poverty Bay, New Zealand*. In: D.N.B. Skinner (Ed.), Geological Society of New Zealand 1997 Annual Conference. Geological Society of New Zealand, Wellington, p. 49.	Mud volcanism

Author(s)	Location	Reference	Source
de Lange, W.P. Healy, T.	Poverty Bay	(1997) *Numerical modelling of tsunamis associated with marl diapirism off Poverty Bay, New Zealand*, Combined Australasian Coastal Engineering and Ports Conference, Christchurch: 1043-1047.	Mud volcanism
Magill, C.	Poverty Bay	(2001) *Numerical modelling of tsunami generated by mass movement.* MSc thesis, University of Waikato, 198.	Landslides
Cochran, U. G. Downes, G. Walters, R. et al.	Southland	EQC report (in preparation)	Earthquakes on the southern portion of the Alpine fault and within the Puysegur trench.
Magill, C.R.	Lake Tarawera, Poverty Bay	(2001) Numerical modelling of tsunami generated by mass movement. MSc Thesis, University of Waikato, Hamilton, 198 pp.	Pyroclastic flow (Tarawera), Landslide (Poverty Bay).
de Lange, W.P. Magill, C.R. Nairn, J.A. Hodgson, K.	Lake Tarawera	(2002) *Tsunami generation by pyroclastic flows entering Lake Tarawera,* Eos, 83(22:supplement): WP54.	Tarawera volcano
de Lange, W.P. Chicks, L. Healy, T.	Firth of Thames	(2001) *Potential tsunami hazard associated with the Kerepehi Fault, Firth of Thames, New Zealand.* Natural Hazards, 24(3): 309-318. (1999) *Tsunami hazard and inundation modelling for the Firth of Thames,* Tephra, October: 51-55.	Kerepehi fault, South America, Auckland Volcanic Field
Chick, L.M.	Firth of Thames, Hauraki Gulf	(1999) *Potential tsunami hazard associated with the Kerepehi Fault, Hauraki Gulf, New Zealand*. MSc Thesis, The University of Waikato, Hamilton, 284 pp.	Earthquakes on Kerepehi fault
Butcher, C.N. Gilmour, A.E.	Wellington and Lyttleton Harbours	(1987) *Free oscillations in Wellington and Lyttelton Harbours*. DFMS Reports, 1: 3-10.	Chile 1960 and Alaska 1964 earthquakes
Abraham, E.R.C.	Wellington Harbour	(1997) *Seiche modes of Wellington Harbour, New Zealand.* New Zealand Journal of Marine and Freshwater Research, 31(2): 191-200.	
Barnett, A. Beanland, S. Taylor, R.G.	Wellington Harbour (Te Papa)	(1991) *Tsunami and Seiche Computation for Wellington Harbour,* Proceedings of Pacific Conference on Earthquake Engineering, Vol. 2, Auckland.	Crustal earthquakes in Cook Strait and South American earthquakes.

Author(s)	Location	Reference	Source
Gilmour, A. Stanton, B.	Wellington Region	(1990) *Tsunami Hazards in the Wellington Region,* Report for Wellington Regional Council, by DSIR.	Crustal earthquakes in Cook Strait and South American earthquakes.
Power, W. Downes, G. McSaveney, M. Beavan, J. Hancox, G.	West Coast	(2003) *The Fiordland earthquake and tsunami, New Zealand, 21 August 2003,* Proceedings of the IUGG Tsunami Workshop 2003 and the International Workshop, Tsunamis in the South Pacific, Kluwer.	2003 Fiordland earthquake
Power, W.L. Reyners, M.E. Wallace, L.M.	East Coast	(2005) Source models of tsunamigenic earthquakes on the Hikurangi Plate interface. 1 p. In: *USGS Tsunami Sources Workshop 2006: Great Earthquake Tsunami Sources: Empiricism & Beyond, April 21-22, 2005.* US Geological Survey.	Hikurangi Margin
Leonard, G.S. Johnston, D.M. Downes, G.L. Power, W.L. Paton, D.	All New Zealand	(2005) Understanding effective societal response to warnings and development of national guidelines for tsunami evacuation mapping. p. 24-25 In: *Living on the edge: coastal sustainability: NZCS Conference, Kaikoura 2005.* [Auckland]: New Zealand Coastal Society.	Locations around the Pacific Ocean
Leonard, G.S. Johnston, D.M. Downes, G.L. Power,W.L. Lukovic, B. Paton, D. Brounts, H.	All New Zealand	(2005) Tsunami evacuation zone mapping for rapid national use: a draft method allowing for varied risk, evolving tsunami models and human behaviour. p. 36-37 In: *Conference proceedings: 7th New Zealand Natural Hazards Management Conference, Christchurch, 23-24 August 2005.* Lower Hutt, GNS Science. GNS Science miscellaneous series 8	Locations around the Pacific Ocean
Power, W.L.	Wellington Harbor	(2007) Response of Wellington Harbour to the 2007 Solomon Islands and Peru tsunamis. p. 133 In: Mortimer, N.; Wallace, L.M. (Eds.) *Geological Society of New Zealand & New Zealand Geophysical Society Joint Annual Conference: launching International Year of Planet Earth, 26-29 November 2007, Tauranga: programme and abstracts.* Geological Society of New Zealand. Geological Society of New Zealand miscellaneous publication 123A.	Solomon Islands, Peru

Author(s)	Location	Reference	Source
Power, W.L. Lukovic, B.	All New Zealand	(2008) Using cluster analysis to optimize tsunami evacuation zones. Abstract NG23A-1113 In: *2008 AGU Fall Meeting, 15-19 December, San Francisco: abstracts.* Washington, DC: American Geophysical Union. Eos 89(53:supplement)	subduction zone earthquakes
Power, W.L.; Cousins, W.J.; King, A.B.; Destegul, U.	Cook Strait	(2008) Tsunami hazards of Cook Strait. p. 72 In: Wysoczanski, R. (comp.) *Geological Society of New Zealand, New Zealand Geophysical Society, New Zealand Geochemical & Mineralogical Society joint annual conference: Geosciences '08: programme and abstracts.* Lower Hutt: Geological Society of New Zealand. Geological Society of New Zealand miscellaneous publication 125A.	Faults within Cook Strait, e.g., Wairarapa Fault, Hikurangi subduction zone, Wellington fault
Wang, X. Prasetya, G. Power, W.L.	Poverty Bay, Gisborne	(2009) Tsunami inundation modeling in Poverty Bay, New Zealand: preparedness for potential tsunamis from distant and local sources. Abstract SE58-A011 In: *6th Annual Meeting AOGS, 11 to 15 August 2009, Singapore: abstracts.* Singapore: Asia Oceania Geosciences Society.	South America, Hikurangi subduction interface/Outer rise, Ariel Bank fault, Gable End fault, Lachlan fault
Wang,X. Power, W.L. Bell, R.E. Downes, G.L. Holden, C.	Gisborne	(2009) Slow rupture of the March 1947 Gisborne earthquake suggested by tsunami modelling. p. 221 In: Barrell, D.J.A.; Tulloch, A.J. (Eds.) *Geological Society of New Zealand & New Zealand Geophysical Society Joint Annual Conference, Oamaru, 23-27 November 2009: programme and abstracts.* Wellington: Geological Society of New Zealand. Geological Society of New Zealand miscellaneous publication 128A.	Hikurangi Margin
Power, W.L. Prasetya, G. Wang, X. Wilson, K.J.	Southland	(2009) The Fiordland 2009 tsunami: observations and interpretation. p. 173 In: Barrell, D.J.A.; Tulloch, A.J. (eds) *Geological Society of New Zealand & New Zealand Geophysical Society Joint Annual Conference, Oamaru, 23-27 November 2009: programme and abstracts.* Wellington: Geological Society of New Zealand. Geological Society of New Zealand miscellaneous publication 128A.	Fiordland fault

Author(s)	Location	Reference	Source
Bell, R.E. Wang, X. Power, W.L. Downes, G.L. Holden, C.	East Coast, Gisborne	(2009) Hikurangi Margin tsunami earthquake generated by slip over a subducted seamount. p. 18 In: Barrell, D.J.A.; Tulloch, A.J. (Eds.) *Geological Society of New Zealand & New Zealand Geophysical Society Joint Annual Conference, Oamaru, 23-27 November 2009: programme and abstracts.* Wellington: Geological Society of New Zealand. Geological Society of New Zealand miscellaneous publication 128A.	Hikurangi Margin
Leonard, G.S. Johnston, D.M. Power, W.L. Coetzee, D. Downes, G.L. Lukovic, B.	All New Zealand	(2010) A national tsunami evacuation mapping framework: warning preparedness for communities integrating social and geoscience best practice. p. 168 In: Hoskin, P.; Hikuroa, D.; Eccles, J. (conveners) *GeoNZ 2010: geoscience, geothermal: abstract volume: Auckland, 21-24 November 2010.* Wellington: Geoscience Society of New Zealand. Geoscience Society of New Zealand miscellaneous publication 129A.	All sources
Gale, N.H. Gledhill, K.R. Power, W.L.	All New Zealand	(2010) Tsunami threats: evaluation and advice. p. 101 In: Hoskin, P.; Hikuroa, D.; Eccles, J. (conveners) *GeoNZ 2010: geoscience, geothermal: abstract volume: Auckland, 21-24 November 2010.* Wellington: Geoscience Society of New Zealand. Geoscience Society of New Zealand miscellaneous publication 129A.	All sources
Power, W.L. Clark, K.J. Beavan, R.J. Wang, X. Prasetya, G. Holden, C. Wallace, L.M.		(2011) The 2009 South Pacific tsunami: implications for tsunami hazard in the South Pacific. Abstract 4610 In: *XXV IUGG General Assembly, Melbourne, Australia, 28 June - 7 July 2011: abstracts.* IUGG.	Tonga trench
Leonard, G.S. Power, W.L. Johnston, D.M. Coetzee, D. Downes, G.L.	All New Zealand	(2011) The New Zealand National Tsunami Evacuation Mapping Framework: from modelling and warning to community preparedness. Abstract 4601 In: *XXV IUGG General Assembly, Melbourne, Australia, 28 June - 7 July 2011: abstracts.* IUGG.	All sources

Author(s)	Location	Reference	Source
Cousins, W.J. Power, W.L. Destegul, U. King, A.B.	Wellington Region	(2008) Earthquake and tsunami losses from major earthquakes affecting the Wellington Region. Benfield Limited. 18 p.	Wellington fault, Wairarapa fault, Booboo fault, Hikurangi subduction zone
Leonard, G.S. Power, W.L. Lukovic, B. Smith, W.D. Langridge, R.M. Johnston, D.M. Downes, G.L.	All New Zealand	(2008) Interim tsunami evacuation planning zone boundary mapping for the Wellington and Horizons regions defined by a GIS-calculated attenuation rule. Lower Hutt: GNS Science. GNS Science report 2008/30. 18 p.	All Sources
Power, W.L. Gale, N.H. Lukovic, B. Gledhill, K.R. Clitheroe, G. Berryman, K.R. Prasetya, G.	All New Zealand	(2010) Use of numerical models to inform distant-source tsunami warnings. Lower Hutt: GNS Science. GNS Science report 2010/11. 22 p.	Distant Sources
Smith, W.D. Power, W.L. Lukovic, B. Cousins, W.J.	Wanganui	(2007) Wanganui tsunami risk assessment. GNS Science consultancy report 2007/308. 10 p.	All Sources
Wright, K.C. Baldi, M. Van Dissen, R.J. Salinger, J. Dellow, G.D. Page, M.J. Power, W.L. King, D. Lindsay, J.	Auckland Region	(2009) Natural hazards and their impacts, Auckland region. Auckland Regional Council Technical Report No.010 February 2009.	Local, Regional and distant sources
Power, W.L. Reyners, M.E. Wallace, L.M.	East Coast	(2008) Tsunami hazard posed by earthquakes on the Hikurangi subduction zone interface. GNS Science consultancy report 2008/40. 58 p.	Hikurangi subduction interface
Cousins, W.J. Power, W.L. Destegul, U. King, A.B.	Wellington Region	(2007) Combined earthquake and tsunami losses for major earthquakes affecting the Wellington region. GNS Science consultancy report 2007/280. v, 83 p.	Wellington fault, Wairarapa fault, subduction zone to Cook Strait
Berryman, K.R. Power, W.L. Saunders, W.S.A. Cousins, W.J.	Wairarapa Coast	(2008) Tsunami hazard and mitigation in relation to proposed rural subdivision at Flat Point, Wairarapa Coast. GNS Science consultancy report 2008/225. 28 p.	All Sources

Author(s)	Location	Reference	Source
Wang, X. Prasetya, G. Power, W.L. Lukovic, B. Brackley, H.L. Berryman, K.R.	Gisborne, Poverty Bay	(2009) Gisborne District Council tsunami inundation study. GNS Science consultancy report 2009/233. 117 p.	Distant Source from Peru, local sources from Hikurangi margin, Arieal Bank fault, Gable End fault, Lachlan fault
Cousins, W.J. Power, W.L. Destegul, U. King, A.B. Trevethick, R. Blong, R. Weir, B. Miliauskas, B.	Wellington Region	(2009) Earthquake and tsunami losses from major earthquakes affecting the Wellington region. Paper 24 In: Why do we still tolerate buildings that are unsafe in earthquakes: New Zealand Society for Earthquake Engineering 2009 Conference, 3-5 April, Christchurch, New Zealand. Wellington, NZ: New Zealand Society for Earthquake Engineering.	Wellington fault, Wairarapa fault, subduction zone to Cook Strait
Power, W.L. Downes, G.L. McSaveney, M.J. Beavan, R.J. Hancox, G.T.	South Coast	(2006) The Fiordland earthquake and tsunami, New Zealand, 21 August 2003. p. 31-42 In: Satake, K. (Ed.) Tsunamis : case studies and recent developments. Berlin: Springer Dordrecht. Advances in natural and technological hazards research 23.	Fiordland fault
Power, W.L. Downes, G.L. Stirling, M.W.	All New Zealand	(2007) Estimation of tsunami hazard in New Zealand due to South American earthquakes. Pure and applied geophysics, 164(2/3): 547-564; doi: 10.1007/s00024-006-0166-3.	South America
Fry, B. Bannister, S.C. Beavan, R.J. Bland, L. Bradley, B.A. Cox, S.C. Cousins, W.J. Gale, N.H. Hancox, G.T. Holden, C. Jongens, R. Power, W.L. Prasetya, G. Reyners, M.E. Ristau, J. Robinson, R. Samsonov, S. Wilson, K.J. GeoNet team	South Coast	(2010) The Mw 7.6 Dusky Sound earthquake of 2009: preliminary report. Bulletin of the New Zealand Society for Earthquake Engineering, 43(1): 24-40.	Dusky Sound

Author(s)	Location	Reference	Source
Uslu, B. Power, W.L. Greenslade, D. Eble, M. Titov, V.	South Coast	(2011) The July 15, 2009 Fiordland, New Zealand tsunami: real-time assessment. Pure and applied geophysics 168(11): 1963-1972.	Fiordland fault
Tolkova, E. Power, W.L.	Monterey Bay, Poverty Bay	(2011) Obtaining natural oscillatory modes of bays and harbors via Empirical Orthogonal Function analysis of tsunami wave fields. Ocean Dynamics, 61(6): 731-751, doi:10.1007/s10236-011-0388-5	Hikurangi margin, Distant sources
Prasetya, G. Beavan, R.J. Wang, X. Reyners, M.E. Power, W.L. Wilson, K.J. Lukovic, B.	South Coast	(2011)Evaluation of the 15 July 2009 Fiordland, New Zealand tsunami in the source region. Pure and applied geophysics 168(11): 1973-1987.	Fiordland fault
Power, W.L. Wallace, L.M. Wang, X. Reyners, M.E.	North Island	(2012) Tsunami hazard posed to New Zealand by the Kermadec and southern New Hebrides subduction margins: an assessment based on plate boundary kinematics, interseismic coupling, and historical seismicity. Pure and applied geophysics 169(1/2): 1-36.	Kermadec and southern New Hebrides subduction margins
Wang, X. Power, W.L. Bell, R.E. Downes, G.L. Holden, C.	Gisborne	(2009) Slow rupture of the March 1947 Gisborne earthquake suggested by tsunami modelling. p. 221 In: Barrell, D.J.A.; Tulloch, A.J. (Eds.) *Geological Society of New Zealand & New Zealand Geophysical Society Joint Annual Conference, Oamaru, 23-27 November 2009: programme and abstracts.* Wellington: Geological Society of New Zealand. Geological Society of New Zealand miscellaneous publication 128A.	Hikurangi margin
Prasetya, G. Wang, X. Palmer, N.G.	Tiwai Point	(2010) Tsunami inundation modelling for Tiwai Point. GNS Science consultancy report 2010/293, 75 p.	Subduction zone in Peru, Puysegur trench, Fiordland fault
Prasetya, G. Wang, X. Palmer, N.G. Grant, G.	Riverton	(2011) Tsunami inundation modelling for Riverton and New River Estuary Southland. GNS Science consultancy report 2011/150, 79 p.	Subduction zone in Peru, Puysegur trench, Fiordland fault

Author(s)	Location	Reference	Source
Prasetya, G. Wang, X.	Coromandel and Waikato Region	(2011) Tsunami frequency analysis for eastern Coromandel and Waikato Region from Kermadec Trench and local sources within the Bay of Plenty. GNS Science consultancy report 2011/135, 56 p.	Kermadec Trench and local sources within the Bay of Plenty
Prasetya, G. Wang, X.	Bay of Plenty	(2011) Review of tsunamigenic sources of the Bay of Plenty region. GNS Science consultancy report 2011/224, 65 p.	South America, Kermadec and Hikurangi margin, New Hebrides, local faults
Chague-Goff, C., Goff, J.	East Coast	(2007) East coast tsunami hazard study - Stage 1, NIWA Technical Report CHC2007-074.	All Sources
Goff, J. Walters, R. Callaghan, F.	Northland Region, Auckland Region, Waikato Region, Bay of Plenty Region	(2006) Tsunami Source Study. Environment Waikato Technical Report 2006/49 // NIWA Client Report: CHC2006-082.	South America, Solomon Islands, New Hebrides, Tonga-Kermadec Trench, Bay of Plenty local faults, submarine landslides
Chagué-Goff, C.; Goff, J.R.	Northland Region	(2006) Tsunami hazard assessment for the Northland region. NIWA Client Report CHC2006-069.	South America, Aleutian Islands, Tonga-Kermadec, Kuril Islands, Krakatau eruption
Lane, E. Walters, R.A. Arnold, J. Roulston, H.	Northland Region	(2007) Northland Regional Council Tsunami Modelling Study 1. NIWA Client Report: CHC2007-109. Report for Northland Regional Council. 88 pp.	South America (Peru/Chile), Tonga-Kermadec
Gillibrand, P Lane, E. Arnold, J et al.	Northland Region	(2008) Northland Regional Council Tsunami Modelling Study 2. NIWA Client Report: CHC 2008-115. Report for Northland Regional Council 111 pp.	South America (Peru/Chile), Tonga-Kermadec
Arnold, J. Carter, J. Dumas, J. Gillibrand, P	Northland Region	(2009) Northland Regional Council Tsunami Modelling Study 3, NIWA Client Report: CHC 2009-042. Report for Northland Regional Council, 116 pp.	South America (Peru/Chile), Tonga-Kermadec
Arnold, J. Gillibrand, P. Sykes, J	Northland Region	(2010) Northland Regional Council Numerical Modelling of Tsunami Inundation for Whangarei Harbour and Environs, NIWA Client Report: CHC 2010-133. Report for Northland Regional Council 80 pp.	South America (Peru/Chile), Tonga-Kermadec

Author(s)	Location	Reference	Source
De Lange, W.P.; Hansford, A.J. Moon, V.	North Island	(2006) Tsunami generation by island edifice failure at White Island and Motuhora Volcanos, New Zealand. Proceeding of New Zealand Geotechnical Society 2006 Symposium: Earthquakes and Urban Development.	White Island and Motuhora Volcanos
De Lange, W.P. Moon, V.	All New Zealand	(2005) New Zealand seismic tsunami hazard, Coastal News, No.33:.19-20.	Faults around New Zealand
Goff, J. Walters, R.	Auckland Region	(2005) Tsunamis in the Auckland region: Where? How big? How often? Coastal News, No.31: 6-7.	South America, Hikurangi-Kermadec
De Lange, W.P. McSaveney, E.	All New Zealand	(2007) Tsunamis - New Zealand's Underrated Hazard. In Life on the Edge - New Zealand's Natural Hazards and Disasters.	South America, Wairarapa fault, Hikurangi margin, volcanoes and landslides
de Lange, W.P. Moon, V.G.	Tawharanui Peninsula	(2007) Tsunami washover deposits, Tawharanui, New Zealand. Sedimentary Geology, 200 (3/4): 232-247.	Eruption from the submarine Mt Healy caldera
De Lange, W.P. Prasetya, G.S. Spiers, K.C. Moon, V.G.	Bay of Plenty	(2007) Palaeotsunami sources for the Bay of Plenty. Abstract of Geological Society of New Zealand & New Zealand Geophysical Society Joint Annual Conference, 2007	Palaeotsunami sources
Lane, E. Walters, R. Arnold, J. Enright, M. Roulston, H.	Auckland Region	(2009) Auckland Regional Council Tsunami Inundation Study. Prepared by National Institute of Water & Atmospheric Research Ltd for Auckland Regional Council. Auckland Regional Council Technical Report 2009/113	Peru 1868 Event (South America)
Goff, J. Walters, R. Lamarche, G. Wright, I. Chagué-Goff, C.	Auckland Region	(2005) Tsunami Overview Study. Auckland Regional Council Technical Publication No.280.	South America, Aleutian Islands, Kuril Islands, Solomon Islands, Kamchatka, Krakatau Volcano, Kermadec trench, Local sources inside Hauraki Gulf such as Hauraki graben and Rangitoto Volcano
Walters, R. Barnes, P. Goff, J.	Kaikoura coast	(2006) Locally generated tsunami along the Kaikoura coastal margin: Part 1. Fault ruptures, New Zealand Journal of Marine and Freshwater Research, 40(1): 1-16	Local faults in Kaikoura margin

Author(s)	Location	Reference	Source
Walters, R. Barnes, P. Lewis, K. Goff, J.R. leming, J.	Kaikoura coast	(2006) Locally generated tsunami along the Kaikoura coastal margin: Part 2. Submarine landslides, New Zealand Journal of Marine and Freshwater Research, 40:1, 17-28.	Landslide in Kaikoura Canyon
Walters; R. Goff; J. Wang, K.	Bay of Plenty	(2006) Tsunamigenic Sources in the Bay of Plenty, New Zealand. Science of Tsunami Hazards, Vol. 24(5): 339.	Local faults and landslides inside Bay of Plenty
Goff, J.R. Lane, E. Arnold, J.	Otago coastline	(2009) The tsunami geomorphology of coastal dunes. Nat. Hazards Earth Syst. Sci., 9, 847–854.	tsunami geomorphology,
Goff, J.R.	All New Zealand	(2008) The New Zealand palaeotsunami database, NIWA Technical Report 131, National Institute of Water & Atmospheric Research, Christchurch, New Zealand, ISBN 978-0-478-23280-6.	Palaeotsunami
Goff, J.R. Hicks, D.M. Hurren, H.	many coastal areas around New Zealand	(2006) Tsunami geomorphology in New Zealand, NIWA Technical Report No. 128, National Institute of Water & Atmospheric Research, Christchurch, New Zealand,	tsunami geomorphology,
Goff, J. Nichol, S. Kennedy, D..		(2010) Development of a palaeotsunami database for New Zealand. Natural Hazards 54: 193-208.	Palaeotsunami
Goff, J. Pearce, S. Nichol, S.L. Chagué-Goff, C. Horrocks, M. Strotz, L.	Kaituna Bay, Mimiwhangata	(2010) Multi-proxy records of regionally-sourced tsunamis, New Zealand. Geomorphology, 118(3/4): 369-382.	Palaeotsunami
McFadgen, B.G. Goff., J.R.	Wairau	(2007) Tsunamis in the New Zealand archaeological record. Sedimentary Geology, 200(3/4), Issues 3-4: 263-274.	archaeological record
Gillibrand, P. Power, W. Lane, E. Wang, X. Arnold, J.	Auckland Region	(2010) Probabilistic hazard analysis and modelling of tsunami inundation for the Auckland Region from regional Source Tsunami. NIWA/GNS-Joint Consultancy Report.	Kermadec subduction zone, New Hebrides subduction zone
Hayes; G.P. Furlong, K.P.	South Coast	(2010) Quantifying potential tsunami hazard in the Puysegur subduction zone, south of New Zealand. Geophysical Journal International, 183(3): 1512–1524.	Puysegur subduction zone

Author(s)	Location	Reference	Source
Power, W. Gale, N.	All New Zealand	(2011) Tsunami Forecasting and Monitoring in New Zealand. Pure Appl. Geophys. 168: 1125-1136.	Distant sources around Pacific, Solomon Islands, Tonga-Kermadec
Hayes, G.P. Furlong, K.P. Ammon, C.J.	South coast	(2009) Intraplate deformation adjacent to the Macquarie Ridge south of New Zealand—the tectonic evolution of a complex plate boundary, Tectonophysics, 463, 1-14. doi:10.1016/j.tecto.2008.09.024.	Macquarie Ridge
Kukowski; N. Greinert, J. Henrys, S.	East coast	(2010) Morphometric and critical taper analysis of the Rock Garden region, Hikurangi Margin, New Zealand: Implications for slope stability and potential tsunami generation. Marine Geology, 272(1-4): 141-153	Landslides in Rock Garden region of Hikurangi margin
Kennedy, D.M. Tannock, K.L. Crozier, M.J. Rieser, U.	Otago	(2007) Boulders of MIS 5 age deposited by a tsunami on the coast of Otago, New Zealand. Sedimentary Geology. Volume 200,(3/4): 222-231.	Palaeotsunami
Goff, J, Nichol, S. Chagué-Goff, C. Horrocks, M. McFadgen, B. Cisternas, M.	Chatham Island	(2010) Predecessor to New Zealand's largest historic trans-South Pacific tsunami of 1868 AD. Marine Geology. Volume 275(1-4): 155-165.	1868 South America event (Peru-Chile border)
Dykstra, J.L.	South coast	(2009) Landslide-Generated Tsunami Hazards in Fiordland, New Zealand and Norway. American Geophysical Union, Spring Meeting 2009, abstract CG11A-07.	Potential landslides in Fiordland
Cochran, U.A. Berryman, K.R. Mildenhall, D.C. Hayward, B.W. Southall, K. Hollis, C.J.	Northern Hawke's Bay	(2005) Towards a record of Holocene tsunami and storms for northern Hawke's Bay, New Zealand, New Zealand Journal of Geology and Geophysics, 48(3): 507-515.	Paleotsunami
Berryman, K. Ota, Y. Miyauchi, T. Hull, A. Clark, K. Ishibashi, K. Iso, N. Litchfield, N.	Wairarapa coast	(2011) Holocene Paleoseismic History of Upper-Plate Faults in the Southern Hikurangi Subduction Margin, New Zealand, Deduced from Marine Terrace Records. Bulletin of the Seismological Society of America 101(5): 2064-2087.	Paleotsunami

Author(s)	Location	Reference	Source
Leonard, G.S. Power, W. Lukovic, B. Smith, W. Johnston, D. Downes, G.	Wellington and Horizons regions	(2008) Interim tsunami evacuation planning zone boundary mapping for the Wellington and horizons regions defined by a GIS-calculated attenuation rule. GNS Science Report SR2008/30, Lower Hutt 18 pp.	Probabilistic tsunami height with a 500-year return period from regional and distant sources; Probabilistic tsunami height with a 2500-year return period from all sources;

APPENDIX 2: BOLIDE FREQUENCY AND MAGNITUDE

The flux of small near-Earth objects colliding with the Earth follows a power-law distribution (Brown et al., 2002). The cumulative number N of objects colliding with the Earth each year with diameters exceeding D is given by:

$$\log N = 1.57(\pm 0.03) - 2.70(\pm 0.08) \bullet \log D$$ **Equation A 2.1**

or in terms of energy, E (in kilotons):

$$\log N = 0.568(\pm 0.015) - 0.90(\pm 0.03) \bullet \log E$$ **Equation A 2.2**

(One kiloton TNT equivalent is 4.185 x 1012 Joules).

The flux is more-or-less uniformly distributed over Earth's surface, and so the proportion falling on any smaller area is approximately in direct proportion to the ratio of areas. The area within a 1000 km radius of Wellington is ~0.62% of the Earth's surface, and the area within a 3000 km radius is ~5.54% (we choose these two distances arbitrarily for the purpose of illustration). A larger bolide could cause a dangerous tsunami from a more distant ocean impact than a smaller bolide.

To estimate the potential of these bolides to generate tsunami, we use the relationship between kinetic energy, mass and velocity (E=½mv2), and assume that they transfer 50% of their energy to create a water wave (much water is heated and some is vaporised). Hence the mass of water (M kg) displaced is given by:

$$M = 4.185 \times 1012V\text{-}2 \bullet 100.63(\pm 0.04)\text{-}1.11(\pm 0.04)\log N$$ **Equation A 2.3**

In deep water, the wave speed (V) is ~200 m/s. It is unlikely that the efficiency of transfer of kinetic energy on impact with water is as great as 50%. A portion of the energy of the bolide is lost in its passage through the atmosphere; this is 100% for smaller than fist-sized bolides. Above a few tens of metres in diameter, energy is also consumed in forming a crater in the sea floor. Hence the estimation of the probability of displacement of a given volume of water is conservative with respect of public safety. Again to be conservative, we ignore the salt content of sea water to estimate the volume of displaced sea water (Figure A 2.1).

Within the probability horizon of our calculation of risk, out to a probability of once in a few thousand years, bolide-impact tsunami do not feature as a significant risk; they are lost in the background noise below other large and more probable events. But at longer event horizons, bolide tsunami are the largest tsunami waves that can hit large areas of the New Zealand coast. There is, however, a bolide size at which a tsunami is not the most significant effect of the collision. Such large events are not only conceivable, they are known to have occurred a number of times in Earth's history.

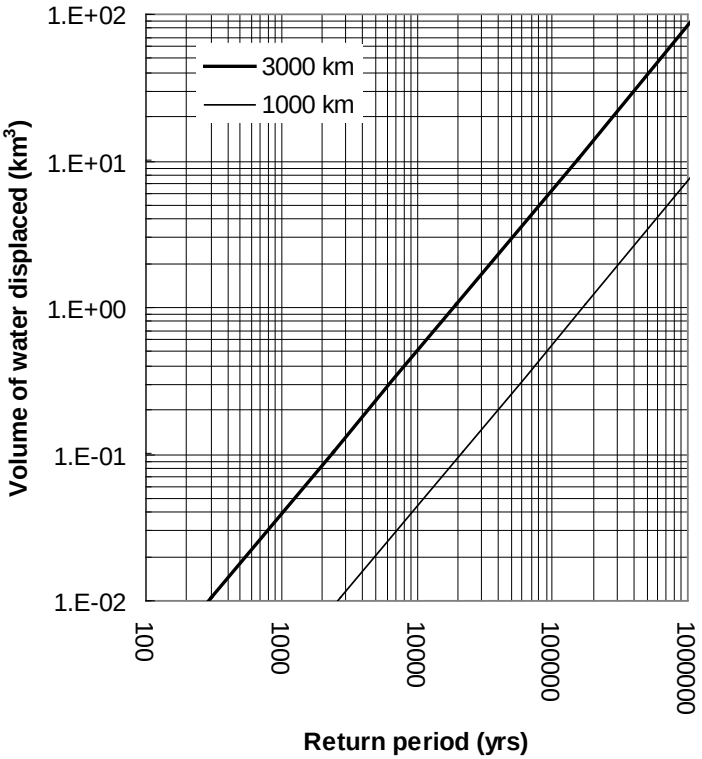

Figure A 2.1 Estimated volume of water displaced by a bolide hitting ocean within 1000 and within 3000 km of Wellington for various return periods. A displaced volume of less than 0.1 cubic kilometres is not likely to produce a damaging tsunami, and hence bolides are not a factor warranting concern in New Zealand's tsunami risk. In the rare event of a large Near Earth Object colliding with the Earth, a warning time of weeks to months is available with current technology.

Because all larger Near Earth Objects are identified and tracked, warnings can be issued. Hence, unlike any other tsunami, the possibility exists to know of the likelihood of generation of a specific bolide tsunami weeks or months in advance of the event.

APPENDIX 3: SUBDUCTION ZONE PARAMETERS, AS USED IN THE TSUNAMI SOURCE MODEL

Table A 3.1 Properties of subduction zone sources. Mmax is the maximum value of M_W, C is the coupling coefficient, and B-value is the Gutenberg-Richter B-value. Left and Right REL_VEL are the relative velocities between the converging plates in mm/yr at the two ends of the subduction zone. Width-pref is the preferred estimate of the subduction zone width in km. A worldwide upper limit on seismic moment of M_W 9.7 was assumed in the probabilistic model in Chapter 6 (this only affects those subduction zones where the tabulated Mmax-max is greater than 9.7). The B-value range was set to include the possibility that subduction plate-interfaces may have low b-values relative to the global B-value of 1 (Bayrak et al., 2002). Mmax-max is based on the assumption that the only ultimate constraint on the maximum magnitude is the length of the subduction zone (McCaffrey, 2007). Mmax-min is based on the magnitude of the largest known historical or paleo-tsunami.

Subduction Zone	Mmax – pref	Mmax – min	Mmax – max	C – pref	C – min	C – max	B-value – pref	B-value – min	B-value - max	Left_REL_VEL	Right_REL_VEL	Length (km)	Width – pref
Alaska	9.77	9.50	10.05	0.50	0.30	0.70	0.75	0.50	1.00	74.60	49.00	4130.00	116.00
Cascadia	9.00	8.80	9.20	0.80	0.70	0.90	0.75	0.50	1.00	47.80	32.70	1415.00	77.00
Japan	9.07	9.00	9.14	0.70	0.60	0.90	0.75	0.50	1.00	93.00	91.10	742.00	158.00
Kanto	8.22	8.00	8.43	0.90	0.80	1.00	0.75	0.50	1.00	36.00	34.10	312.00	77.00
Nankai	8.73	8.50	8.95	0.90	0.80	1.00	0.75	0.50	1.00	55.70	44.40	762.00	77.00
Kurile-Kamchatka	9.36	9.00	9.72	0.80	0.70	0.90	0.75	0.50	1.00	90.90	78.70	2223.00	131.00
Ryukyu	8.54	8.00	9.09	0.20	0.10	0.70	0.75	0.50	1.00	134.00	58.00	1440.00	35.00
Izu-Bonin	8.20	7.20	9.21	0.20	0.10	0.70	0.75	0.50	1.00	47.10	61.40	1128.00	85.00
Marianas	8.34	7.20	9.48	0.20	0.10	0.70	0.75	0.50	1.00	76.30	49.10	1822.00	85.00
North Yap	8.11	7.20	9.01	0.20	0.10	0.70	0.75	0.50	1.00	3.00	9.00	290.00	116.00
Palau-South Yap	8.04	7.20	8.88	0.20	0.10	0.70	0.75	0.50	1.00	1.60	7.10	554.00	116.00
Hikurangi	8.50	8.00	9.00	0.54	0.40	0.70	0.75	0.50	1.00	19.50	65.50	660.00	130.00
Kermadec	8.74	8.10	9.39	0.30	0.20	0.75	0.75	0.50	1.00	45.30	98.10	1627.00	77.00
Tonga	8.57	8.00	9.14	0.20	0.10	0.70	0.75	0.50	1.00	112.60	269.50	1125.00	68.00
Puysegur	8.43	7.80	9.07	0.70	0.50	0.80	0.75	0.50	1.00	36.60	29.90	834.00	97.00
Hjort	7.78	7.20	8.36	0.50	0.30	0.70	0.75	0.50	1.00	25.20	18.90	493.00	24.00
Solomon NW	8.36	8.10	8.62	0.70	0.60	0.80	0.75	0.50	1.00	91.10	107.00	465.00	66.00
Solomon SE	8.58	8.10	9.06	0.70	0.60	0.80	0.75	0.50	1.00	98.10	88.40	995.00	66.00
New Hebrides North	8.01	7.60	8.43	0.25	0.15	0.70	0.75	0.50	1.00	94.70	90.70	400.00	46.00

Subduction Zone	Mmax – pref	Mmax – min	Mmax – max	C – pref	C – min	C – max	B-value – pref	B-value – min	B-value - max	Left_REL_VEL	Right_REL_VEL	Length (km)	Width – pref
New Hebrides Central	8.49	8.30	8.69	0.70	0.60	0.80	0.75	0.50	1.00	33.70	102.30	500.00	72.00
New Hebrides South	8.11	7.60	8.62	0.25	0.15	0.70	0.75	0.50	1.00	102.30	174.90	560.00	46.00
New Hebrides Mat. Hunt.	8.40	8.00	8.49	0.25	0.15	0.70	0.75	0.50	1.00	49.10	45.80	463.00	43.00
New Britain	8.41	8.00	8.82	0.70	0.60	0.80	0.75	0.50	1.00	48.70	160.00	660.00	66.00
New Guinea Trench East	8.27	7.60	8.93	0.70	0.60	0.80	0.75	0.50	1.00	92.60	84.10	600.00	116.00
New Guinea Trench West	8.64	8.20	9.07	0.70	0.60	0.80	0.75	0.50	1.00	28.10	22.10	764.00	116.00
Manus East	8.30	7.50	9.10	0.50	0.30	0.70	0.75	0.50	1.00	10.00	6.90	809.00	116.00
Manus West	8.33	7.50	9.17	0.50	0.30	0.70	0.75	0.50	1.00	16.90	8.70	900.00	116.00
Esuador-Colombia	9.15	8.80	9.51	0.80	0.70	0.90	0.75	0.50	1.00	53.00	60.90	1329.00	174.00
Peru	9.43	9.00	9.87	0.80	0.70	0.90	0.75	0.50	1.00	70.00	63.90	2502.00	169.00
Northern Chile	9.04	8.60	9.48	0.80	0.70	0.90	0.75	0.50	1.00	79.50	80.50	1394.00	143.00
Central Chile	9.51	9.50	9.51	0.80	0.70	0.90	0.75	0.50	1.00	80.50	78.70	1301.00	183.00
Patagonia North	8.52	8.00	9.04	0.50	0.30	0.70	0.75	0.50	1.00	21.30	19.30	731.00	116.00
Potagonia South	8.74	8.00	9.49	0.50	0.30	0.70	0.75	0.50	1.00	15.10	10.80	1577.00	116.00
Mexico Jalisco	8.33	8.20	8.45	0.50	0.30	0.70	0.75	0.50	1.00	13.60	36.30	396.00	51.00
Mexico Michoa	8.58	8.00	9.17	0.70	0.50	0.90	0.75	0.50	1.00	44.00	78.80	1710.00	33.00
Central America ElSalv	8.29	8.00	8.58	0.30	0.10	0.70	0.75	0.50	1.00	71.30	80.00	546.00	42.00
Central America CoRica	8.22	7.70	8.74	0.50	0.30	0.70	0.75	0.50	1.00	70.80	79.10	533.00	77.00
Philippine	8.43	7.60	9.25	0.25	0.10	0.75	0.75	0.50	1.00	43.00	29.40	1633.00	47.00
East Luzon Trough	7.86	7.30	8.43	0.50	0.30	0.70	0.75	0.50	1.00	14.20	11.90	290.00	88.00
Cotabato Trench	8.21	8.00	8.42	0.50	0.30	0.70	0.75	0.50	1.00	18.80	18.20	250.00	116.00

References

Bayrak, Y., Yılmazturk, A., and Ozturk, S. (2002). Lateral variation of the modal (a/b) values for the different regions of the world, *J. Geodyn*., 34, 653–666.

McCaffrey, R. (2007). The Next Great Earthquake, *Science* 315: 1675-1676.

APPENDIX 4: CRUSTAL FAULT PARAMETERS, AS USED IN THE TSUNAMI SOURCE MODEL

Table A 4.1 Crustal faults properties. Fault Name and NZSHM_Number are as used in the National Seismic Hazard Model (Stirling et al., 2012). NZSHM_Number can be used to identify fault locations using the figures in Stirling et al. (2012). MWMN, MW, MWMX are minimum, preferred, and maximum moment magnitudes. RECINTMN, RECINT, RECINTMX are minimum, preferred and maximum recurrence intervals (in years).

FaultName	NZSHM_Number	MWMN	MW	MWMX	RECINTMN	RECINT	RECINTMX
Wairaka02	2	6.6	6.6	6.7	936	906	990
KerepehiO	3	7.2	7.2	7.3	18954	19860	22903
NgatoroS03	4	6.1	6.5	6.6	241	434	474
NgatoroS05	6	6.3	6.5	6.5	376	522	571
Ohena04	7	5.9	6.5	6.5	202	499	546
Ohena02	8	6.7	6.8	6.9	530	653	714
Ohena03	9	6.2	6.5	6.6	307	518	567
Wairaka05	13	6.4	6.8	6.9	626	1173	1283
AldermanE06	17	6.3	6.5	6.6	2177	2859	3014
Astrolabe07	24	6	6.7	6.8	234	693	730
Ohena01	27	6	6.6	6.6	1243	3467	3791
OtaraEast03	28	6.5	6.7	6.8	708	1026	1121
Astrolabe05	31	6.2	6.7	6.8	292	687	724
TaurTrE03	32	6	6.5	6.6	251	562	614
TaurTrE02	37	6.2	6.7	6.7	246	530	580
TuhuaN03	38	6.2	6.4	6.5	1277	1745	1840
TaurTrE01	40	6.2	6.5	6.6	238	388	424
OtaraEast04	41	6.4	6.4	6.5	853	825	902
AldermanW01	43	6.1	6.5	6.5	5960	10967	11563
Tuakana11	48	6.1	6.4	6.5	536	860	941
AldermanE02	49	6.1	6.4	6.5	1905	2996	3159
Tuakana10	54	6.1	6.6	6.6	514	1034	1131
TuhuaN01	55	6.3	6.6	6.7	1282	2162	2279
Wairaka01	56	6.6	6.6	6.7	3769	3647	3987
Tuakana05	58	6	6.7	6.7	381	1302	1423
OtaraEast02	61	6.4	6.4	6.5	317	307	336
Astrolabe02	62	6.1	6.7	6.7	795	1786	1884
OtaraWest02	68	5.9	6.6	6.6	188	517	565
AldermanE07	69	6.1	6.5	6.6	1890	4122	5704
Matatara04	72	6.1	6.8	6.8	892	2766	3025
Astrolabe01	73	6.1	6.6	6.6	941	2027	2138
MaungatiW02	74	6	6.5	6.5	646	1346	1471
Tuakana04	76	6.1	6.5	6.6	720	1547	1692
TuhuaS02	77	6.1	6.4	6.5	2072	3473	3662
Tuakana03	78	6.2	6.5	6.5	924	1310	1433
MaungatiW01	80	6.6	6.6	6.7	518	714	978
Tuakana02	81	6.3	6.6	6.7	754	1209	1321
WhiteIsN01	82	6.5	6.5	6.6	9182	8884	9714
KerepehiN	83	6.7	6.8	6.8	8521	8928	10296

FaultName	NZSHM_Number	MWMN	MW	MWMX	RECINTMN	RECINT	RECINTMX
Volkner04	86	6.1	6.7	6.7	124	351	384
Matatara03	87	6.1	6.5	6.6	520	992	1084
TeArawa03	88	6.4	6.4	6.5	222	268	367
Volkner03	96	6.1	6.5	6.6	230	459	502
Tauranga05	98	6.1	6.6	6.7	491	1123	1227
Tumokemoke02	99	6.4	6.5	6.5	773	842	921
Maketu02	106	5.9	6.5	6.6	592	1756	2286
Okurei02	107	6	6.7	6.7	1895	5466	5586
Tumokemoke01	108	6.2	6.5	6.6	527	886	969
Maketu03	110	6.1	6.4	6.5	2805	4335	4430
Okurei01	112	6.5	6.6	6.7	2361	2868	2932
Volkner01	113	6.6	6.6	6.6	865	837	915
Tauranga03	114	6.3	6.6	6.6	718	1000	1006
Maketu01	120	6.4	6.4	6.5	1284	1285	1318
Pokare02	126	6.1	6.5	6.6	473	1207	1881
Nukuhou01	127	6.1	6.5	6.5	649	1104	1056
RaukumaraF22	129	7	7.2	7.3	24445	27161	59754
Tarawera05	130	6	6.5	6.6	785	1865	1911
Ohae01	135	6.9	7	7.1	19760	26347	43472
Opotiki03	136	6.6	7	7.1	2582	7773	25650
Tarawera03	137	6.2	6.5	6.6	1434	2351	2410
Moutoki02	139	6.3	6.6	6.6	1681	2571	3163
Tokata01	140	6	6.4	6.5	418	1014	1974
RaukumaraF23	142	6.5	6.6	6.7	120000	125000	130000
Pokare01	145	6	6.6	6.6	445	1273	1984
WhiteIs01	146	6.6	6.7	6.8	602	879	1262
Tarawera01	147	6.3	6.5	6.6	975	1314	1346
Moutoki01	149	6.2	6.6	6.6	1413	2589	3184
Wkm-1	150	6.6	6.6	6.7	423	454	766
Ohae02	151	6.8	6.9	7	16892	22522	37162
RaukumaraF15	155	6.9	7	7.2	9500	10000	10500
RaukumaraF21	156	6.5	6.6	6.7	28205	41786	13789354
WhakataneN	158	7.4	7.5	7.6	1516	2374	4420
Opotiki02	161	5.9	6.5	6.6	810	3372	11127
Urewera3	162	7.2	7.3	7.4	4925	7661	14045
Matata	163	6.6	6.7	6.8	497	812	829
RaukumaraF13	164	6.7	6.8	7	3134	3482	19152
Waikaremoana	165	7.4	7.5	7.6	6716	10446	19152
WaimanaN	166	7.4	7.5	7.6	6805	10586	19407
RaukumaraF19	167	6.6	6.7	6.8	31339	46429	15321505
RaukumaraF18	168	6.6	6.7	6.8	10000	67500	125000
RaukumaraF17	170	6.3	6.4	6.5	10000	67500	125000
Houtunui	175	7.1	7.2	7.4	1671	2786	6129
RuatoriaS2	180	6.7	7	7.2	1003	1857	6129
RuatoriaS1	182	7	7.3	7.5	1805	3343	11031
ArielBank	202	7.3	7.4	7.6	449	723	1087

FaultName	NZSHM_Number	MWMN	MW	MWMX	RECINTMN	RECINT	RECINTMX
GableEnd	206	7.1	7.2	7.4	386	763	1502
ArielNorth	207	6.7	6.8	7	766	1641	4304
TuriN	208	6.7	6.8	6.8	3698	3154	10518
WhakataneS	213	7.2	7.3	7.4	1092	1709	3182
TuriC	224	6.8	6.8	6.9	4189	3573	11913
PovertyBay	225	6.4	6.5	6.7	150	358	1408
ArielEast	227	6.4	6.6	6.8	334	716	1878
TuaheniR	228	6.2	6.5	6.7	710	1184	2605
TuriS	230	6.7	6.8	6.8	3698	3154	10518
Lachlan3	231	7.3	7.5	7.7	665	1068	2114
ParituW	238	6.2	6.5	6.7	710	1184	2605
HawkeBay4	241	6.5	6.6	6.8	2037	3018	9959
Napier1931	242	7.4	7.6	7.7	1692	2821	6205
HawkeBay7	245	6.4	6.5	6.7	3761	8357	9193
ParituR	247	6.6	6.9	7.1	815	1358	2988
HawkeBay5&11	248	6.5	6.7	6.9	2350	3482	5746
Mahia2	249	6.5	6.7	6.9	1985	3308	7278
HawkeBay6&12	250	6.4	6.6	6.7	3761	8357	9193
RitchieR	257	6.9	7.1	7.3	1429	2646	8733
HawkeBay1	258	6.6	6.7	6.9	1332	2368	6512
HawkeBay2	260	7	7.1	7.3	1639	2960	8682
CEgmontN	262	6.7	6.8	6.9	1577	1682	1869
KidnappersR	263	7.3	7.4	7.6	1755	2600	4290
RitchieW1	266	7.3	7.5	7.7	3761	6268	13789
Lachlan1&2	269	7	7.2	7.4	752	1170	2145
RitchieW2	277	6.8	7	7.2	903	1671	5516
CEgmontC	278	6.7	6.8	6.8	1479	1577	1753
WaverOkaia1	281	6.9	7	7.1	29755	40988	73293
MotuokuraN	282	7	7.1	7.3	1630	2716	5975
MoumahOkaia4	284	6.9	6.9	7	8565	7866	26724
RidgeROkaia2	285	6.9	7	7.1	59509	81977	146586
Waitot1011	288	7	7.1	7.1	8088	9285	23718
Waimarama3&4	289	6.6	6.8	6.9	752	1254	2758
PaoanuiRN	291	7.1	7.3	7.5	2800	4666	10265
NukWaitot1to6	292	7	7.1	7.1	15251	26011	162788
MotuokuraE	293	7.3	7.5	7.7	1609	2681	5899
Waimarama1&2	294	6.3	6.5	6.6	460	766	1685
KairakauN	295	6.8	6.9	7.1	1003	1671	3677
CegmontS	296	6.5	6.6	6.6	7244	9267	15450
Kairakau2	297	6.7	6.8	7	878	1463	3218
Waitot8to9	298	7	7	7.1	2466	3798	9072
Okaia5	300	6.6	6.6	6.7	18593	29825	85484
KairakauS	303	7	7.1	7.3	533	789	1302
MotuokuraR	312	7	7.1	7.3	1222	1811	2988
Rangioffsh	315	7.1	7.2	7.3	2758	3830	8427
Madden	316	7.5	7.6	7.8	1540	2396	4392
Mascarin	317	7.3	7.4	7.5	1110	1439	3166

FaultName	NZSHM_Number	MWMN	MW	MWMX	RECINTMN	RECINT	RECINTMX
OmakereR	318	7	7.2	7.4	2215	3691	8120
PoranagR	320	7.1	7.2	7.4	2424	4039	8886
Onepoto	322	7.3	7.4	7.5	3604	4805	8810
OmakereS	323	6.8	7	7.1	2865	4457	8171
PaoanuiRS	325	7	7.2	7.4	2173	3621	7967
Fisherman	331	7.4	7.5	7.6	4126	5502	10087
Mataikona	335	7.2	7.3	7.5	614	853	1251
Manaota	336	7.5	7.6	7.7	14259	21125	34856
PoranagW1	338	7	7.2	7.4	1922	3204	7048
PoranagW2	339	6.8	7	7.1	852	1579	5209
Okupe	344	7.3	7.4	7.5	3886	5397	11874
WairarapNich	345	7.9	8.2	8.3	785	1199	1851
Riversdale	351	7.1	7.2	7.4	527	731	1073
UrutiE	354	6.9	7.1	7.3	1755	2925	6435
UrutiN	356	6.7	6.9	7.1	1003	1671	3677
KekNeed	360	7.3	7.4	7.6	1463	2438	5363
UrutiR2	363	6.5	6.7	6.9	439	731	1609
DryHuang	366	7.1	7.3	7.4	2946	4676	9001
Wharekauhau	367	7.2	7.3	7.5	913	1421	2605
Otaraia	368	7	7.1	7.2	10969	16250	26813
UrutiBasin	369	7.1	7.2	7.3	558	853	1502
WhareamaBank	370	7.3	7.5	7.7	1655	3064	10112
OpouaweUruti	371	7.7	7.8	8	3560	6593	21757
PalliserKai	372	7.5	7.6	7.8	716	1114	2043
JorKekCha	373	7.4	7.6	7.8	1410	2089	3447
JorKekNeed	374	7.4	7.6	7.8	313	389	455
Honeycomb	375	7	7.1	7.3	1504	2507	5516
Pahaua	377	7.7	7.9	8	3660	6779	22369
AwatNEVerCl	379	7.6	7.7	7.8	2528	4213	9270
AwatNEVer	380	7.6	7.7	7.8	2486	4604	9116
WharaToCampB	385	7	7.2	7.4	655	1091	1964
HopeTeRapa1n2	389	7.3	7.4	7.6	802	1254	2006
KekerenguBF	390	7.4	7.6	7.8	3265	6122	14692
UpperSlope	391	7	7.2	7.4	1553	2911	6987
MS05	399	6.7	6.8	7	5571	13393	208930
MS04	400	7.1	7.3	7.5	6351	13232	47636
MS01	402	6.8	7	7.2	3789	9471	28414427
Hundalee	405	7.1	7.3	7.4	1444	3076	10150
MS02	406	6.3	6.5	6.6	527	1163	5934
NorthCant13	408	6.7	6.9	7.1	2953	7382	2214654
NorthCant10	412	6.6	6.8	7	403	756	1814
NMFZM	413	7.1	7.3	7.5	13642	27283	81850
MS09	415	6.4	6.5	6.7	1683	3756	25239
NMFZK1	416	7.2	7.4	7.6	10188	20731	66857
NMFZ1819	418	6.9	7.1	7.3	14597	34212	328437
NMFZK2	423	6.8	7	7.2	4776	9718	31339
NorthCant8	426	6.9	7.1	7.3	5376	10753	32259

FaultName	NZSHM_Number	MWMN	MW	MWMX	RECINTMN	RECINT	RECINTMX
NMFZF1	427	6.8	7	7.2	4776	9286	25072
NMFZB0	429	7	7.2	7.4	25796	32245	55277
NMFZ4647	430	7	7.2	7.4	7540	17672	169651
NMFZE1	431	7	7.2	7.4	4569	10982	171322
NMFZE2	433	6.9	7.1	7.3	3900	9375	146251
NMFZF2	434	6.9	7.1	7.2	5412	10524	28414
NorthCant11	438	6.4	6.5	6.7	1560	3250	11700
NMFZB1	439	6.6	6.8	7	11477	14347	24594
NMFZB2	443	7.1	7.3	7.5	27913	34891	59814
NorthCant2	444	6.5	6.7	6.9	5321	9501	19953
NorthCant4	445	6.2	6.4	6.6	4364	8183	19639
NorthCant1	448	6.6	6.8	7	6407	12814	38443
Pegasus1nw	449	6.8	7	7.2	6110	9165	13748
MilfordB1	469	7.4	7.6	7.8	765	1416	4673
Swedge6to10	474	7.1	7.3	7.6	529	882	1941
MilB5GeoR2	475	7.8	7.9	8	15461	25768	56690
CaswellH8	476	7	7.1	7.2	2051	3582	9193
CaswellH10	480	6.8	6.9	7	1302	2350	6895
CaswellH9	481	6.6	6.8	6.9	998	1802	5286
GeorgeR1	482	7.9	8.1	8.4	3836	7104	23442
FiordMar1&2	489	7.1	7.2	7.3	56411	62679	68947
CaswellH67	490	7.1	7.2	7.4	2300	4152	12181
Cwedge123	491	7	7.2	7.4	3029	5049	11108
Swedge5	492	7.5	7.7	7.9	1017	1695	3728
Cw4Swedge411	497	7.3	7.5	7.8	752	1254	2758
Caswell5	498	7.1	7.2	7.3	3064	6129	33707
Swedge2	499	7.2	7.4	7.7	577	1068	3524
Caswell4	503	7.1	7.3	7.4	2849	4975	12768
Swedge3	508	7	7.1	7.4	390	650	1430
Swedge1	510	7	7.2	7.4	2159	4318	23748
SFiordMg13	511	7	7.1	7.2	878	1463	3218
Caswell3	513	6.7	6.9	7	1425	2487	6384
Caswell1	517	7.4	7.5	7.6	4331	7561	19407
Caswell211	521	6.8	7	7.1	1652	2885	7405
Chalky4to8	522	6.8	6.9	7	1170	1950	4290
SFiordMg1to9	523	6.6	6.6	6.7	1033	1762	8157
FiveFingers	526	6.9	7	7.1	4137	7661	25280
Chalky1to3	530	6.7	6.8	7	3009	5571	18386
Akatore	531	7.3	7.4	7.6	1852	3482	7114
HumpR	532	7.5	7.6	7.7	37942	63236	139119
Hauroko	533	7.5	7.6	7.7	1943	3238	7124
Solander	534	7.1	7.2	7.3	19096	31827	70019
Settlement	535	6.7	6.8	7	2403	4004	8810
CBalleny	536	7.3	7.4	7.5	699	932	1281

This page is intentionally left blank.

APPENDIX 5: TENTATIVELY IDENTIFIED LOCAL FAULTS

A5.1 OUTER RISE FAULTS

Earthquakes on Outer Rise faults were proposed as tsunami sources affecting the Raukumara Peninsula in an EQC report by Power et al. (2008) and commercial studies for Gisborne District Council. These posited a fault capable of earthquakes of M_W ~8.0, sited close to the trench, with an estimated recurrence interval of ~1300 years. Subsequently it has been argued that for such a large slip rate, there should be faults evident in the bathymetry; for this reason the estimated characteristic magnitude was reduced here to M_W 7.8, halving the slip rate. It is suggested here that similar sources may exist along the length of the Hikurangi Trench, but with recurrence intervals that lengthen to the south. These important tsunami sources warrant further study.

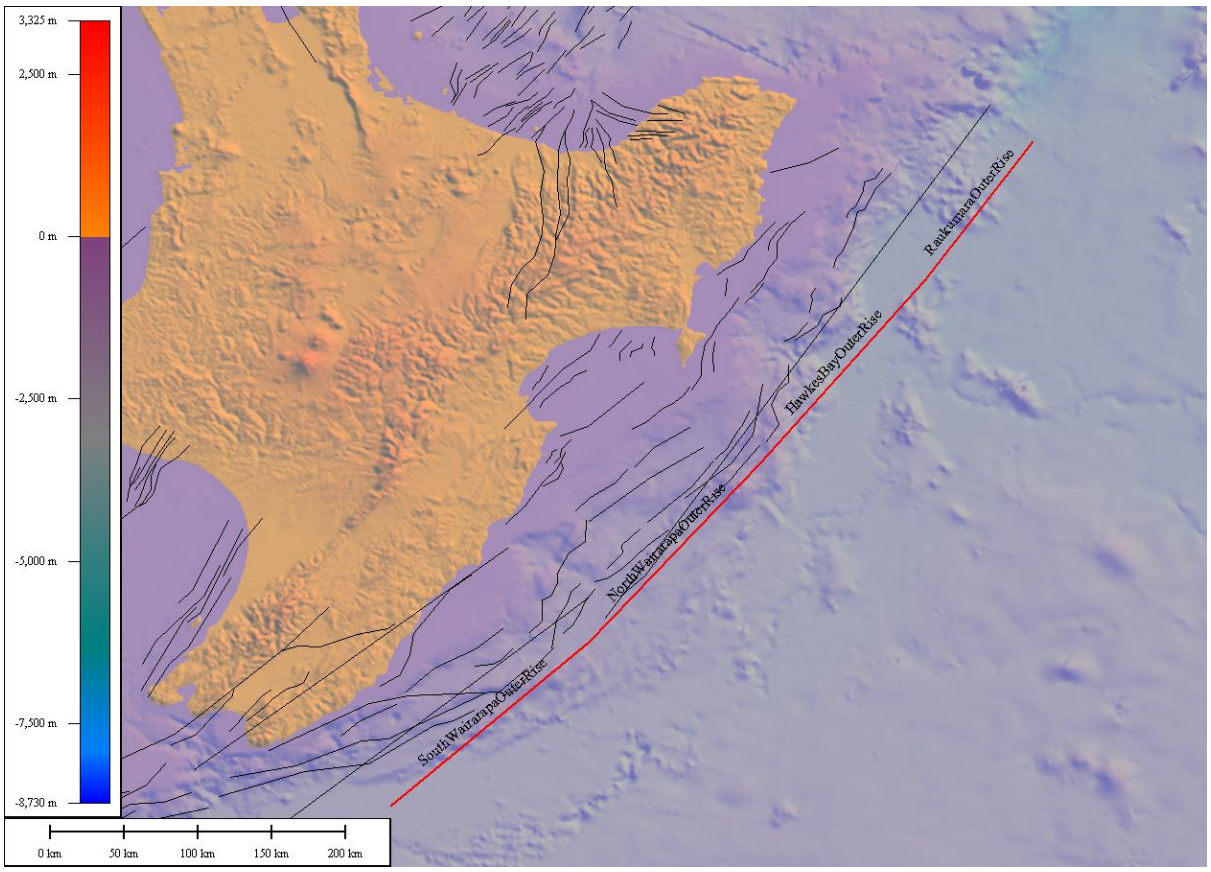

Figure A 5.1 Assumed location of Hikurangi Outer Rise faults as used for this study.

Table A 5.1 Assumed Hikurangi Outer Rise fault properties. Type 'Nn' implies a normal fault mechanism, SR is short for Slip Rate.

Name	Type	Length (km)	Dip	Dip direction	Depth	M_W	Recurrence Interval (years)	SR (mm/yr)
Raukumara Outer Rise	Nn	150	58°	301°	25	7.8	1300	3.5
HawkesBay Outer Rise	Nn	150	58°	305°	25	7.8	1460	3.15
North Wairarapa Outer Rise	Nn	150	58°	305°	25	7.8	1640	2.85
South Wairarapa Outer Rise	Nn	150	58°	311°	25	7.8	1900	2.5

A5.2 TARANAKI BASIN FAULTS

The following faults in the Taranaki Basin are believed to exist and are probably active, but with long recurrence intervals. Parameters are highly uncertain, and most are estimated by extrapolation from properties of onshore faults. The Cape Egmont Fault is already present in the National Seismic Hazard Model, but a non-segmented model was added to indicate the possibility of a larger rupture.

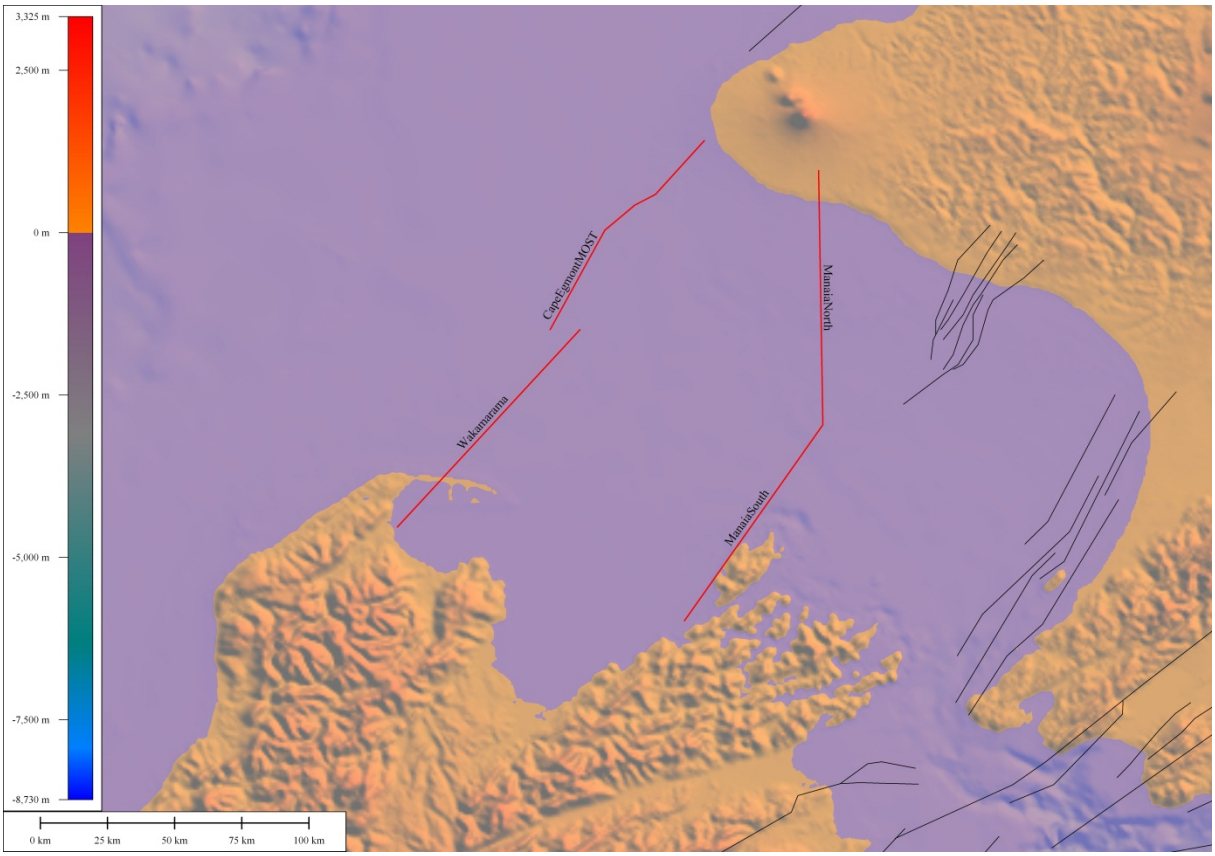

Figure A 5.2 Assumed locations of tentatively identified Taranaki Basin faults.

Table A 5.2 Assumed Taranaki Basin fault properties. Type 'nn' implies a normal fault mechanism, 'rv' a reverse mechanism, 'rs' is combined reverse and strike-slip. SR is short for Slip Rate.

Name	Type	Length (km)	Dip	Dip direction	Depth	M_W	Recurrence Interval (years)	SR (mm/yr)
ManaiaSouth	Rs	83	90°	120°	12	7.2	12000	0.2
ManaiaNorth	Rs	95	90°	90°	12	-	Inactive	Inactive
Wakamarama	Rv	90	45°	305°	12	7.6	30000	0.2
CapeEgmont MOST	Nn	85	60°	295°	12	7.6	20000 (3000)	0.4 (1)

(Numbers in brackets are recurrence interval and slip rate for all ruptures on Cape Egmont Fault. The tsunami hazard model uses only the unbracketed numbers for multi-segment ruptures)

A5.3 OFFSHORE WEST COAST FAULTS

The following faults were tentatively added; they are assumed to accommodate a portion of the dip-slip component of movement along the plate boundary convergence. The Alpine Fault accommodates the strike-slip movement and some portion of the dip slip. Indirect evidence for these faults comes from marine terraces along the West Coast.

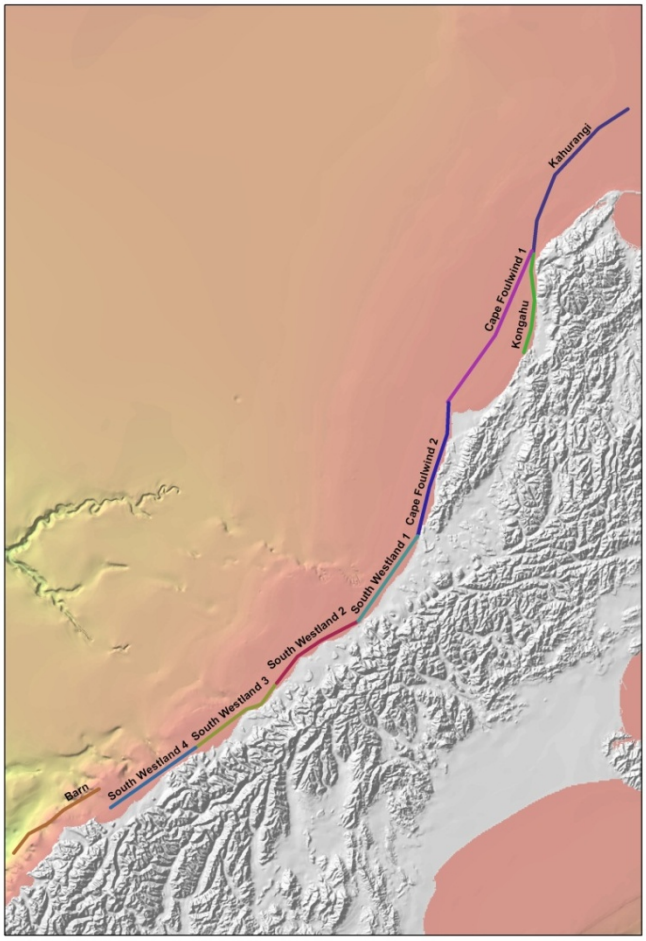

Figure A 5.3 Assumed locations of west coast South Island faults.

Table A 5.3 Assumed west coast South Island fault properties. Type 'rv' implies a reverse fault mechanism, SR is short for Slip Rate

Name	Type	Length (km)	Dip	Dip direction	Depth	M_W	Recurrence Interval (years)	SR (mm/yr)
Barn	Rv	68	25°	143°	15	7.6	2400	2
SouthWestland1	Rv	65	25°	150°	15	7.6	4900	1
SouthWestland2	Rv	65	25°	140°	15	7.6	4900	1
SouthWestland3	Rv	67	25°	143°	15	7.6	4900	1
SouthWestland4	Rv	65	25°	126°	15	7.6	9700	0.5
CapeFoulwind1	Rv	109	25°	105°	15	7.6	9700	0.5
CapeFoulwind2	Rv	86	25°	139°	15	7.6	9700	0.5
Kongahu	Rv	63	25°	93°	15	7.6	15000	0.3
Kahurangi	Rv	112	25°	138°	15	7.6	15000	0.3

APPENDIX 6: A PROBABILISTIC METHODOLOGY FOR ESTIMATING HAZARD FROM TSUNAMI GENERATED BY SUBMARINE LANDSLIDES

Central New Zealand (the Cook Strait-Wellington area) was identified as a priority area to quantify landslide-generated tsunami hazard in the 2005 *Review of Tsunami Hazard and Risk in New Zealand* (IGNS client report 2005/104). Funding through the Natural Hazards Research Platform enabled preliminary work on this problem to be undertaken (Power et al., 2011), and has subsequently funded the second phase of the project with the objective of determining the probabilistic hazard from landslide tsunami to the Wellington region. This second phase of the project was initiated in mid-2012. The results of the first phase of work are summarised below.

Landslides are documented as widespread in the Cook Strait Canyon area (Mountjoy et al., 2009; Micallef et al., 2012). Analysis of landslide morphology demonstrates that the majority of landslides have some dependence on canyon incision. Several landslides are perched on the canyon walls and are likely to have resulted solely from the action of earthquake ground motion. It is inferred that the mapped population of landslides is representative of failures during earthquakes, with the majority of landslides affected by canyon erosion of the lower slope. This enables a model for landslide triggering to be developed based on return intervals for earthquake ground motion using the National Probabilistic Seismic Hazard Model (Stirling et al., 2012).

A model workflow has been developed in ArcGIS that uses pseudo-static slope-stability equations to determine the level of strong ground motion required to trigger failure, using data points on a 1 km grid across the canyon system. The result is compared with the time-varying levels of ground motion expected from the national Probabilistic Seismic Hazard Model to determine the time interval over which slopes within the canyon system can be expected to fail. The model is verified against commercial slope stability modelling software, and will underpin future probabilistic assessments of landslide-tsunami hazard.

The numerical hydrodynamic code Gerris has been adapted to model submarine landslides as tsunami sources (Popinet et al., 2011). The 2D vertical slice model has been validated against benchmark tests and demonstrates satisfactory performance with published laboratory-based benchmarks. Landslide scenarios have been modelled for Cook Strait Canyon based on evidence from previous slope failures of the canyon walls. These scenarios have been modelled in 2D and 3D using techniques from published code (TOPICS), as well as the newly developed code, to determine the most effective and realistic method of modelling landslide-tsunami sources. The effects of the generated waves on the coast have been modelled to assess whether a hazard exists from these landslide-generated tsunami. The results demonstrate the existence of a landslide-tsunami hazard to the Wellington/South Wairarapa coastal region. Modelling results indicate that initialisation of the tsunami over complex submarine topography (e.g., submarine canyons versus simple open slopes) can have significant influence on where tsunami energy is guided and focussed. The results demonstrate that the characteristics of the generated tsunami waves are not, however, particularly sensitive to incremental changes in the density or volume of the landslides.

Landslide-generated tsunami cannot be incorporated into the New Zealand hazard and risk model at this stage. However, development of a probabilistic tsunami hazard assessment is in progress and is planned for completion in 2014. The probabilistic landslide-tsunami model

will be based on a landslide-initiation model incorporating return times for varying levels of earthquake-generated ground motions. From this a synthetic catalogue of landslide-triggered tsunami events will be used to assess the probabilistic hazard from landslide tsunami to coastal areas of the Wellington region. This model is being developed as a workflow that can be applied to other regions of New Zealand to assess landslide-generated tsunami hazard. The model will be able to be incorporated with the tectonic-source tsunami model to assess the complete tsunami hazard to New Zealand coastal areas.

A6.1 REFERENCES

Micallef, A.; Mountjoy, J.J.; Canals, M.; Lastras, G. (2012). Deep-Seated Bedrock Landslides and Submarine Canyon Evolution in an Active Tectonic Margin: Cook Strait, New Zealand. In *Submarine Mass Movements and Their Consequences*, Advances in Natural and Technological Hazards Research 31, Springer, 201-212.

Mountjoy, J.J.; Barnes, P.M.; Pettinga, J.R. (2009). Morphostructure and evolution of submarine canyons across an active margin: Cook Strait sector of the Hikurangi Margin, New Zealand. *Marine Geology* 260(1-4), 45-68.

Power, W., et al. (2011) Towards a probabilistic landslide tsunami model for New Zealand. Unpublished project completion report to the Natural Hazards Research Platform contract CS GNS 25.

Stirling, M.W.; McVerry, G.; Gerstenberger, M.; Litchfield, N.; Van Dissen, R.; Berryman, K.; Barnes, P.; Beavan, J.; Bradley, B.; Clark, K.; Jacobs, K.; Lamarche, G.; Langridge, R.; Nicol, A.; Nodder, S.; Pettinga, J.; Reyners, M.; Rhoades, D.; Smith, W.; Villamor, P.; Wallace, L. (2012). National seismic hazard model for New Zealand: 2010 update. *Bulletin of the Seismological Society of America* 102(4), 1514-1542.

Popinet, S. et al. (2011). Gerris – Landslide-generated tsunamis. http://gfs.sourceforge.net/wiki/index.php/Landslide-generated_tsunamis.

APPENDIX 7: ADDITIONAL HAZARD MODEL INFORMATION

This appendix provides additional information on parameters and assumptions used in the tsunami hazard model.

A7.1 SUMMARY TABLE OF UNCERTAINTIES AND VARIABILITIES

The treatment of uncertainty and variability in the tsunami hazard model is quite complicated. Table A 7.1 was constructed to provide a quick summary and pointers to further information.

Table A 7.1 Summary table of uncertainties and variabilities.

	Uncertainties	**Variabilities**
Earthquake Magnitude-Frequency	Subduction zones: Maximum magnitudes, B values, coupling coefficients Crustal Faults: Characteristic magnitudes, recurrence intervals Section 6.4; Appendix 7.2	Sequence of earthquake moment magnitudes (M_W) Section 6.4; Appendix 7.2
Earthquake locations within source regions		Local subduction zones: source location Regional and Distant Subduction zones: effect of varying location is represented in σB Appendix 7.4
Geophysical properties at tsunami source	Uncertain fault geometry (e.g. dip and strike angles), uncertain material properties (e.g. rigidity). Section 6.5; Appendix 7.3	Non-uniform slip distribution, variations in rupture dimensions. Section 6.5; Appendix 7.3
Tsunami Modelling	Unknown biases in tsunami models. For crustal faults: uncertainty in equivalence of maximum 'tsunami height'. Uncertainty/errors in bathymetric data. Appendix 7.3	

A7.2 GENERATION OF SYNTHETIC CATALOGUES

Sampling of epistemic uncertainty in Magnitude-Frequency distributions

Epistemic uncertainty in the characteristic magnitudes of local crustal faults from the New Zealand Seismic Hazard Model (NZSHM) is modelled as normally distributed with a standard deviation of 0.1 magnitude units (M_W), and the adjusted characteristic magnitude is truncated to lie between the minimum and maximum moment magnitudes MWMN and MWMX, as specified in Appendix 4.

Epistemic uncertainty in the characteristic magnitudes of tentatively identified local crustal faults (Appendix 5) is modelled as normally distributed with a standard deviation of 0.2 and truncated at ±0.4 magnitude units.

Epistemic uncertainty in the magnitude-frequency distribution of subduction zone tsunami sources is represented by sampling from the parameters in Table A 3.1. A uniform random distribution is assumed between the minimum and maximum tabulated values. The sampled values of Mmax and B-value enter directly into the equation for a truncated Guttenberg-Richter distribution. The other parameters are used to determine the A-value via a process of balancing the overall seismic moment release rate.

Variability in the magnitude of earthquakes

Variability in the magnitudes of earthquakes on local crustal faults is modelled as normally distributed with a standard deviation of 0.1 magnitude units, and the sampled magnitude is truncated to lie between minimum and maximum moment magnitudes MWMN and MWMX as specified in Appendix 4. In the NZSHM earthquakes with magnitudes below MWMN are regarded as part of the background seismicity, here it is assumed that earthquakes below MWMN make a negligible contribution to the tsunami hazard.

Variability in the magnitudes of earthquakes on tentatively identified local crustal faults (Appendix 5) is modelled as normally distributed with standard deviation of 0.1 magnitude units, and the sampled magnitude is truncated to lie within ±0.4 magnitude units of the corresponding tabulated characteristic magnitude in Appendix 5.

Variability in the magnitudes of earthquakes on subduction zones is modelled by random sampling from a truncated Gutenberg-Richter (GR) distribution, parameterised by A-value, B-Value and Maximum magnitude as described in the previous section. The truncation of the GR distribution is implemented as a sharp truncation in the incremental GR distribution, which leads to a gentle tapering off in the cumulative distribution (see Chapter 3 of McGuire, 2004). Note that this may not be a good representation of subduction zones like Cascadia (Section 5.1.1.3) that experience low seismicity in the intervals between large (M_W>8) earthquakes, many of which are whole-margin events.

Global maximum magnitude cut-off

In epistemic sampling of the maximum magnitude of subduction zone tsunami sources, a global upper bound on Mmax is set at M_W 9.7, slightly larger than the largest historically observed earthquake globally. This global cut-off only affects those subduction zones where Mmax-max is greater than 9.7 in Table A 3.1 (Alaska, Peru, Kuril-Kamchatka).

Minimum magnitudes for subduction zone earthquakes

In constructing the synthetic catalogues of subduction zone earthquakes we do not consider earthquakes of less than the following thresholds:

Distant earthquakes, M_W 8.5

Regional earthquakes, M_W 8.0

Local earthquakes, M_W 7.5

Below these magnitudes it is assumed that the tsunami generated are too small to significantly influence the tsunami hazard curves.

A7.3 EXPLANATION AND DERIVATION OF COEFFICIENTS DESCRIBING VARIABILITY AND UNCERTAINTY USING AN 'EFFECTIVE MAGNITUDE' APPROACH

There are several areas of uncertainty and variability that ought to be included in a tsunami hazard analysis. A complete Monte-Carlo analysis of all factors for all sources would be computationally very demanding, as well as challenging to construct. The approach taken here, which is original to this report, is to approximate the effects of these variables through an 'effective magnitude'. The idea is that variations and uncertianties in the parameters that control tsunami generation have an effect on reducing or enhancing the tsunami height which, from the point of view of an observer at one section of the coast, are approximately equivalent to an increase or decrease in the magnitude of the source earthquake relative to a baseline model.

The parameters used for this uncertainty/variability modelling are tabulated in Table A7.2. The parameters describe the standard deviations of (zero-mean) normally distributed random variables that are added to the synthetic earthquake catalogue magnitudes. The interpretation and assumed values of these parameters will be described below. It is useful to know that, when using Abe's (1979,1995) equations to estimate tsunami heights, a 0.1 increase in 'effective magnitude' is equivalent to an increase in tsunami height of 26%, a 0.2 increase is equivalent to 58%, and a 0.3 increase is equivalent to 100% (i.e., a doubling in height).

Table A 7.2 Standard deviations associated with stochastic adjustments to the synthetic catalogue to create a catalogue of 'effective magnitudes'. The fault-specific uncertainty covers uncertainties that are specific to the modelling of each fault, while the method bias covers uncertainties that cause a systematic bias across all faults. Units are in the M_W scale.

	Local Crust Fault (empirical model)	**Local Subduction Zone (numerical model)**	**Distant Subduction Zone (numerical model)**
Variability (e.g. non-uniform slip) σ_v	0.25	0.25	0.1
Modelling uncertainty (fault specific) σ_u	0.2	0.1	0.1
Modelling uncertainty (method bias) σ_b	0.14	0.05	0.05

The application of these parameters, which describe the uncertainties and variabilities that affect tsunami heights, by using them to estimate an 'effective magnitude' can be described as follows:

$$Mw_{ijk}(effective) = Mw_{ijk} + \sigma_v N(0,1)_{ijk} + \sigma_u N(0,1)_{jk} + \sigma_b N(0,1)_k \qquad \textbf{Equation A 7.1}$$

where i represents individual earthquakes on fault j, described in synthetic catalogue k. N(0,1) represents a number sampled from the normal distribution with mean of zero and standard deviation of 1. The subscript to N(0,1) describes the set over which individual samples are made, e.g., $N(0,1)_{jk}$ is sampled for each fault in each catalogue, but has the same value for all earthquakes on a particular fault in a particular catalogue.

The parameters describing variability represent the effects of variations in earthquake properties, other than magnitude, that vary from event to event even in the same location. Most prominent among these is the effect of 'variable slip', which research by Geist (2002) and Mueller et al. (2012) have shown to have a significant effect on tsunami heights. This parameter describes a random difference to the synthetic catalogue magnitude which is independently sampled from a zero-mean normal distribution for every earthquake.

The assumed values for these parameters are best explained starting with the case for local subduction zones. In the work of Geist (2002) the peak nearshore tsunami amplitudes varies over a factor of approximately three from lowest to highest, when local subduction zone slip distributions are randomly sampled. Assuming this variation corresponds to ±1σ of variation, we conclude that σ is approximately 0.24. In the preliminary work of Mueller et al. (2012), an increase in magnitude of 0.5 was needed to cover the total spread of inundation from 60 events with randomly varying slip. Assuming this corresponds to 2σ of variation (since ~98% of events do not exceed the inundation of an event with magnitude 0.5 units higher), we conclude that σ is approximately 0.25. Hence the value assumed for this parameter was σ_v =0.25.

In the absence of studies, we have assumed the same level of variability, i.e., 0.25 magnitude units, for other local faults; further research is required to produce a better estimate. The variability caused by non-uniform slip in distant and regional earthquakes also requires more research. It is generally assumed that the role of non-uniform slip in these events is minor or negligible, though this may perhaps not be the case if the slip distribution affects the direction of the 'beam' of the main tsunami energy, or if the down-dip distribution of slip affects the depth of water in which the tsunami is generated. Variations in the length and width of rupture may also have an influence, particularly if the sudbuction zone has changes in strike. For now it has been assumed that the effect is small compared to that of local events and therefore σ_v=0.1 was used.

Fault-specific uncertainty concerns fault properties that are fixed in time, but are not known with full accuracy. Examples include aspects of fault geometry, such as dip and rake angles, as well as uncertainty in elastic properties such as rigidity[23]. Titov et al. (1999) examined the sensitivity of tsunami amplitudes in Hawaii to variations in dip and rake angles of subduction earthquake tsunami sources in the Alaskan-Aleutian Arc. Over realistic ranges of uncertainty in those angles they found relatively modest variations in tsunami amplitude of 20-30%, hence our assumed value of σ_u=0.1 for these parameters as applied to distant and local subduction zones. Uncertainty in estimated tsunami heights as a consequence of fault properties is expected to be greater for tsunami generated by faults not on the subduction interface because: (a) the Abe equation used to estimate the tsunami heights does not include any variables other than magnitude and distance, and (b) there is generally a greater variation in fault properties and earthquake mechanisms among non-subduction inteface earthquakes. Hence σ_u=0.2 was assumed. These parameters describe a random difference to the synthetic catalogue magnitude which is independently sampled from a zero-mean normal distribution for every fault, but which is given the same value for every earthquake on the fault.

Modelling bias consists of systematic bias in our modelling methods that potentially affect all tsunami height estimates made with a technique. In the case of subduction zone modelling this could represent any tendency for the COMCOT model to systematically under- or over-estimate tsunami heights. Systematic deviations from the Okada method for calculating seabed displacements would fall into this category too. As these methods are not known to have strong biases, a relatively low σ_b=0.05 has been assumed. The potential bias in the Abe formula used for local non-subduction sources has two identified components: (a) the possibility that New Zealand conditions represent a systematic difference in elastic properties (see section A7.4), and (b) the uncertainty over the relationship between how the maximum tsunami height is defined where hydrodynamic modelling is used and how it is interpreted in the local source Abe equation (see Section 6.6). Each of these effects were estimated as σ_b=0.1, but as they are independent a combined value of σ_b=0.14 was assumed. These parameters describe a random difference to the synthetic catalogue magnitudes which is independently sampled for each catalogue, but which is given the same value for every event of the same category (i.e., Local crust, Local subduction zone, or Distant subduction zone) within a catalogue.

The effect of inaccurate bathymetric data could either be described as a fault-specific uncertainty, or as a modelling bias, depending on where the errors occur. Errors close to the coast for which the hazard curve is being calculated may act as a general bias, while those that are on the tsunami propagation paths only for certain sources may be fault-specific. More research is required to understand and quantify these effects.

[23] The treatment of rigidity as an uncertainty is problematic in the tsunami hazard model. For this study a rigidity of 50 GPa, typical of hard rock, has been assumed throughout. Shallow dipping subduction zones, such as Hikurangi and parts of the Kermadec Trench, may have lower rigidities at shallow depths (see Bilek and Lay, 1999). The effect of a lower rigidity on an earthquake of fixed magnitude is to increase its tsunami generation potential (this is one possible explanation for 'tsunami earthquakes', such as the 1947 Gisborne events; see Section 3.2), but it will also reduce the frequency with which such earthquakes occur in our model based on plate-rate balancing. As these two effects tend to counteract each other in the hazard curves this effect is not well described by the current uncertainty model. Ideally a location-specific rigidity model could be used—this is a topic for further research.

A7.4 ESTIMATION OF TSUNAMI HEIGHTS

Interpretation of 'maximum tsunami height'

The maximum tsunami height within a coastal section is the maximum at any offshore point in the area over the duration of the simulation. The time periods of the simulations are typically 30 hours for distant sources, 24 hours for regional sources, and 12 hours for local sources, and are intended to be sufficiently long to capture the largest waves in most situations likely to contribute to the hazard curves (the quality of simulation results degrades over time elapsed since the first wave arrivals, hence running the models for longer would not necessarily improve the results).

Faults that are partially on-shore

The following set of crustal faults, labelled with the Fault Name and NZSHM_Number (see Appendix 4), were identified as extending a significant distance onshore for at least half of their length. In the estimation of tsunami heights for earthquakes on these faults, it was assumed that only half of the seismic moment release contributes to tsunami generation, i.e., the effective magnitude was reduced by 0.2 magnitude units.

WairarapNich_345, AwatNEVerCl_379, AwatNEVer_380, Matata_163, WhakataneN_158, WaimanaN_166, Waikaremoana_165, Urewera3_162, Otaraia_368, JorKekCha_373, JorKekNeed_374, Hundalee_405

Estimation of tsunami heights – Distant and Regional subduction zones

Models from the New Zealand tsunami forecast database (Power, unpublished; an earlier version of this database is described in Power and Gale, 2011) were used to fit parameters of a semi-empirical model (Abe, 1979, 1994). The form of the empirical equation is:

$$Ht = 10^{M_W - B_{ij}}$$ **Equation A 7.2**

where the coefficients B_{ij} (and their standard deviations σB_{ij}) were estimated using the data from the forecast models. i represents each particular source region, and j represents each particular coastal zone. M_W is the moment magnitude.

Abe (1979, 1994) calculated coefficients B_{ij} using historical data, but given the sparsity of New Zealand historical data, the approach used here is to fit these coefficients using modelled scenario data.

For this purpose 312 models were used from the forecast database, which for distant sources includes simulations at M_W 8.7, 9.0, 9.3, located at intervals of 400 km around the subduction zones of the Pacific Rim. Regional events were similarly modelled at M_W 8.1, 8.4, 8.7, 9.0, 9.3 and 400 km intervals. Source models for distant earthquakes in the forecast database were based on the subduction zone unit sources given by NOAA (see for example, Tang et al., 2010). Regional earthquake sources were modelled using additional unit sources compiled within GNS Science.

Rupture dimensions were typically 1000 x 100 km for M_W9.3, 600 x 100 km for M_W9.0, 400 x 100 km for M_W8.7, 200 x 100 km for M_W8.4, and 200 x 50 km for M_W8.1. Variations around these dimensions were made for scenario events located near the ends of subduction zones. In reality, variations in the dimensions of rupture vary considerably even between

earthquakes of the same magnitude, and this affects the degree of tsunami generation; this variation contributes to the variability coefficients in Table A 7.1.

Once the coefficients B_{ij} and σB_{ij} have been determined, estimation of wave heights proceeds using equation A 7.2, specifically:

$$Ht = 10^{M_W - (B_{ij} + \overline{\sigma B_{ij}})}$$ **Equation A 7.3**

where $\overline{\sigma B_{ij}}$ is randomly sampled from a normal distribution with mean of zero and standard deviation σB_{ij}. This corresponds primarily to the variability in tsunami height associated with different earthquake locations within the source region.

Abe (1979) successfully calibrated and applied equation A 7.2 in the context of earthquakes spanning a wide range of magnitudes (large events such as the 1960 M_W9.5 Chile earthquake and the 1960 M_W9.2 Alaska tsunami were among those used for calibration), suggesting that A7.2 is suitable for use over a broad range of tsunamigenic magnitudes.

Estimation of tsunami heights – Local subduction zones

Tsunami heights from the local subduction zone sources, i.e., Hikurangi, Kermadec and Puysegur, were estimated by searching for the closest analogue in a pre-calculated catalogue and scaling the results to accommodate the difference between the synthetic catalogue earthquake magnitude and the magnitude of the closest analogue scenario.

The pre-calculated catalogue of tsunami scenarios consisted of a scenario for rupture of the whole subduction margin, two half margin scenarios, and three one-third margin scenarios. Due to the length of the Kermadec Trench, six scenarios, each spanning one-sixth of the trench, were also used for that source. The magnitudes of these scenarios are tabulated in Table A7.3

Table A 7.3 Magnitudes of scenario events used for modelling of local subduction zones.

	Hikurangi	**Kermadec**	**Puysegur**
Whole margin	9.0	9.3	9.0
Half margin	8.6	9.0	8.6
Third of margin	8.3	8.7	8.3
Sixth of margin	-	8.3	-

For any given local subduction zone earthquake in the synthetic catalogue, the earthquake location was uniformly randomly distributed across the margin, i.e., if the magnitude was closest to that of a one-third of margin event, the wave heights were equally likely to be modelled by scaling any one of the three corresponding scenarios. This amounts to an assumption that the subduction zones are homogeneous in the spatial distribution of earthquakes. The Hikurangi margin, however, is known to have strong variations in geophysical properties along its length, which may well correlate with the distribution of large earthquakes; if so, this would be in contradiction to this assumption used here. Further research is therefore required to better understand and quantify these relationships, and to incorporate the heterogeneity of the local subduction zones into the tsunami hazard model.

Once the appropriate scenario is selected the estimation of tsunami heights proceeds using:

$$Ht = 10^{M_W - (B_{ij} + \overline{\sigma B_{ij}})}$$ **Equation A 7.4**

where B_{ij} are estimated using only the results from the chosen analogue scenario. As σB_{ij} cannot be estimated from a single scenario, a fixed value of 0.1 has been assumed (this is approximately the average value of σB_{ij} found for the distant and regional sources), further research is needed to better quantify this parameter.

Note that this scaling is consistent with Abe's (1979, 1995) empirical equations for local and distant source tsunami.

The approach to estimating tsunami heights for local subduction events by scaling the catalogue is not without limitations. In particular, the discretization of events in the catalogue into adjacent equal size ruptures may produce inconsistencies around the borders between the modelled events. Improvements to this methodology should probably accompany research into the variation in geophysical properties along the length of the subduction zones.

Estimation of tsunami heights – Local crustal and outer rise faults

Estimation of tsunami heights from the local non-subduction zone faults follows the methods of Abe (1995). The tsunami height is estimated as:

$$Ht = 10^{M_W - logD - 5.55 + C}$$ **Equation A 7.5**

where M_W is the earthquake moment magnitude, D is the distance between the fault and the coastal section, and C is a constant.

If D < $10^{\frac{M_W}{2} - 2.25}$ (when the coastal section is approximately above the fault plane) then

$$Ht = 10^{\frac{M_W}{2} - 3.3 + C}$$ **Equation A 7.6**

is used instead.

The constant C is taken here to be 0.1; in Abe's work C is either 0.0 or 0.2 according to the specific geophysical properties of the location, here this uncertainty is instead expressed using the 'effective magnitude' approach described in the next section.

Because equation A 7.5 uses only magnitude and distance from the fault to determine tsunami height, it can give poor results in situations where the bathymetry is unfavourable for tsunami propagation. For instance, equation A 7.5 may overestimate tsunami heights at the Kapiti coast caused by earthquakes near the Wairarapa coast, since the throttling effect of the narrow part of Cook Strait is not taken into account.

Construction of hazard curves

Hazard curves are constructed from the synthetic catalogues of tsunami heights in the following way:

For a chosen 20 km coastal section, the catalogue of tsunami heights is sorted into descending order. Within a catalogue covering N years, the tsunami with return period RP is expected to occur at least N/RP times. The (N/RP)th entry in the sorted synthetic catalogue of tsunami heights is therefore the estimated tsunami height at the desired return period.

This process is repeated for several different return periods to construct a single hazard curve.

Epistemic uncertainty is accounted for by creating a different hazard curve for each set of the sampled epistemically-uncertain parameters. The distribution of different hazard curves can then be used to quantify the uncertainty in the hazard curves. In our results this is achieved by identifying the 16th and 84th percentile from the distribution of curves at each return period.

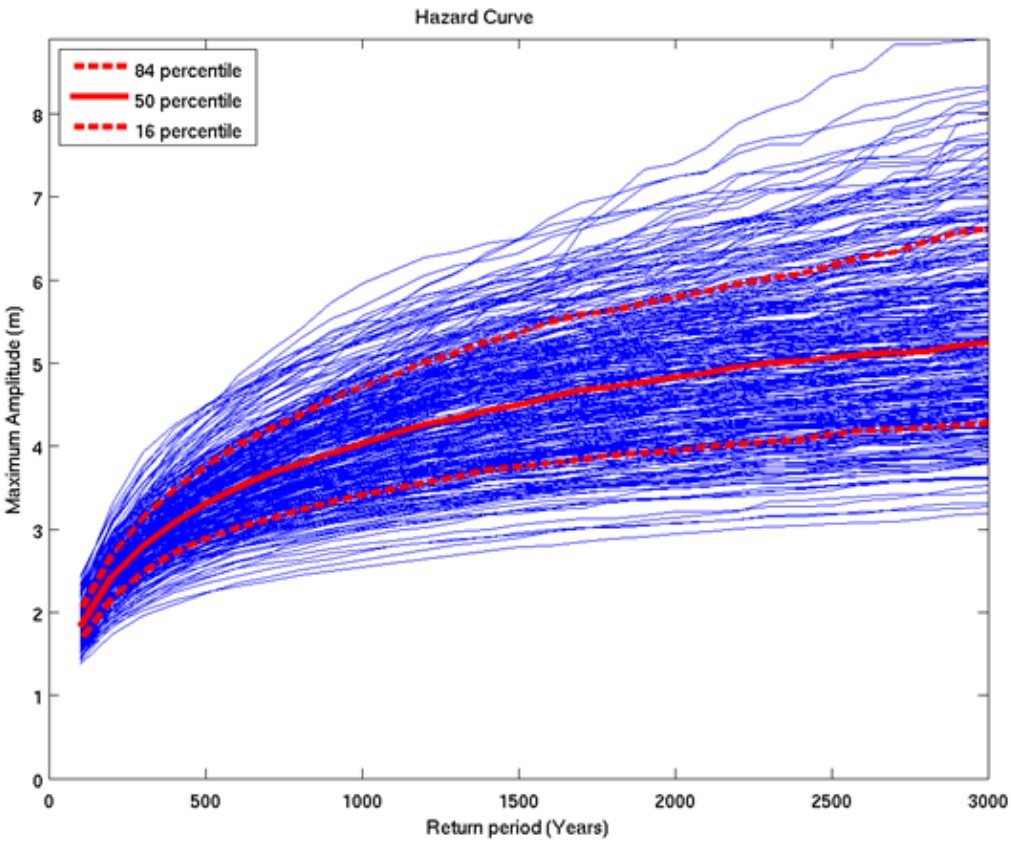

Figure A 7.1 Hazard curves for 300 samples of epistemic uncertainty, illustrating how the 16th, 50th and 84th percentiles of uncertainty are calculated.

A7.5 REFERENCES

Abe, K. (1979). Size of great earthquakes of 1837–1974 inferred from tsunami data. *Journal of Geophysical Research*, 84: 1561-1568.

Abe, K. (1995). Estimate of tsunami run-up heights from earthquake magnitudes. In Tsunami: Progress in Prediction, Disaster Prevention and Warning, Adv. Nat. Technol. Hazards Res., vol. 4, Y. Tsuchiya and N. Shuto (eds.), Kluwer Acad.: 21-35.

Bilek, S.L., and Lay, T. (1999). Rigidity variations with depth along interpolate megathrust faults in subduction zones, *Nature*, 400, 443– 446.

Geist, E.L. (2002). Complex earthquake rupture and local tsunamis, *J. Geophys. Res*. 107, doi 10.1029/2000JB000139.

McGuire, R.K. (2004). Seismic hazard and risk analysis, EERI Monograph MNO-10, Earthquake Engineering Research Institute, Oakland, California.

Mueller, C.;, Power, W.; Fraser, S.; Wang, X. (2012). Towards a Robust Framework for Probabilistic Tsunami Hazard Assessment (PTHA) for Local and Regional Tsunami in New Zealand.Abstract volume of the Geosciences 2012 conference, Hamilton, New Zealand. p. 64.

Power, W.L. and Gale, N.H. (2011). Tsunami forecasting and monitoring in New Zealand. *Pure and Applied Geophysics*, 168(6/7): 1125-1136. doi: 10.1007/s00024-010-0223-9.

Tang, L., Titov, V.V., and Chamberlin, C.D. (2010). A Tsunami Forecast Model for Hilo, Hawaii. PMEL Tsunami Forecast Series: Vol. 1, NOAA OAR Special Report.

Titov, V.V., Mofjeld, H.O., Gonzalez, F.I., and Newman, J.C. (1999). Offshore forecasting of Hawaiian tsunamis generated in Alaskan-Aleutian subduction zone, NOAA Technical Memorandum ERL, Pacific Marine Environmental Laboratory (PMEL), Seattle, Washington, 26 pp.

www.gns.cri.nz

Principal Location

1 Fairway Drive
Avalon
PO Box 30368
Lower Hutt
New Zealand
T +64-4-570 1444
F +64-4-570 4600

Other Locations

Dunedin Research Centre
764 Cumberland Street
Private Bag 1930
Dunedin
New Zealand
T +64-3-477 4050
F +64-3-477 5232

Wairakei Research Centre
114 Karetoto Road
Wairakei
Private Bag 2000, Taupo
New Zealand
T +64-7-374 8211
F +64-7-374 8199

National Isotope Centre
30 Gracefield Road
PO Box 31312
Lower Hutt
New Zealand
T +64-4-570 1444
F +64-4-570 4657